S S R P   2 0 2 4

23. Steirisches Seminar über Regelungstechnik und Prozessautomatisierung

23rd Styrian Workshop on Automatic Control

presentation slides

September 9 - 11, 2024

Schloss Retzhof, Leitring/Wagna, Austria

IRT

http://www.irt.tugraz.at

TU Graz

Graz University of Technology

I. Model Predictive Control of a Metal Hydride Hydrogen Storage
presenter: Daniel Schwingshackl

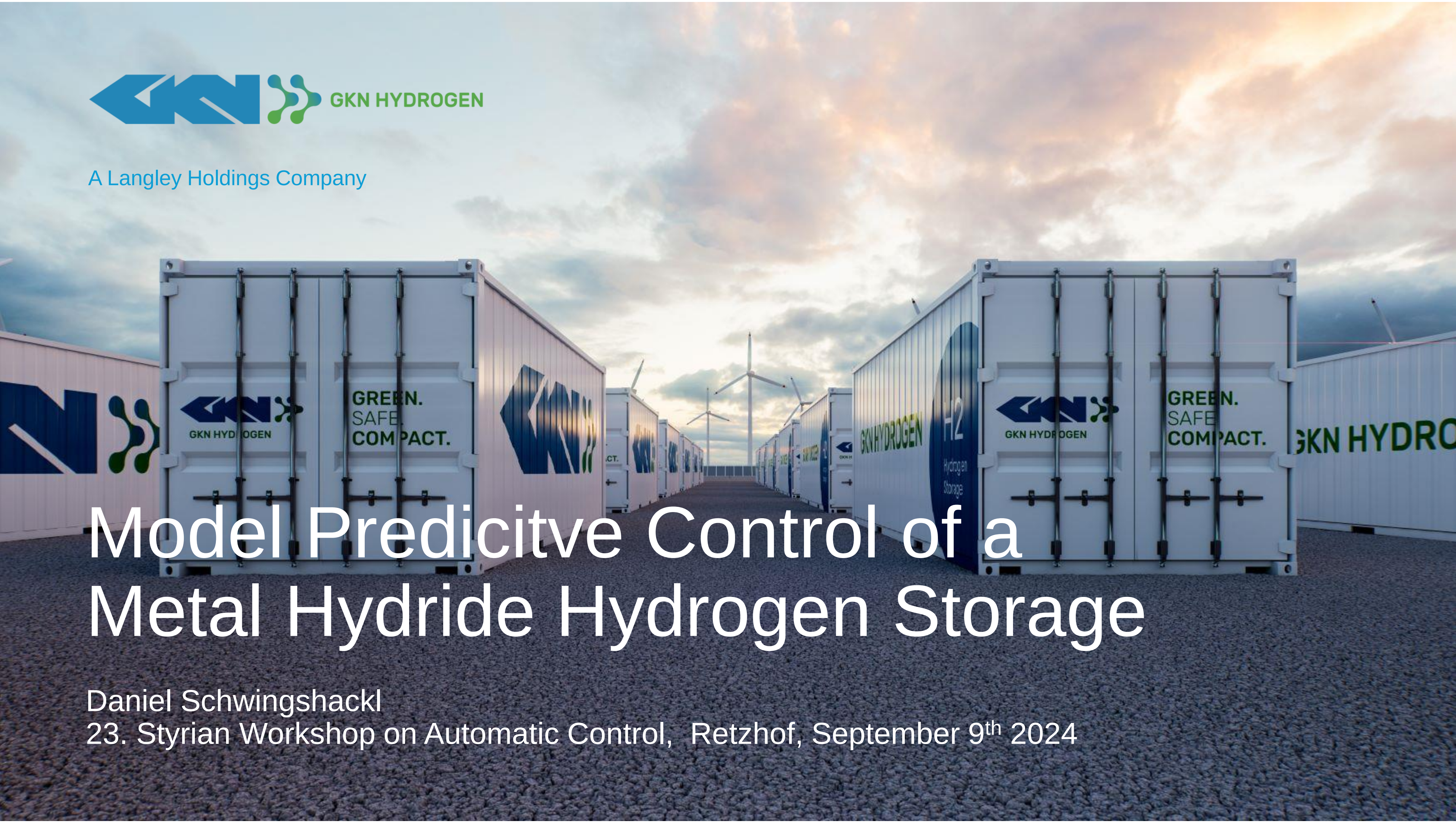

GKN HYDROGEN

A Langley Holdings Company

Model Predicitve Control of a Metal Hydride Hydrogen Storage

Daniel Schwingshackl

23. Styrian Workshop on Automatic Control, Retzhof, September 9th 2024

Content

Introduction

- The company GKN Hydrogen
- Metal Hydride - How it works
- Metal Hydride Hydrogen Storage (MHHS)

MPC of a MHHS

- Motivation
- Control strategy
- Modelling approach
- Simulation results
- Outlook

GKN Powder Metallurgy – Origin of GKN Hydrogen

PEOPLE

6,600+

MANUFACTURING LOCATIONS

29

SALES REVENUE

1.05 bn

Tn

HOEGANAES

World # 2 24% global share

300,000 tons/year

LANGLEY

Langley Holdings plc acquires GKN Hydrogen 1st August 2024

LAUNCH MAY 2021

GKN HYDROGEN

NEW Business since 2022

GKN HYDROGEN
A Langley Holdings Company

GREEN. SAFE. **COMPACT.**

GKN Hydrogen = Green H_2 Energy Storage

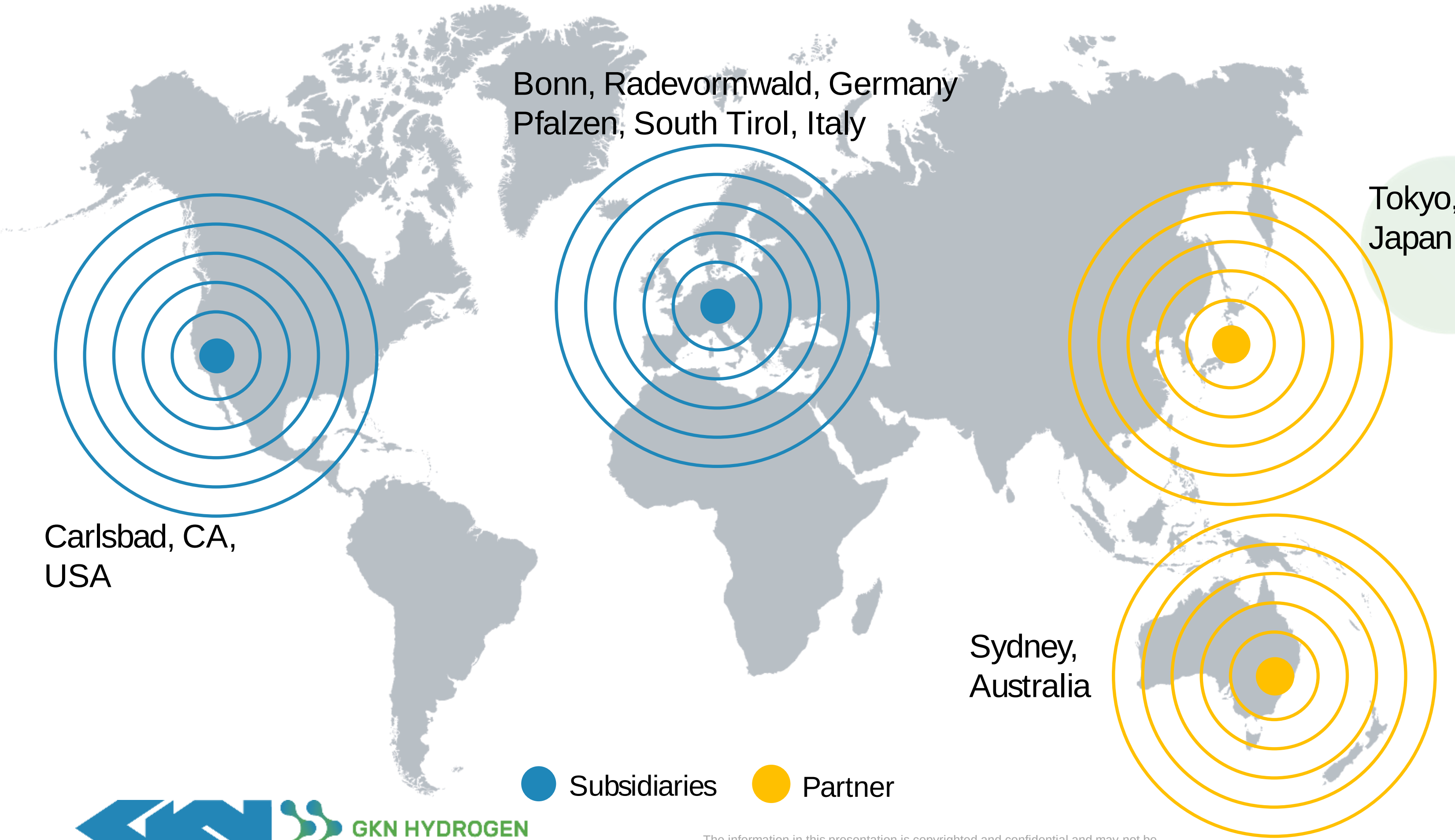

Europe
- Research & Development
- Application Engineering
- Supply Chain
- Manufacturing
- Project Management
- Service

USA
- Application Engineering
- Project Management
- Service

Australia
- Application Engineering
- Project Management
- Service

Japan
- MOU in place

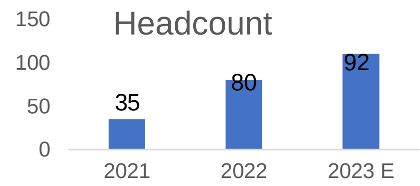

GKN HYDROGEN
A Langley Holdings Company

GREEN. SAFE. COMPACT.

Hydrogen Timeline - From R&D to Industrial Scale

2013

R&D launch in partnership with GKN Powder Metallurgy

GKN POWDER METALLURGY

#1 Global Producer of Powder Metal Parts

#2 Global Producer of Metal Powder

2019

Installation of initial proof of concept product

Power-2-Power

2021

Virtual launch of GKN Hydrogen and HY2 product suite HY2MINI, HY2MEDI & HY2MEGA storage

2022

Launch of digital monitoring platform

GKN Hydrogen becomes a separate legal entity

2023 & Beyond

New Commercial product groups

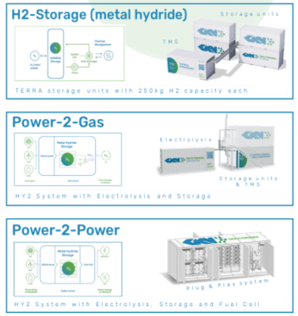

2024

Langley Holdings plc acquires GKN Hydrogen 1st August

LANGLEY

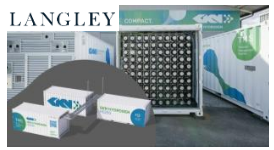

Launch of GKN HYDROGEN

GKN HYDROGEN
A Langley Holdings Company

GREEN. SAFE. COMPACT.

Metal Hydride Storage = How it works

Hydrogen Charge

- H_2 gas is fed to the metal alloy at pressure up to 40 bar
- Alloy reacts with hydrogen, creating a metal hydride and releases heat

Hydrogen Discharge

- Metal hydride is heated
- H_2 is released safely

<20℃ (68°F)
Usable Heat

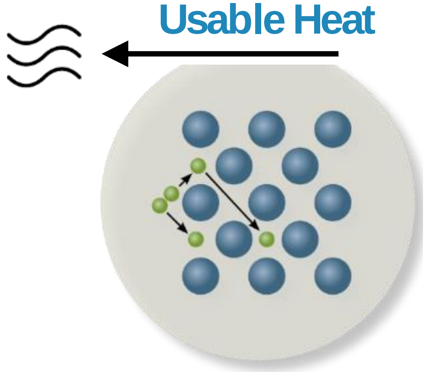

LONG-DURATION STORAGE

- Stored without losses indefinitely until needed
- **~96% chemically bonded/ solid and safe, only 4% is gaseous H2**

>60℃ (140°F)
Heat In

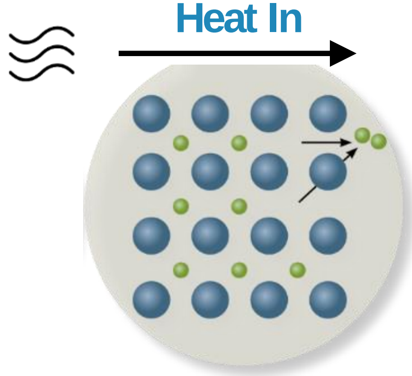

GKN HYDROGEN
A Langley Holdings Company

GREEN. SAFE. COMPACT.

What we offer

Hydrogen Storage

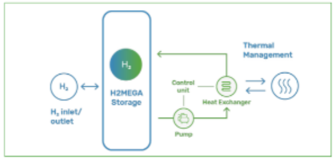

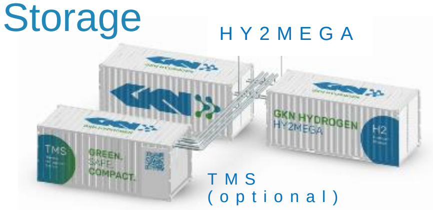

HY2MEGA storage units with 250 kg H2 capacity each

Power-2-Gas

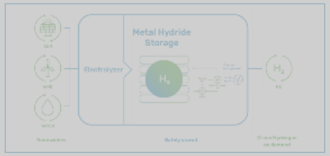

HY2 Systems with Electrolysis and Storage

Power-2-Power

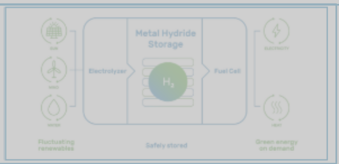

HY2 Systems with Electrolysis, Storage and Fuel Cell

Modular System

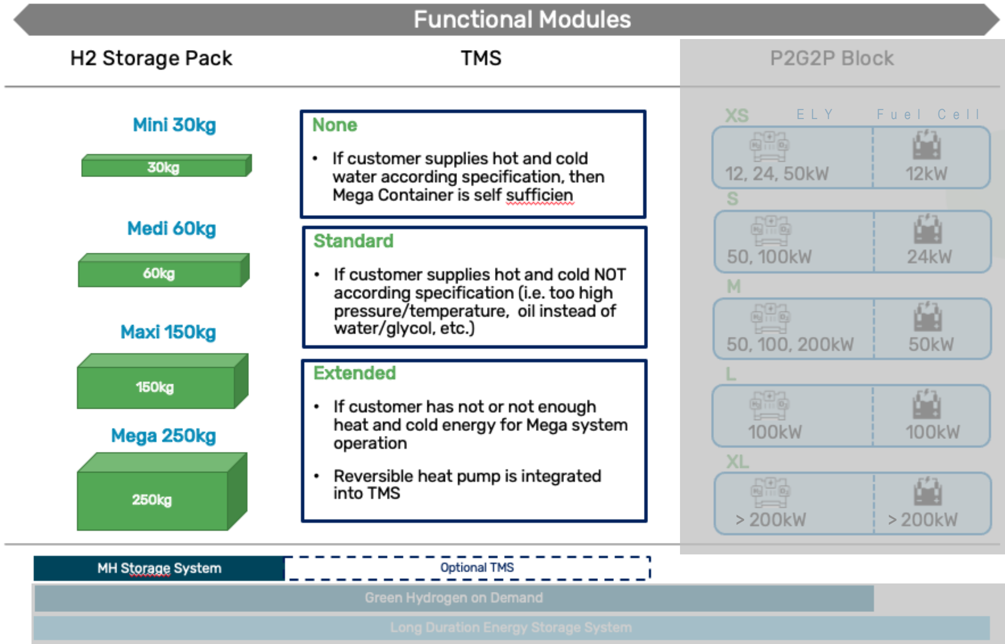

GKN HYDROGEN

GREEN. SAFE. COMPACT.

Metal Hydride Hydrogen Storage (MHHS)

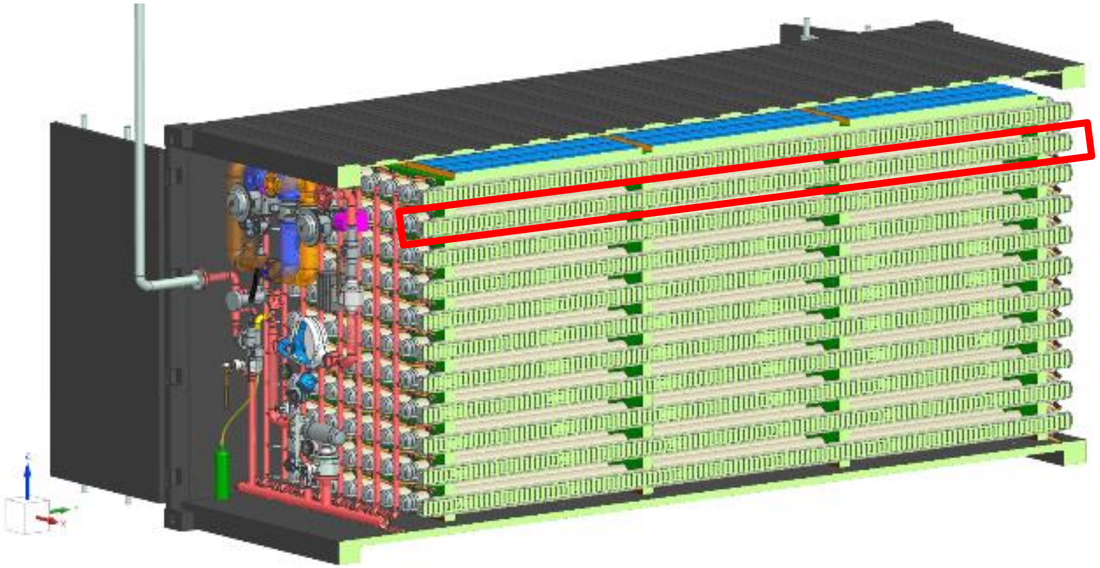

Outer tube
Heating/Cooling shell

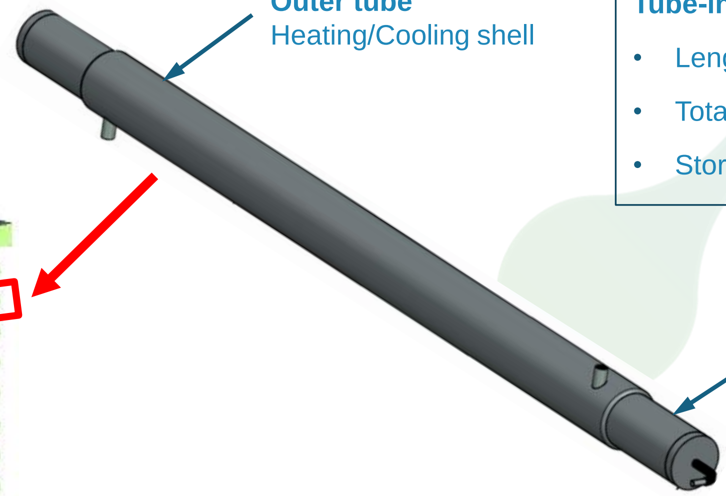

Inner tube
Discs of Metal Hydrid

Tube-in-tube concept

- Length: 5,1 m
- Total weight: ~230kg
- Storage capacity: 2,5 kg H2

- 100 tubes
- Collector for H2
- Collector for heating/cooling fluid
- Total weight: ~35 tons
- Storage capacity: 250 kg H2

Metal Hydride Hydrogen Storage (single tube)

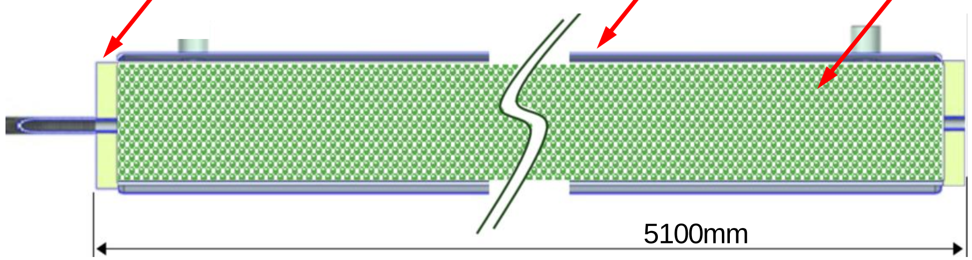

Void volume inner tube:

$V_{VT} = \pi/4 \times d_i^2 \times L = 45.26 dm^3$

Mass of FeTi filled into the tube:

130 discs x 1.091kg/disc= 141.83kg

Volume of FeTi :

Density FeTi = $6.05 kg/dm^3$

$V_{FeTi} = m/\rho = 23.44 dm^3$

Gaseous H2 volume:

$21.82 dm^3$

MH volume:

$23.44 dm^3$

Ratio gaseous H2/total volume:

~ 48.2%

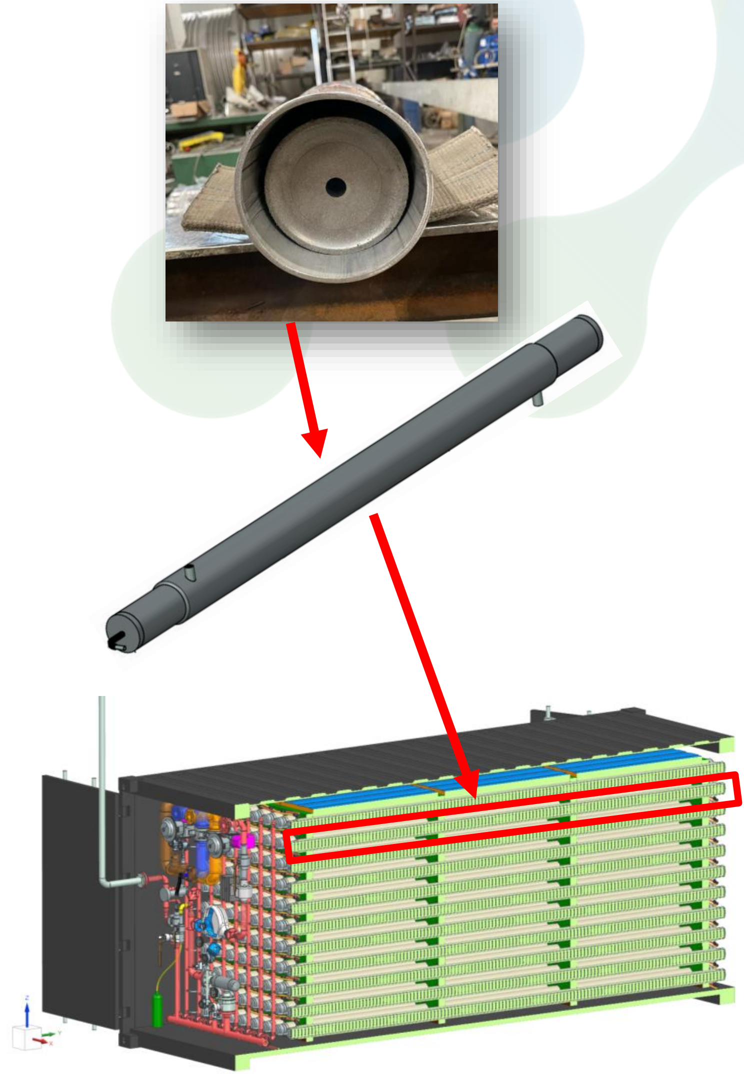

Motivation

For loading/unloading actions

- Storage to be prepared upfront in order to minimize reaction times
- Time and energy consuming
- Storage behaviour heavily depends on current operating point
- Heating power is limited

Challenges

- Reduce undesired waiting times
- Avoid H2 overfilling
- Ensure H2 customer flow
- Minimize self-consumptions
- Applicability on PLC

Idea

- By having future information on customers H2 demand/production
- Predict storage behavior based on mathematical model
- Keep storage pressure within its limits
- Minimize required heating power using optimization

Model Predictive Control (MPC) and Local Linear Neuro Fuzzy Model (LLNFM) [1,2]

State of the art

- Currently applied
  - ON/OFF control combined with thresholds (temperature/pressure)

- Literature
  - PI/PID-Control strategies [3,4,5,6]
    - No prediction of storage behaviour
    - Future load profile not taken into account

  - Model Predictive Control [7,8,9]
    - multi-reactor application
    - Offline optimization

Control strategy

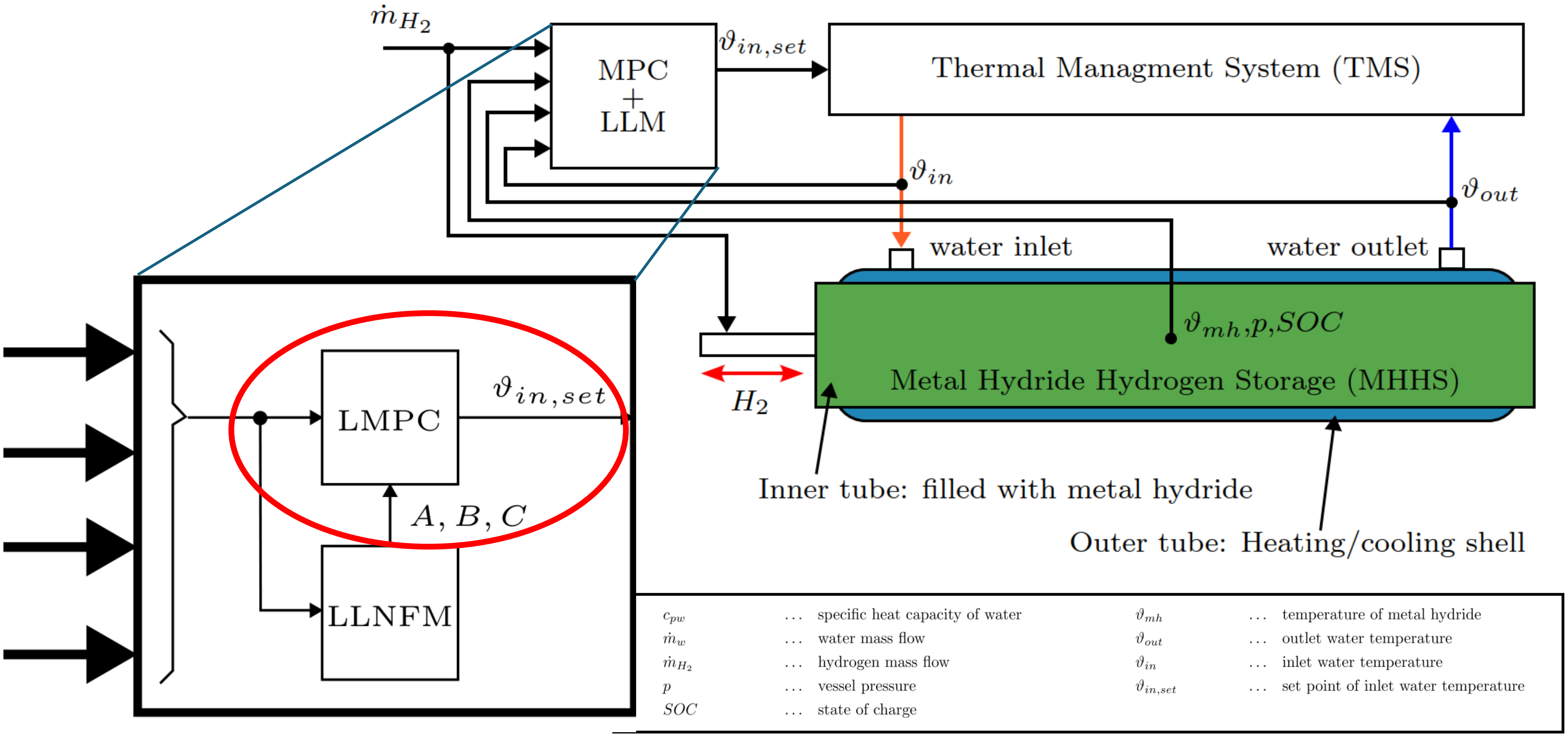

Linear MPC [12,13]

Linear discrete time system

$$\mathbf{x}_{k+1} = \mathbf{A}\mathbf{x}_k + \mathbf{B}\mathbf{u}_k$$
$$\mathbf{y}_k = \mathbf{C}\mathbf{x}_k$$

with

$$\mathbf{u}_k = \mathbf{u}_{k-1} + \mathbf{\Delta}\mathbf{u}_k$$

Prediction:

$$\bar{\mathbf{y}}^T = \begin{bmatrix}\mathbf{y}_{k+1}^T & \mathbf{y}_{k+2}^T & \cdots & \mathbf{y}_{k+n_p}^T\end{bmatrix}$$

Optimization:

$$\min_{\mathbf{\Delta}\bar{\mathbf{u}}} \left(\bar{\mathbf{e}}^T\mathbf{Q}\bar{\mathbf{e}} + \mathbf{\Delta}\bar{\mathbf{u}}^T\mathbf{R}\mathbf{\Delta}\bar{\mathbf{u}}\right)$$
$$\begin{aligned} s.t.: \quad \bar{\mathbf{u}} &\leq \bar{\mathbf{u}}_{max} \\ \bar{\mathbf{u}} &\geq \bar{\mathbf{u}}_{min} \\ |\mathbf{\Delta}\bar{\mathbf{u}}| &\leq \mathbf{\Delta}\bar{\mathbf{u}}_{max} \end{aligned}$$

with

$$\bar{\mathbf{e}} = \bar{\mathbf{y}} - \bar{\mathbf{y}}_r$$
$$\bar{\mathbf{u}}^T = \begin{bmatrix}\mathbf{u}_k^T & \cdots & \mathbf{u}_{k+n_c-1}^T\end{bmatrix}$$

Linear MPC [12,13]

$$\mathbf{x}^T = [x_1 \quad x_2 \quad x_3 \quad x_4 \quad x_5] = [\vartheta_{out} \quad p \quad \vartheta_{mh} \quad SOC \quad P_{th}]$$
$$u^T = \vartheta_{in}$$
$$d^T = \dot{m}_{H_2}$$
$$\mathbf{y}^T = [y_1 \quad y_2] = [p \quad P_{th}]$$

Linear discrete time system

$$\mathbf{x}_{k+1} = \mathbf{A}\mathbf{x}_k + b_1 u_k + b_2 d_k$$
$$\mathbf{y}_k = \mathbf{C}\mathbf{x}_k$$

with

$$u_k = u_{k-1} + \Delta u_k$$

Prediction:

$$\bar{\mathbf{y}}^T = [\mathbf{y}_{k+1}^T \quad \mathbf{y}_{k+2}^T \quad \cdots \quad \mathbf{y}_{k+n_p}^T]$$

Optimization:

$$\min_{\Delta\bar{u}} \left(\bar{e}^T Q \bar{e} + \Delta\bar{u}^T R \Delta\bar{u}\right)$$
$$\begin{aligned} s.t.: \quad \bar{u} &\leq \bar{u}_{max} \\ \bar{u} &\geq \bar{u}_{min} \\ |\Delta\bar{u}| &\leq \Delta\bar{u}_{max} \\ \bar{y}_1 &\leq \bar{p}_{max} \\ \bar{y}_1 &\geq \bar{p}_{min} \end{aligned}$$

with

$$\bar{e} = \bar{y}_2$$
$$\bar{u}^T = [u_k^T \quad \ldots \quad u_{k+n_c-1}^T]$$

Control strategy

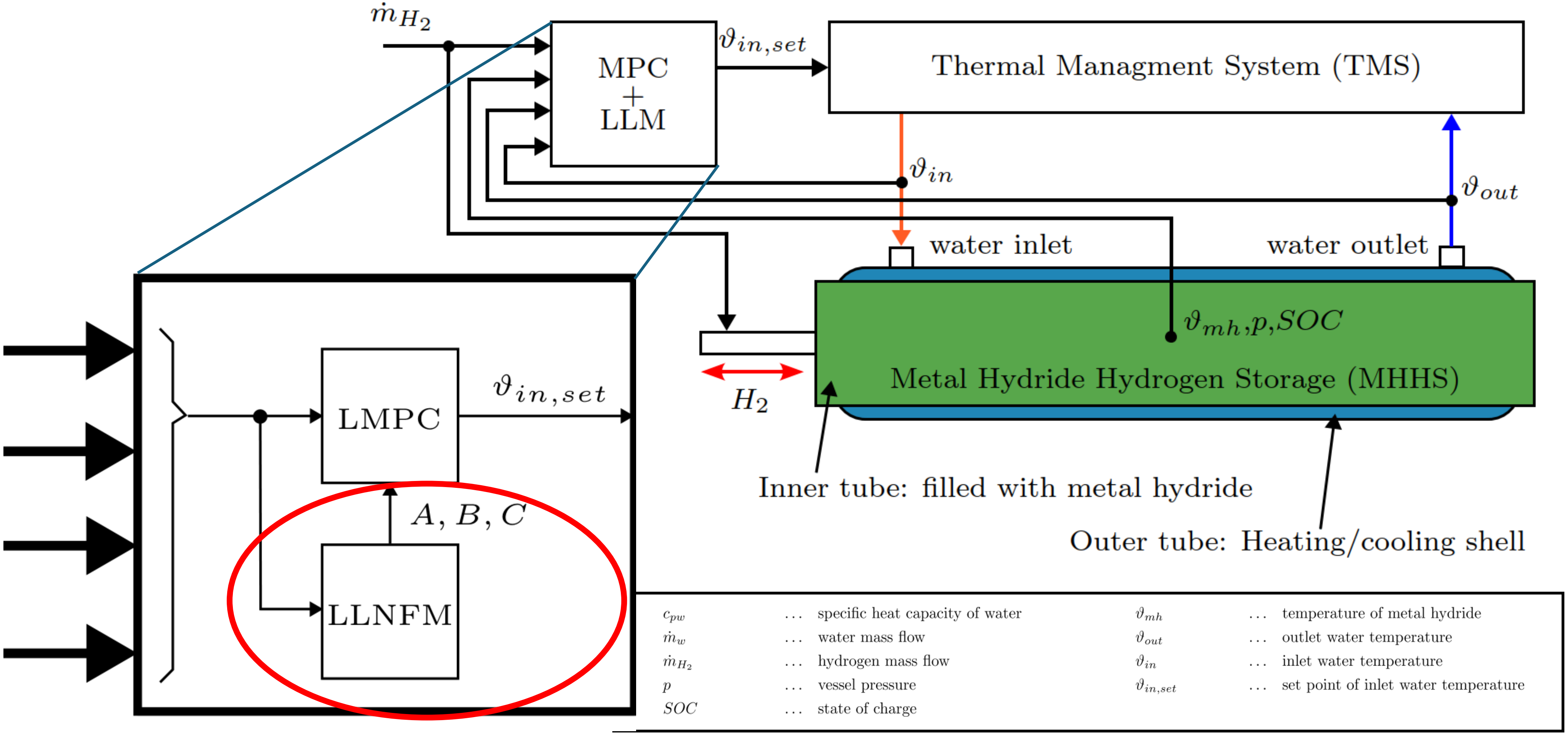

GKN HYDROGEN
A Langley Holdings Company

GREEN. SAFE. COMPACT.

Local Linear Neuro Fuzzy Model (LLNFM)

1 output of the form:

$$y_k = \sum_{l=1}^{M} \left(w_{l0} + \sum_{i=1}^{n} \left[w_{li}^{y} y_{k-i} + \sum_{j=1}^{m} w_{li}^{u_j} u_{j,k-i} \right] \right) \Phi_l(\mathbf{u}^*{}_k)$$

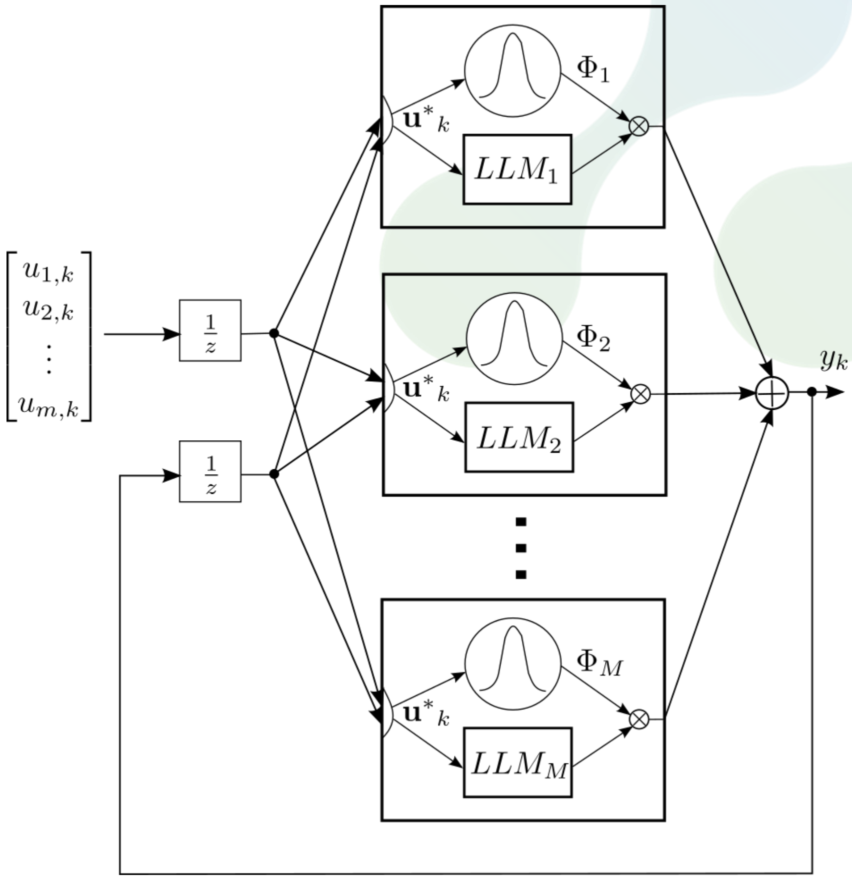

- m inputs
- M local models of order n
- LoLiMoT-algorithm [10]
- 1 LLNFM for each control variable

State space model based on LLNFM

Rewriting:

$$y_k = \sum_{l=1}^{M}\left(w_{l0} + \sum_{i=1}^{n}\left[w_{li}^{y} y_{k-i} + \sum_{j=1}^{m} w_{li}^{u_j} u_{j,k-i}\right]\right)\Phi_l(\mathbf{u}^*{}_k)$$

Parameters:

$$w_k^d = \sum_{l=1}^{M} w_{l0}\Phi_l(\mathbf{u}^*{}_k)$$

$$b_{n-i,k}^{u_j} = \sum_{l=1}^{M} w_{li}^{u_j}\Phi_l(\mathbf{u}^*{}_k)$$

$$a_{n-i,k} = -\sum_{l=1}^{M} w_{li}^{y}\Phi_l(\mathbf{u}^*{}_k)$$

Extension:

$$u_d = 1$$

$$y_k = \sum_{i=1}^{n}\left(-a_{n-i,k} y_{k-i} + \sum_{j=1}^{m} b_{n-i,k}^{u_j} u_{j,k-i}\right) + w_k^d u_d$$

State space model based on LLNFM

$$y_k = \sum_{i=1}^{n} \left(-a_{n-i,k} y_{k-i} + \sum_{j=1}^{m} b_{n-i,k}^{u_j} u_{j,k-i} \right) + w_k^d u_d$$

State space representation:

$$\mathbf{x}_{k+1} = \mathbf{A}_k \mathbf{x}_k + \mathbf{B}_k \mathbf{u}_k + \mathbf{b}_{1k} u_d$$
$$y_k = \mathbf{c}_k^T \mathbf{x}_k$$

System parameters:

$$\mathbf{A}_k \approx \begin{bmatrix} 0 & \cdots & \cdots & 0 & -a_{0,k} \\ 1 & \ddots & & \vdots & -a_{1,k-1} \\ 0 & \ddots & \ddots & \vdots & \vdots \\ \vdots & \ddots & \ddots & 0 & -a_{n-2,k-n+2} \\ 0 & \cdots & 0 & 1 & -a_{n-1,k-n+1} \end{bmatrix} \quad \mathbf{B}_k \approx \begin{bmatrix} b_{0,k}^{u_1} & \cdots & b_{0,k}^{u_m} \\ \vdots & & \vdots \\ b_{n-1,k-n+1}^{u_1} & \cdots & b_{n-1,k-n+1}^{u_m} \end{bmatrix} \quad \mathbf{b}_{1k} \approx \begin{bmatrix} 0 \\ \vdots \\ 0 \\ w_{k-n+1}^d \end{bmatrix}$$

Modelling approach

- Performance depends on model quality
- Proper excitation over entire operating range required
- <u>Problem:</u>
  - excitation on real world system exceeds available capacities (cost & time)
- <u>Solution:</u>
  - Generation of identification data via simulation using a detailed physical model

Simulation Model for MHHS [14]

$$\dot{m}_R = k \cdot exp\left(\frac{E}{R \cdot T}\right) \cdot \left(\frac{p_{EQ} - p}{p_{EQ} + \epsilon}\right) \cdot \begin{cases} \rho_{max} - \rho & for\ absorption \\ \rho - \rho_{min} & for\ desorption \end{cases}$$

- Dynamic behaviour: release of hydrogen
  - Heating of storage by glycol
  - "self cooling" due to chemical reaction of releasing hydrogen

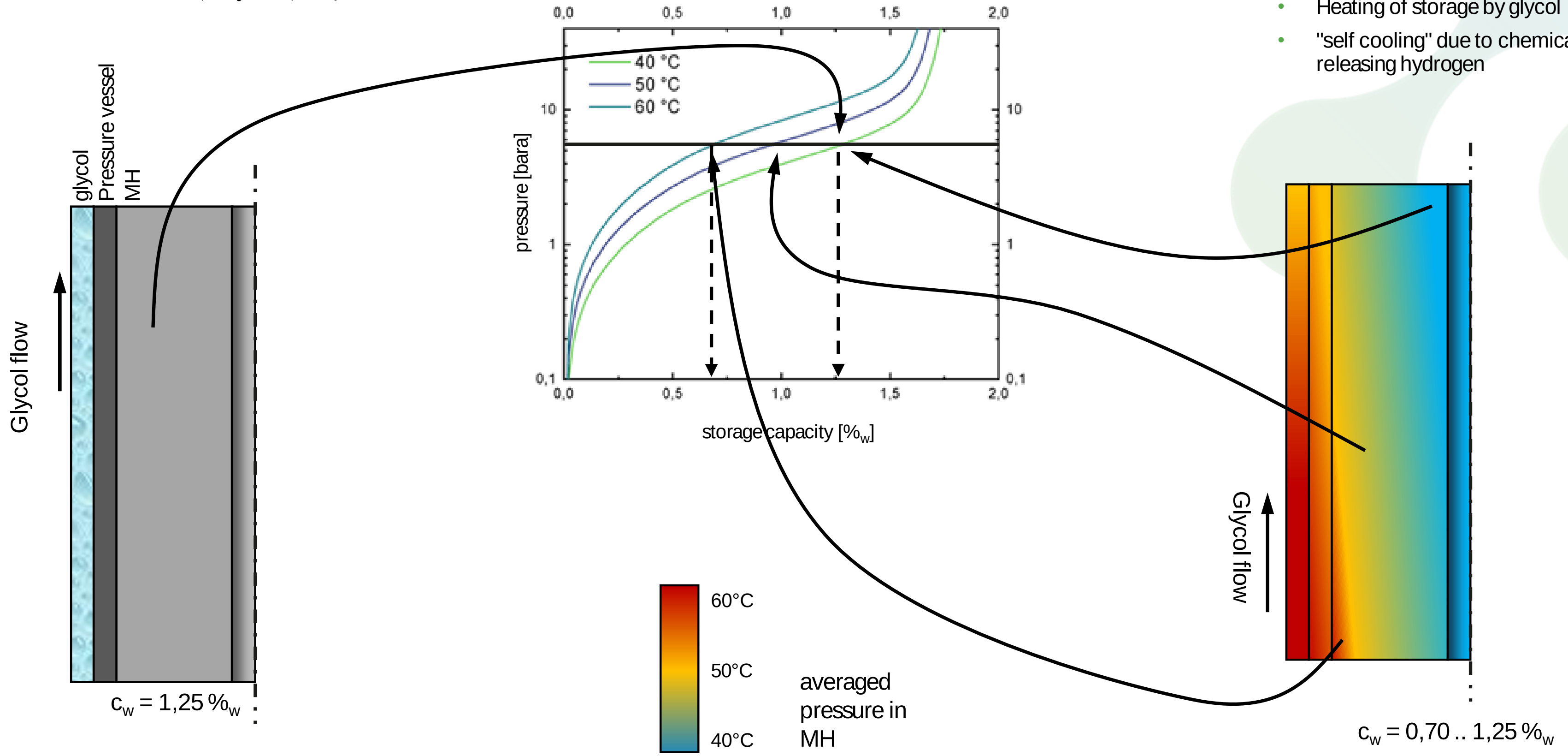

Modelling approach: work flow [1]

- Modeling of the MHHS in Matlab according specification
- Generation of the identification data by simulation
- Identification of LLNFM using LoLiMoT [10]

Identification of the LLNFM

- Excitation based on 3211 piecewise constant sequence [11]

- Applied on several operating points

- Further signal types to be considered
  - APRB signal (open)
  - Shifted chirp (open)

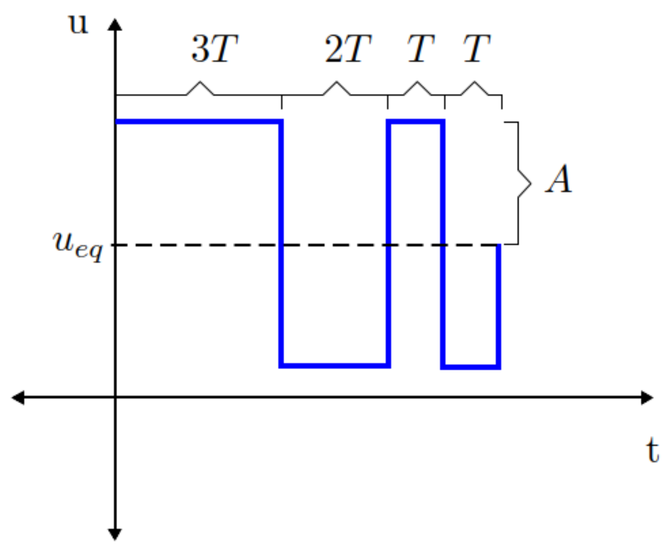

Problem configuration

<u>Inputs:</u>

- Inlet water temperature $\vartheta_{in,set}$

<u>Outputs:</u>

- Vessel pressure p
- Outlet water temperature ϑ_{out}
- Temperature of the metal hydride ϑ_{mh}
- Hydrogen state of charge SOC

<u>Measurable disturbance:</u>

- Desired hydrogen flow $\dot{m}_{H_2}$

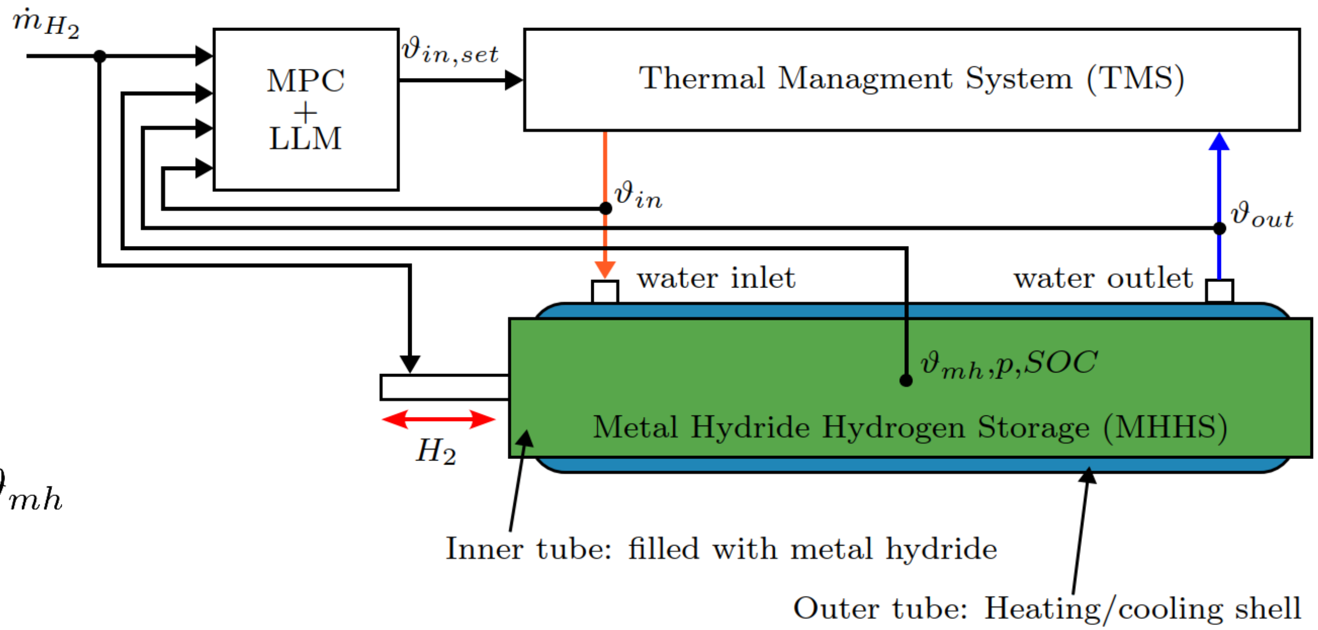

Validation of the physical model

Comparison:

- Measurement vs. phys. model

Error:

- Water outlet temp.: <5°C
- Metal hydride temp.: <9°C
- Pressure: <7bar

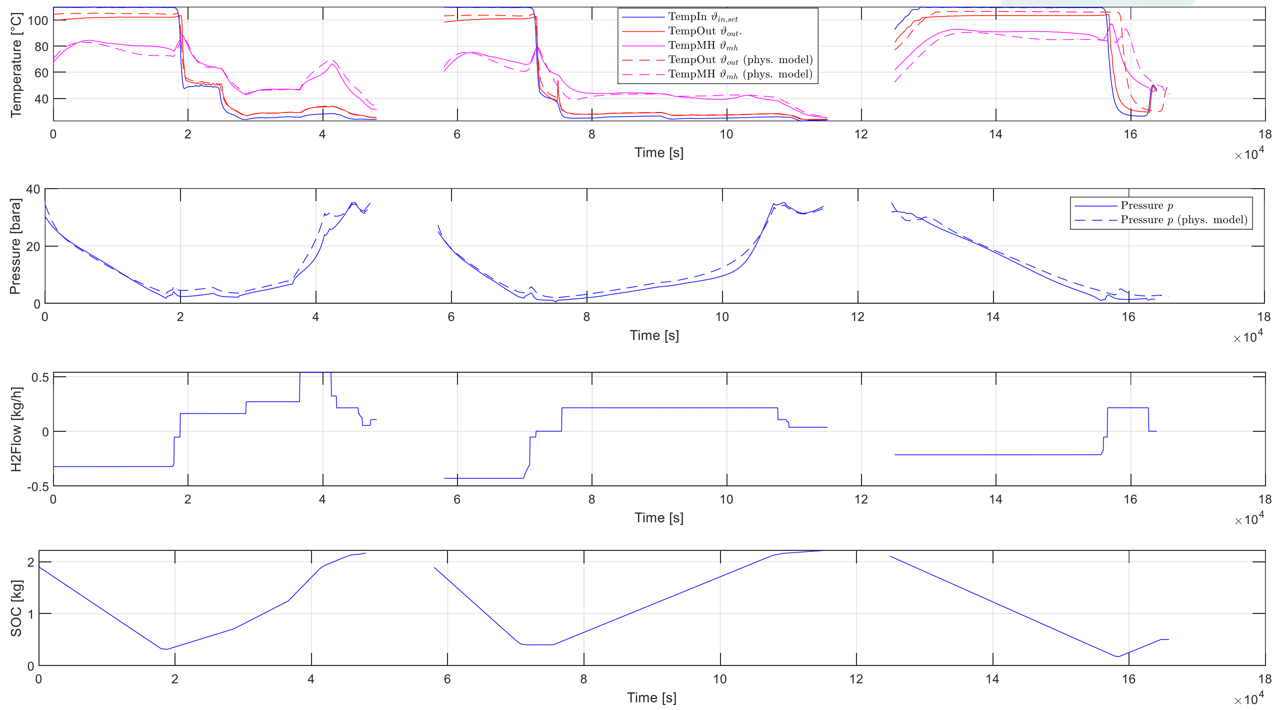

Generation of LLNFM

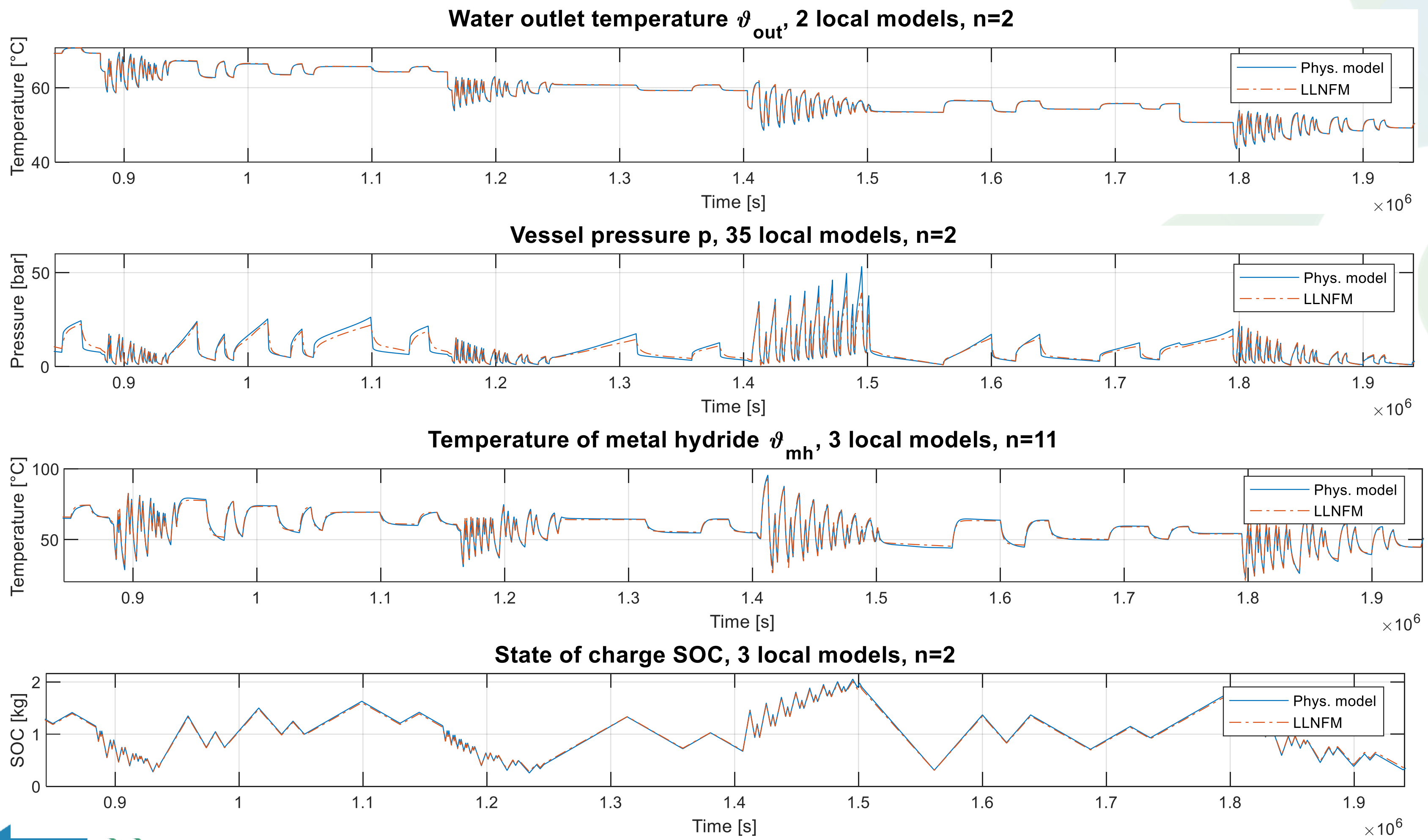

Simulation results

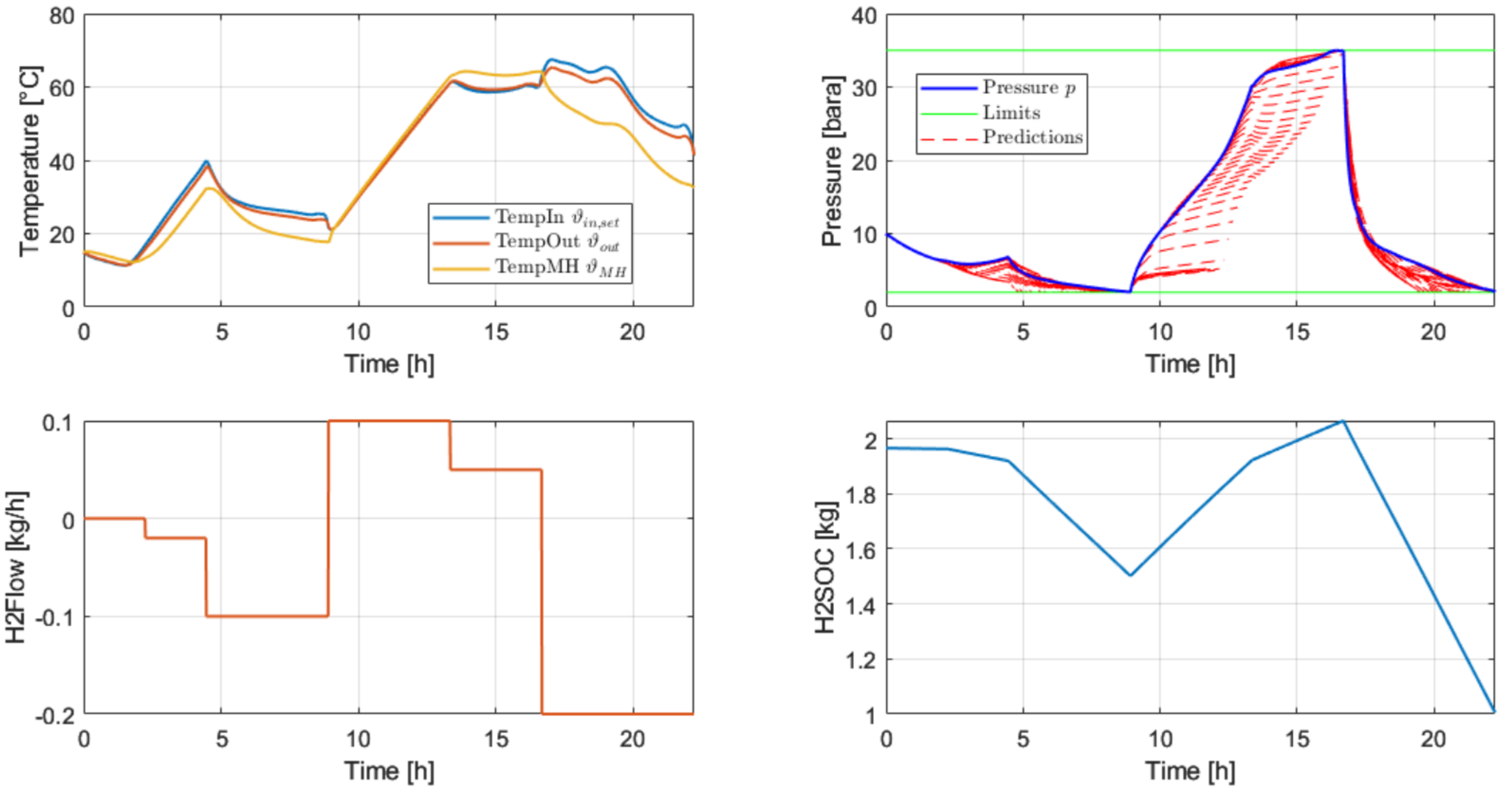

Simulation results

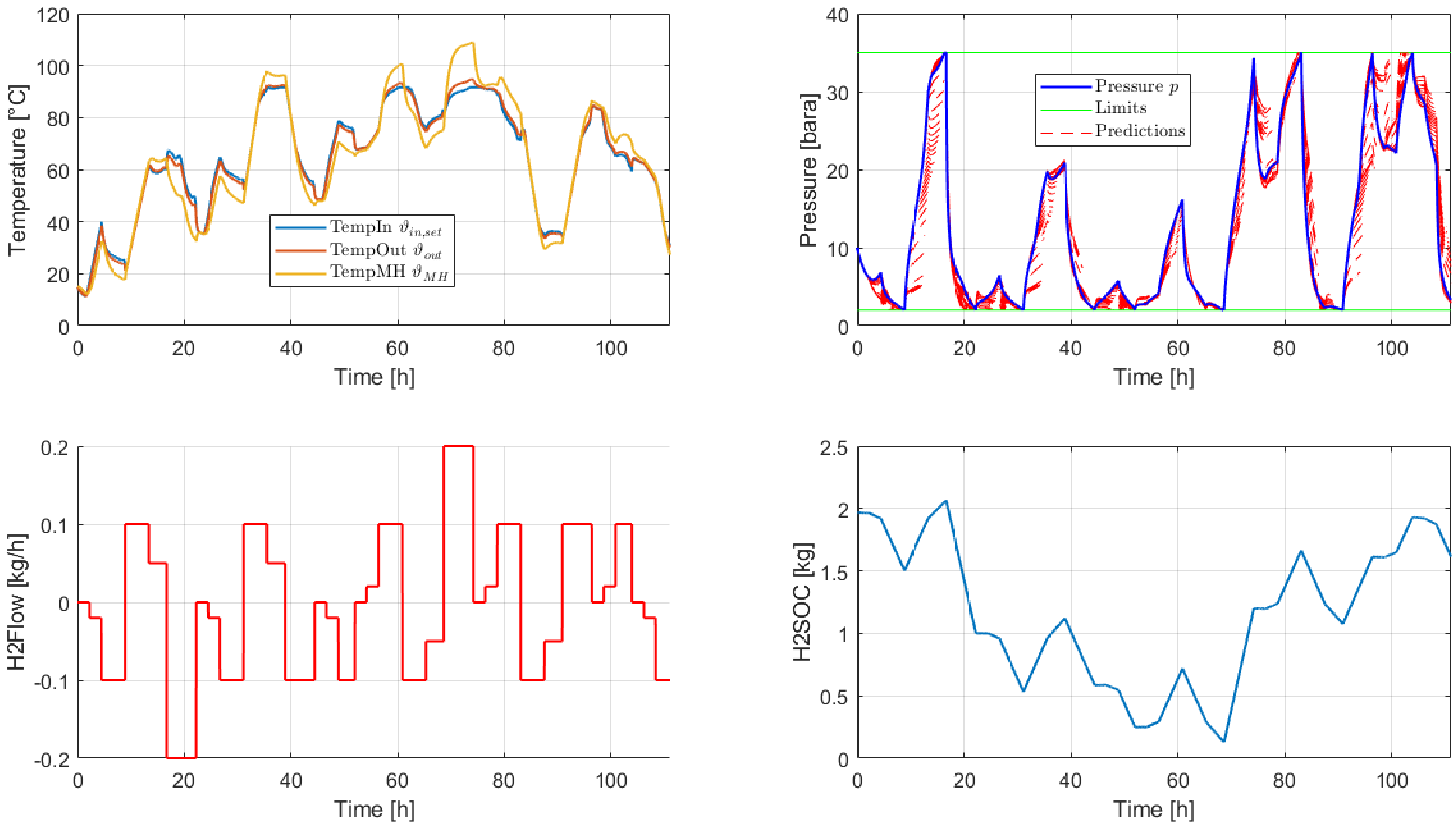

Outlook

Short term

- Validation on the physical model (model deviations)
- Validation on real world system

- Mid term
  - Extension for customer applications
  - Extension for variable water mass flow

- Long term
  - Online application for model adaption

GKN HYDROGEN

A Langley Holdings Company

Thank you for your attention!

Daniel Schwingshackl, Advanced Engineering

Daniel.Schwingshackl@gknhdyrogen.com

GREEN. SAFE. COMPACT.

II. A Path Following Model Predictive Controller for Autonomous Truck Navigation in Off-Road Environments

presenter: Hamid Didari

Hamid Didari, Gerald Steinbauer-Wagner

TU Graz

SCIENCE
PASSION
TECHNOLOGY

A Path Following Model Predictive Controller for Autonomous Truck Navigation in Off-Road Environments

September 9th 2024

Bundesministerium Landesverteidigung
Bundesministerium Finanzen
UNSER HEER
FFG Forschung wirkt.
FORTE

Introduction

- Challenges of Using Human Operators in Truck Logistics
  - Health Impact:
    - Increased risk of musculoskeletal disorders from vibrations and poor seating posture in off-road environments.[1]
  - Regulatory Restrictions:
    - Limited to a maximum of 9 hours of driving per day.
    - Mandatory break of at least 45 minutes after every 4.5 hours of driving.

[1] Influence of particle damping on ride comfort of mining dump truck. In 2020.

Introduction

- Benefits of Autonomous Trucks in Logistics
  - Continuous Operation
  - Cost Reduction
  - Safety Improvements

AIS Navigation Stack[2]

- Global Planner
  - Utilizes earth observation data to plan a path toward the goal.

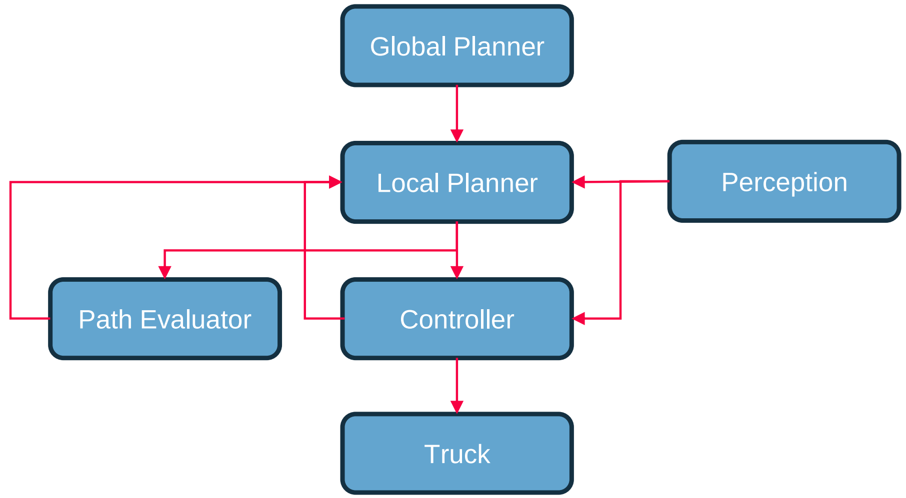

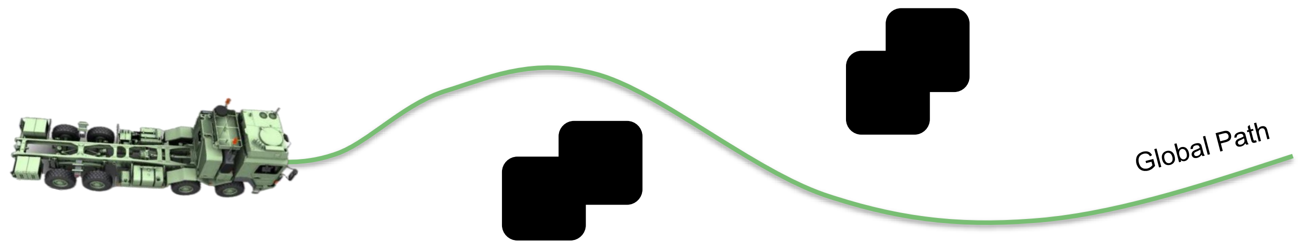

[2] An event-based approach to autonomous navigation. In 2023

AIS Navigation Stack[2]

- Global Planner
- Local Planner
  - Considers obstacles detected through perception and plans a path that follows the route provided by the Global Planner.

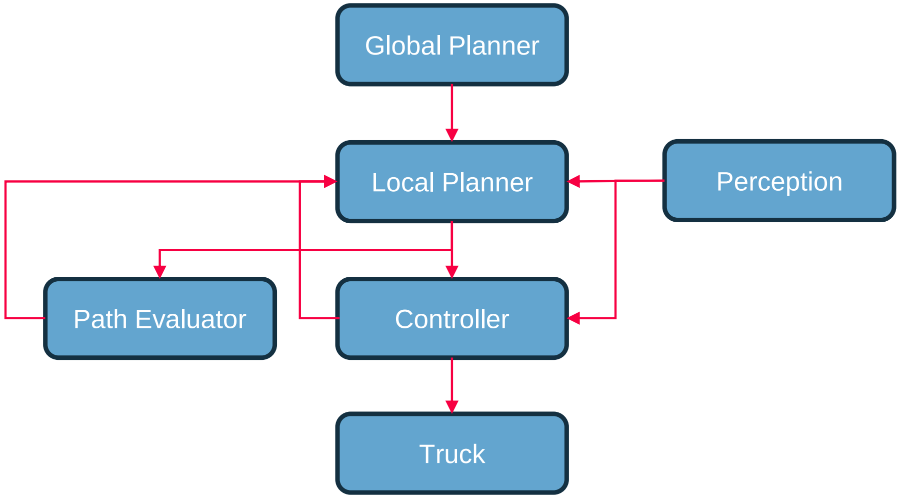

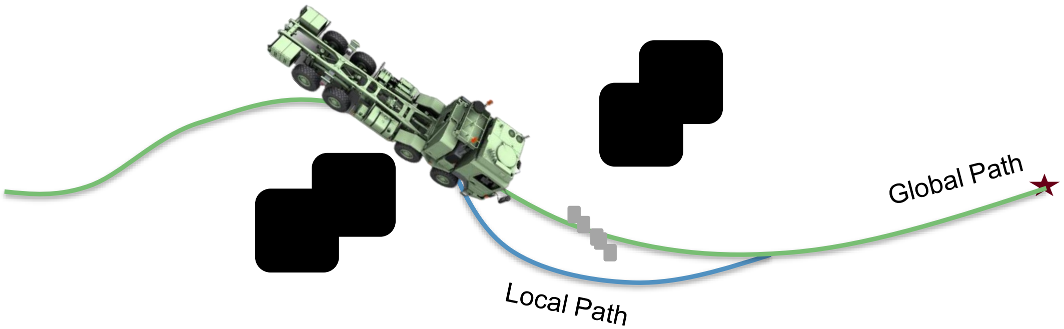

[2] An event-based approach to autonomous navigation. In 2023

AIS Navigation Stack[2]

- Global Planner
- Local Planner
- Controller
  - Generate the control command to follow the local Path
- Path Evaluator:
  - checks if the current local path is safe.

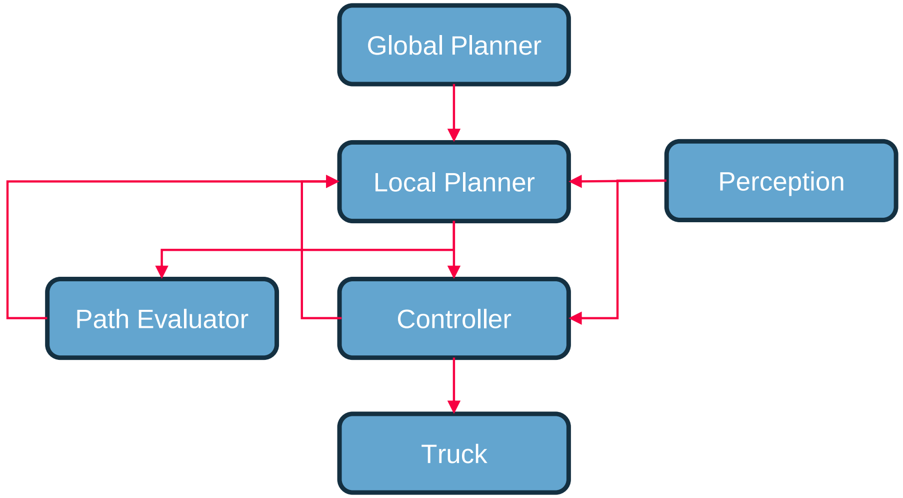

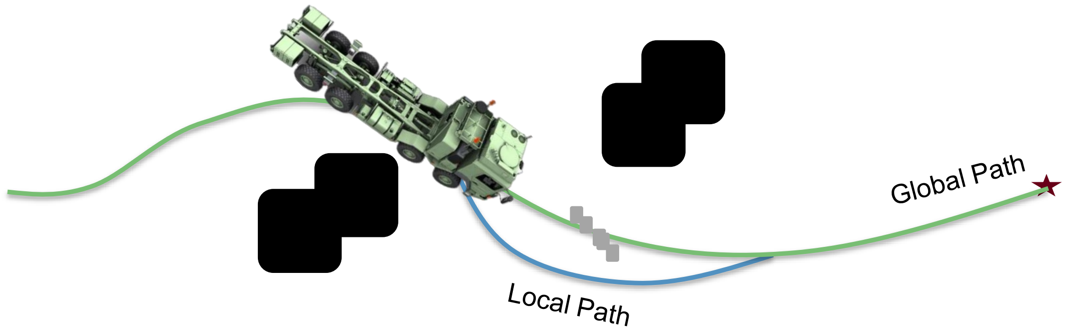

[2] An event-based approach to autonomous navigation. In 2023

Controller

- Standard controller for AD from DARPA Grand Challenge[3]
    - Computes the cross-track error and heading error.
    - Combines cross-track and heading errors to generate a steering command.

- Limitations
    - Control gains must tuned manually.
    - Ignores future trajectory points.
    - Does not handle constraints such as acceleration limitations.

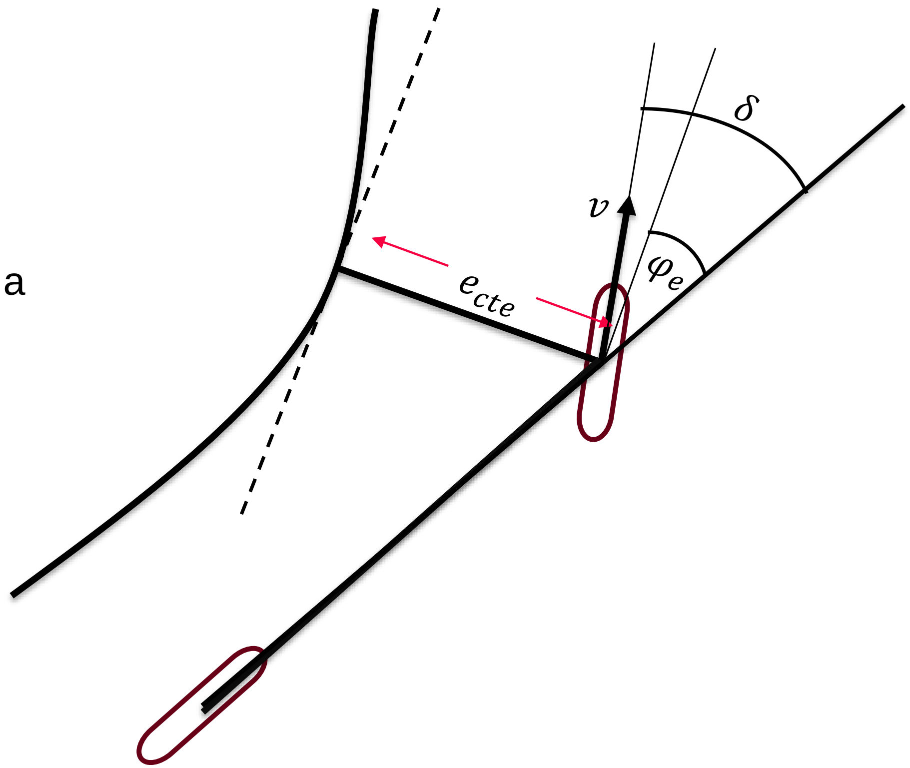

[3] Autonomous automobile trajectory tracking for off-road driving: Controller design, experimental validation and racing. In 2007

Controller

- Model predictive control (MPC)
  - Model
    - Truck can be modeled as a bicycle (Inertial symmetry, Rigid body)

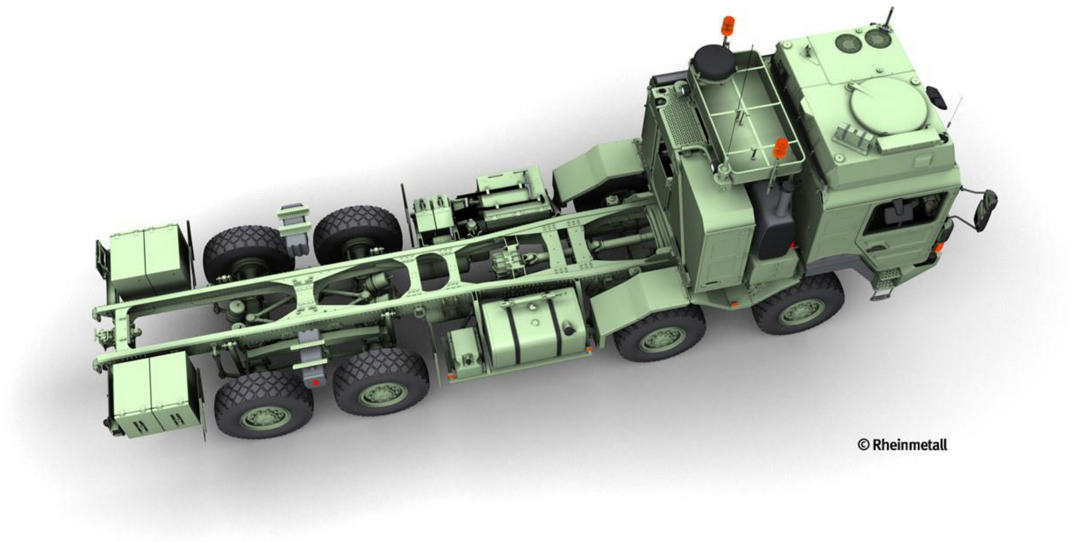

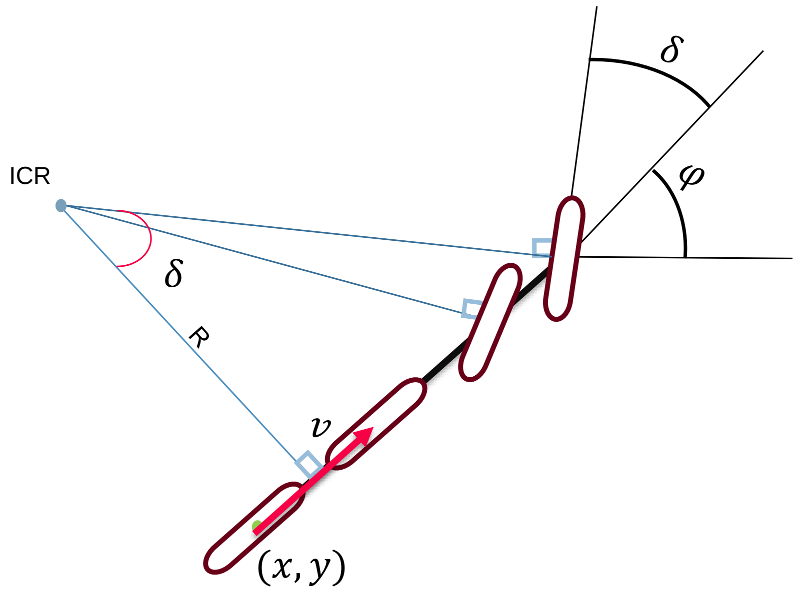

Controller

- Model predictive control (MPC)
  - Model
    - Truck can be modeled as a bicycle (Inertial symmetry, Rigid body)

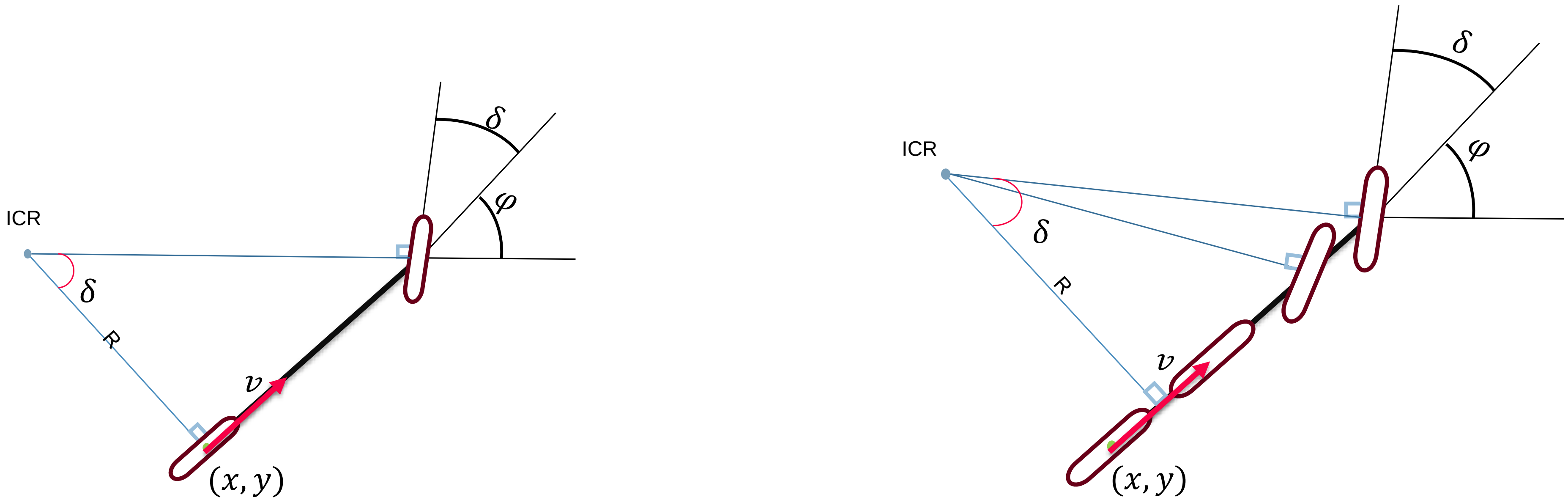

Controller

- Model predictive control (MPC)
  - Model
    - Truck can be modeled as a bicycle (Inertial symmetry, Rigid body)
    - Bicycle Model Position Update Equations:

$$\delta_{k+1} = \delta_k + \Delta\delta\ \Delta t$$

$$x_{k+1} = x_k + v_k \cos(\varphi_k + \delta_k)\,\Delta t$$

$$y_{k+1} = y_k + v_k \sin(\varphi_k + \delta_k)\Delta t$$

$$\varphi_{k+1} = \varphi_k + \frac{v_k}{L} \tan(\delta_k)\Delta t$$

$$v_{k+1} = v_k + a_k \Delta t$$

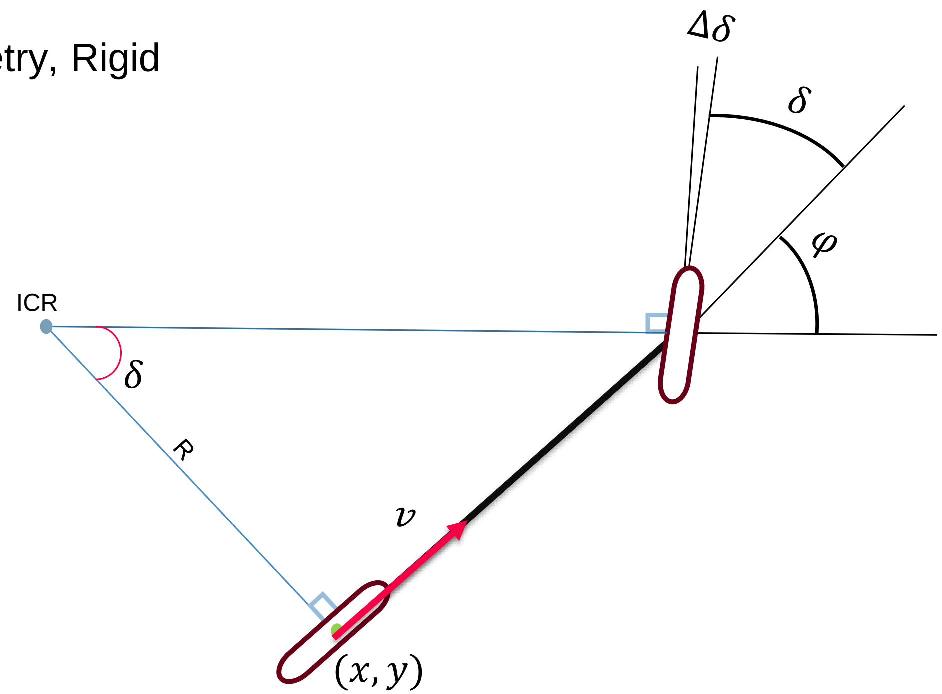

Controller

- Model predictive control (MPC)
  - Model
    - Truck can be modeled as a bicycle (Inertial symmetry, Rigid body)
    - Bicycle Model Position Update Equations
    - Error Definition

$$\theta_\rho \triangleq \arg min_\theta \, (x - x^{path}(\theta_\rho), y - y^{path}(\theta_\rho))$$

$$e^c \triangleq \sin\psi_{(\theta_\rho)} \left(x - x^{path}(\theta_\rho)\right) - \cos\psi_{(\theta_\rho)} \left(y - y^{path}(\theta_\rho)\right)$$

$$\theta_a \approx \theta_{\rho_{t-1}} + v\Delta t$$

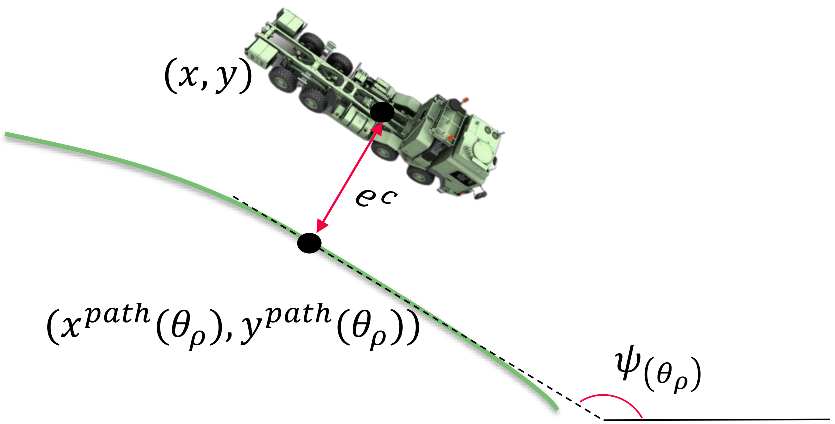

Controller

- Model predictive control (MPC)
  - Model
    - Truck can be modeled as a bicycle (Inertial symmetry, Rigid body)
    - Bicycle Model Position Update Equations
    - Error Definition

$$\theta_p \approx \theta_{\rho_{t-1}} + v\Delta t$$

$$e^l \triangleq \theta_a - \theta_\rho \approx -\cos\psi_{(\theta_a)}\left(x - x^{path}(\theta_a)\right) - \sin\psi_{(\theta_a)}\left(y - y^{path}(\theta_a)\right)$$

$$e^c \approx \sin\psi_{(\theta_a)}\left(x - x^{path}(\theta_a)\right) - \cos\psi_{(\theta_a)}\left(y - y^{path}(\theta_a)\right)$$

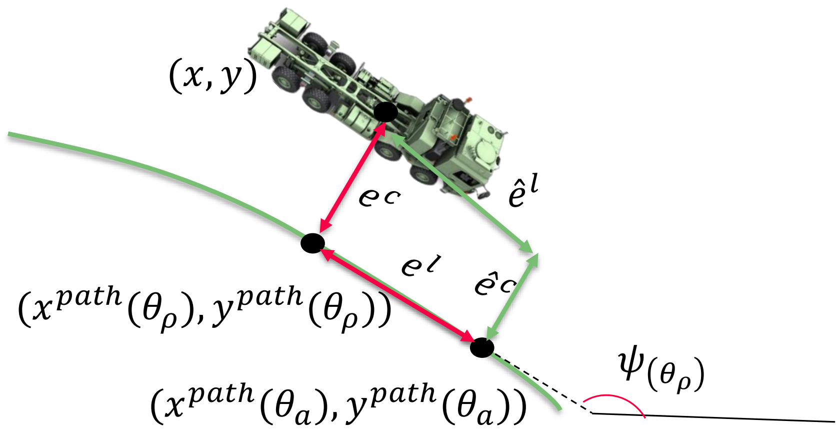

Controller

- Model predictive control (MPC)
  - Model
    - Truck can be modeled as a bicycle (Inertial symmetry, Rigid body)
    - Bicycle Model Position Update Equations
    - Objective for MPC Cost Function:

$$\min \sum_{k=1}^{N} \left[\begin{pmatrix} \hat{e}_k^c \\ \hat{e}_k^l \\ \hat{e}_k^v \end{pmatrix}^T \begin{pmatrix} q_c & 0 & 0 \\ 0 & q_l & 0 \\ 0 & 0 & q_v \end{pmatrix} \begin{pmatrix} \hat{e}_k^c \\ \hat{e}_k^l \\ \hat{e}_k^v \end{pmatrix} + \begin{pmatrix} a_k \\ \delta_k \end{pmatrix}^T \begin{pmatrix} r_a & 0 \\ 0 & r_\delta \end{pmatrix} \begin{pmatrix} a_k \\ \delta_k \end{pmatrix} \right]$$

$$\underline{a} < a_k < \overline{a}\,,\ \underline{\delta} < \delta_k < \overline{\delta}\,,\ \underline{\Delta\delta} < \Delta\delta_k < \overline{\Delta\delta}$$

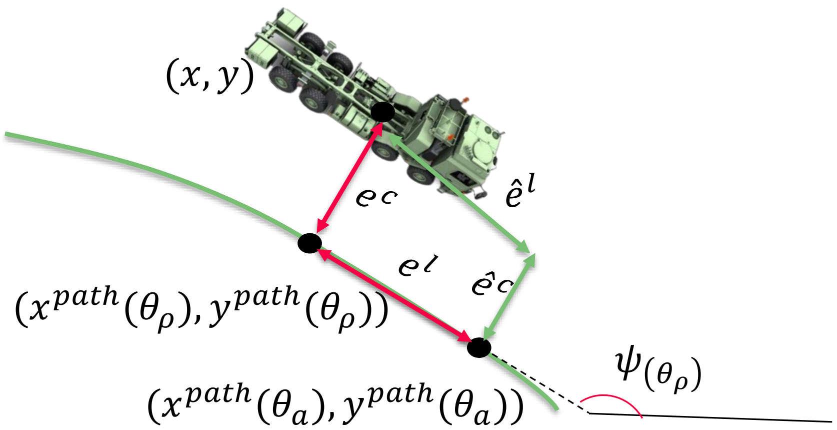

Controller

- Model predictive control (MPC)
  - Model
  - Velocity Adaptation

$$\delta_{avg} = \sum |\delta_k| / N$$

$$v_{scale} = \frac{\delta_{max} - \delta_{avg}}{\delta_{max}}$$

$$v_{Ref} = (1 - v_{scale}) * v_{Ref}$$

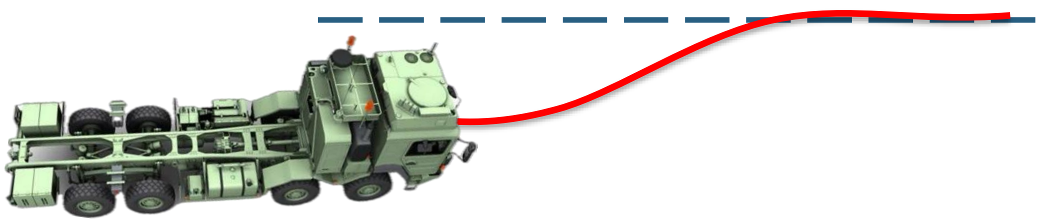

Simulation Environments

- The simulation is done in Model.Connect.

- CARLA
  - Simulates the off-road environments.

- AVL VSM^{TM}
  - Simulates the truck's physics.

- ROS
  - Runs the navigation stacks.

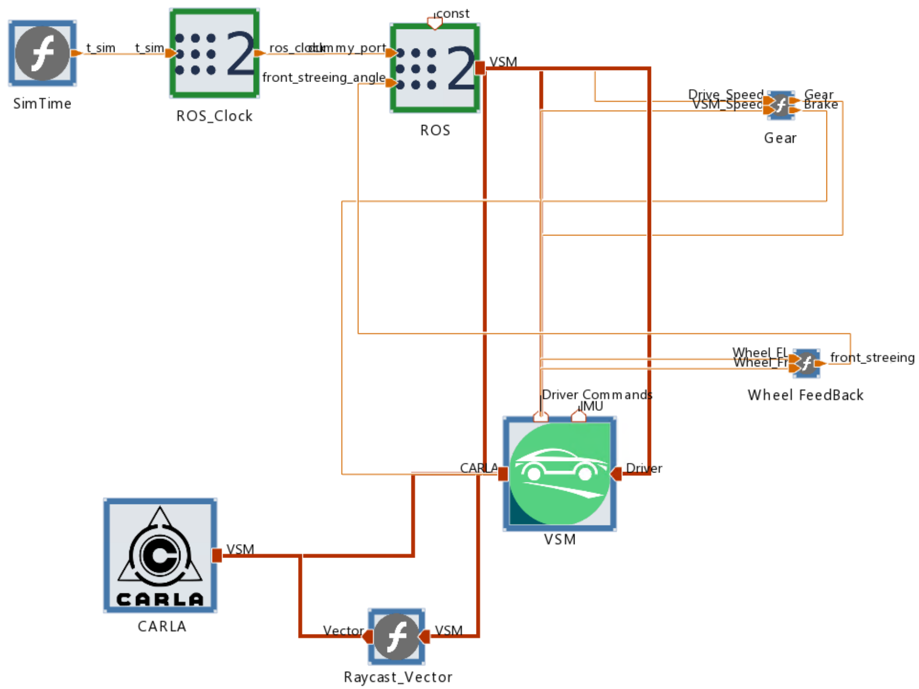

Controller Results

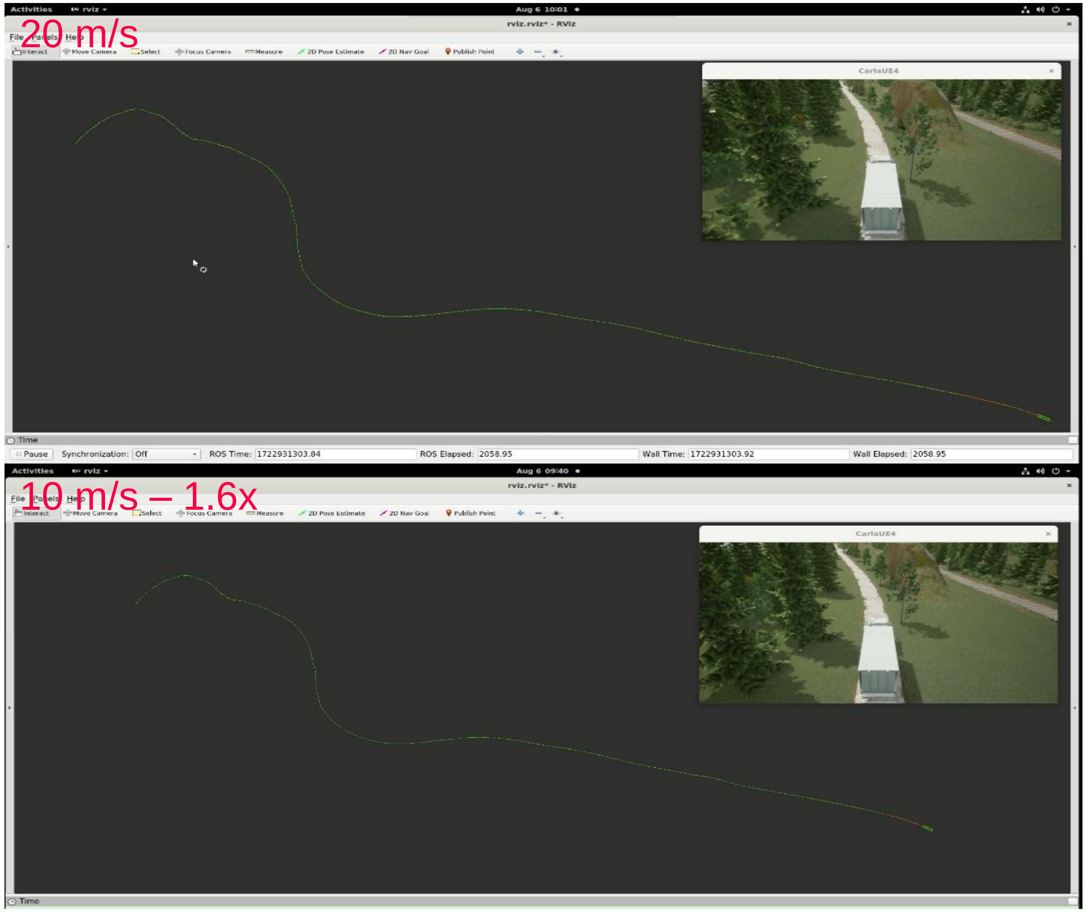

Controller Results

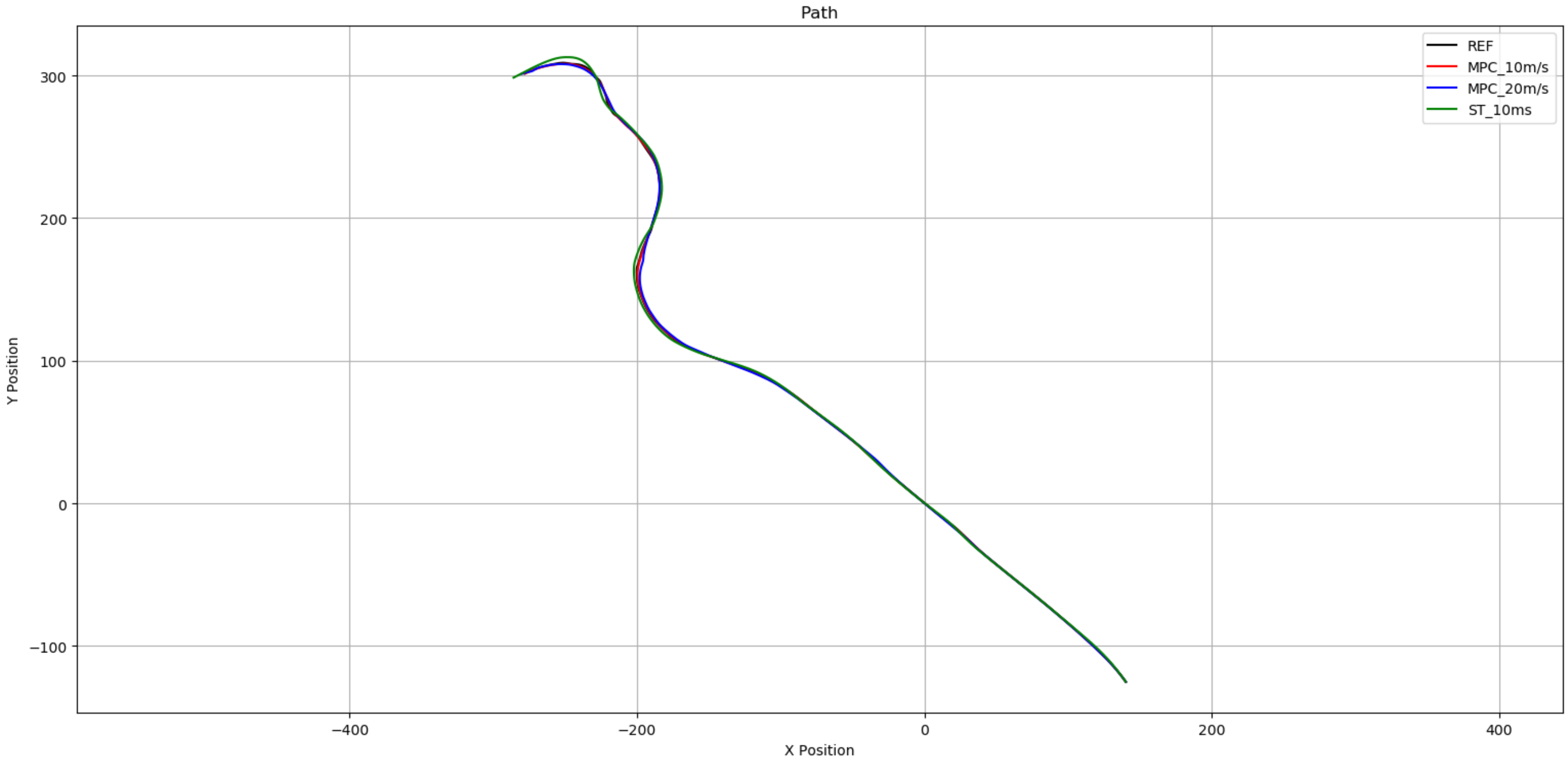

Controller Results

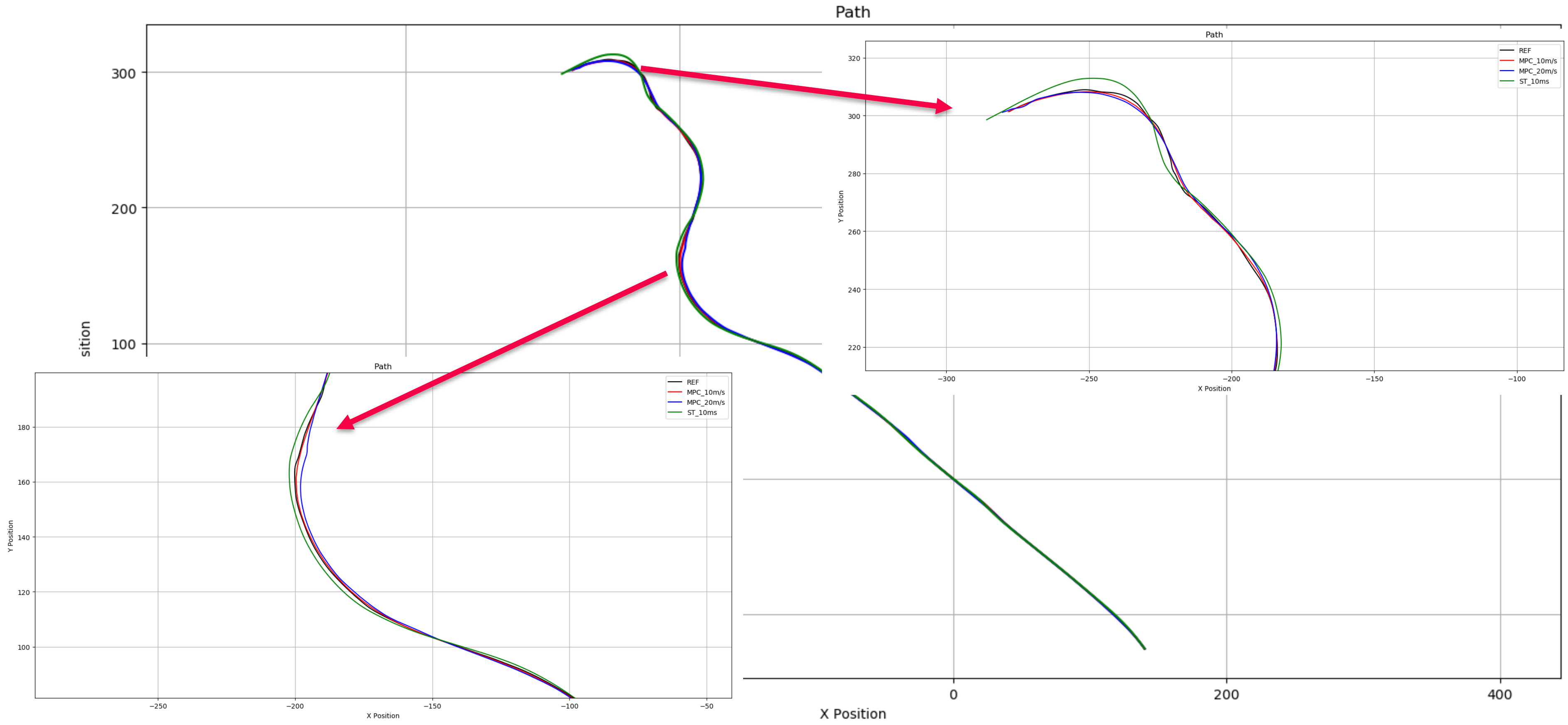

Controller Results

	Stanley	MPC(20m/s)	MPC(10m/s)
Max e_{cte}	4.12 m	2.7 m	1.04m
RMS e_{cte}	1.12 m	0.72 m	0.3m

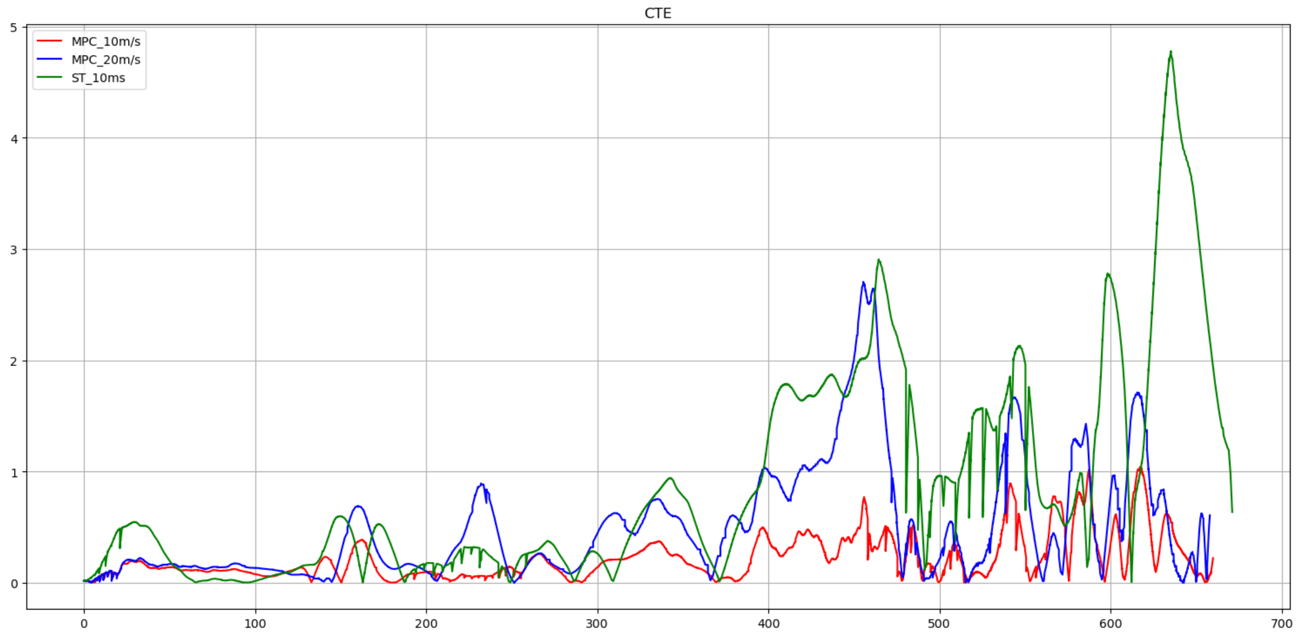

Controller Results – Delay

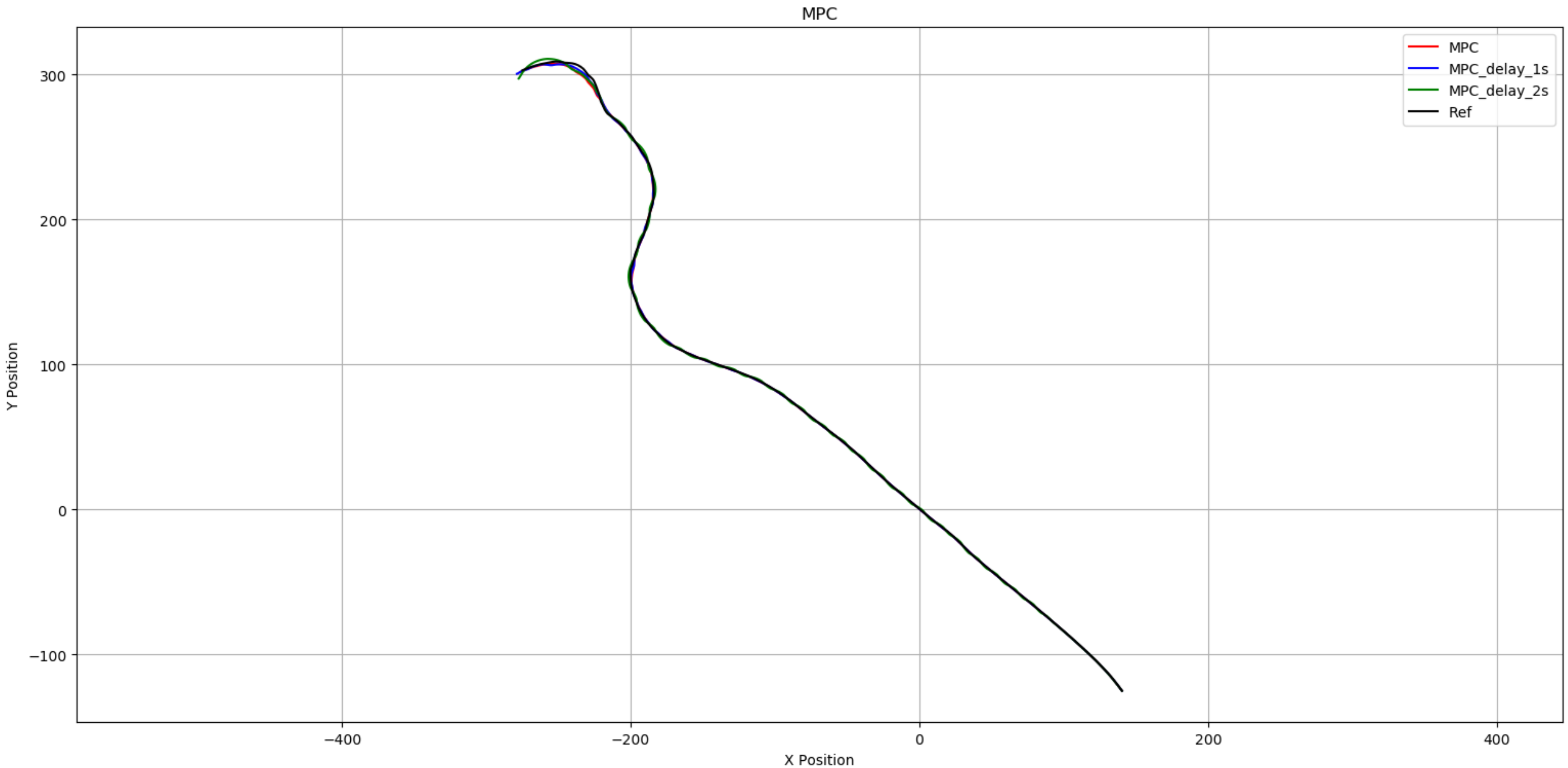

Controller Results – Delay

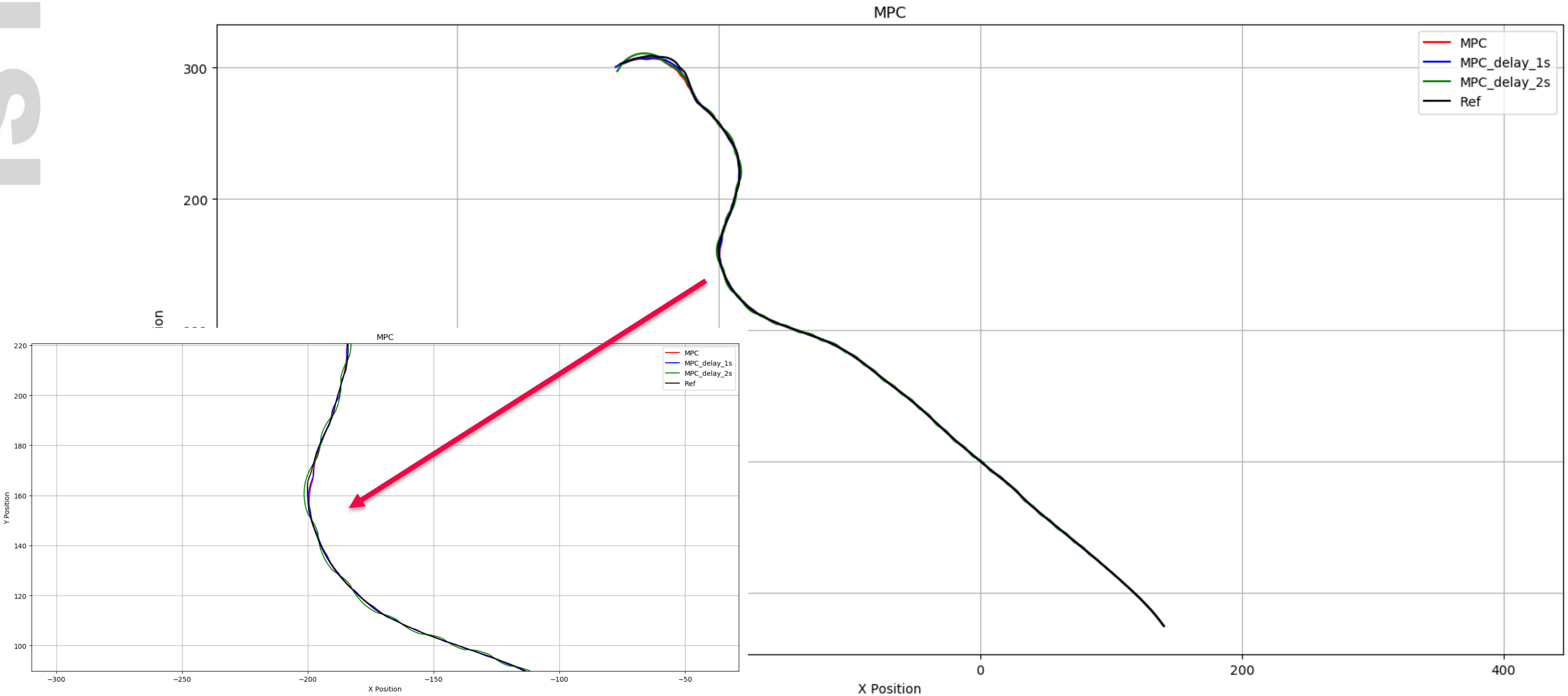

Controller Results – Delay

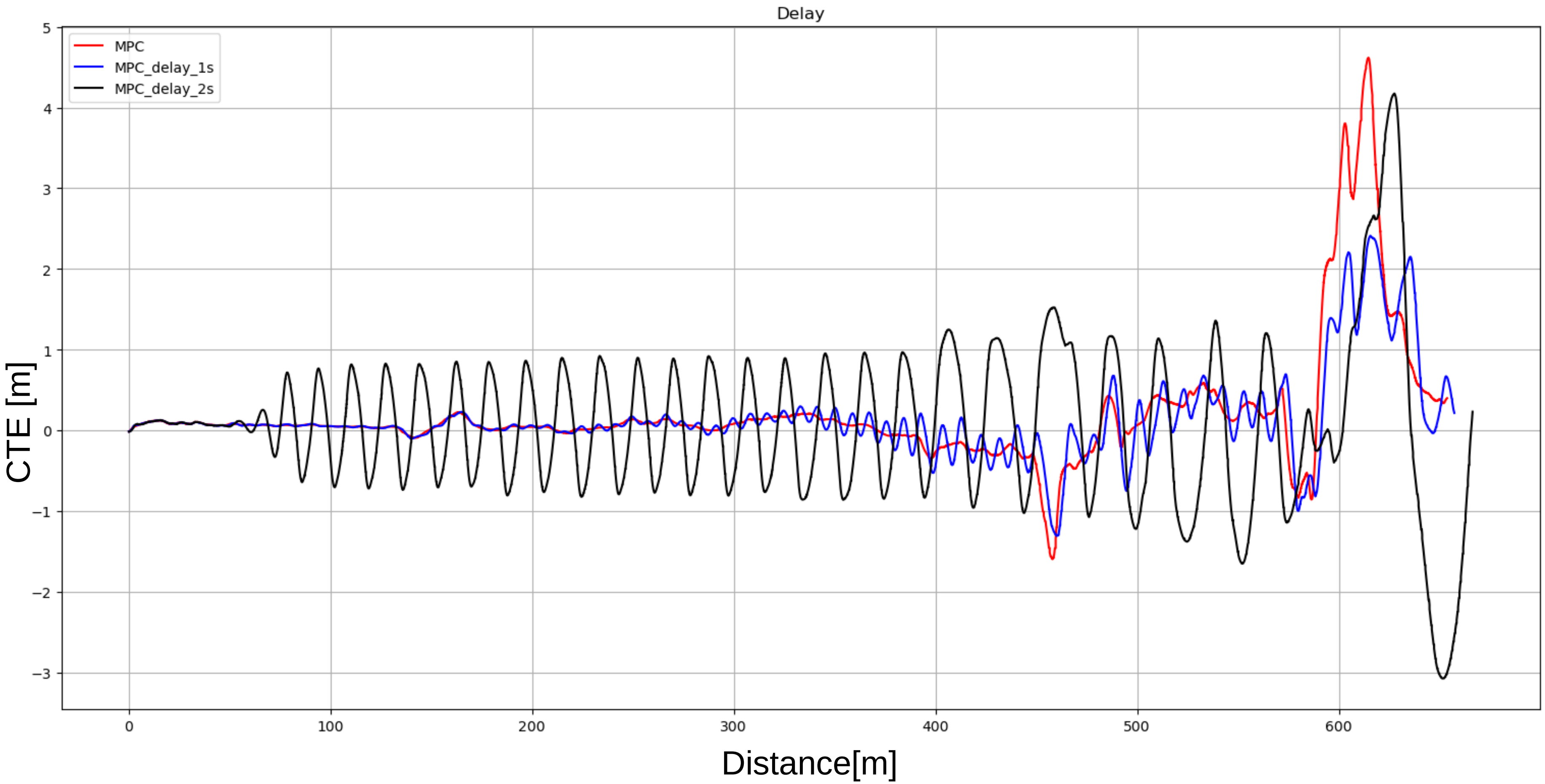

Obstacle Avoidance

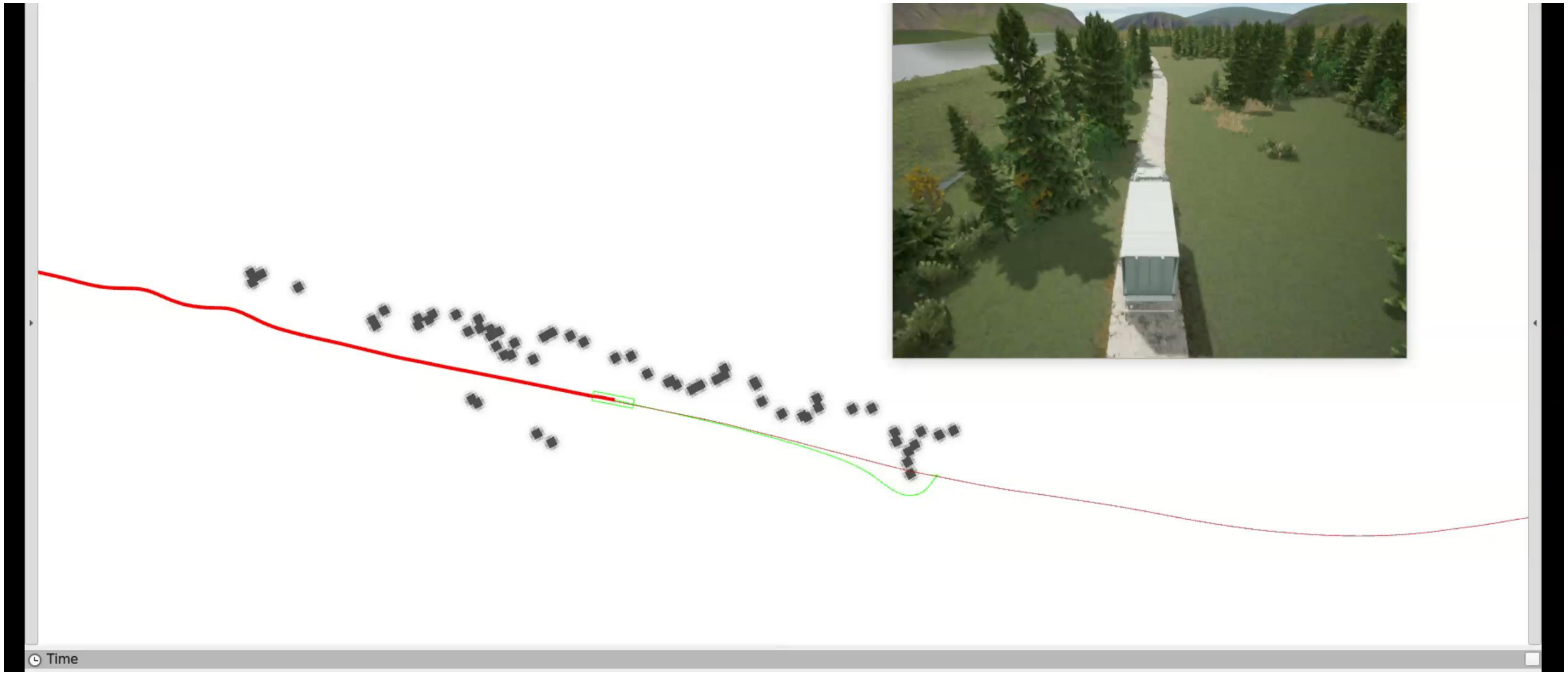

Future Works

- Utilize a more accurate model for the truck that considers tire friction.
- Apply Model Predictive Path Integral (MPPI) for the local planner to account for truck dynamics.
- Include obstacles in MPC optimization to ensure they are avoided in the lower-level controller.

This work has been funded by the Austrian defense research program FORTE of the Federal Ministry of Finance (BMF), as part of the SIMPAS project.

III. Innovative control to suppress sloshing in fast transport of liquids
presenter: Stefan Jakubek

Innovative control to suppress sloshing in fast liquid transport maneuvers

Stefan Jakubek, Alexander Schirrer, Christoph Hametner


Link to the full
Presentation Video

Sloshing occurs when transporting liquids quickly

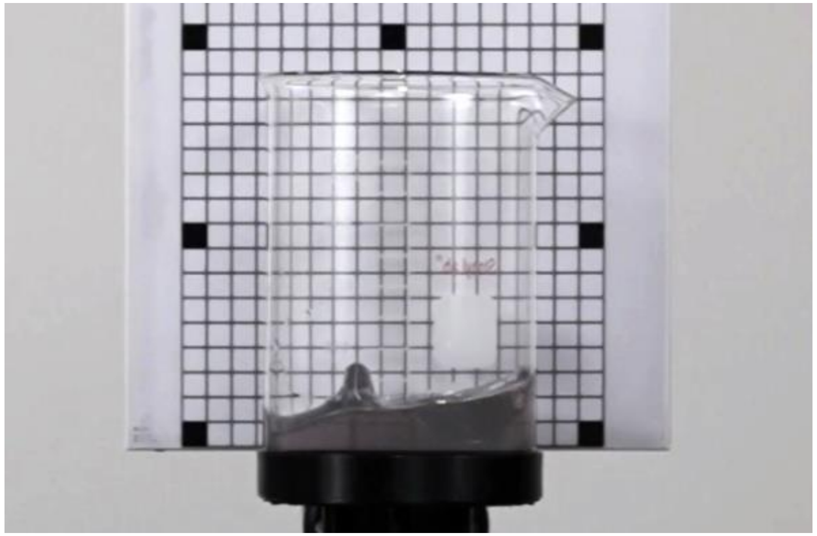

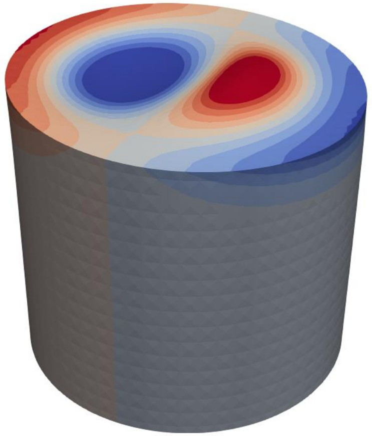

- Sloshing is a complex phenomenon in fluid mechanics
- Sloshing can be problematic in applications, such the **handling of liquid cargo** or **industrial production involving liquids**:
  - **Chemical Industry**
  - **Food Industry**
  - **Biotechnology**
  - **Pharmaceutical Industry**
- Understanding and controlling sloshing is crucial for ensuring the safety and efficiency of liquid-carrying systems, as uncontrolled sloshing can lead to instability.

Sloshing occurs when transporting liquids quickly

ACOPOS 6D by B&R Industrial Automation GmbH

Sloshing sensitivity of liquid containers is high

Even small movements of a liquid container cause significant sloshing!

Liquid sloshing modes generally have very little damping!

Modeling liquid sloshing dynamics: Fluid field equations

Assumptions: irrotational, incompressible fluid with negligible viscous dissipation

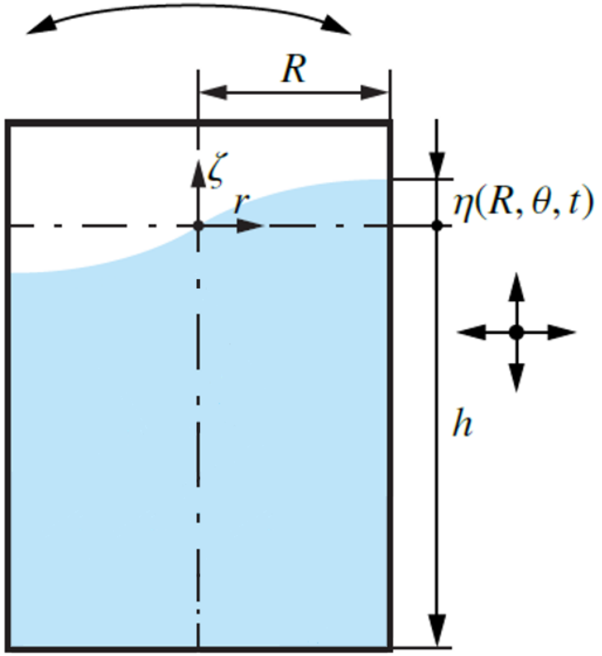

Velocity potential function
$$\boldsymbol{q} = -\nabla \Phi$$

Continuity equation
$$\nabla \cdot \boldsymbol{q} = 0$$

Laplace's equation
$$\nabla^2 \Phi = 0$$

Euler equation: $\nabla \left(\frac{P}{\rho} + \frac{1}{2} q^2 + g Z' - \frac{\partial \Phi}{\partial t} \right) = 0$

Boundary conditions:

- at cylinder walls and bottom: $\left.\frac{\partial \tilde{\Phi}}{\partial r}\right|_{r=R} = 0 \qquad \left.\frac{\partial \tilde{\Phi}}{\partial \zeta}\right|_{\zeta=-h} = 0$

- linearized free surface:
$$\left.\begin{aligned} \frac{\partial \eta}{\partial t} &= -\frac{\partial \tilde{\Phi}}{\partial \zeta} \\ \frac{\partial \tilde{\Phi}}{\partial t} - g\eta &= 0 \end{aligned}\right\} \text{ at } \zeta = \eta(r, \varphi, t)$$

Natural frequencies of the *i*-th asymmetric sloshing mode:

$$\omega_{1i}^2 = \frac{g\xi_{1i}}{R} \tanh\left(\xi_{1i} \frac{h}{R}\right) \quad \text{with} \quad \xi_{1i} = 1.841,\ 5.335,\ 8.535,\ \ldots$$

Eigenmodes of liquid sloshing dynamics

Animation of different sloshing modes

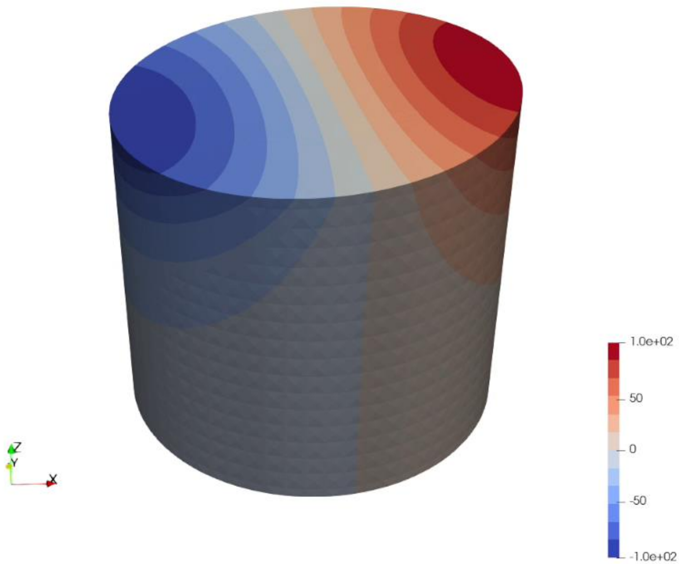

Excitation of the 2nd sloshing mode

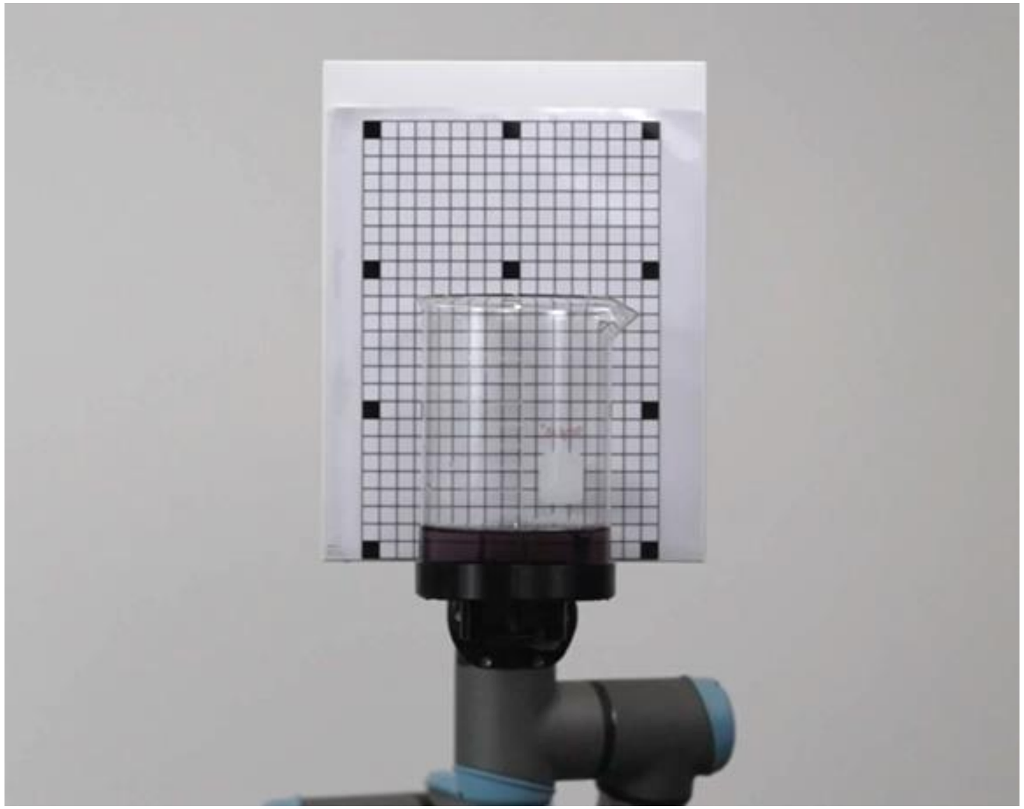

Control-oriented modeling of sloshing: Forced container oscillation

Forced harmonic oscillations of container:

The hydrodynamic pressure at any point due to liquid sloshing is determined from

$$
\begin{aligned}
p &= \rho \frac{\partial \tilde{\Phi}}{\partial t} \\
&= \rho X_0 \Omega^2 \cos\theta \cos\Omega t \cdot \\
&\cdot \left\{ r + \sum_{n=1}^{\infty} \frac{2R\,\Omega^2}{(\xi_{1n}^2 - 1)(\omega_{1n}^2 - \Omega^2)} \frac{J_1(\xi_{1n} r/R) \cosh[\xi_{1n}(z+h)/R]}{J_1(\xi_{1n}) \cosh(\xi_{1n} h/R)} \right\}
\end{aligned}
$$

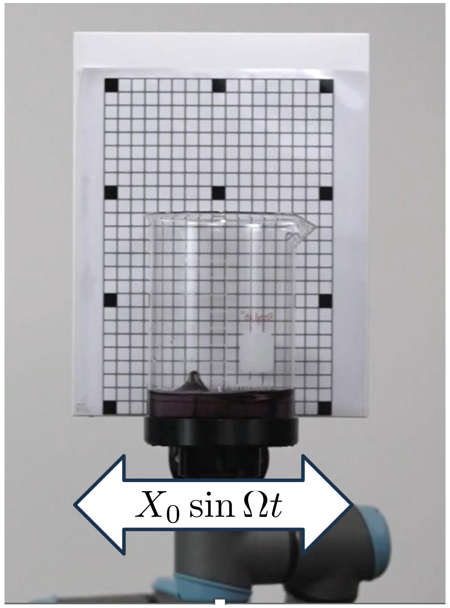

The overall lateral force on the container wall then becomes

$$
F_x = \int_0^{2\pi} \int_{z=-h}^{0} p \cos\theta \, R \, d\theta \, dz = m_f X_0 \Omega^2 \sin\Omega t \left[1 + \sum_{n=1}^{\infty} \frac{1}{\xi_{1n} h (\xi_{1n}^2 - 1)} \frac{2R\,\Omega^2}{(\omega_{1n}^2 - \Omega^2)} \tanh(\xi_{1n} h/R) \right]
$$

Ibrahim, R. A. *Liquid Sloshing Dynamics,(Theory and Applications)*. Cambridge University Press, 2005.

Control-oriented modeling of sloshing : Forced pendulum oscillations

Pendulum with harmonic excitation of pivot:

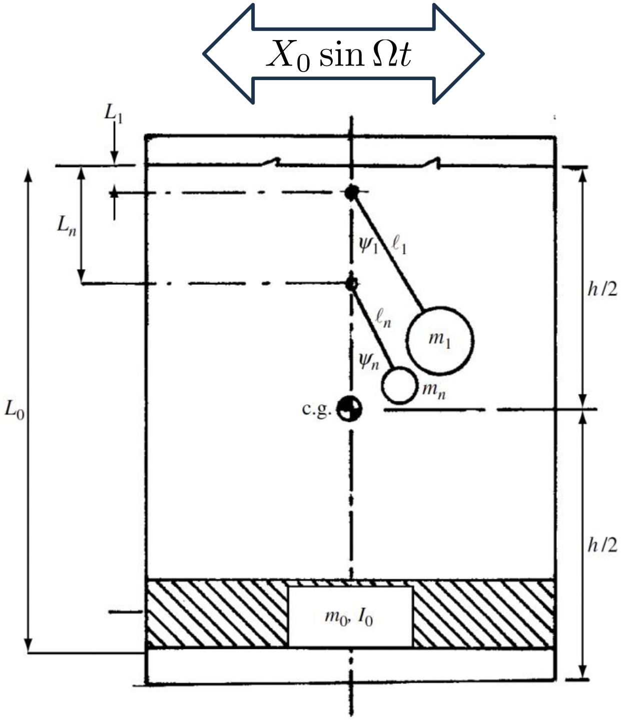

$$\frac{d}{dt}\left(\frac{\partial L}{\partial \dot{q}_i}\right) - \frac{\partial L}{\partial q_i} = -\frac{\partial \mathcal{S}}{\partial \dot{q}_i} + Q_i$$

$$\begin{aligned} F_x &= X_0 \Omega^2 \sin \Omega t \left\{ m_0 + \sum_{n=1}^{\infty} m_n \left[\frac{\Omega^2}{\omega_n^2 - \Omega^2} + 1 \right] \right\} \\ &= m_F X_0 \Omega^2 \sin \Omega t \left\{ 1 + \sum_{n=1}^{\infty} \frac{m_n}{m_F} \left(\frac{\Omega^2}{\omega_n^2 - \Omega^2} \right) \right\} \end{aligned}$$

Ibrahim, R. A. *Liquid Sloshing Dynamics, Theory and Applications*. Cambridge University Press, 2005.

Control-oriented modeling of sloshing : Equivalent pendulum model

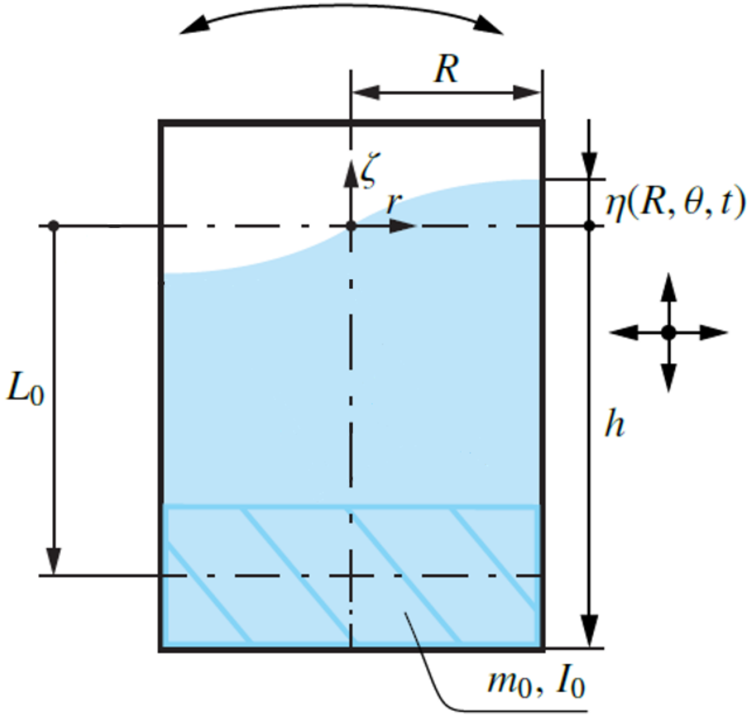

- Some part of the liquid acts as if it was a rigid body (m_0, I_0).
- The rest undergoes complex liquid motion, which can be expressed by several eigenmodes, each represented via 2nd-order dynamics
  → interpretation as mathematical pendulums!
- First and second mode are sufficient to describe the dominant motion well!
- Pendulum parameters (m_i , l_i , L_i) are obtained from:
  1. eigenfrequencies
  2. total mass and total inertia
  3. center of gravity
  4. reproduce total reaction forces and torques between liquid and container walls

An old but effective idea: The Moroccan waiter‘s tray

Support the container by a freely moving tray (pendulum-like motion):

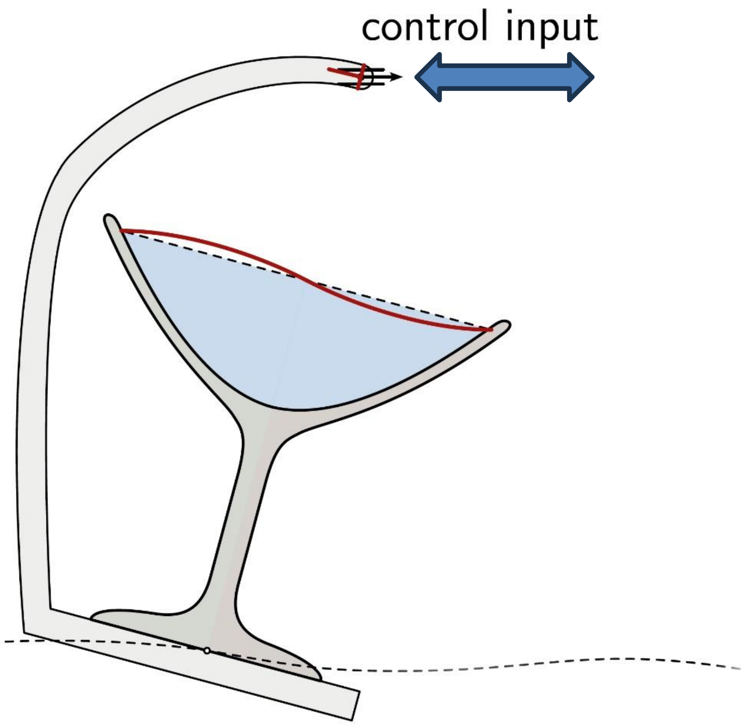

When only the pivot is moved, then sloshing is greatly inhibited!

Solution: Let's suspend the container on a *virtual* pendulum!

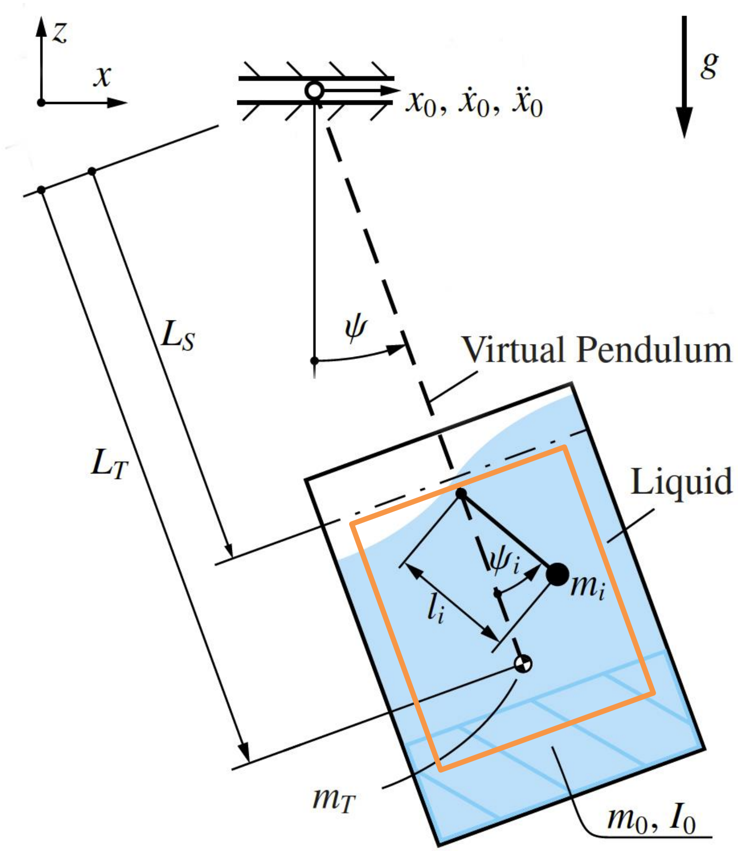

Control input = acceleration of pivot: $u = \ddot{x}_0$

State vector: $\boldsymbol{x} = \begin{bmatrix} \psi & \boxed{\psi_1 \quad \psi_2} & x_0 & \dot{\psi} & \dot{\psi}_1 & \dot{\psi}_2 & \dot{x}_0 \end{bmatrix}^T$

liquid sloshing modal coordinates

Effects:

1. The resulting dynamic system is differentially flat, the flat output coordinate is found as:

$$y_f = x_0 + \alpha\psi + \alpha_1\psi_1 + \alpha_2\psi_2$$

2. Selecting the virtual pendulum length L_T appropriately makes the 1st sloshing mode uncontrollable by x_0 i.e. the first sloshing mode is eliminated!

Virtual tray length L_T is adjusted to suppress 1st sloshing mode

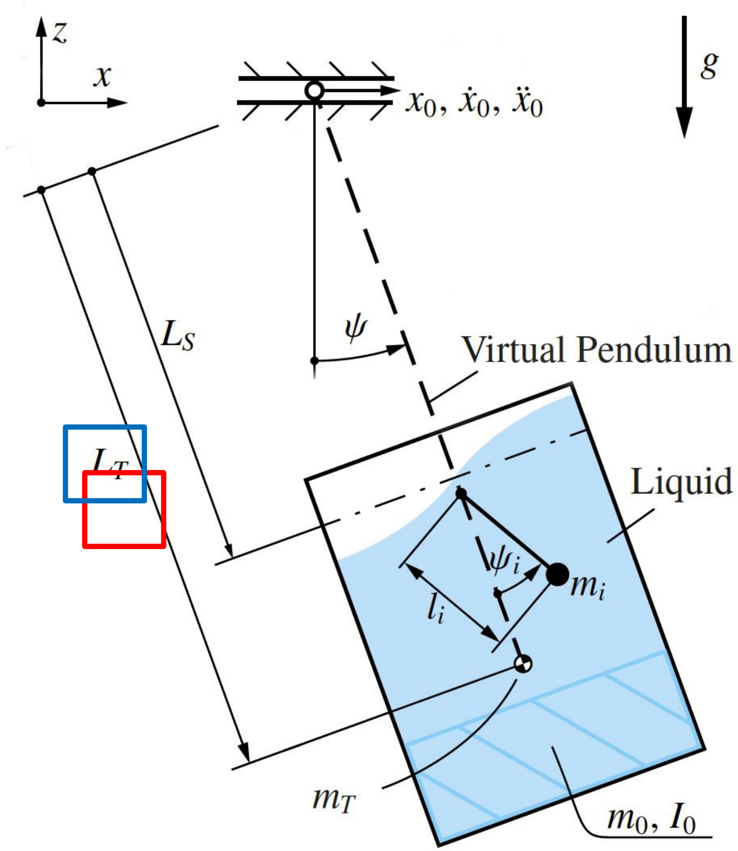

Equations of motion:

$$\dot{\boldsymbol{x}} = \boldsymbol{A}(\boxed{L_T})\,\boldsymbol{x} + \boldsymbol{b}(\boxed{L_T})\ddot{x}_0(t)$$

Key idea:

1. Modal analysis to identify dominant sloshing mode:

Find mode with largest magnitude in ψ_1

→ eigenvalue $\lambda_s(L_T)$, left eigenvector $\boldsymbol{z}_s^{\mathrm{T}}(L_T)$

2. Adjust virtual pendulum (tray) length L_T to *violate* Hautus controllability criterion for this mode:

$$\boxed{L_T}: \ \boldsymbol{z}_s^{\mathrm{T}}(L_T)\,\boldsymbol{b}(L_T) = 0$$

→ This mode is now **uncontrollable** by $u = \ddot{x}_0$

Virtual tray length L_T is adjusted to suppress 1st sloshing mode

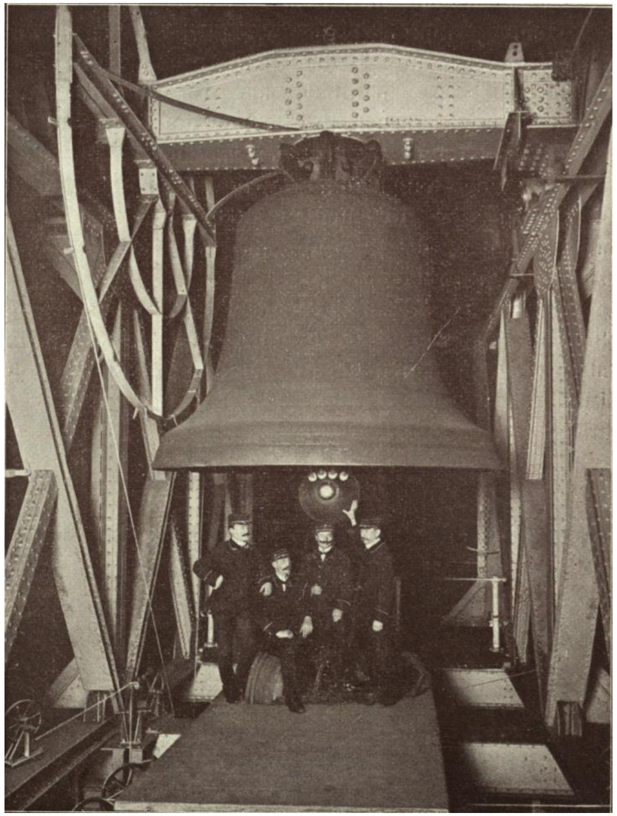

$$\ddot{x}_0(t) = \delta(t)$$

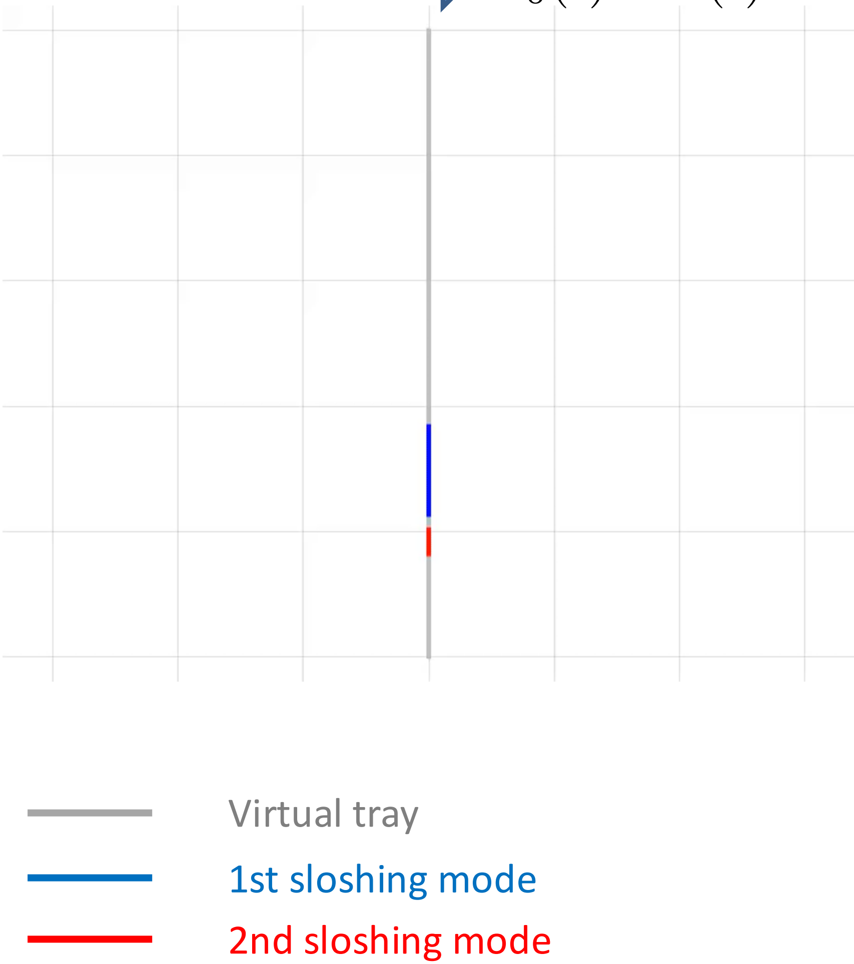

1st sloshing mode is controllable:

$$\boldsymbol{z}_S^{\mathrm{T}}(L_T)\,\boldsymbol{b}(L_T) \neq 0$$

1st sloshing mode is uncontrollable:

$$\boldsymbol{z}_S^{\mathrm{T}}(L_T)\,\boldsymbol{b}(L_T) = 0$$

→ Analogous to a silent/muted bell

Virtual tray pendulum approach: Experimental validation

Model of sloshing modes → Virtual tray suspension → Elimination of 1st sloshing mode → Flat output formulation → Rest-to-rest trajectory planning

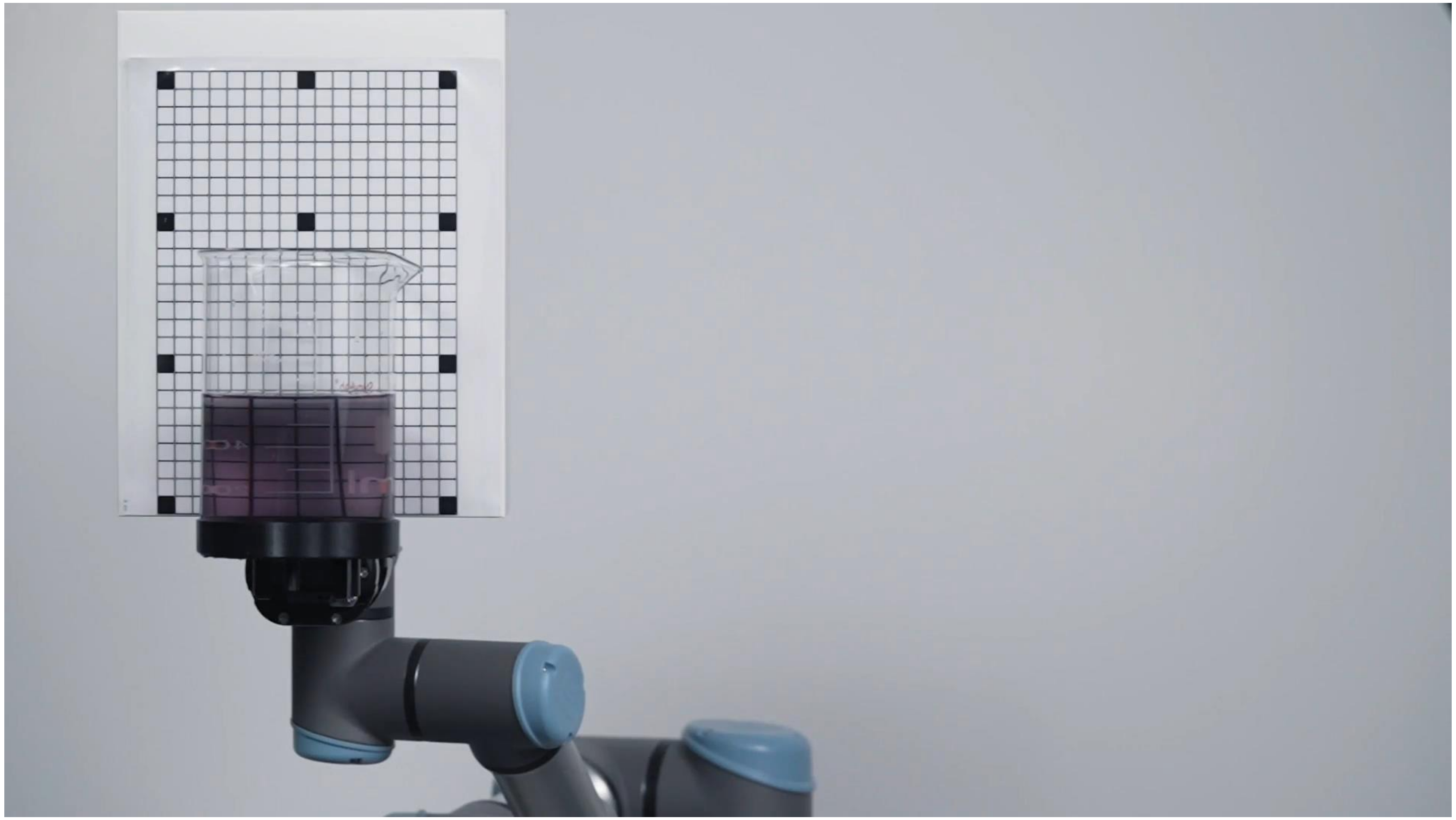

Analysis of dynamic liquid pressure distribution during transit

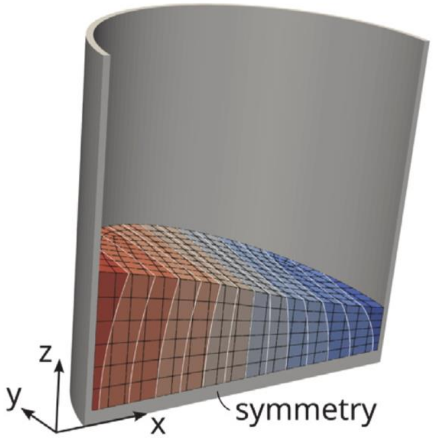

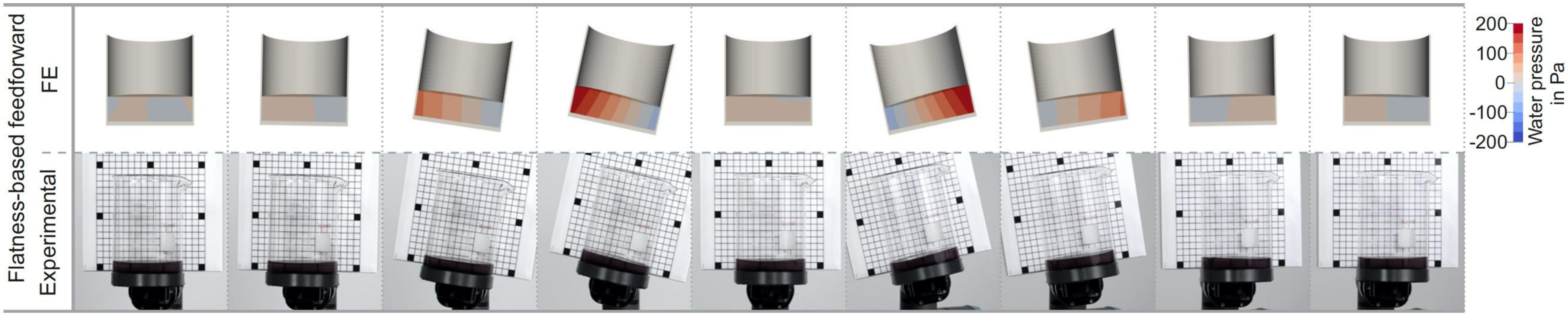

What if... the container shape is more complex?

© Adobe

- Wave motion decisivly depends on container geometry
- Sloshing motion can easily become unstable in shallow liquid containers
- Owing to their boundary conditions, complex container geometries do generally not have analytic sloshing models
- Control oriented pendulum models can be created from high-fidelity finite element (FE) models through matching in the frequency domain

Complex FE sloshing dynamics is used to calibrate pendulum model

Complex FE sloshing dynamics is used to calibrate pendulum model

Reaction forces and moments during harmonic sway/pitch motion of container are extracted from FE-model, e.g.

$$F_x = \int_{\partial\Omega} p \cdot (\mathbf{e}_x \cdot \mathbf{n}) d\Omega$$

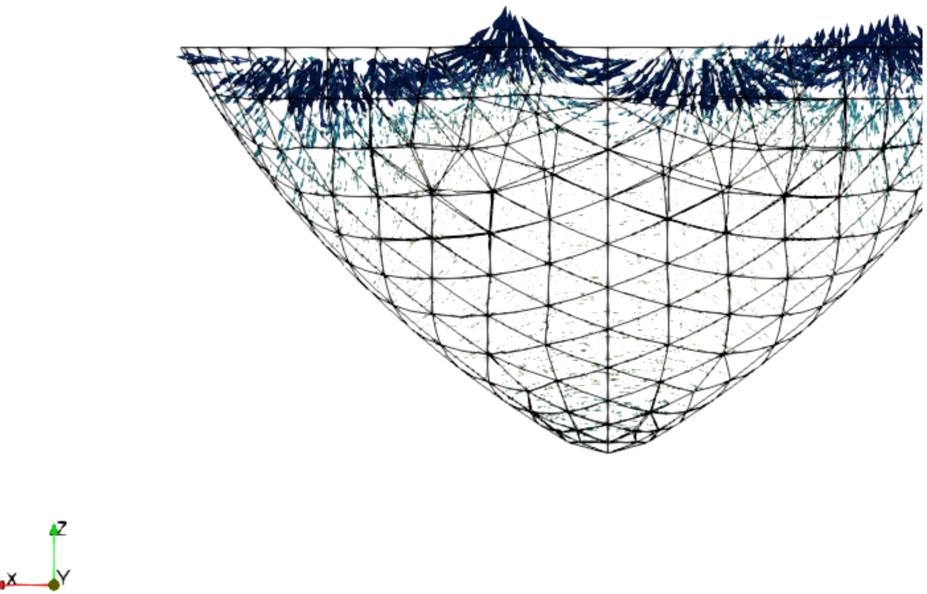

Pendulum model parameters are fitted to achieve equivalent force/moment frequency responses:

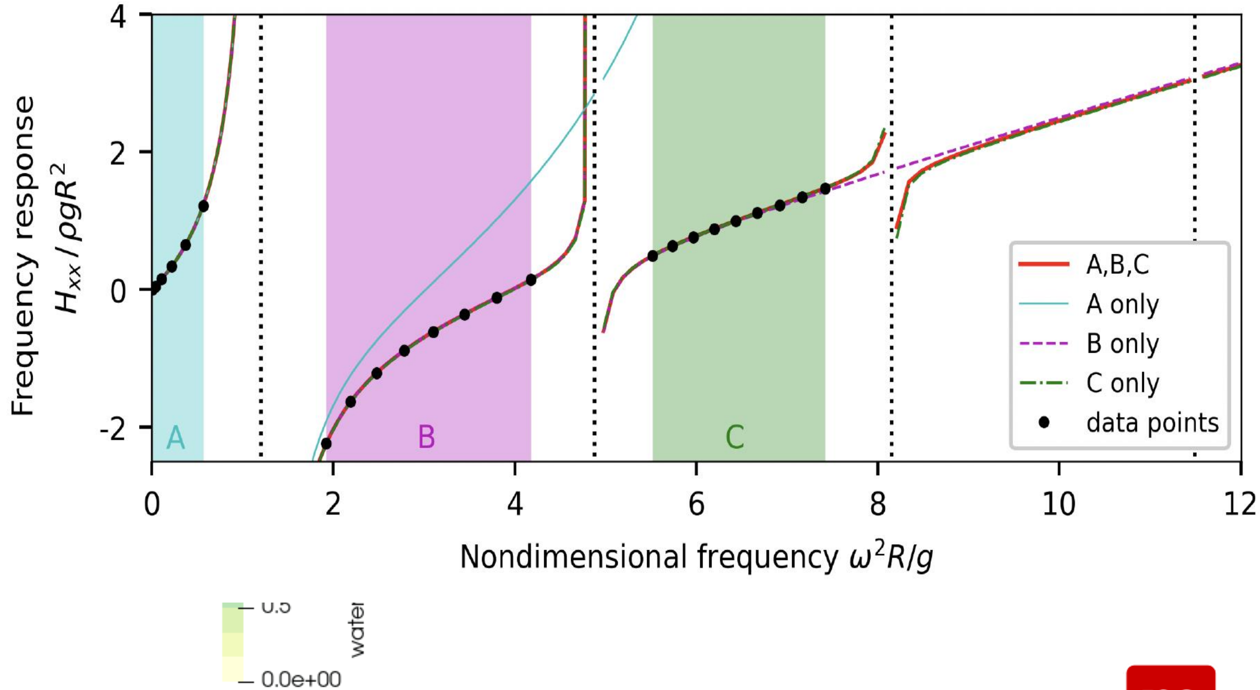

Complete FE sloshing dynamics is used to calibrate pendulum model

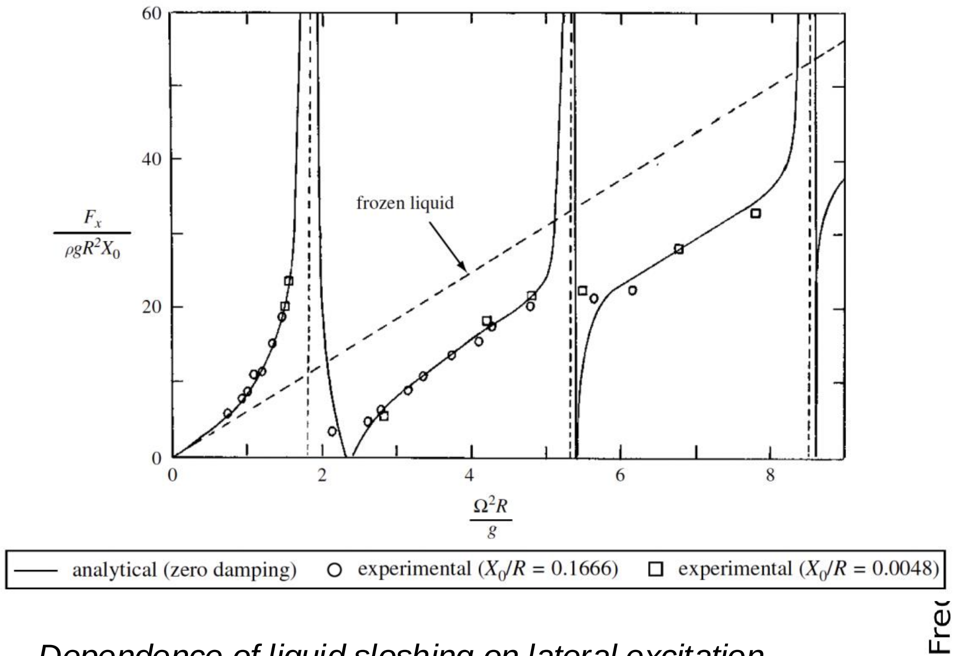

Dependence of liquid sloshing on lateral excitation frequency in a circular tank for h/R.2.0.
in Abramson, H. et al. "Representation of fuel sloshing in cylindrical tanks by an equivalent mechanical model." *ARS Journal* 31, no. 12 **(1961)**: 1697-1705.

Pendulum model parameters are fitted to achieve equivalent force/moment frequency responses:

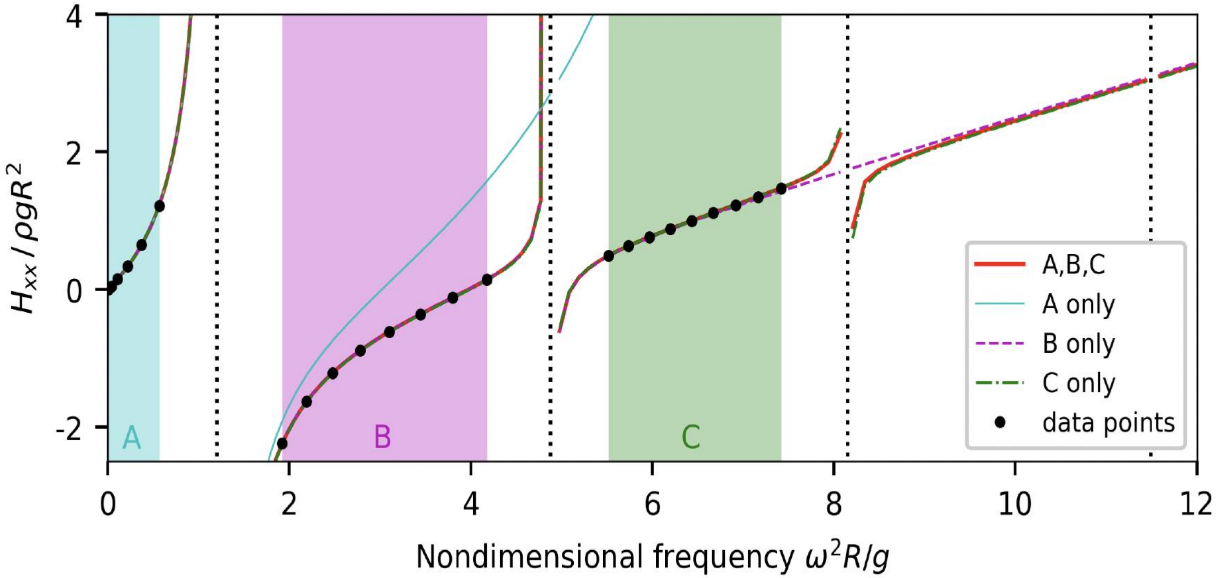

The resulting virtual tray pendulum motion

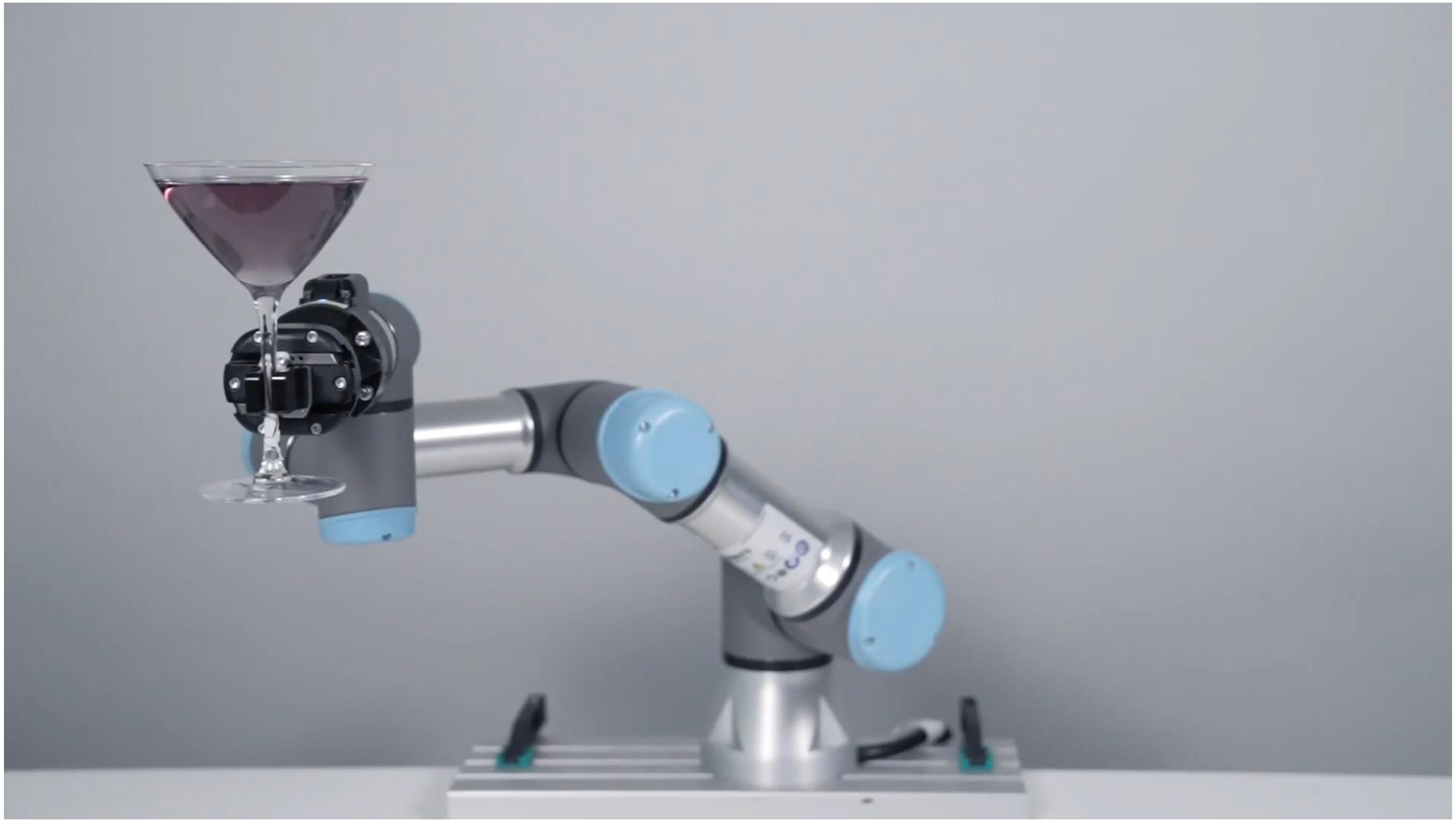

Analysis of dynamic liquid pressure distribution during transit

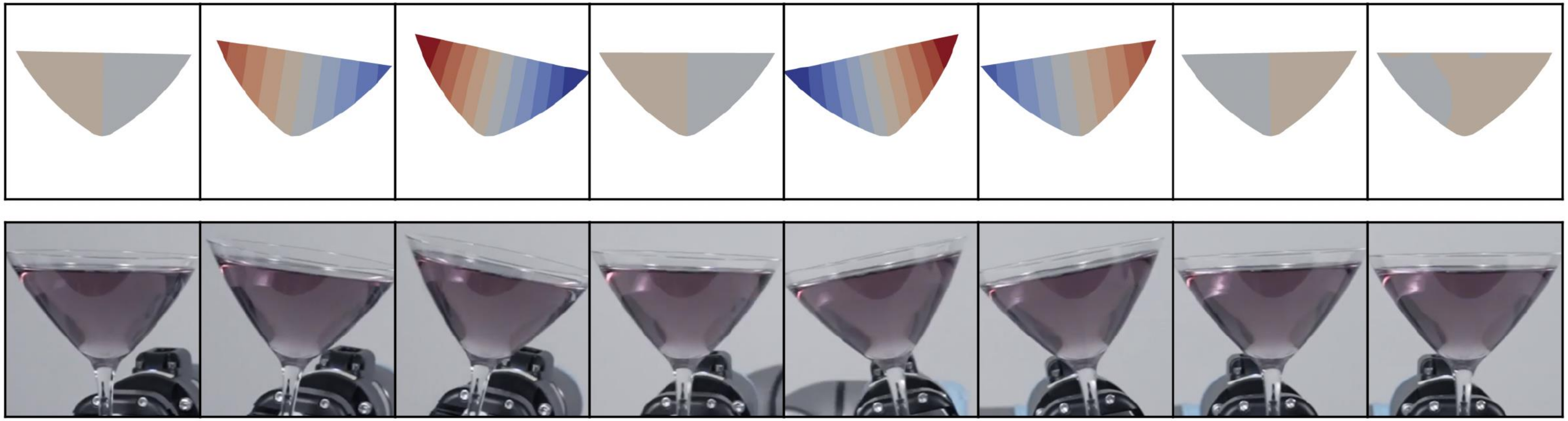

Example of high sloshing sensitivity: The Martini cocktail glass

A small disturbance of the robot trajectory causes massive spilling:

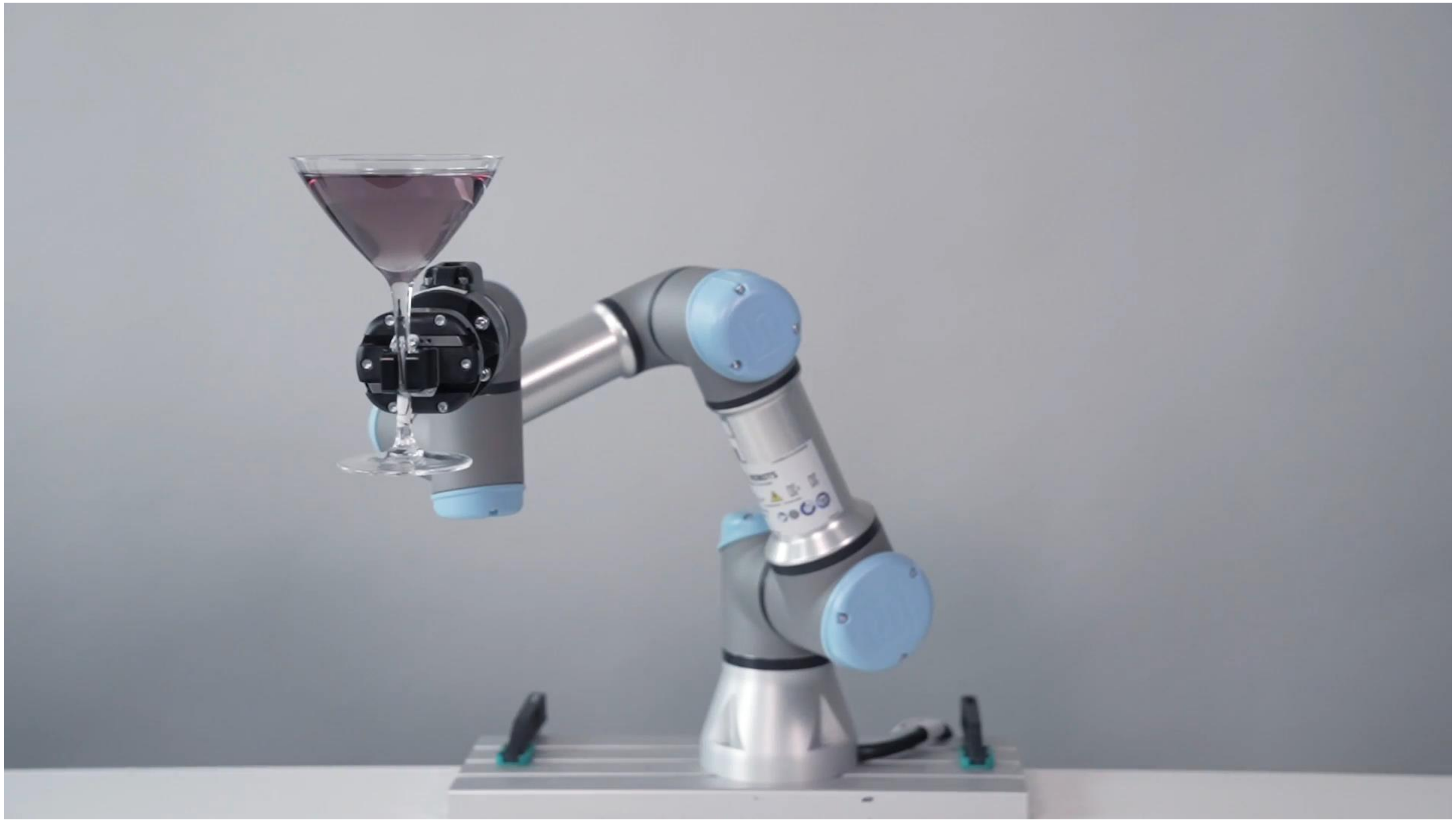

What if... the container cannot be pitched?

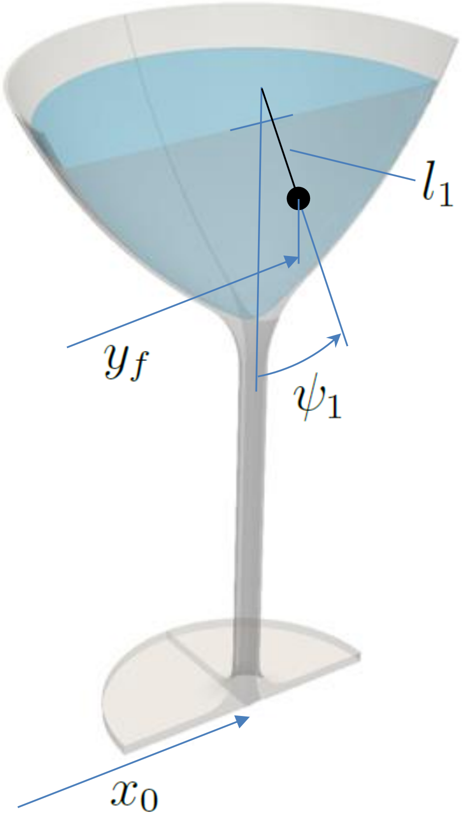

- Container motion is restricted to translation, i.e. ψ=*0* !
- Therefore, the first sloshing mode cannot be fully eliminated anymore during container motion.

But:

- Flat output can still be found: $y_f = x_0 + \alpha_1\psi_1 + \alpha_2\psi_2$
- Rest-to-rest trajectories now show excitation of first sloshing mode during transit, but all sloshing is stopped when the container has reached its final position

Rest-to-rest maneuver without pitching the glass: 1D case

The concept can be easily extended to two-dimensional motion

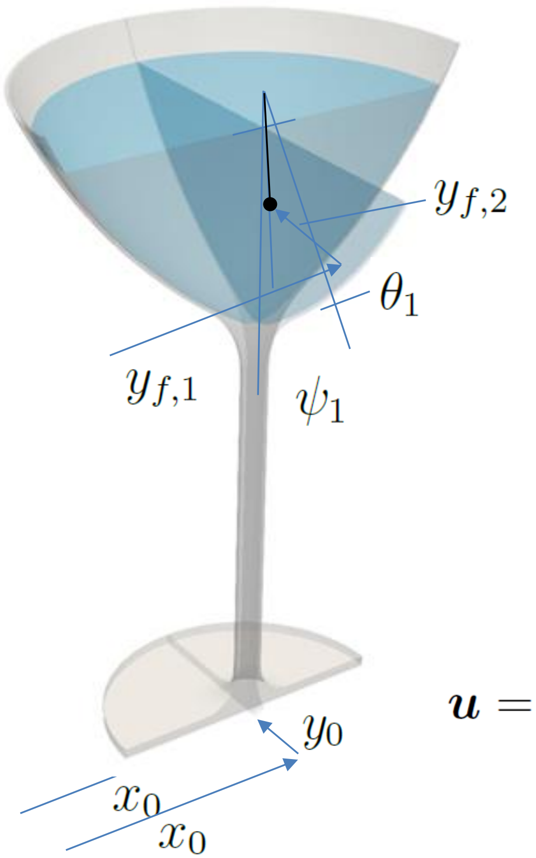

$$\boldsymbol{u} = \begin{bmatrix} \ddot{x}_0 & \ddot{y}_0 \end{bmatrix}^T$$

An industrial application: The ACOPOS 6D system

B&R A member of the ABB Group

- A product of **B&R Industrial Automation GmbH**
- Magnetic levitation transport system
- Mainly planar movements
- Maximum speed $v_{max} = 1\frac{m}{s}$
- Maximum acceleration: $a_{max} = 10\frac{m}{s^2}$

Spatial expansion: Flatness-based feedforward control without pitching

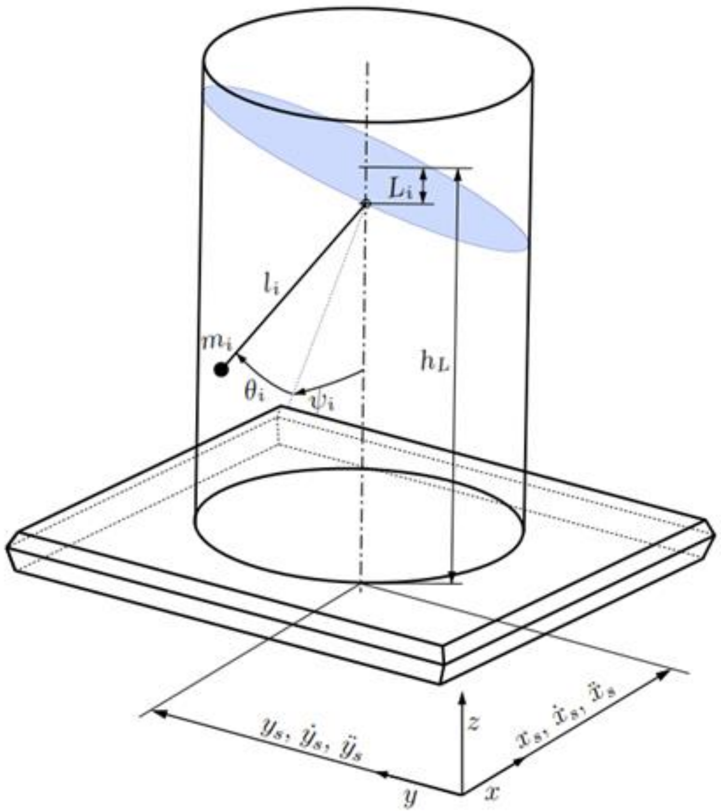

$$\boldsymbol{u}_s = \begin{bmatrix} \ddot{x}_s & \ddot{y}_s \end{bmatrix}^T$$

Two flat outputs:

$$y_{f,1} = x_s + l_1\psi_1 \qquad y_{f,2} = y_s + l_1\theta_1$$

→ Decoupled and physically interpretable:
linearized tip position of the liquid pendulum

Container motion can also subjected to constraints:

Examples:

$$|\ddot{x}_s^2 + \ddot{y}_s^2| \leq a_{max}$$ → Maximum shuttle acceleration

$$|\psi_1| \leq \psi_{1,max}$$
$$|\theta_1| \leq \theta_{1,max}$$
→ Maximum sloshing excitation during transit

High dynamic sloshing control: The “swifty eight”

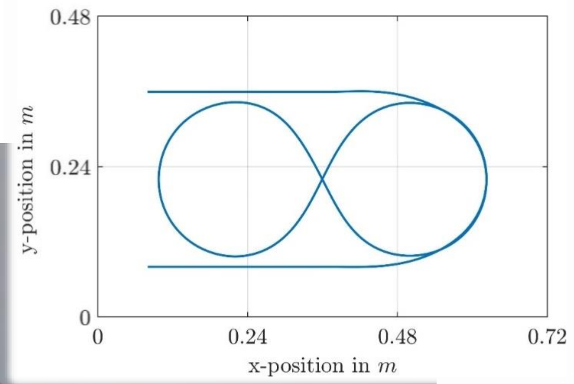

The “swifty eight”: Comparison with uncontrolled case

1999 European Control Conference (ECC)
31 August – 3 September 1999, Karlsruhe, Germany

MOTION PLANNING AND NONLINEAR SIMULATIONS FOR A TANK CONTAINING A FLUID

François Dubois

Nicolas Petit, Pierre Rouchon

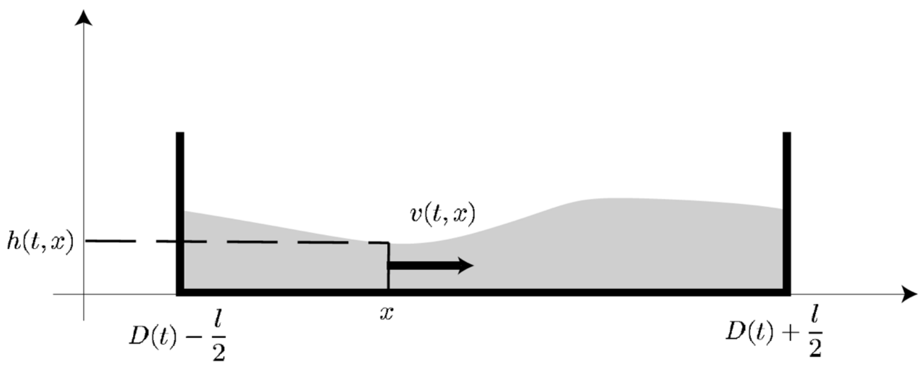

Parameterization of the motion Every quantity of the system writes in terms of $\mathcal{V}$ and $\dot{\mathcal{V}}$. Thus $\mathcal{V}$ is a "flat output" – see [5] and [9] for details. At first order:

$$D(t) = \frac{1}{2}\left[\mathcal{V}(t+\frac{\Delta}{2}) + \mathcal{V}(t-\frac{\Delta}{2})\right] \tag{13}$$

$$v(t,x) = \frac{1}{2}\left[\dot{\mathcal{V}}(t+\frac{x-D(t)}{c}) + \dot{\mathcal{V}}(t-\frac{x-D(t)}{c})\right] \tag{14}$$

$$h(t,x) = \overline{h} + \frac{\sqrt{\overline{h}}}{2\sqrt{g}}\left(\dot{\mathcal{V}}(t-\frac{x-D(t)}{c}) - \dot{\mathcal{V}}(t+\frac{x-D(t)}{c})\right)$$

Thank you for your Attention!

Rothenbuchner, Lukas, Christoph Neudorfer, Markus Fallmann, Florian Toth, Alexander Schirrer, Christoph Hametner, and Stefan Jakubek. *"Efficient feedforward sloshing suppression strategy for liquid transport."* Journal of Sound and Vibration (2024): 118542.

Toth, Florian, Andreas Scharner, Alexander Schirrer, Christoph Hametner, and Stefan Jakubek. *"Rapid sloshing-free transport of liquids in arbitrarily shaped containers."* Acta Mechanica, in press.

IV. Modelling, Control and Monitoring of a Renewable Flow Battery
presenter: Thomas Reiter-Nigitz

Modelling, Control and Monitoring of a Renewable Flow Battery

Retzhof, 09.09.2024

Thomas Reiter-Nigitz, Johannes Niederwieser, Uwe Poms, Dominik Wickenhauser, Stefan Spirk, Markus Gölles

Why renewable flow batteries?

- Flow batteries have large storage capacity and can balance the electric grid regarding fluctuating renewable energy sources and fluctuating energy sinks

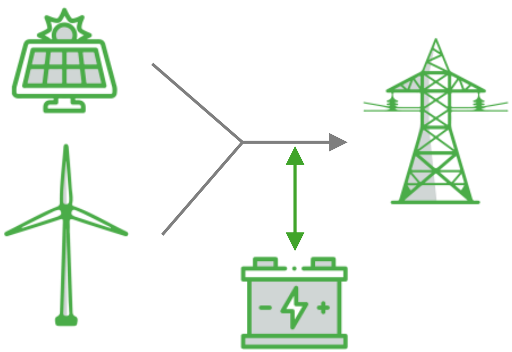

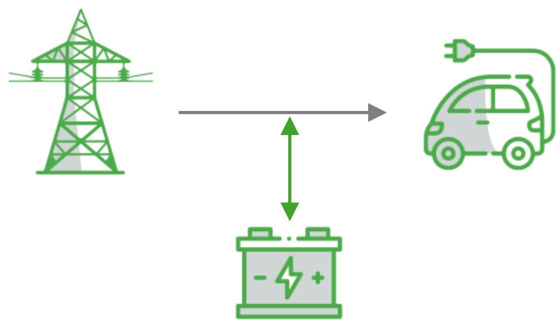

- But flow batteries typically use materials that are not renewable and not local

➢ **Ongoing research to develop renewable flow batteries**

Aim

- BPTI from TU Graz found electrolyte that can be synthesized from plant-based resources

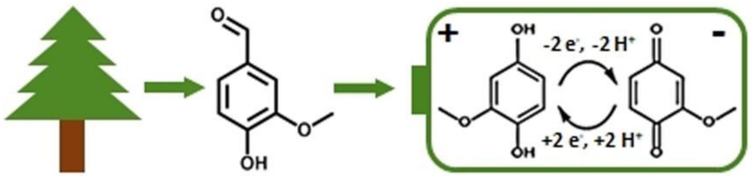

- Further research for electrolyte at demonstration level requires a control and monitoring strategy

> **Aim: Develop control and monitoring strategy for research demonstrator of renewable flow battery**

Research demonstrator 1/2

Output 5kW

Storage capacity 20kWh

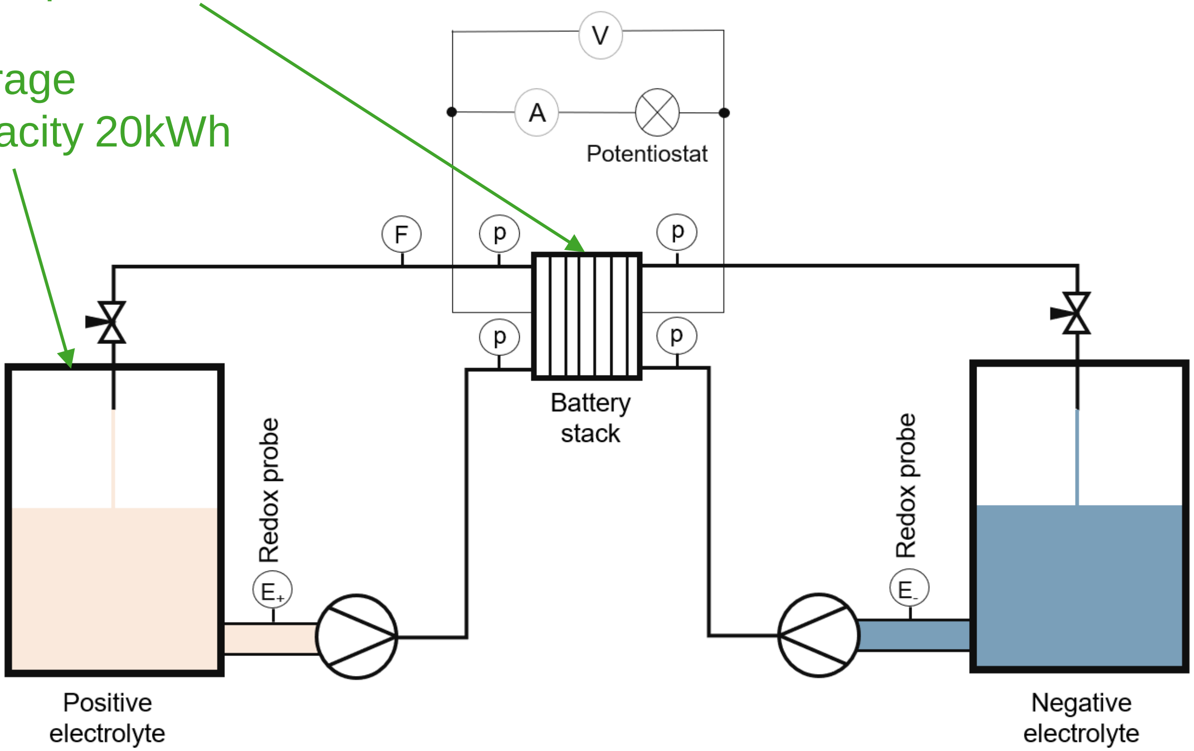

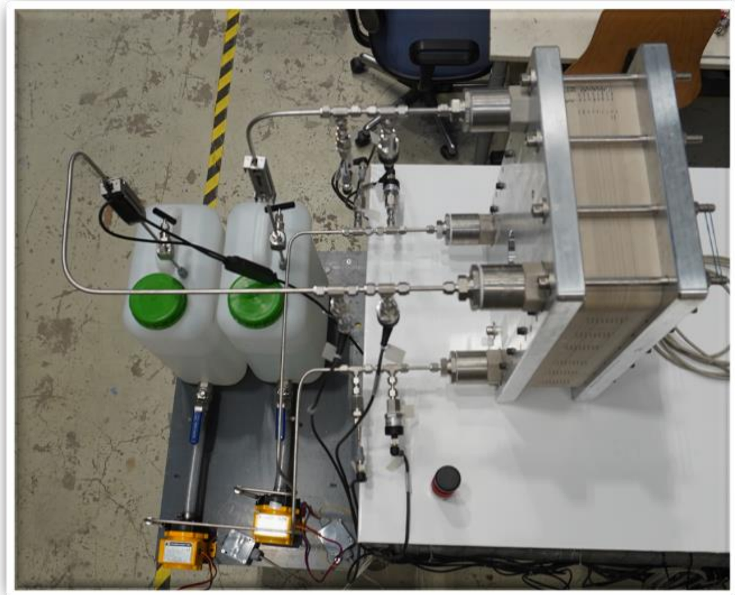

Research demonstrator 2/2

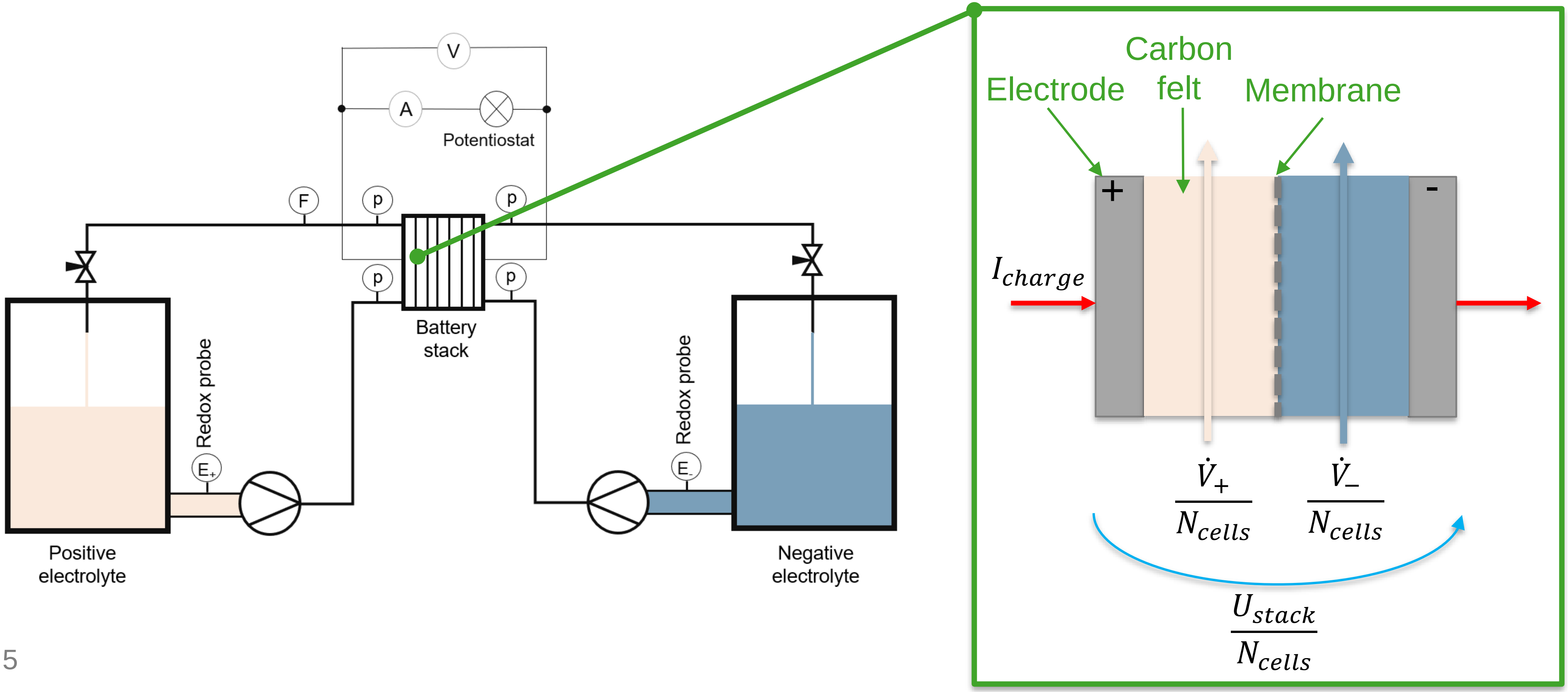

Control and monitoring tasks 1/2

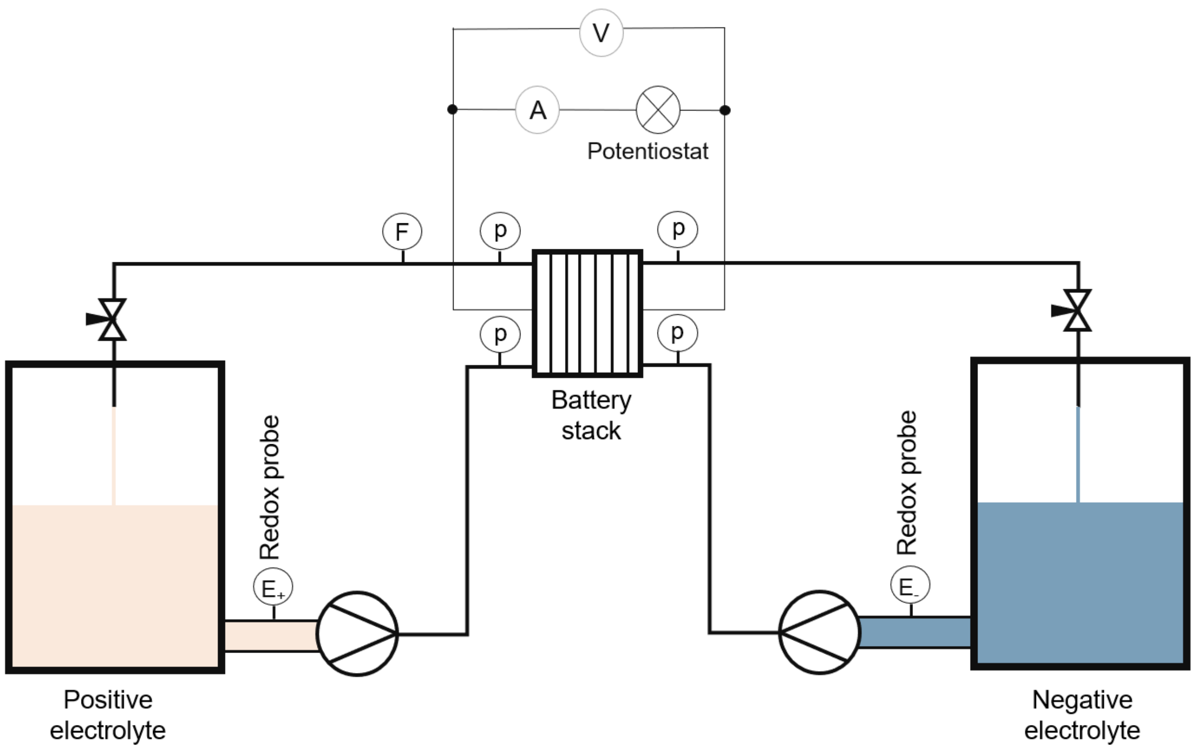

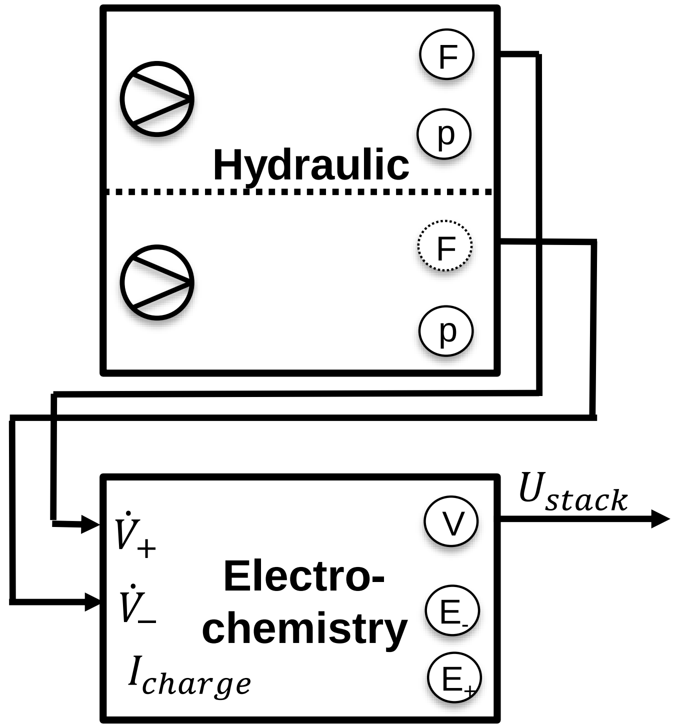

Plant

Control and monitoring tasks 2/2

- Potentiostat controls the electric circuit
  - ➢ Simplification compared to grid operation

- Control task:
  Develop hydraulic control

- Monitoring task:
  Develop state-of-charge (SOC) estimator

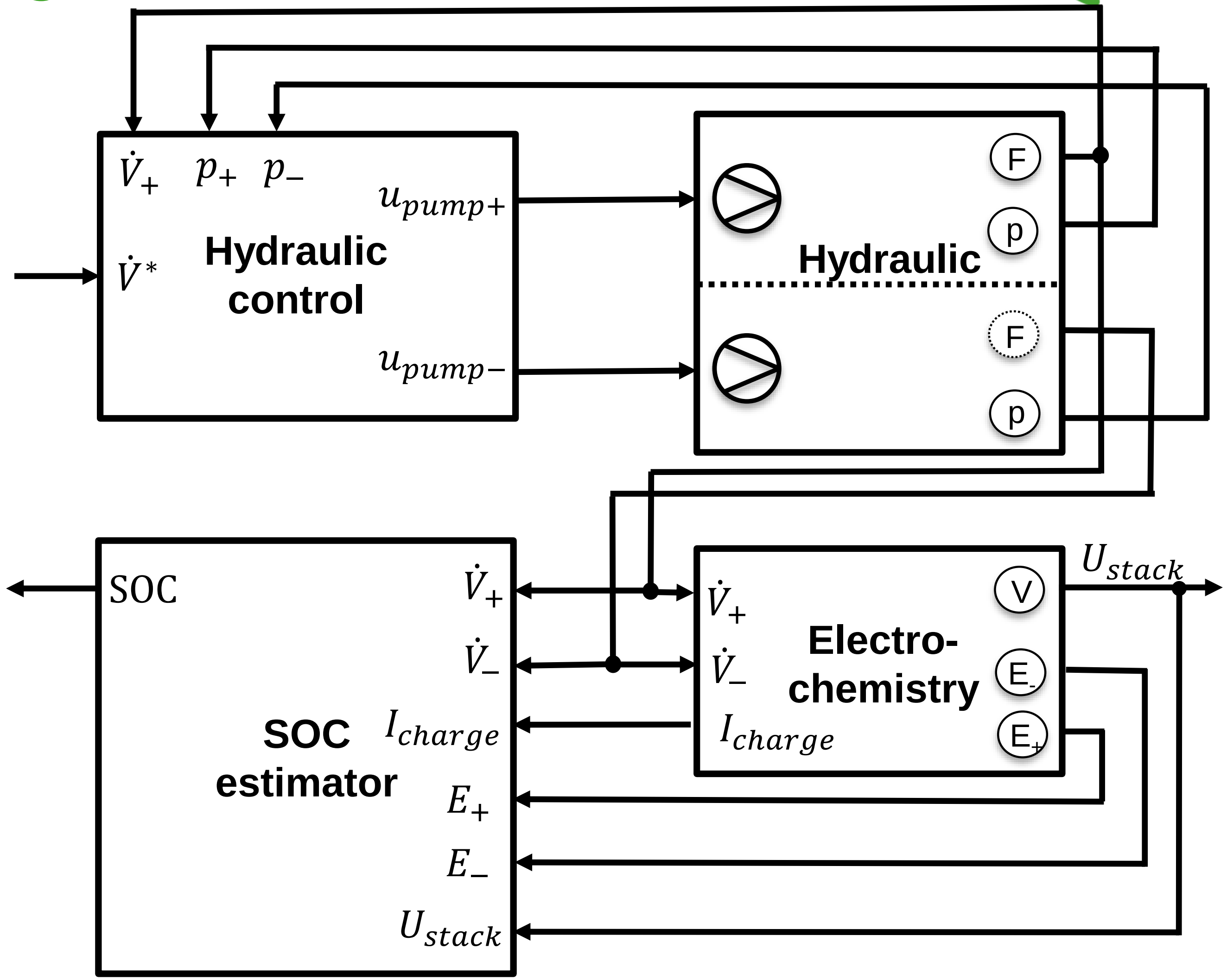

Main content

- **Hydraulic control**
  - Hydraulic model
  - Control design
  - Validation of hydraulic control

- **SOC estimator**
  - SOC definition
  - Concentration model
  - Electrochemistry model
  - SOC observer
  - Validation of SOC estimator

Hydraulic model:
Overview for one hydraulic side

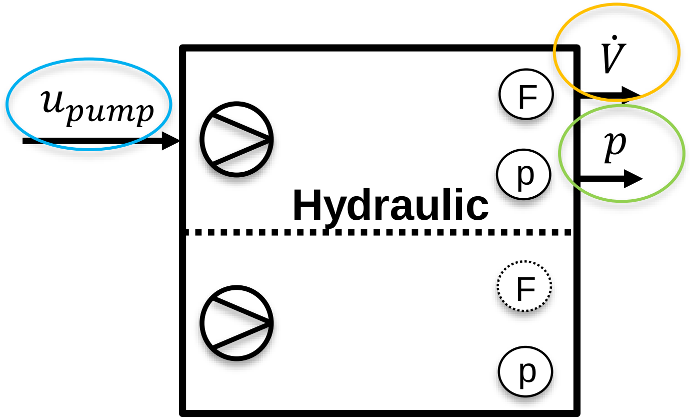

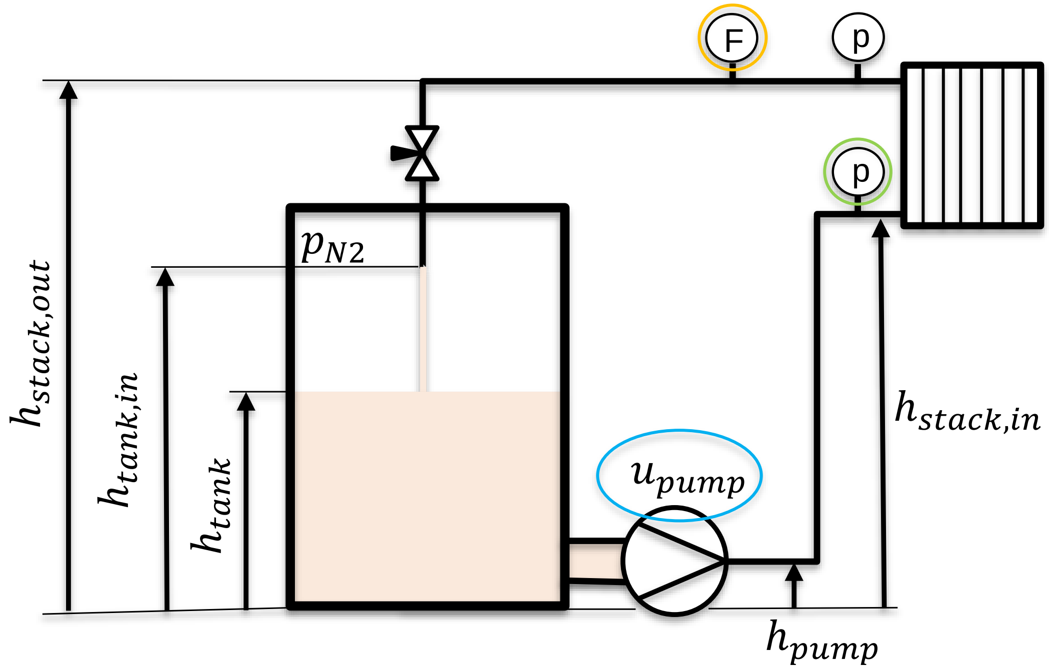

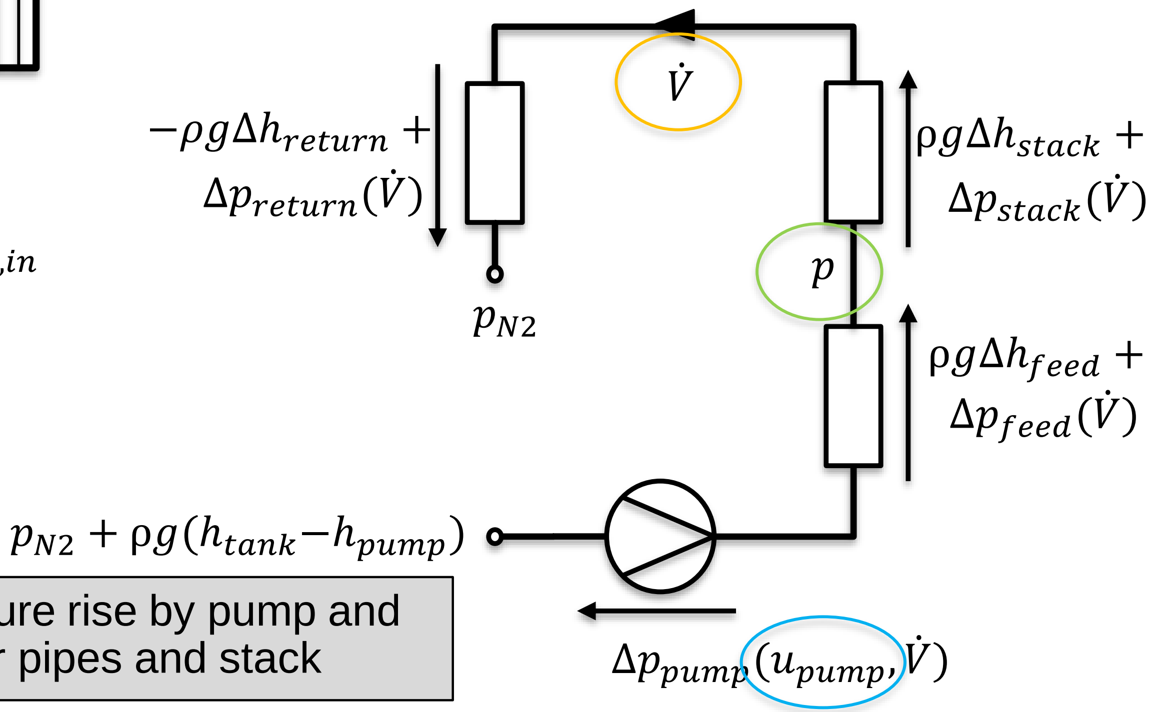

- Next: Model pressure rise by pump and pressure drop over pipes and stack

Hydraulic model: Pressure rise by pump

- Model based on affinity law:

$$\Delta p_{pump}(u_n, \dot{V}) = \alpha u_n^2 + \beta u_n \dot{V} + \gamma \dot{V}^2$$

- with non-linear correction, most likely necessary due to pure feedforward pump controller

$$u_n = u_{pump}^{\delta}$$

$$\delta = 0.9$$

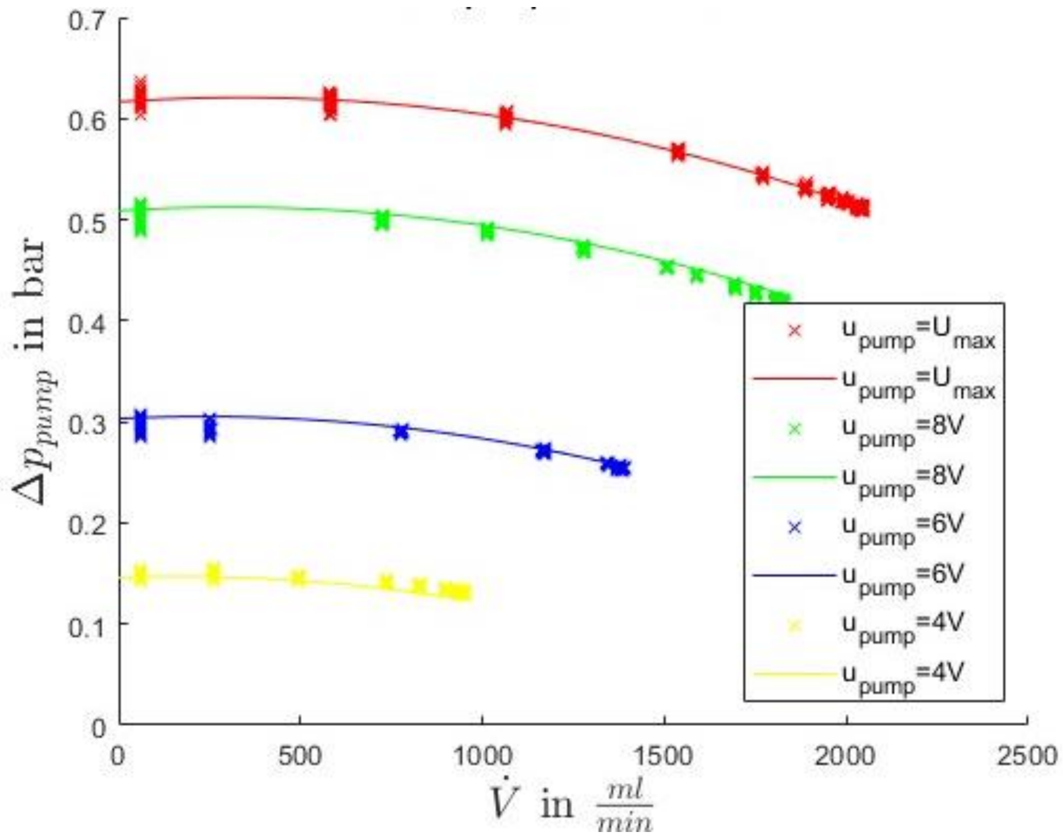

Hydraulic model:
Pressure drop over pipes and stack

- Model pipes with turbulent flow

$$\Delta p_{pipe}(\dot{V}) = R_{quad}\dot{V}^2$$

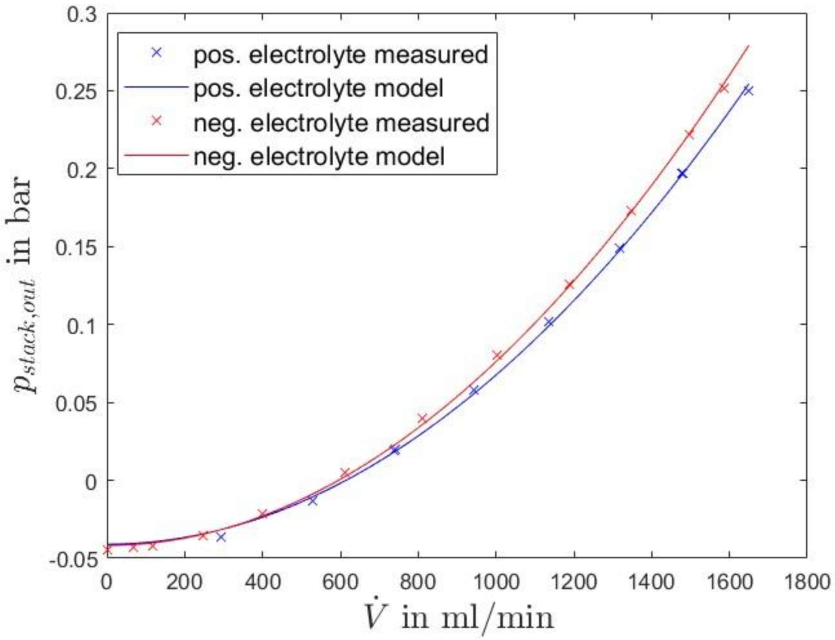

- Model stack with combination of laminar and turbulent flow

$$\Delta p_{stack}(\dot{V}) = R_{lin}\dot{V} + R_{quad}\dot{V}^2$$

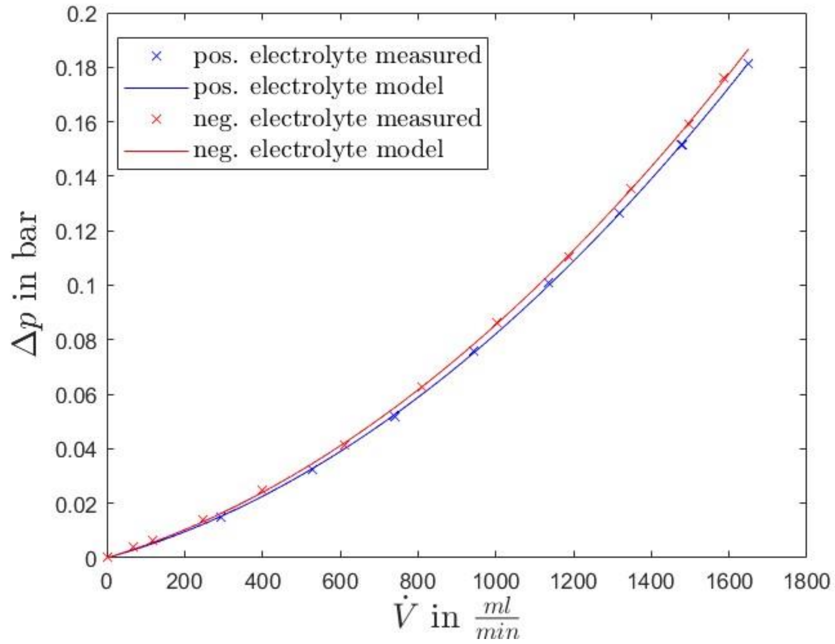

Hydraulic model: Quasi-stationary case

- Sum of the pressure differences along the hydraulic circuit

$$\rho g\left(h_{\text{tank}} - h_{\text{tank,in}}\right) + \alpha u_n^2 + \beta u_n \dot{V} - R_{\text{stack,lin}} \dot{V} + \underbrace{\left(\gamma - R_{\text{feed}} - R_{\text{stack,quad}} - R_{\text{return}}\right)}_{R_{\text{ges,quad}}} \dot{V}^2 = 0$$

- Solve equation for quasi-stationary volume flow

$$\dot{V}_s(u_n) = \frac{\beta u_n - R_{\text{stack,lin}}}{2R_{\text{ges,quad}}} + \sqrt{\left(\frac{\beta u_n - R_{\text{stack,lin}}}{2R_{\text{ges,quad}}}\right)^2 + \frac{\alpha u_n - \rho g\left(h_{\text{tank}} - h_{\text{tank,in}}\right)}{R_{\text{ges,quad}}}}$$

$$u_n = u_{\text{pump}}^{\delta}$$

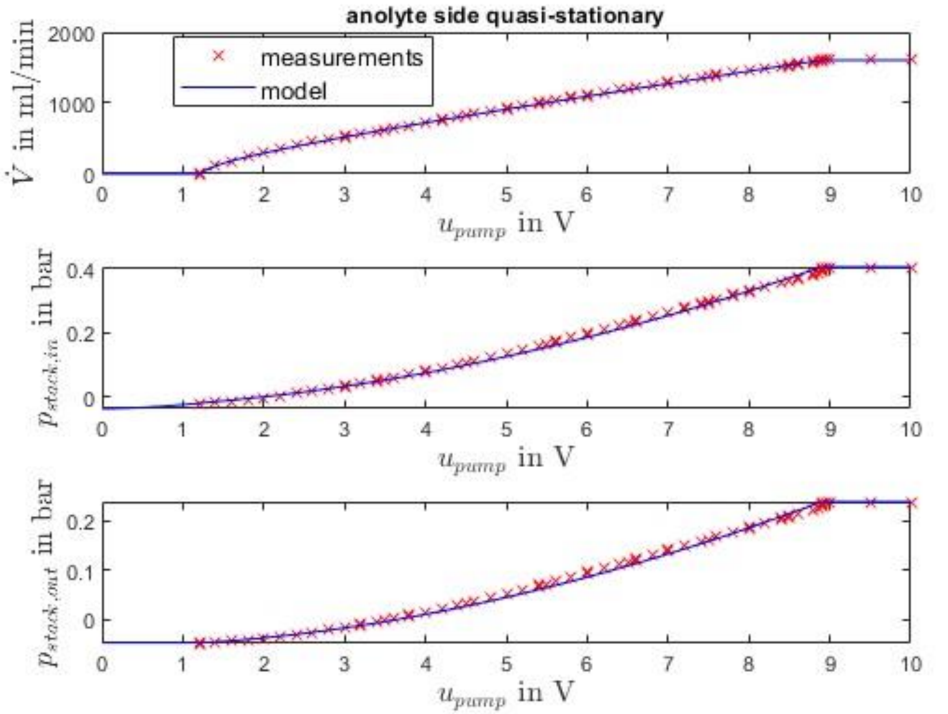

- ➢ **Hydraulic model describes quasi-stationary case sufficiently well**

Hydraulic model: Dynamic case

- Dynamics are approximated by second order delay

$$\dot{V}_s\big(u_n(t - t_{\text{dead}})\big) = \dot{V} + 2TD\frac{d\dot{V}}{dt} + T^2\frac{d^2\dot{V}}{dt^2}$$

➢ **Hydraulic model describes dynamic case sufficiently well and can be used for control design**

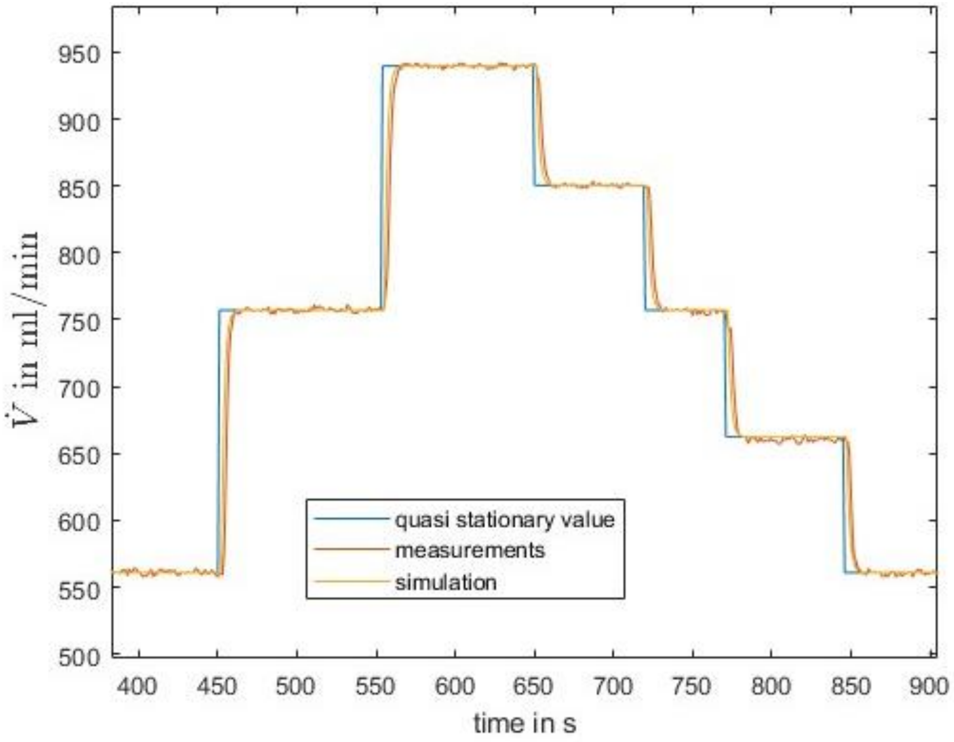

Hydraulic model:
Summary of overall model

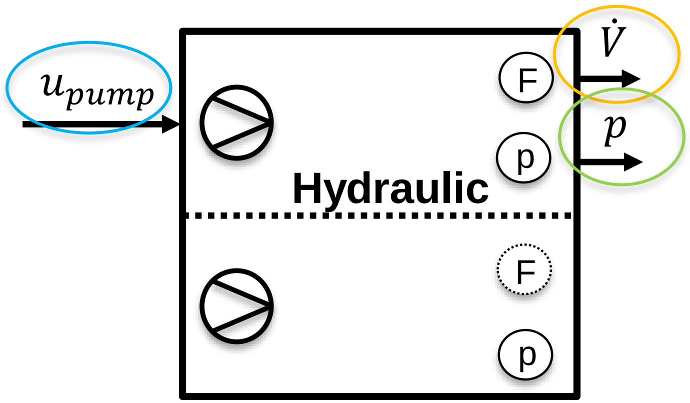

- Influence of the pump speed on the volume flow

$$u_n = u_{\text{pump}}^{\delta}$$

$$\dot{V}_s(u_n) = \frac{\beta u_n - R_{\text{stack,lin}}}{2R_{\text{ges,quad}}} + \sqrt{\left(\frac{\beta u_n - R_{\text{stack,lin}}}{2R_{\text{ges,quad}}}\right)^2 + \frac{\alpha u_n - \rho g\left(h_{\text{tank}} - h_{\text{tank,in}}\right)}{R_{\text{ges,quad}}}}$$

$$\dot{V}_s\left(u_n(t - t_{\text{dead}})\right) = \dot{V} + 2TD\frac{d\dot{V}}{dt} + T^2\frac{d^2\dot{V}}{dt^2}$$

- Influence of the volume flow on the pressure

$$p_{\text{stack,in}} = p_{\text{N}_2} + \rho g(h_{\text{tank}} - h_{\text{stack,in}}) + \Delta p_{\text{pump}}(u_{\text{pump}}, \dot{V}) - R_{\text{feed}}\dot{V}^2$$

Control design: Goals

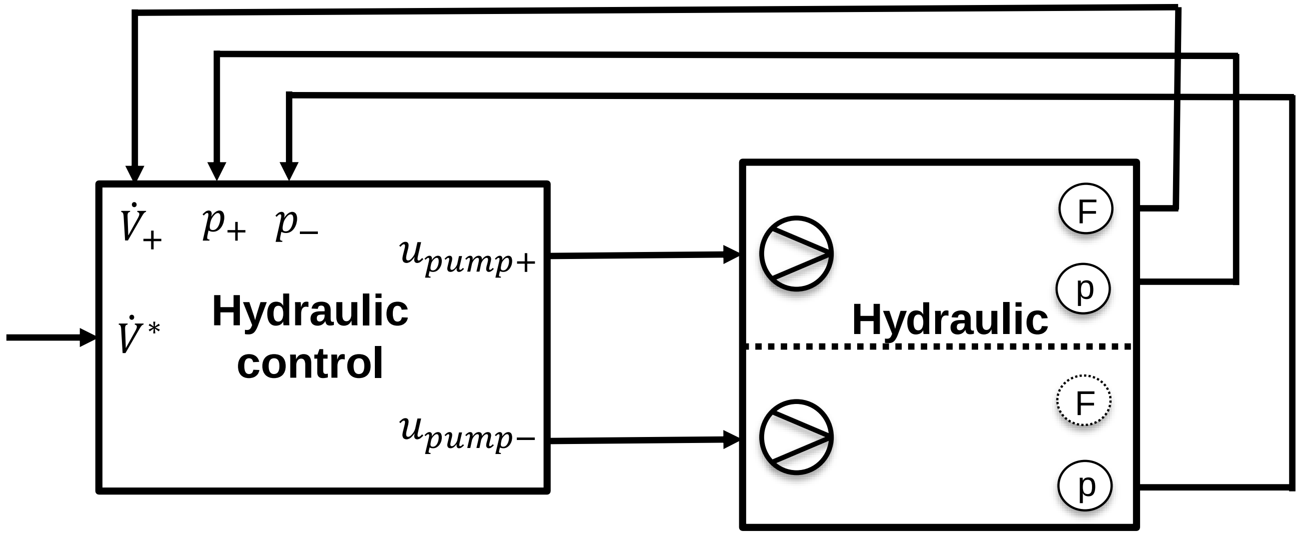

- Reference tracking of a desired volume flow
  - Ensure enough reactants in the stack
  - Avoid unnecessary power consumption at the pumps
- ➢ **Develop flow control**

- Reducing pressure difference across the membrane
  - Avoid mechanical stress
  - Avoid inverse osmosis
- ➢ **Develop pressure control**

Control design: Structure

$$u_n(\dot{V}) = -\frac{\beta\dot{V}}{2\alpha} + \sqrt{\left(\frac{\beta\dot{V}}{2\alpha}\right)^2 - \frac{1}{\alpha}\left(\rho g\left(h_{\text{tank}} - h_{\text{tank,in}}\right) - R_{\text{stack,lin}}\dot{V} - R_{\text{ges,quad}}\dot{V}^2\right)}$$

$$u_{\text{ff}}(\dot{V}) = [u_n(\dot{V})]^{\frac{1}{\delta}}$$

Consider process dynamics in set point for PI-controller

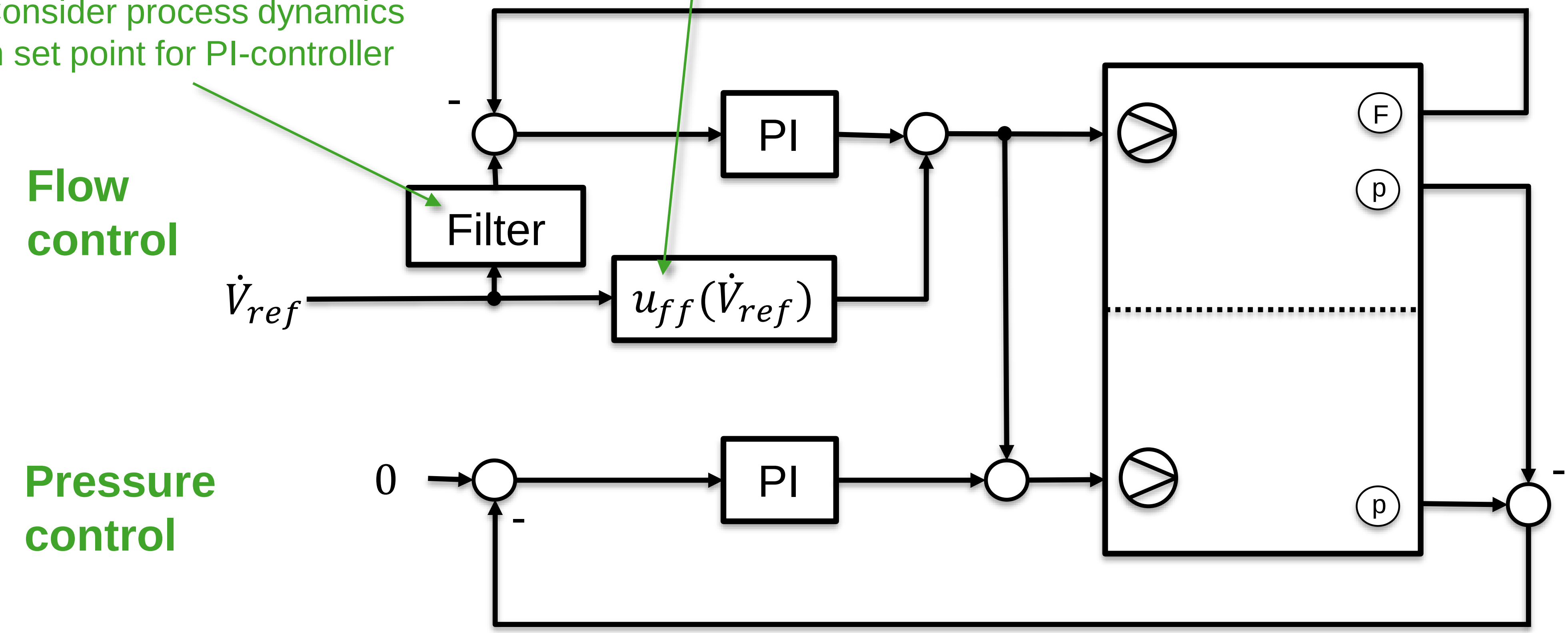

Validation of hydraulic control

- Setpoint for volume flows changes stepwise
- Flow control ensures good reference tracking
- Pressure control keeps pressure differences small

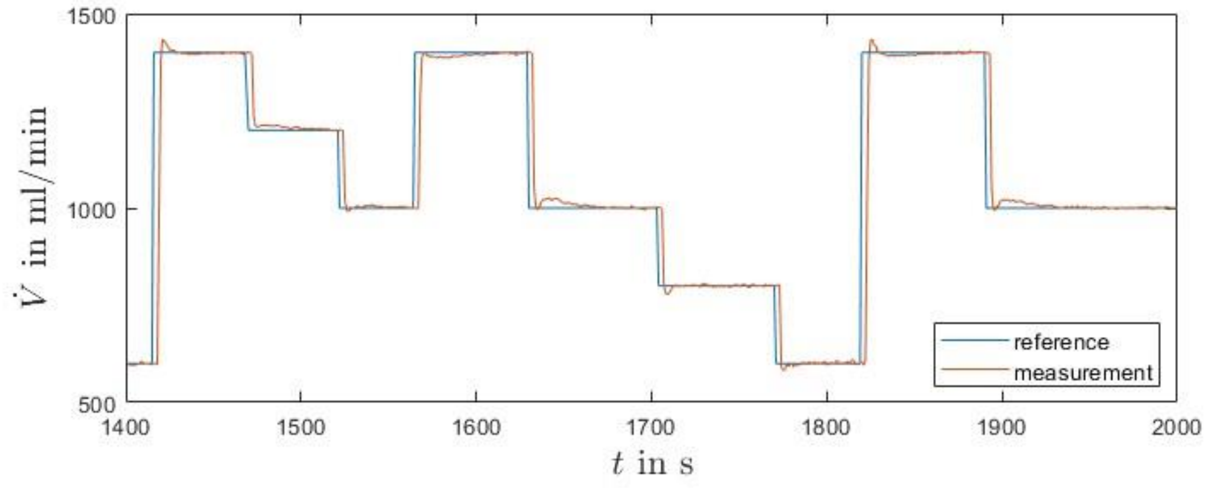

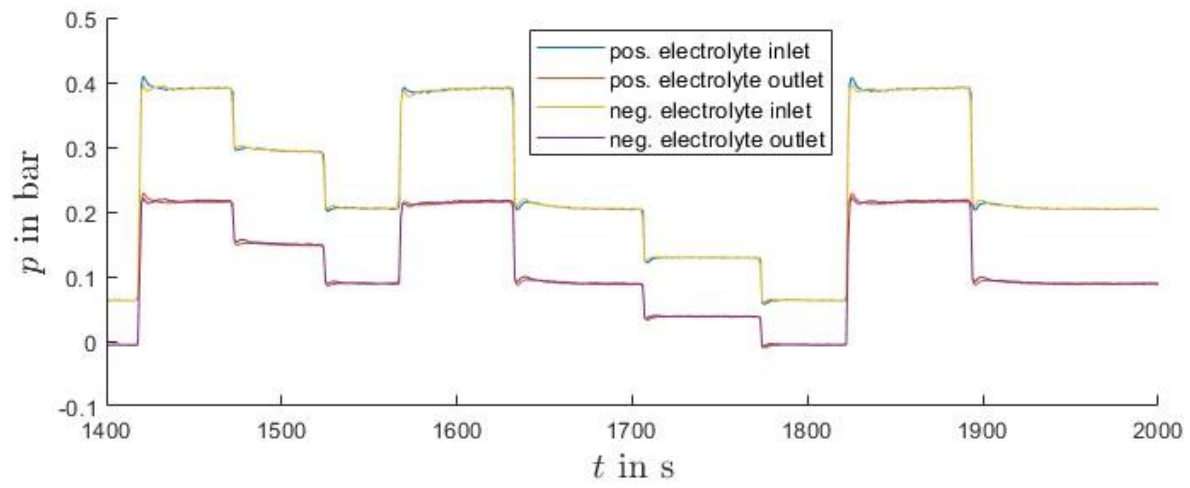

Main content

- **Hydraulic control**
  - Hydraulic model
  - Control design
  - Validation of hydraulic control

- **SOC estimator**
  - SOC definition
  - Concentration model
  - Electrochemistry model
  - SOC observer
  - Validation of SOC estimator

SOC definition: General description

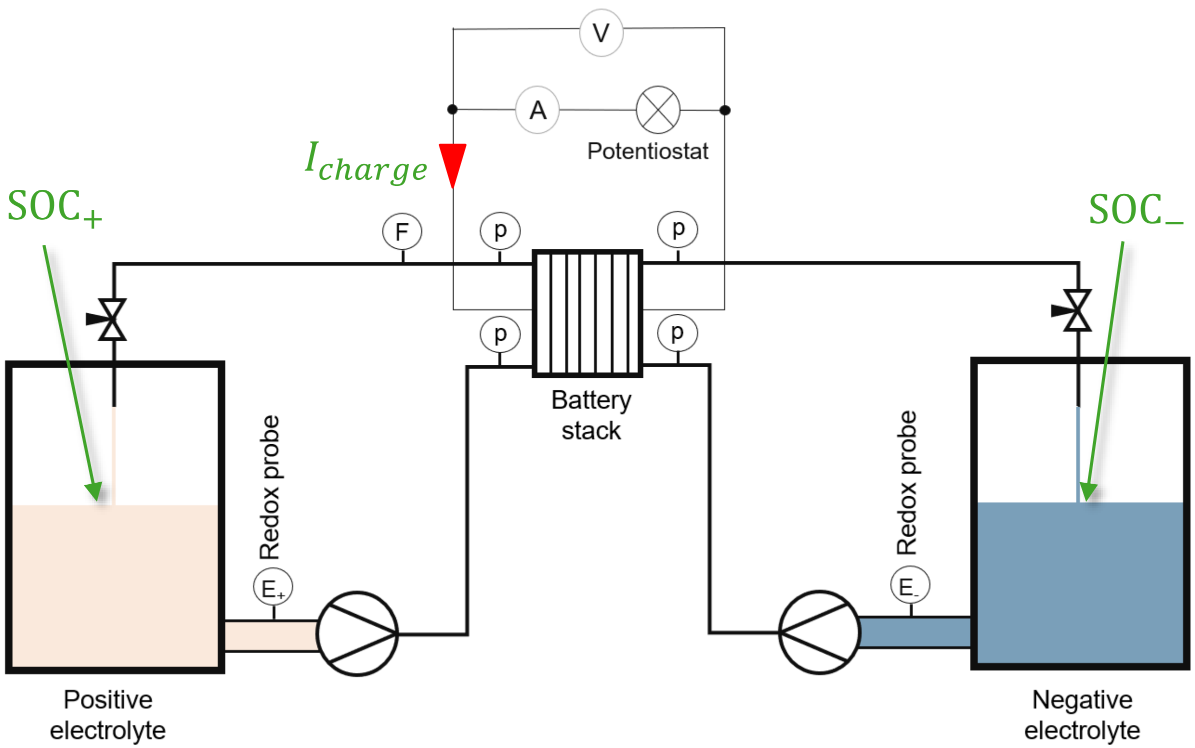

$$SOC := \frac{\text{charge currently stored}}{\text{maximal storable charge}} = \frac{Q}{Q_{max}}$$

- The SOC is NOT directly measurable
- The SOC changes due to the electric current I_{charge}
- Positive and negative electrolyte hold individual SOCs
- ➢ The lower SOC limits the total storage capacity, i.e.

$$SOC = \min(SOC_+, SOC_-)$$

SOC definition: Detailed description

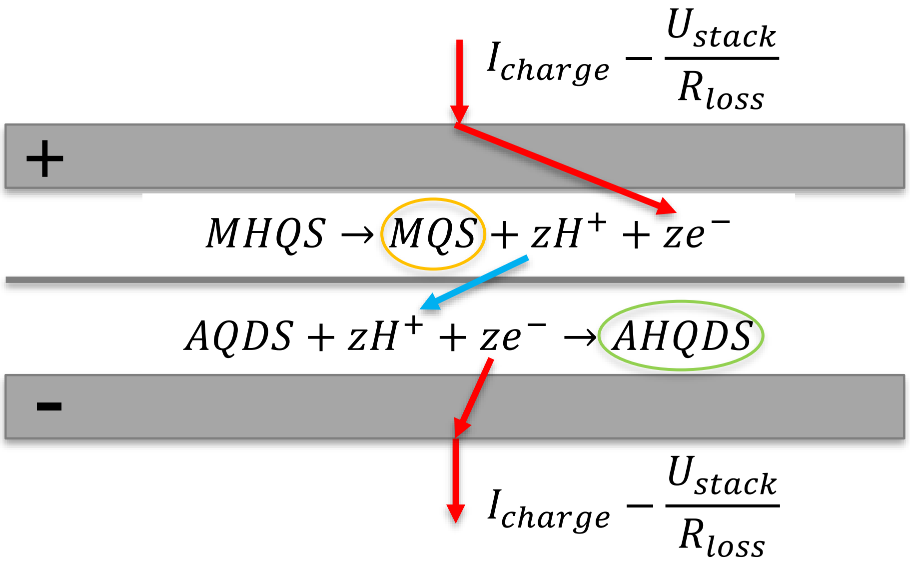

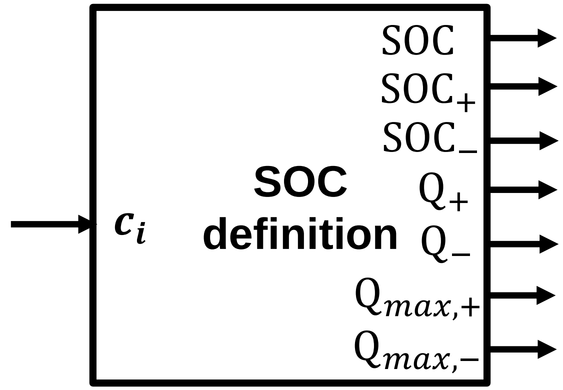

- SOC definition for both sides based on the concentrations of the species

$$\mathrm{SOC}_+ = \frac{c_{\mathrm{MQS,cell}} V_{\mathrm{stack}} + c_{\mathrm{MQS,tank}} V_{\mathrm{tank}}}{(c_{\mathrm{MQS,cell}} + c_{\mathrm{MHQS,cell}}) V_{\mathrm{stack}} + (c_{\mathrm{MQS,tank}} + c_{\mathrm{MHQS,tank}}) V_{\mathrm{tank}}} \cdot \frac{zF}{zF} = \frac{Q_+}{Q_{max,+}}$$

$$\mathrm{SOC}_- = \frac{c_{\mathrm{AHQDS,cell}} V_{\mathrm{stack}} + c_{\mathrm{AHQDS,tank}} V_{\mathrm{tank}}}{(c_{\mathrm{AHQDS,cell}} + c_{\mathrm{AQDS,cell}}) V_{\mathrm{stack}} + (c_{\mathrm{AHQDS,tank}} + c_{\mathrm{AQDS,tank}}) V_{\mathrm{tank}}} \cdot \frac{zF}{zF} = \frac{Q_-}{Q_{max,-}}$$

➢ Next: Model concentration of species in stack and both tanks

Concentration model: Single species in one cell

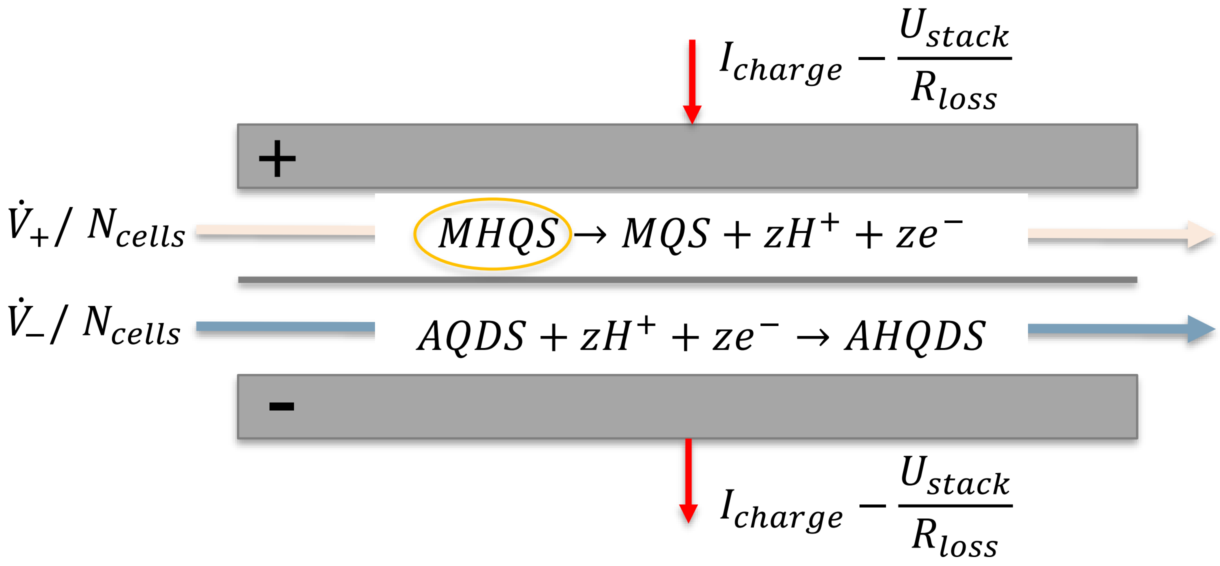

Volume of one electrolyte in one cell

$$\frac{V_{stack}}{N_{cells}} \frac{dc_{MHQS,stack}}{dt} = \overbrace{\frac{\dot{V}_{+}}{N_{cells}} \left(c_{MHQS,tank} - c_{MHQS,stack}\right)}^{\text{Change of concentration due to volume flow}} - \overbrace{\frac{\left(I_{charge} - \frac{U_{stack}}{R_{loss}}\right)}{zF}}^{\text{Change of concentration due to electric current}}$$

$$\cdot \frac{N_{cells}}{V_{stack}}$$

$$\frac{dc_{MHQS,stack}}{dt} = \frac{\dot{V}_{+}}{V_{stack}} \left(c_{MHQS,tank} - c_{MHQS,stack}\right) - \frac{\left(I_{charge} - \frac{U_{stack}}{R_{loss}}\right) N_{cells}}{zFV_{stack}}$$

Concentration model: All species in stack and both tanks

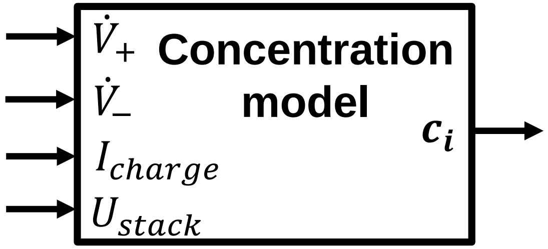

Electric current only acts on concentrations in the stack

$$\frac{d}{dt}\begin{bmatrix} c_{MHQS,stack} \\ c_{MQS,stack} \\ c_{AQDS,stack} \\ c_{AHQDS,stack} \\ c_{MHQS,tank} \\ c_{MQS,tank} \\ c_{AQDS,tank} \\ c_{AHQDS,tank} \end{bmatrix} = \overbrace{\begin{bmatrix} \frac{-\dot{V}_+}{V_{stack}} & 0 & 0 & 0 & \frac{\dot{V}_+}{V_{stack}} & 0 & 0 & 0 \\ 0 & \frac{-\dot{V}_+}{V_{stack}} & 0 & 0 & 0 & \frac{\dot{V}_+}{V_{stack}} & 0 & 0 \\ 0 & 0 & \frac{-\dot{V}_-}{V_{stack}} & 0 & 0 & 0 & \frac{\dot{V}_-}{V_{stack}} & 0 \\ 0 & 0 & 0 & \frac{-\dot{V}_-}{V_{stack}} & 0 & 0 & 0 & \frac{\dot{V}_-}{V_{stack}} \\ \frac{\dot{V}_+}{V_{tank}} & 0 & 0 & 0 & \frac{-\dot{V}_+}{V_{tank}} & 0 & 0 & 0 \\ 0 & \frac{\dot{V}_+}{V_{tank}} & 0 & 0 & 0 & \frac{-\dot{V}_+}{V_{tank}} & 0 & 0 \\ 0 & 0 & \frac{\dot{V}_-}{V_{tank}} & 0 & 0 & 0 & \frac{-\dot{V}_-}{V_{tank}} & 0 \\ 0 & 0 & 0 & \frac{\dot{V}_-}{V_{tank}} & 0 & 0 & 0 & \frac{-\dot{V}_-}{V_{tank}} \end{bmatrix}}^{\text{Linear system, if volume flows are constant}} \begin{bmatrix} c_{MHQS,stack} \\ c_{MQS,stack} \\ c_{AQDS,stack} \\ c_{AHQDS,stack} \\ c_{MHQS,tank} \\ c_{MQS,tank} \\ c_{AQDS,tank} \\ c_{AHQDS,tank} \end{bmatrix} + \frac{N_{cells}}{zFV_{stack}} \begin{bmatrix} -1 \\ 1 \\ -1 \\ 1 \\ 0 \\ 0 \\ 0 \\ 0 \end{bmatrix} \left(I_{charge} - \frac{U_{stack}}{R_{loss}}\right)$$

with $V_{stack} = V_{filling} - V_{tank}$

Electrochemistry model: Overview

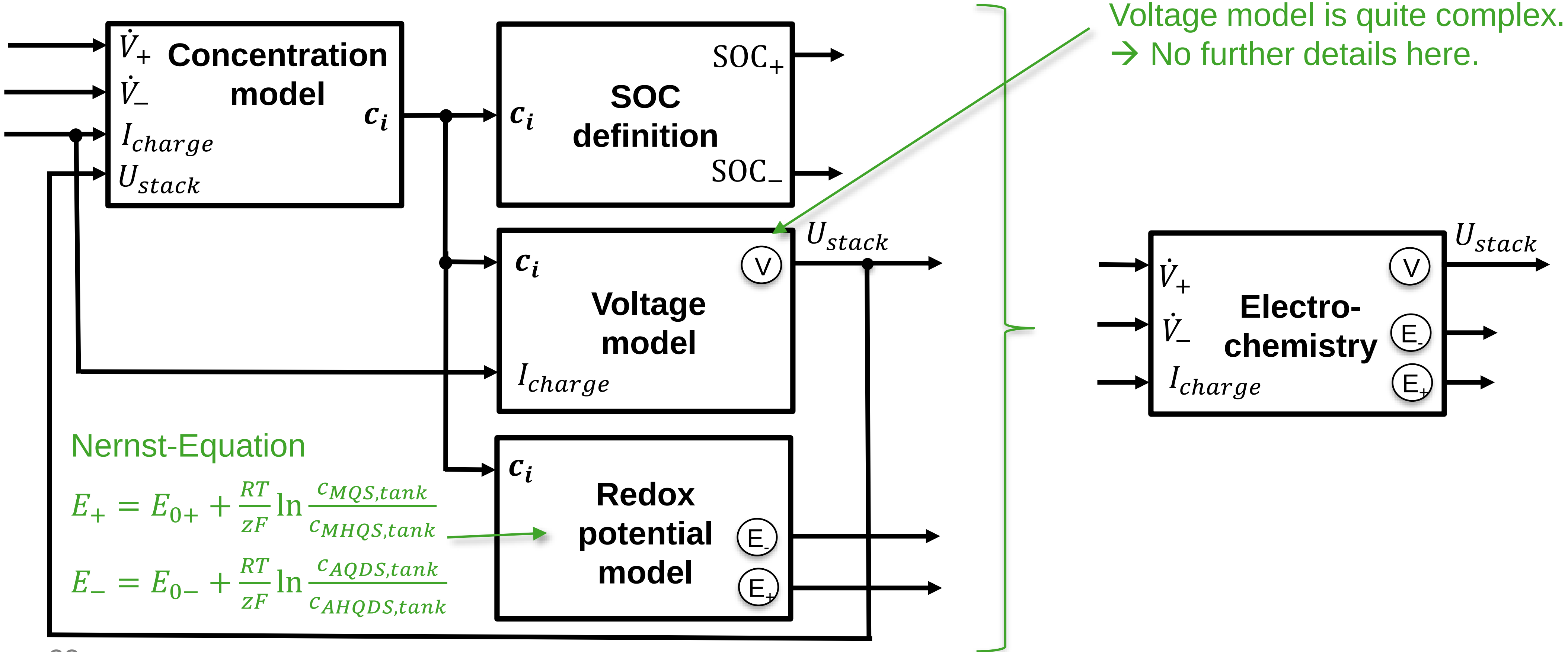

Voltage model is quite complex.
→ No further details here.

Nernst-Equation

$$E_+ = E_{0+} + \frac{RT}{zF} \ln \frac{c_{MQS,tank}}{c_{MHQS,tank}}$$

$$E_- = E_{0-} + \frac{RT}{zF} \ln \frac{c_{AQDS,tank}}{c_{AHQDS,tank}}$$

Electrochemistry model: Validation

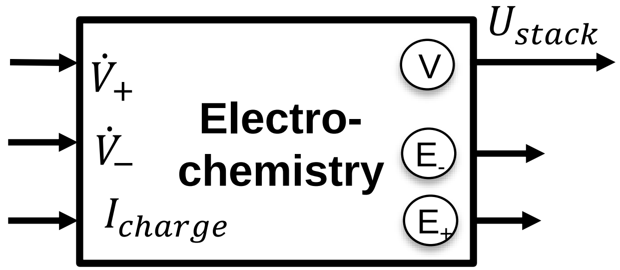

- Volume flows are kept constant
- Electric current alternates between charging and discharging
- Redox potentials and stack voltage can be described by the electrochemistry model
- ➢ **The developed models can be used for SOC estimation via SOC observer**

Model error at high SOCs

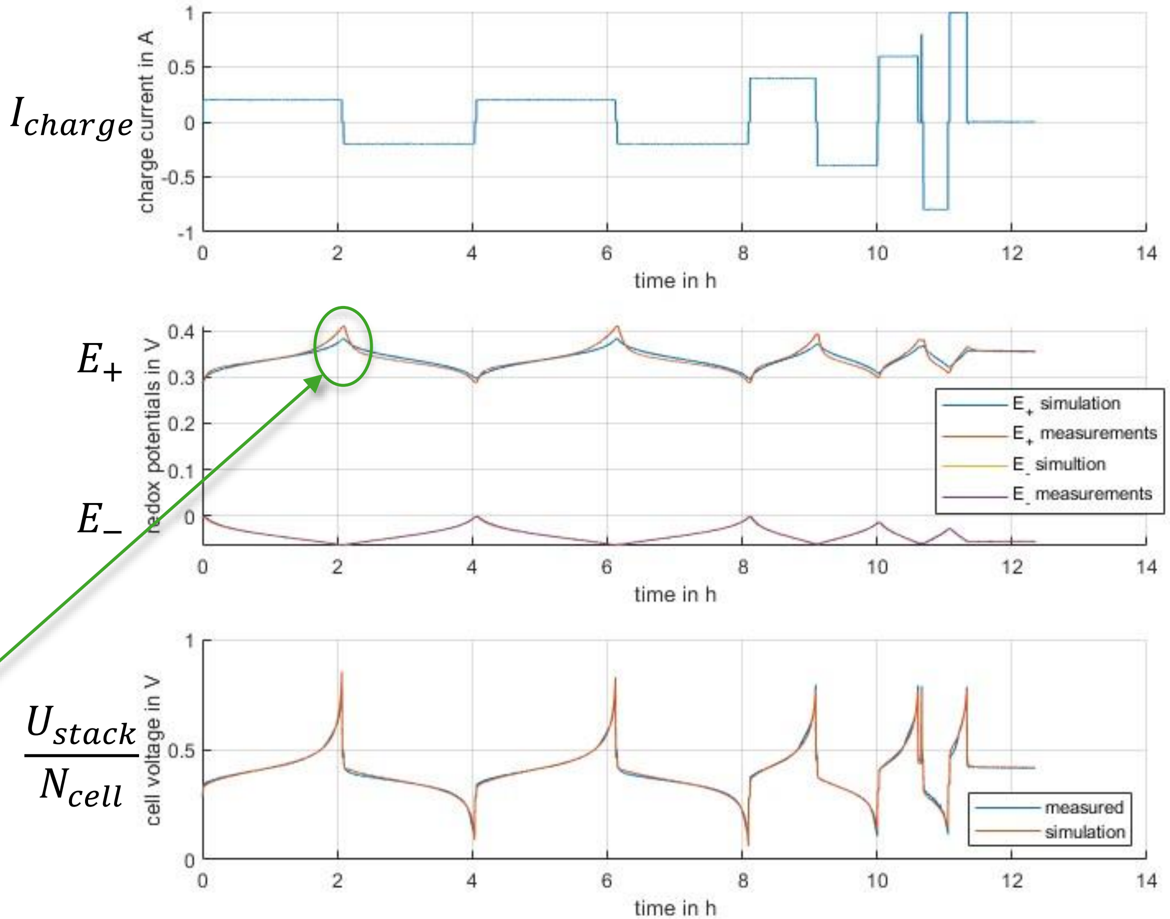

SOC observer: Components

1. Use concentration differences between stack and tank, e.g.: $\Delta c_{MQS} = c_{MQS,stack} - c_{MQS,tank}$

   $$\frac{d\Delta c_{MQS}}{dt} = -\dot{V}_+ \left(\frac{1}{V_{stack}} + \frac{1}{V_{tank}}\right) \Delta c_{MQS} + \frac{N_{cells}}{zFV_{stack}} \left(I_{charge} - \frac{U_{stack}}{R_{loss}}\right)$$

   Asymptotically stable error dynamics
   → Use as **Trivial observer** for all species

2. **Measurement transformation** using Nernst-Equation

   $y_+ = \frac{c_{MQS,tank}}{c_{MHQS,tank}} = e^{\frac{zF}{RT}(E_+ - E_{0+})}$ and $y_- = \frac{c_{AQDS,tank}}{c_{AHQDS,tank}} = e^{\frac{zF}{RT}(E_- - E_{0-})}$

3. **State transformation**

   $$z = \begin{bmatrix} \frac{c_{MQS,tank}}{c_{MHQS,tank}} \\ \frac{1}{c_{MQS,tank} + c_{MHQS,tank}} \\ \frac{c_{AHQDS,tank}}{c_{AQDS,tank}} \\ \frac{1}{c_{AQDS,tank} + c_{AHQDS,tank}} \end{bmatrix} \rightarrow \frac{dz}{dt} = \begin{bmatrix} \frac{\dot{V}_+}{V_{tank}} \Delta c_{MQS}\, z_2 (1 + z_1)^2 \\ 0 \\ \frac{\dot{V}_-}{V_{tank}} \Delta c_{AHQDS}\, z_4 (1 + z_3)^2 \\ 0 \end{bmatrix},$$

   $y_+ = z_1, y_- = z_3$

4. **Non-linear observer** is quite complex → For detailed description see publication

   Thomas Puleston, Andreu Cecilia, Ramon Costa-Castell´o, and Maria Serra. Nonlinear observer for online concentration estimation in vanadium flow batteries based on half-cell voltage measurements. Computers & Chemical Engineering, 185:108664, 2024.

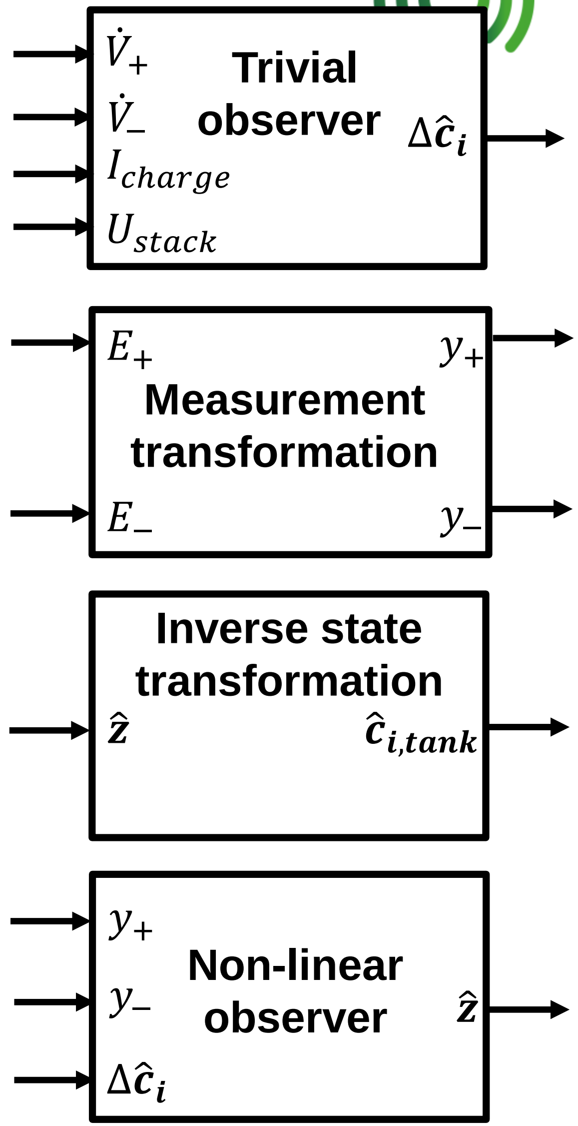

SOC observer:
Structure and combination with SOC definition

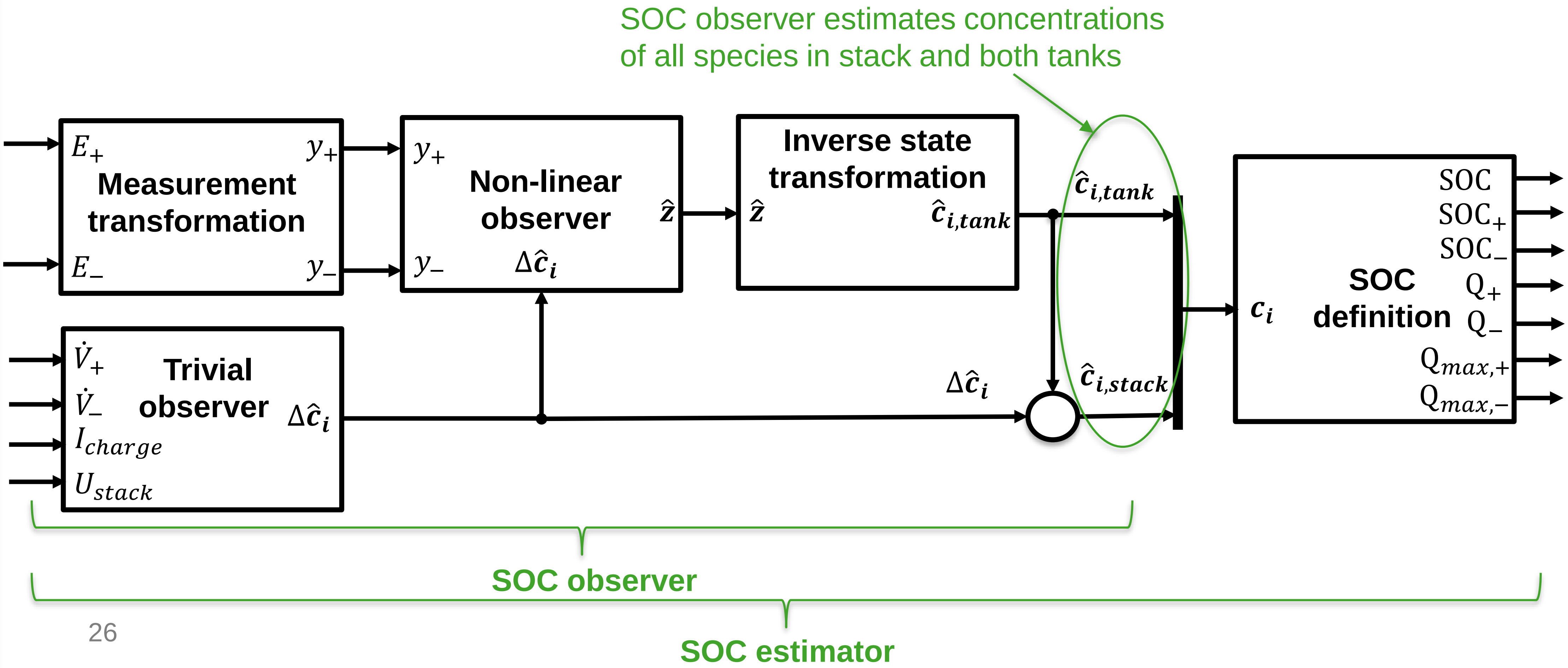

Validation of SOC estimator

- Comparison
  - of charge Q from SOC estimator
  - with charge Q from coulomb counting

$$Q(t) = N_{cells} \int_0^t I_{charge}(\tau)\, d\tau$$

  - Measurement data is chosen such that $Q(0) = 0$ is a valid initial condition for the coulomb counting.
- Electric current alternates between charging and discharging

➢ **SOC estimator provides information about both electrolytes**

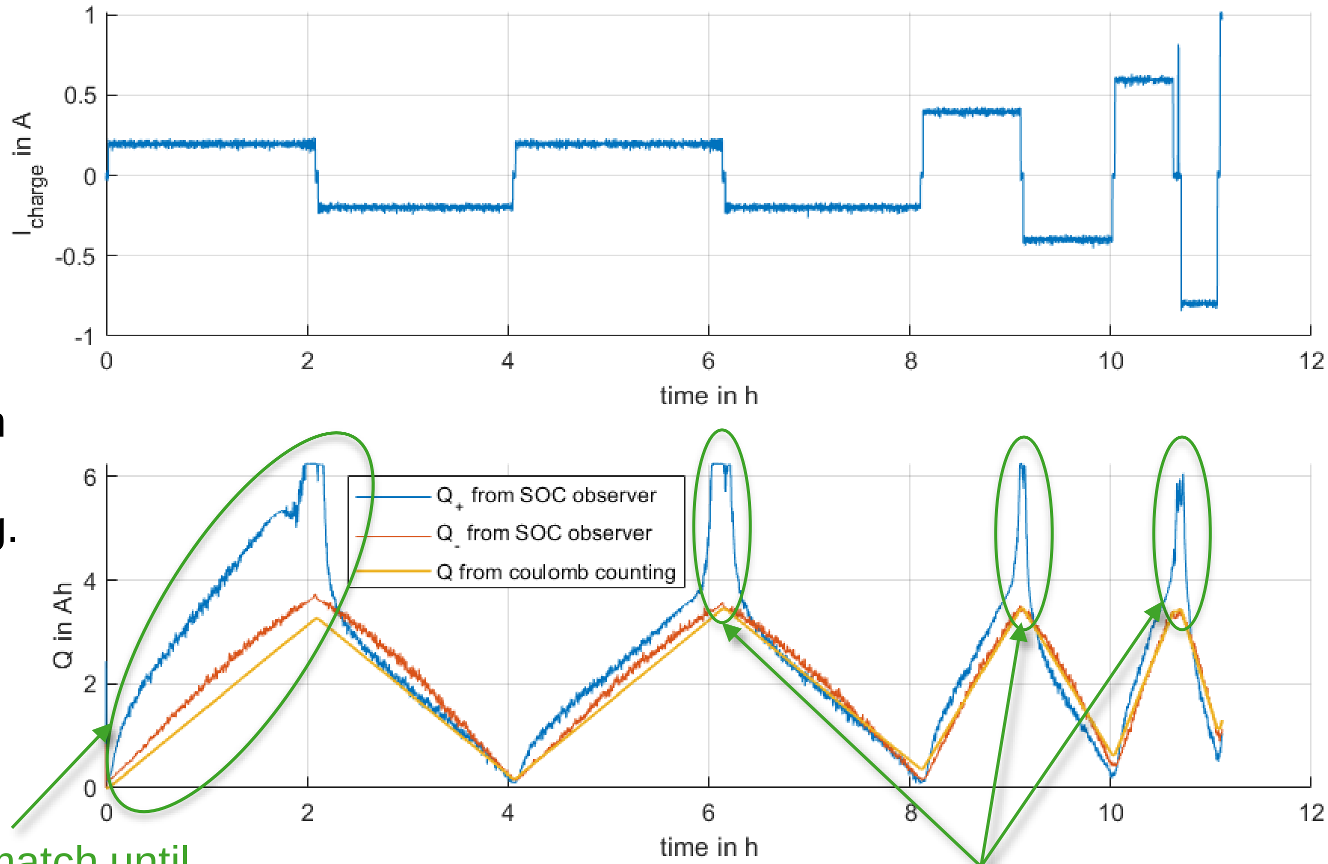

Initial mismatch until
SOC observer converges

Effect of model error at high SOCs

Conclusion and outlook

- Conclusion
  - **Hydraulic control** tracks setpoint of volume flow and keeps pressure difference at membrane around zero
  - **SOC estimator** provides information about both electrolytes
- Outlook
  - Transfer **hydraulic control** to demonstrator with different hydraulic configurations at next scale
  - Use information from **SOC estimator** to provide optimal setpoint for **hydraulic control**

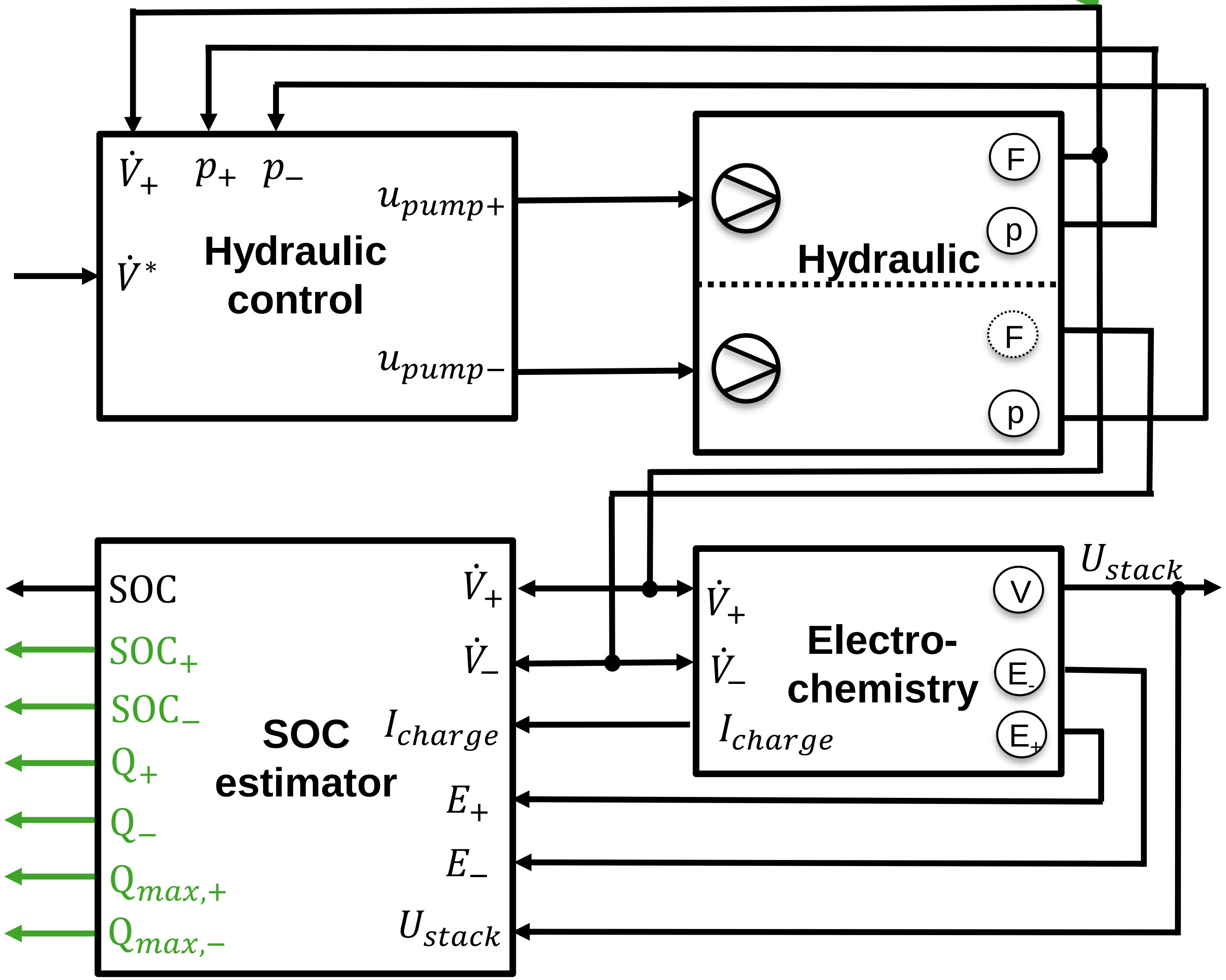

V. Observer design for nonlinear heat and mass transfer systems
presenter: Alexander Schaum

UNIVERSITY OF HOHENHEIM

Process Analytics

23rd Styrian Workshop on Automatic Control, 10.09.2024

OBSERVER DESIGN FOR NONLINEAR HEAT AND MASS TRANSFER SYSTEMS

Prof. Dr. Alexander Schaum,
Chair for Process Analytics, University of Hohenheim
Computational Science Hub (CSH)
alexander.schaum@uni-hohenheim.de

Motivation

$$\rho c_p(T)\frac{\partial T}{\partial t} - \mathrm{div}\,[\lambda(T)\mathrm{grad}\,T] - \phi = 0$$

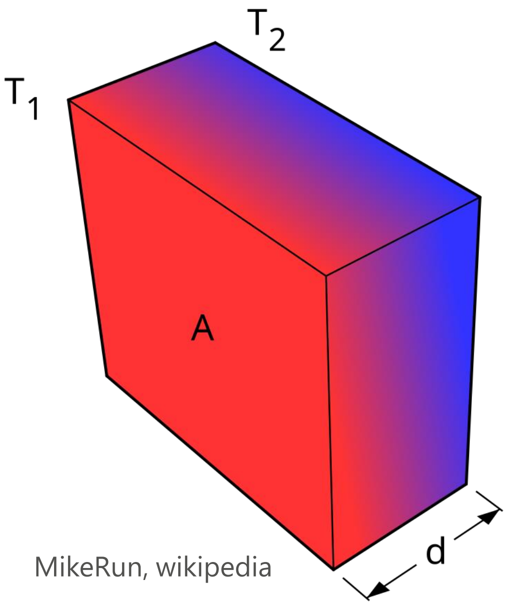

MikeRun, wikipedia

User Stahlkocher, wikipedia

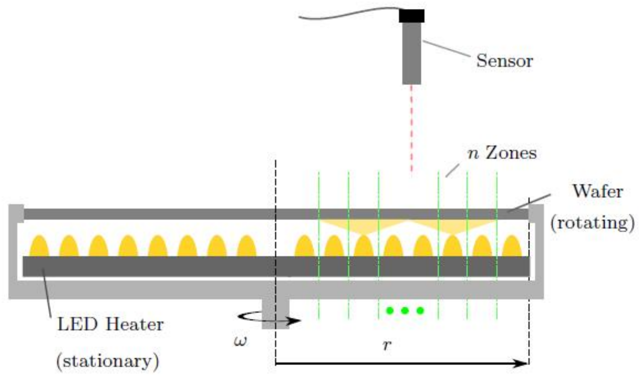

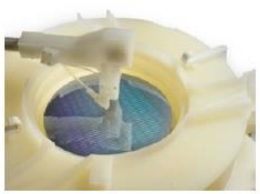

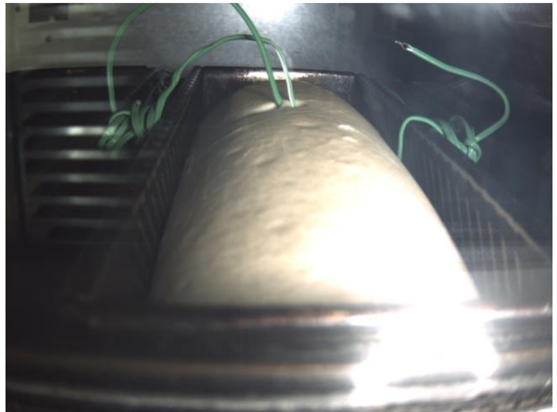

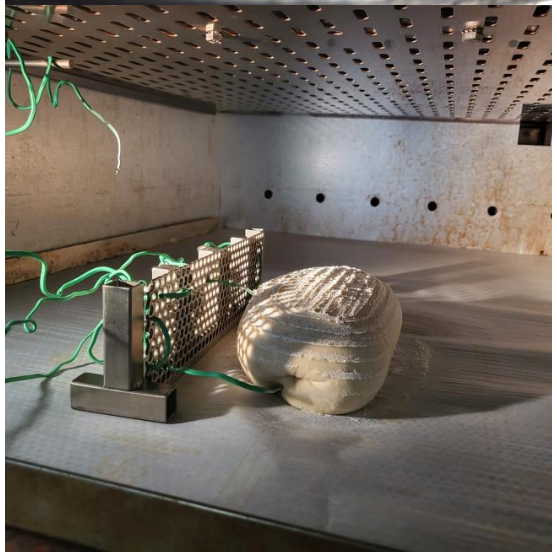

Process modeling

Mass and energy balances

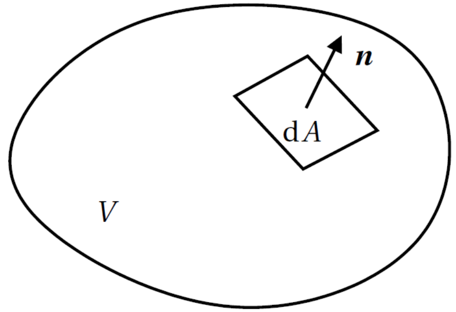

According to the first law of thermodynamics it holds that
$\mathrm{d}U = \mathrm{d}Q + \mathrm{d}W$ with $U = \int_V \rho\, u\, \mathrm{d}V$

Furthermore, it holds that $\mathrm{d}u = c_p(T)\mathrm{d}T$

In consequence one has that $\mathrm{d}U = \int_V \rho\, c_p(T)\mathrm{d}T\mathrm{d}V$
and thus

$$\frac{dU}{dt} = \int_V \rho\, c_p(T)\frac{\partial T}{\partial t}\mathrm{d}V$$

For $\mathrm{dQ} = \int_A dq\, n\, \mathrm{d}A$ and thus $\frac{dQ}{dt} = \int_A \dot{q}\, n\, \mathrm{d}A = \int_V \mathrm{div}\, \dot{q}\, \mathrm{d}V$

Finally, the dissipated power is given by $\frac{dW}{dt} = \int_V \phi\, \mathrm{dV}$,
leading to

$$\int_V \left\{\rho c_p(T)\frac{\partial T}{\partial t} - \mathrm{div}\, \dot{q} - \phi\right\} dV = 0$$

Fourier's law of heat flow states that
$\dot{q} = -\lambda(T)\ \mathrm{grad}\ T$

In summary, one obtains the heat equation

$$\rho c_p(T)\frac{\partial T}{\partial t} - \mathrm{div}\ [\lambda(T)\mathrm{grad}\ T] - \phi = 0$$

plus **boundary conditions**..

UNIVERSITY OF HOHENHEIM

Process modeling

Case example: heat conduction in a rod of radius *R:*

Balancing over cross sections yields

$$\bar{T}(z,t) = \int_0^R \int_0^{2\pi} T(z,r,\varphi)\mathrm{d}r\mathrm{d}\varphi$$

$$\begin{aligned}\rho c_p \frac{\partial \bar{T}}{\partial t} &= \int_0^R \int_0^{2\pi} \frac{\partial T}{\partial t}(z,r,\varphi)\mathrm{d}r\mathrm{d}\varphi \\ &= \frac{\partial}{\partial z}\left(\lambda \frac{\partial \bar{T}}{\partial z}\right) + \bar{\phi}(\bar{T})\end{aligned}$$

Including local control inputs with shape functions, e.g.

$$b_i = \begin{cases} \frac{1}{2\epsilon}, & z \in [\zeta - \epsilon, \zeta + \epsilon] \\ 0, & \text{else} \end{cases}$$

Adding suitable boundary conditions one obtains

$$\rho c_p \frac{\partial \bar{T}}{\partial t} = \frac{\partial}{\partial z}\left(\lambda \frac{\partial \bar{T}}{\partial z}\right) + \bar{\phi}(\bar{T}) + \sum_{i=1}^{p} b_i u_i$$

$$\lambda \frac{\partial \bar{T}}{\partial z}\bigg|_{z=0,1} = \alpha(\bar{T} - T_e)$$

and measurements

$$y_i(t) = \int_0^L c_i(z)\bar{T}(z,t), \quad i = 1,\ldots,m$$

Observer design

Classically, observer design is addressed using a **simulator-corrector structure**, following the **Luenberger observer** design

$$\rho c_p \frac{\partial \hat{\bar{T}}}{\partial t} = \frac{\partial}{\partial z}\left(\lambda \frac{\partial \hat{\bar{T}}}{\partial z}\right) + \bar{\phi}(\hat{\bar{T}}) + \sum_{i=1}^{p} b_i u_i - \sum_{j=1}^{m} l_j(\hat{\bar{T}}(\zeta_j, t) - y_j(t))$$

$$\lambda \frac{\partial \hat{\bar{T}}}{\partial z}\bigg|_{z=0,1} = \alpha(\hat{\bar{T}} - T_e) - \sum_{j=1}^{m} l_{b,j}(\hat{\bar{T}}(\zeta_j, t) - y_j(t))$$

The observer gains are designed using, e.g., backstepping [Smyshlyaev, Krstic, Deutscher, Gering, etc.], spectral decomposition [Curtain, Hagen, Dubljevic, Schaum], or other approaches.

Implementation then uses finite-dimensional approximation using numerical discretization schemes (e.g., finite differences). This approach is called ***late lumping***.

Observer design

Alternatively, so-called **early lumping** is possible, where first the PDE model is approximated in finite dimensions leading to

$$\dot{\boldsymbol{x}} = A_d \boldsymbol{x} + B_d \boldsymbol{u} + \boldsymbol{\phi}_d(\boldsymbol{x})$$
$$\boldsymbol{y} = C\boldsymbol{x}$$

followed by finite-dimensional observer or (extended) Kalman Filter design.

$$\dot{\hat{\boldsymbol{x}}} = A_d \hat{\boldsymbol{x}} + B_d \boldsymbol{u} + \boldsymbol{\phi}_d(\hat{\boldsymbol{x}}) - L(\hat{\boldsymbol{x}}, \boldsymbol{y}, \boldsymbol{u}) \left(C\hat{\boldsymbol{x}} - \boldsymbol{y}\right)$$

Potential **drawbacks** in this approach are

- **loss of information** in the design step due to lumping
- uncertainty regarding **convergence (stability)** with the PDE model
- potentially **high dimensional** lumped system

Pointwise injection observer design

The main idea

Use pointwise measurements as local drivers for the observer by directly imposing the measured value at the measurement location.

Observer

$$\rho c_p \frac{\partial \hat{\bar{T}}}{\partial t} = \frac{\partial}{\partial z}\left(\lambda \frac{\partial \hat{\bar{T}}}{\partial z}\right) + \bar{\phi}(\hat{\bar{T}}) + \sum_{i=1}^{p} b_i u_i$$

$$\lambda \frac{\partial \hat{\bar{T}}}{\partial z}\Big|_{z=0,1} = \alpha(\hat{\bar{T}} - T_e)$$

$$\hat{\bar{T}}(\zeta_i, t) = y_i(t)$$

Observation error dynamics

$$\rho c_p \frac{\partial \tilde{T}}{\partial t} = \frac{\partial}{\partial z}\left(\lambda \frac{\partial \tilde{T}}{\partial z}\right) + \tilde{\phi}(\tilde{T}; T)$$

$$\lambda \frac{\partial \tilde{T}}{\partial z}\Big|_{z=0,1} = \alpha \tilde{T}$$

$$\tilde{\phi}(\tilde{T}; T) := \bar{\phi}(\bar{T} + \tilde{T}) - \bar{\phi}(\bar{T})$$

$$\tilde{T}(\zeta_i, t) = 0$$

Pointwise injection observer design

The main idea

Use pointwise measurements as local drivers for the observer by directly imposing the measured value at the measurement location.

Observation error dynamics

$$\rho c_p \frac{\partial \tilde{T}}{\partial t} = \frac{\partial}{\partial z}\left(\lambda \frac{\partial \tilde{T}}{\partial z}\right) + \tilde{\phi}(\tilde{T}; T)$$

$$\lambda \frac{\partial \tilde{T}}{\partial z}\bigg|_{z=0,1} = \alpha \tilde{T}$$

$$\tilde{\phi}(\tilde{T}; T) := \bar{\phi}(\bar{T} + \tilde{T}) - \bar{\phi}(\bar{T})$$

$$\tilde{T}(\zeta_i, t) = 0$$

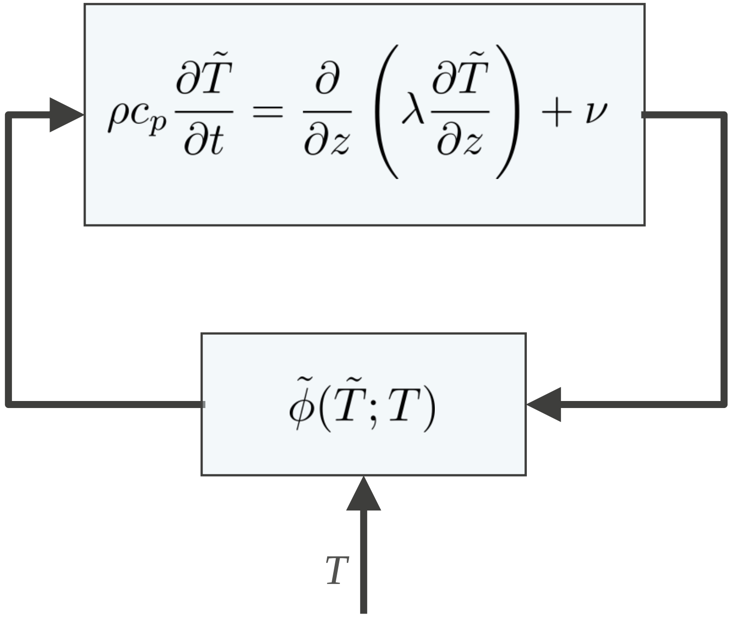

Pointwise injection observer design

By construction the domain is splitted into two parts, so that

$$\tilde{T}(z,t) = \begin{cases} \tilde{T}_1(z,t), & z \in [0,\zeta) \\ 0, & z = \zeta \\ \tilde{T}_2(z,t), & z \in (\zeta, L] \end{cases}$$

where each of the dynamic components satisfies

$$\frac{\partial \tilde{T}_i}{\partial t} = A_i \tilde{T}_i + \tilde{\phi}(\tilde{T}_i)$$

with approciately defined operators A_i, which are assumed to generate C_0- semigroups of contractions S_i with growth bounds $\omega_i < 0$ so that

$$\|S_i(t)\| \leq e^{\omega_i t}$$

It follows that

$$\tilde{T}_i(t) = S_i(t)\tilde{T}_i(0) + \int_0^t S_i(t-\tau)\tilde{\phi}(\tilde{T}_i(\tau); T(\tau))\mathrm{d}\tau$$

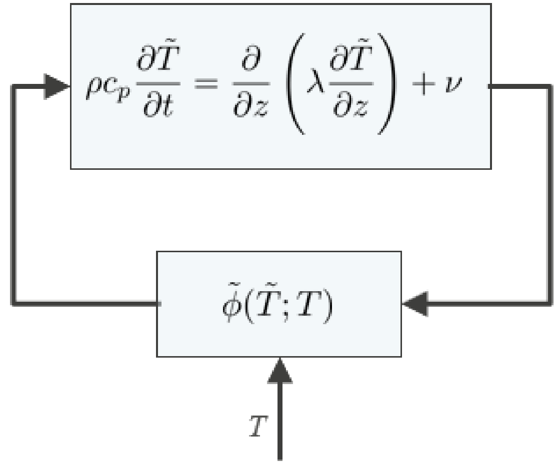

UNIVERSITY OF HOHENHEIM

Pointwise injection observer design

Process Analytics

In consequence it holds that

$$
\begin{aligned}
\|\tilde{T}_i(t)\| &= \left\| S_i(t) \left(\tilde{T}_i(0) + \int_0^t S_i(-\tau)\tilde{\phi}(\tilde{T}_i(\tau); T(\tau))\mathrm{d}\tau \right) \right\| \\
&\leq \|S_i(t)\| \left\| \tilde{T}_i(0) + \int_0^t S_i(-\tau)\tilde{\phi}(\tilde{T}_i(\tau); T(\tau))\mathrm{d}\tau \right\| \\
&\leq e^{\omega_i t} \left(\|\tilde{T}_i(0)\| + \int_0^t e^{-\omega_i \tau} \| \tilde{\phi}(\tilde{T}_i(\tau); T(\tau))\| \mathrm{d}\tau \right)
\end{aligned}
$$

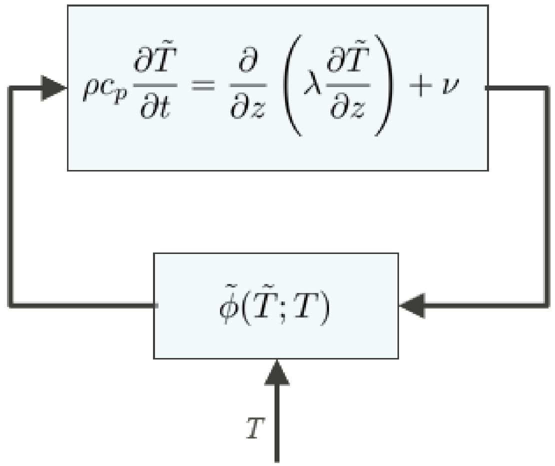

Assuming that $\tilde{\phi}$ is Lipschitz continuous uniformly in T with Lipschitz constant $L_{\tilde{\phi}}$, i.e.,

$$
\|\tilde{\phi}(\tilde{T}_i(t); T(t))\| \leq L_{\tilde{\phi}} \|\tilde{T}_i(t)\|, \quad \forall \quad t \geq 0, T
$$

it follows that

$$
\|\tilde{T}_i(t)\| \leq \underbrace{e^{\omega_i t} \left(\|\tilde{T}_i(0)\| + \int_0^t e^{-\omega_i \tau} \; L_{\tilde{\phi}} \|\tilde{T}_i(\tau)\| \mathrm{d}\tau \right)}_{=:\eta_i(t)}
$$

UNIVERSITY OF HOHENHEIM

Pointwise injection observer design

Process Analytics

For η_i in turn it follows that

$$\dot{\eta}_i = \omega_i \eta_i + e^{\omega_i t} e^{-\omega_i t} L_{\tilde{\phi}} \|\tilde{T}_i\| \leq (\omega_i + L_{\tilde{\phi}})\eta_i$$

From Gronwalls lemma one concludes that for $\omega_i < -L_{\tilde{\phi}}$ one has that in turn it follows that $\eta_i \to 0$ and by definition it thus holds that $0 \leq \|\tilde{T}_i(t)\| \leq \eta_i(t) \to 0$.

The growth bound ω_i in turn depends on the sensor location. Thus, the observer design consists in adequately determining the sensor location ζ so that the above condition holds true.

In case that $L_{\tilde{\phi}}$ is too large, additional sensors can be included to reduce the associated ω_i.

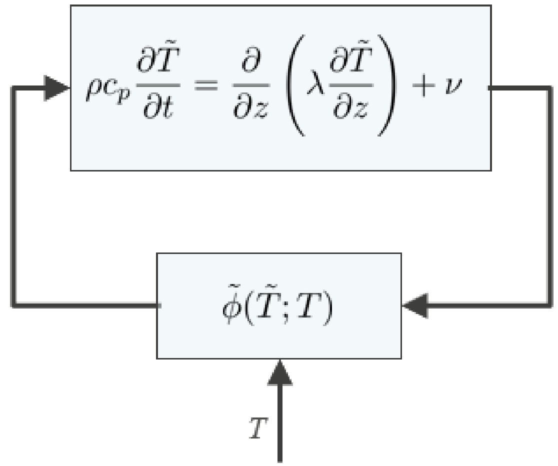

Pointwise injection observer design

Example: Unstable heat equatoin [2015]

$$\frac{\partial \tilde{T}}{\partial t} = \frac{\partial^2 T}{\partial z^2} + kT$$

$$T(0,t) = T(1,t) = 0$$

with $\pi < k < 4\pi^2$. Sensor location at $\zeta = 0.5 \quad (L = 1)$

Without measurement injection

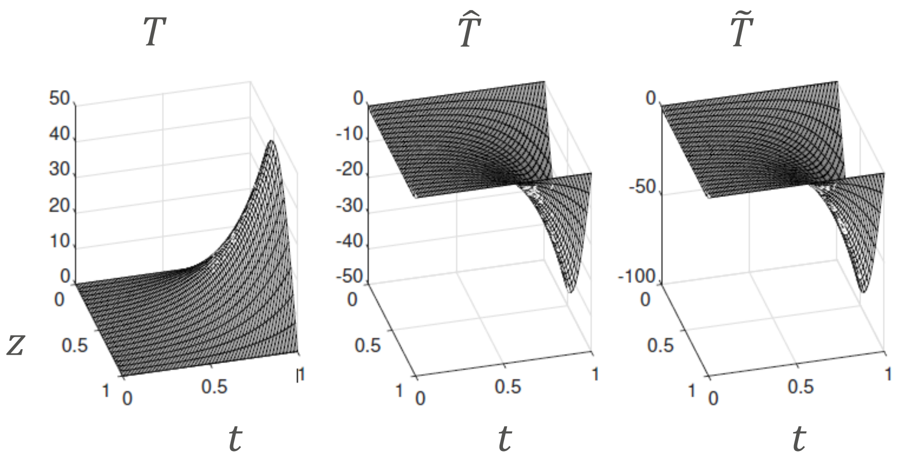

With pointwise measurement injection

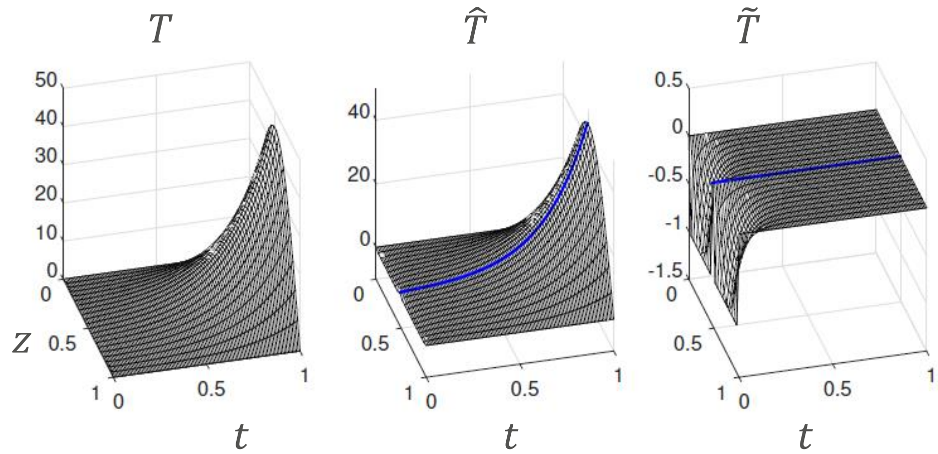

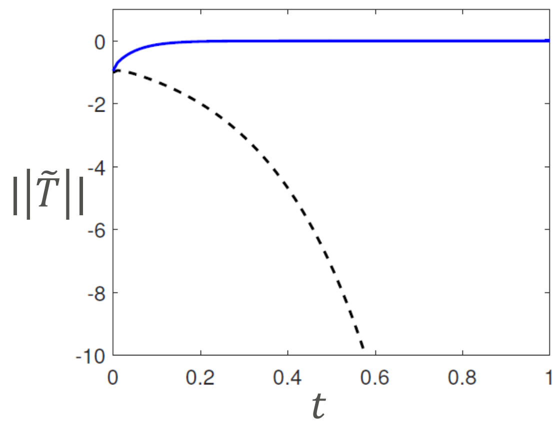

UNIVERSITY OF HOHENHEIM

Pointwise injection observer design

Example: Multistable diffusion-convection-reaction system [2015]

$$\partial_t x(z,t) = \partial_z^2 x(z,t) - \gamma \partial_z x(z,t) - \alpha x(z,t)(1 - x^2(z,t))$$
$$\partial_z x(0,t) = \gamma x(0,t), \quad \partial_z x(1,t) = 0$$
$$x(z,0) = x_0(z), \quad y(t) = x(\zeta, t).$$

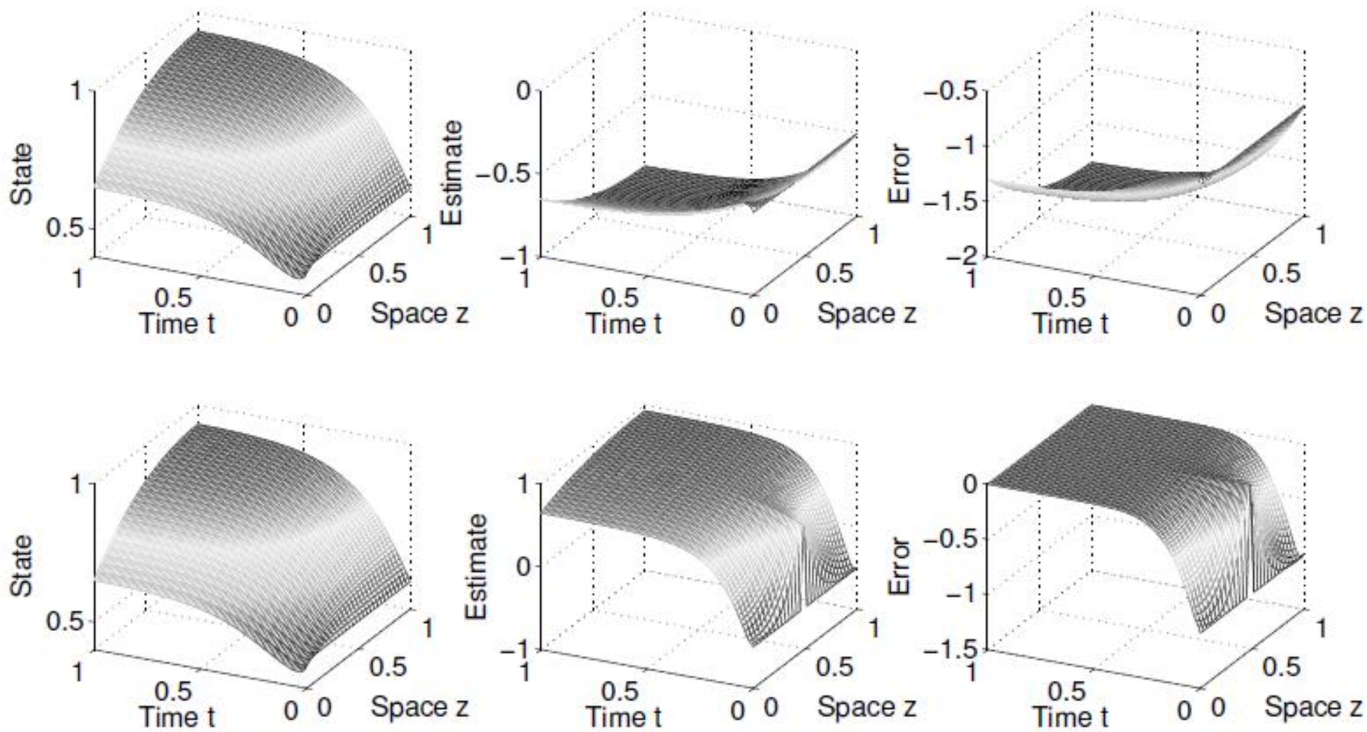

Without measurement injection

With pointwise measurement injection

Transport reaction systems

Adding the mass component

Case study: Tubular reactor models [2016, 2017]

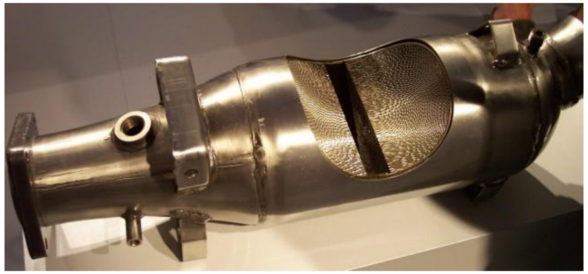

$$\rho V c_p \frac{\partial T}{\partial t} = \frac{\partial}{\partial x}\left(\lambda \frac{\partial T}{\partial x}\right) - v\frac{\partial T}{\partial x} + \eta(u - T) + \delta r(c)e^{-\gamma/T}$$

$$\frac{\partial c}{\partial t} = \frac{\partial}{\partial x}\left(D \frac{\partial c}{\partial x}\right) - v\frac{\partial c}{\partial x} - r(c)e^{-\gamma/T}$$

$$y_i(t) = T(\zeta_i, t)$$

With sensor located before the before the temperature hot spot (ca. 0.3) exponential convergence can be established.

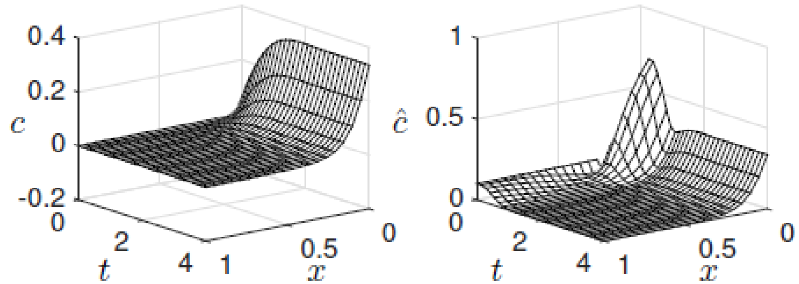

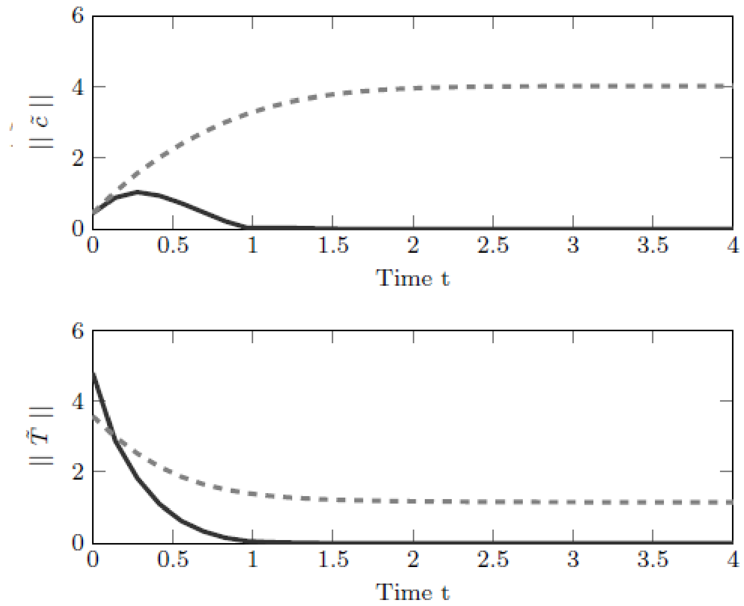

Transport reaction systems

Adding the mass component

Case study: Tubular reactor models [2016, 2017]

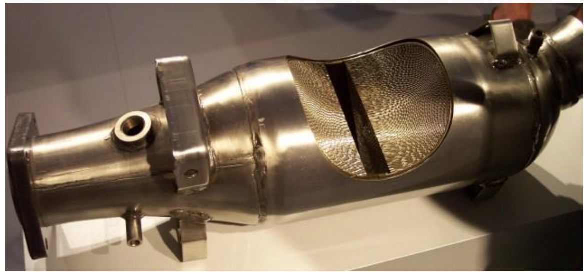

$$\rho V c_p \frac{\partial T}{\partial t} = \frac{\partial}{\partial x}\left(\lambda \frac{\partial T}{\partial x}\right) - v\frac{\partial T}{\partial x} + \eta(u - T) + \delta r(c) e^{-\gamma/T}$$

$$\frac{\partial c}{\partial t} = \frac{\partial}{\partial x}\left(D \frac{\partial c}{\partial x}\right) - v\frac{\partial c}{\partial x} - r(c) e^{-\gamma/T}$$

$$y_i(t) = T(\zeta_i, t)$$

For the case of boundary perturbations, if an additional sensor is put at the corresponding boundary, a perfect cancelation is ensured (*unknown input observer* [Schaum 2018]).

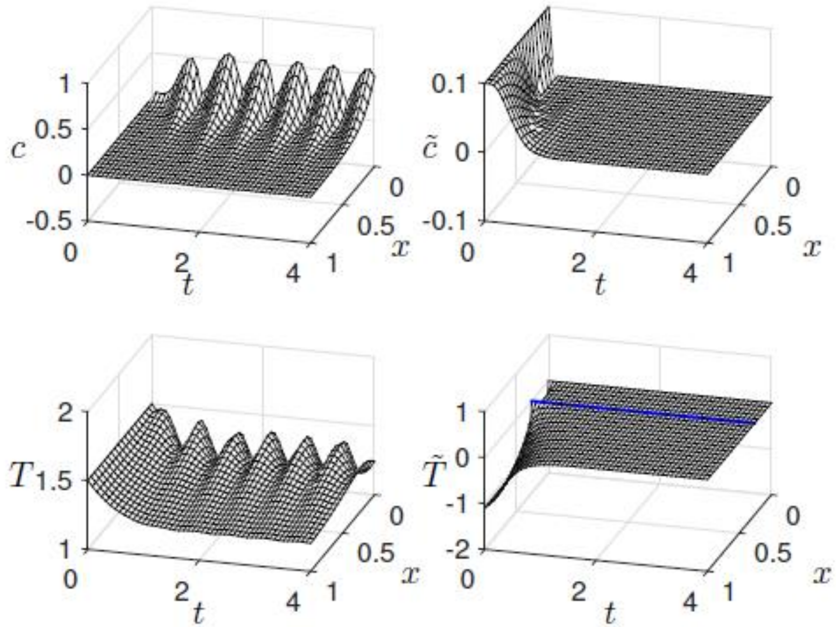

Pointwise injection observer design

Comparison with early-lumping EKF and one single sensor:

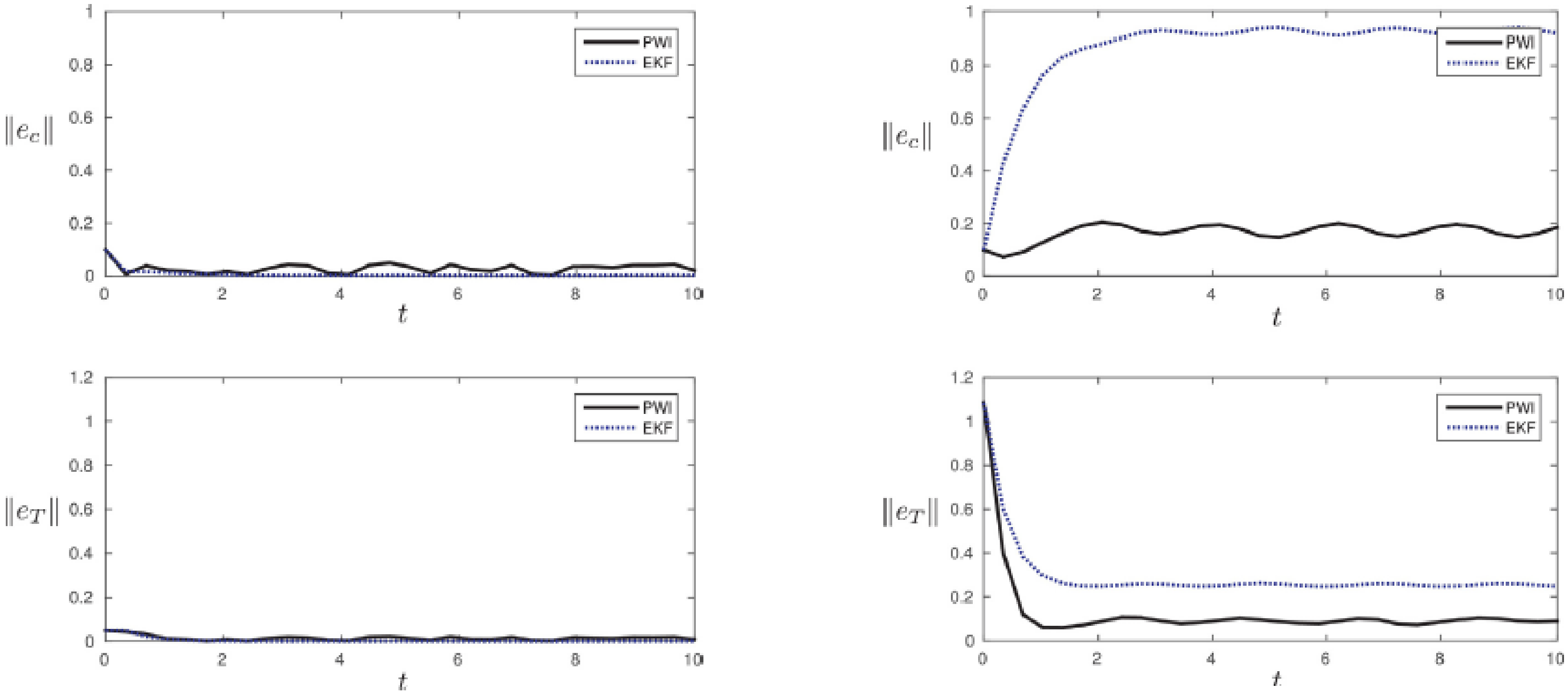

Lack of convergence in some scenarios due to multi-stability of tubular reactor model

Rapid thermal processing of silicon wafers

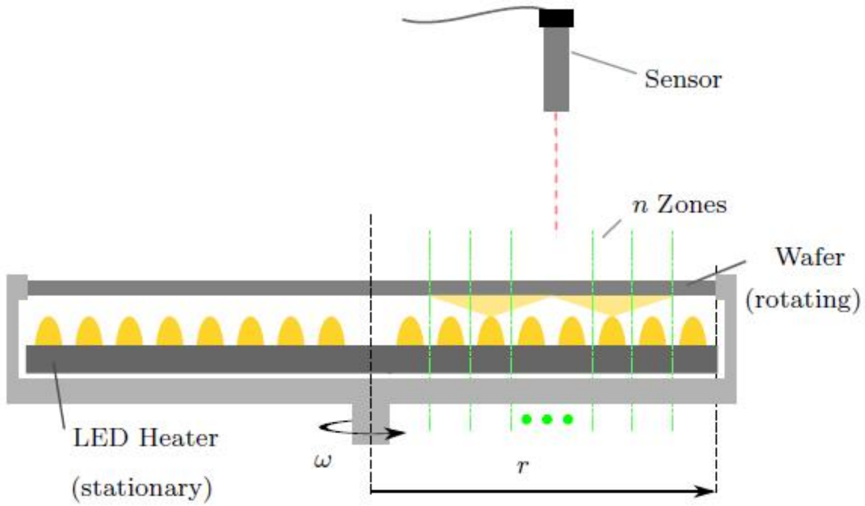

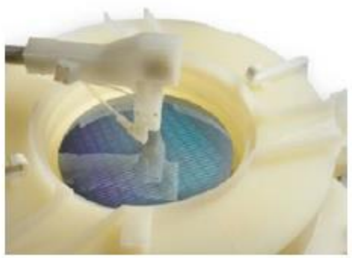

Heat equation in polar coordinates (assuming angular homogeneity) [2021, 2022]:

$$\rho c_p(T)\frac{\partial T}{\partial t} = \frac{1}{r}\frac{\partial}{\partial r}\left(r\,k(T)\frac{\partial T}{\partial r}\right) + \phi(\mathrm{T}) + \sum_{j=1}^{p} b_j u_j$$

$$\frac{\partial T}{\partial r}(0,t) = 0,\ \frac{\partial T}{\partial r}(R,t) = 0, T(r,0) = T_0(r)$$

$$y_i(t) = T(\rho_i,t), \rho_i \in (0,R), i = 1,\dots,m$$

UNIVERSITY OF HOHENHEIM

Rapid thermal processing of silicon wafers

Process Analytics

TU Graz

Kirchhoff transformation: $$k(T)\frac{\partial T}{\partial r} = \frac{\partial \theta}{\partial r} \quad \Leftrightarrow \quad \theta = \int_{T_r}^{T} k(\tau)\mathrm{d}\tau$$

This leads to the simplified model

$$\frac{\partial \theta}{\partial t} = \alpha \frac{1}{r}\frac{\partial}{\partial r}\left(r\frac{\partial \theta}{\partial r}\right) + \psi(\theta), \quad \alpha = \frac{k}{\rho c_p}$$

with the associated transformed measurement

$$y_\theta(t) = \int_{T_r}^{y(t)} k(\tau)\mathrm{d}\tau$$

For θ a pointwise measurement injection observer is designed. Under the assumption that α is constant exponential convergence can be established [Schaum et al 2021].

If α is not constant this assumption leads to a distributed disturbance…

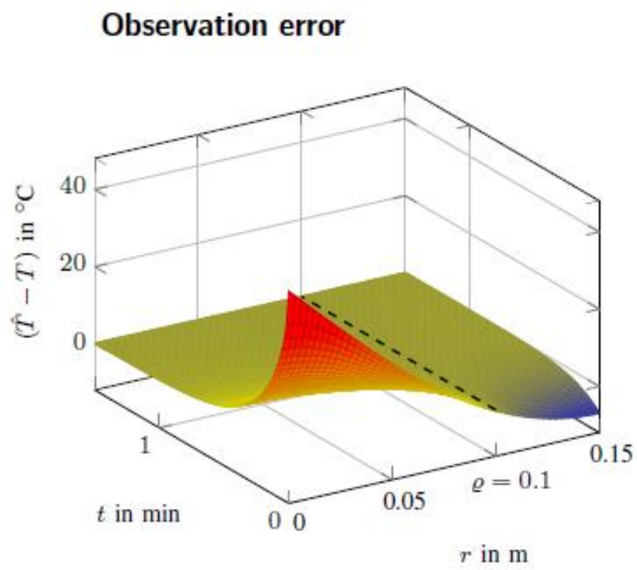

UNIVERSITY OF HOHENHEIM

Rapid thermal processing of silicon wafers

Process Analytics

TU Graz

Based on the previous result, for the case of a distributed disturbance *w*

$$\rho c_p \frac{\partial T}{\partial t} = \frac{\partial}{\partial x}\left(k(T)\frac{\partial T}{\partial x}\right) + \varphi(T) + w$$

using the Lyapunov functional

$$V(\tilde{T}) = \int_0^R r\left(\int_T^{T+\tilde{T}} k(\tau)\mathrm{d}\tau\right)^2 \mathrm{d}r$$

it can be established that, if the sensor locations are appropriately chosen, the observation error dynamics is input-to-state stable (ISS) w.r.t. the disturbance *w*

$$\frac{\mathrm{d}V}{\mathrm{d}t} \leq -(\kappa - \bar{L})\|\tilde{T}\| + \beta(w^+)^2$$

implying robust observer convergence [2022].

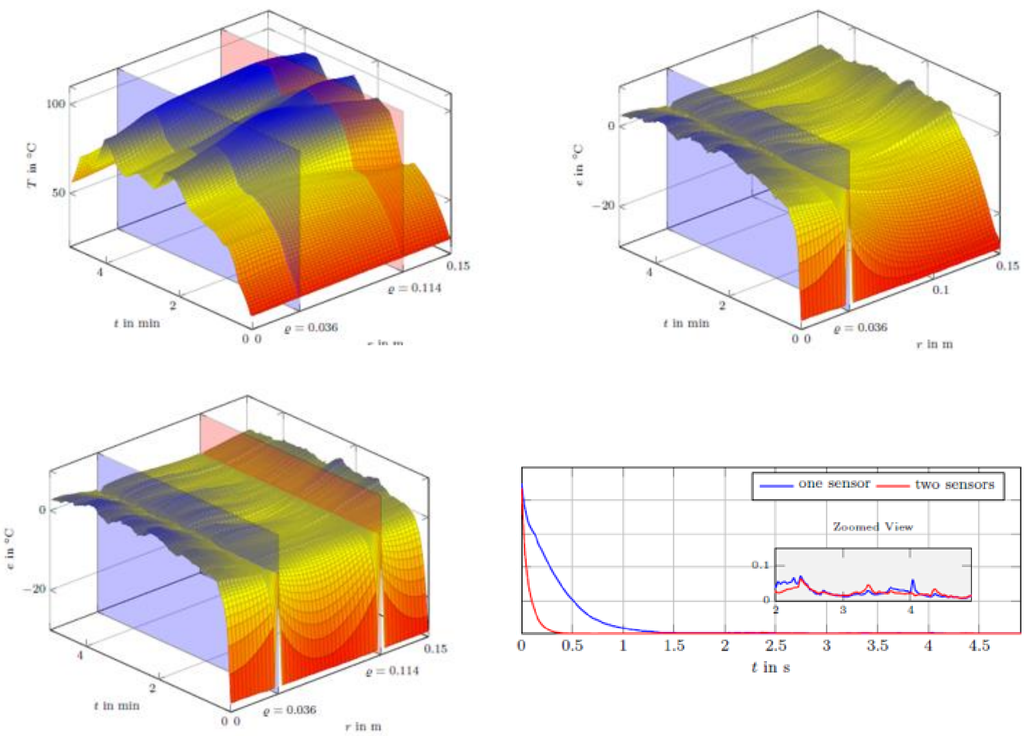

Baking proceses

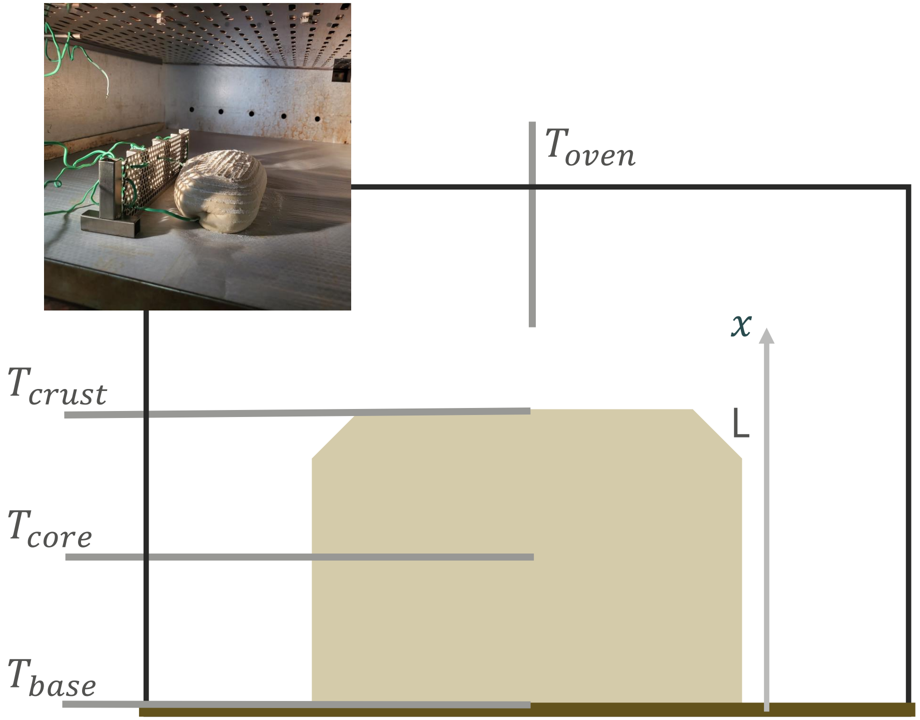

Stefan problem

Under the assumption that parameters only vary on time (only approximately true…) it holds that

$$\frac{\partial T}{\partial t} = \frac{\lambda}{\rho c_p}\frac{\partial}{\partial x}\left(\frac{\partial T}{\partial x}\right), \quad x \in (0, L(t))$$

$$\frac{\lambda}{\rho c_p}\frac{\partial T}{\partial x}(L(t), t) = \alpha L\left(T_{oven}(t) - T(L(t), t)\right)$$

$$T(0, t) = T_{base}(t)$$

Measurement: $y(t) = T(\zeta, t)$
with ζ either fixed or time-varying…

Baking proceses

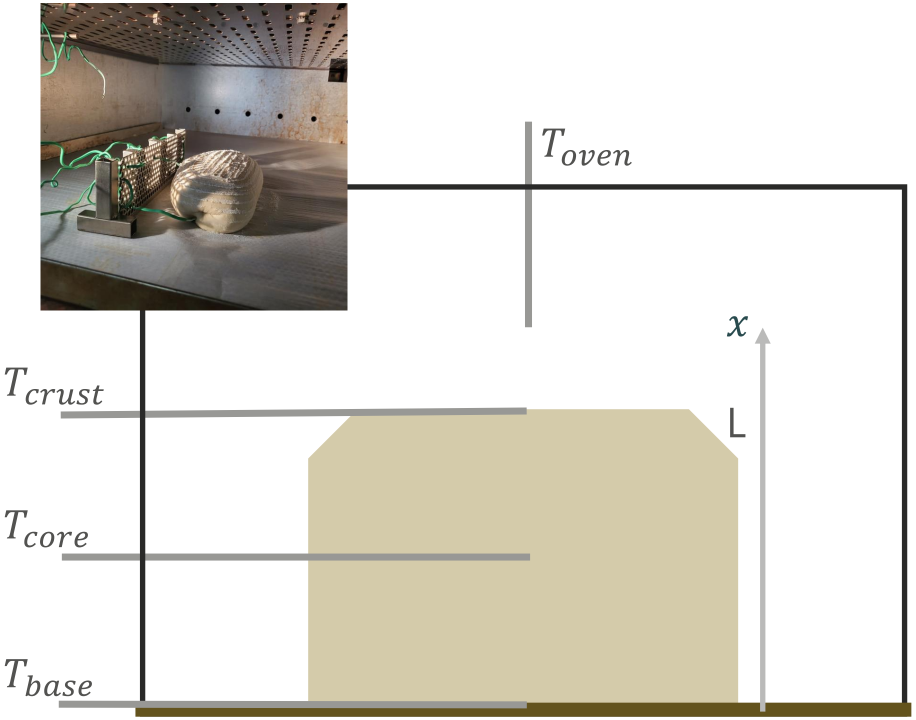

Stefan problem

Normalization of spatial coordinate: $s = \dfrac{x}{L}$

$$
\begin{aligned}
\frac{\partial T}{\partial t} &= \frac{\lambda}{\rho c_p L^2} \frac{\partial^2 T}{\partial s^2} - s \frac{\dot{L}}{L} \frac{\partial T}{\partial s}, \quad s \in (0,1) \\
\frac{\partial T}{\partial s}(1,t) &= \frac{\alpha \rho c_p L}{\lambda} L \left(T_{oven}(t) - T(1,t) \right) \\
T(0,t) &= T_{base}(t)
\end{aligned}
$$

Measurement: $y(t) = T(\sigma, t)$
with σ either fixed or time-varying…

Baking proceses

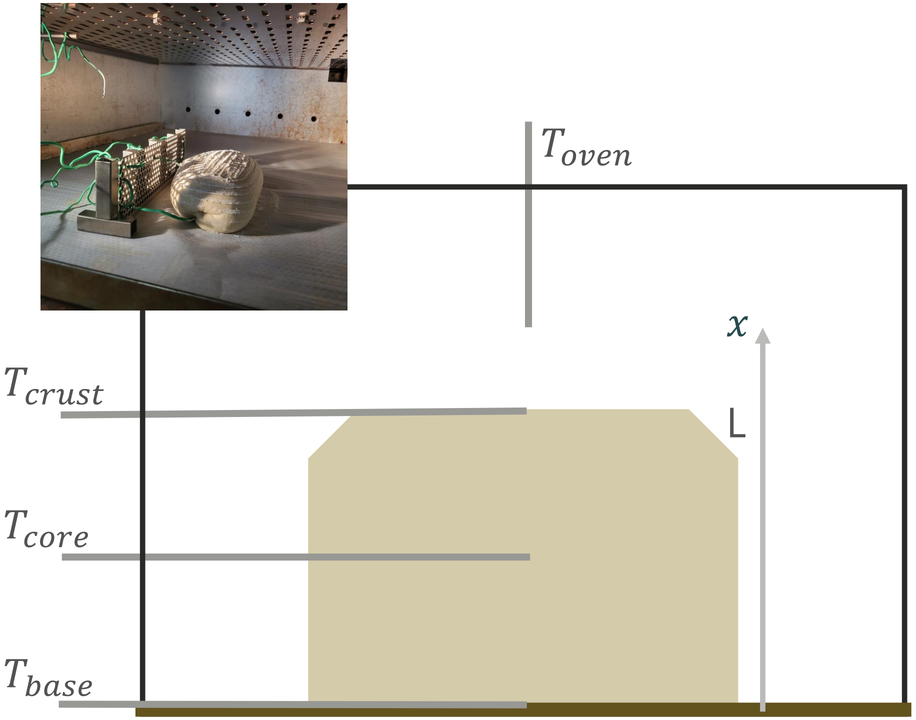

Stefan problem

Assumption: $L, \dot{L}$ are known

$$\frac{\partial T}{\partial t} = \bar{\lambda} \frac{\partial^2 T}{\partial s^2} - s \frac{\dot{L}}{L} \frac{\partial T}{\partial s}$$
$$\frac{\partial T}{\partial s}(1,t) = \bar{\alpha}\,(T_{oven}(t) - T(1,t))$$
$$T(0,t) = T_{base}(t)$$

heat equation with the two unknown time-varying parameters: $\bar{\lambda}, \bar{\alpha}$.

Problem of joint state and parameter estimation for a time-varying PDE system

Baking proceses

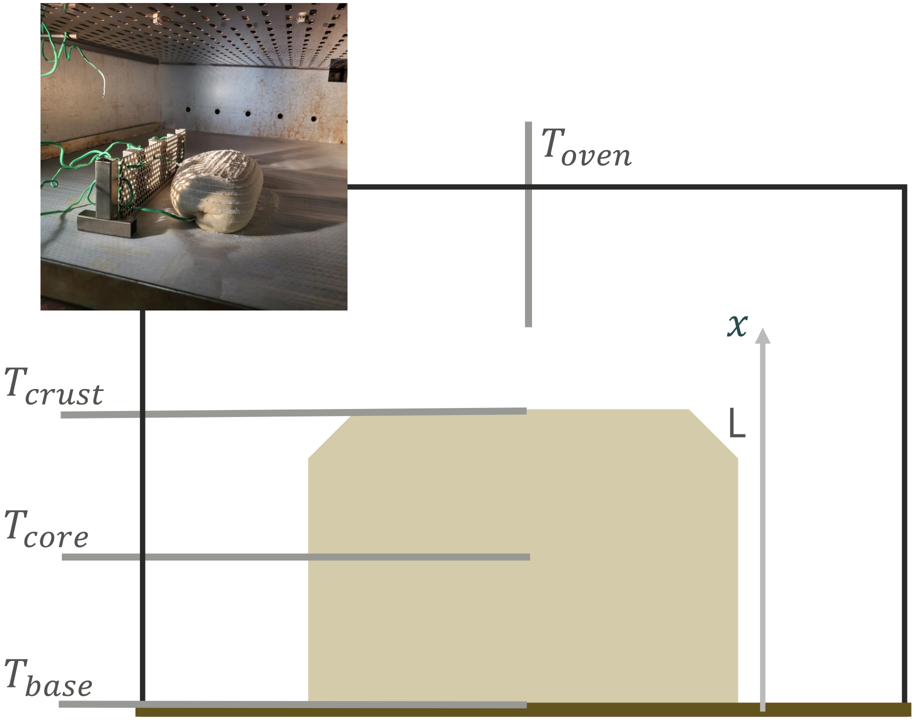

$$\frac{\partial T}{\partial t} = \bar{\lambda}\frac{\partial^2 T}{\partial s^2} - s\frac{\dot{L}}{L}\frac{\partial T}{\partial s}$$

$$\frac{\partial T}{\partial s}(1,t) = \bar{\alpha}\left(T_{oven}(t) - T(1,t)\right)$$

$$T(0,t) = T_{base}(t)$$

Model approximation through finite differences and combination with **extended Kalman Filter for joint state and parameter estimation,** ignoring changes in the size implying a **distributed disturbance**...

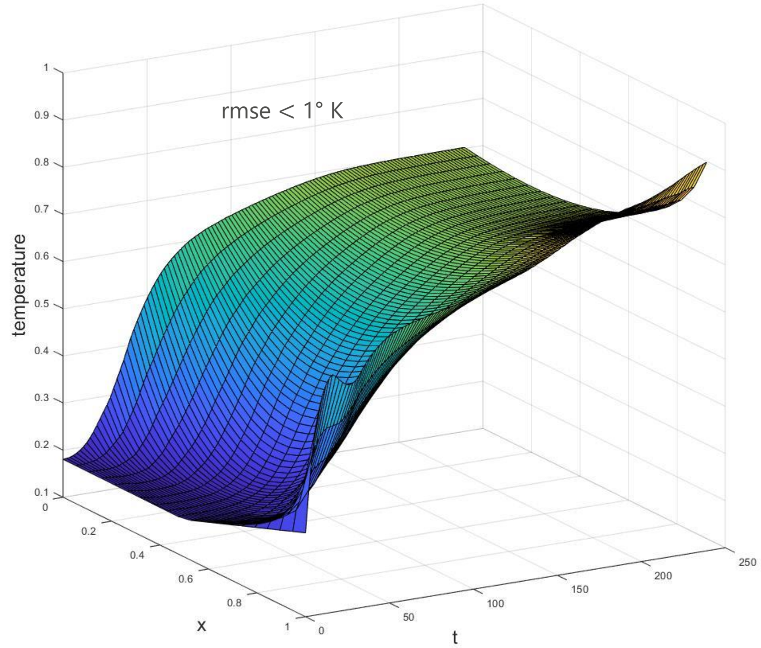

UNIVERSITY OF HOHENHEIM

Baking proceses

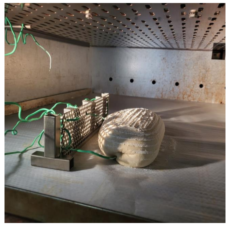

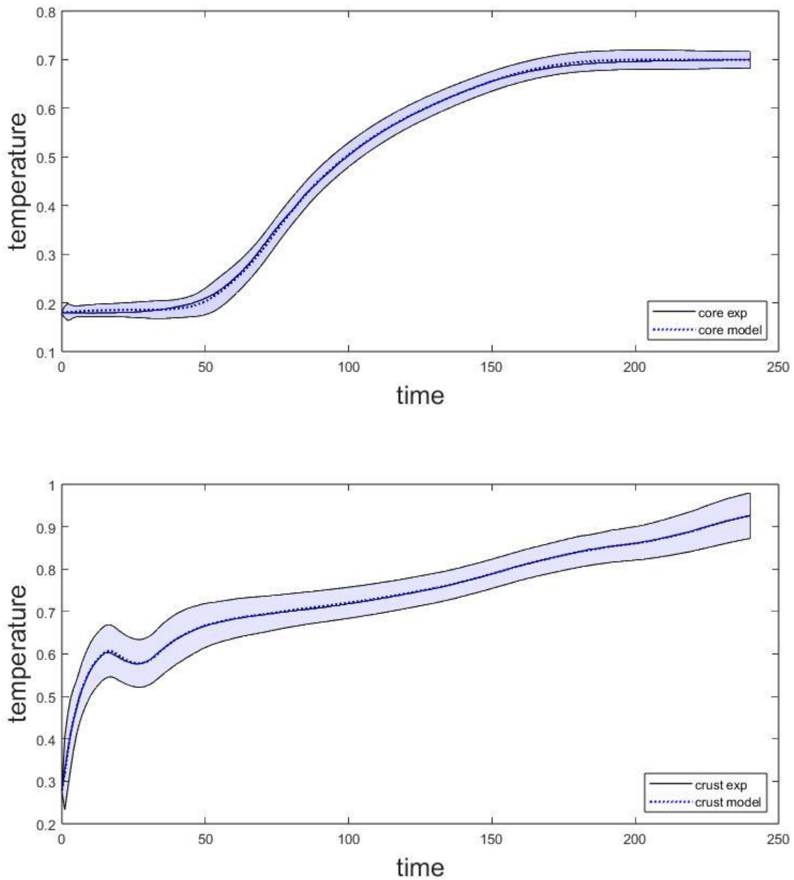

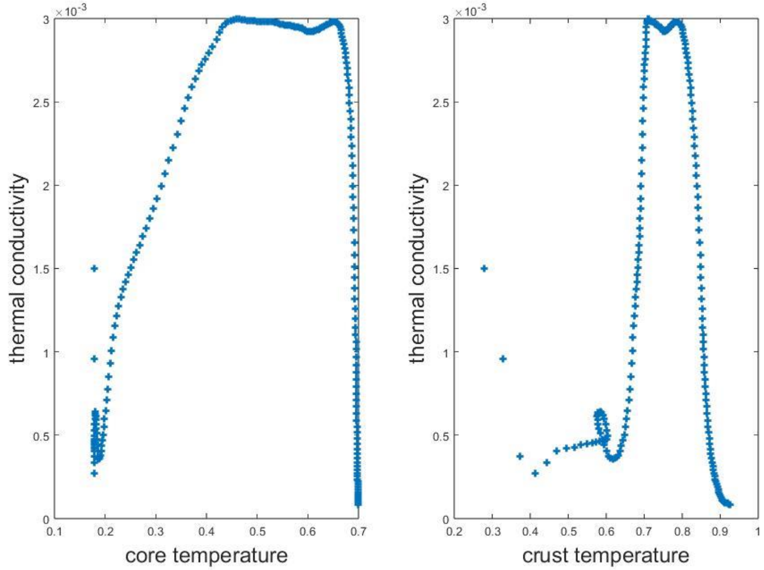

Next steps:

- inclusion of volumetric changes, ISS analysis regarding distributed disturbances,
- different sensor localizations (constant versus time-varying, known versus unknown…)

Conclusions & outlook

Conclusions

- Nonlinear heat and mass transfer models (with time-varying domains) are frequently found in different areas of application
- Different solution strategies can be employed to address such problems, including early and late lumping strategies
- Crucial design degrees of freedom include the sensor location and choice of observer gain
- Pointwise measurement injection observer design provides a direct means for sensor location without the need to design an observer gain, and has been successfully employed for different applications so far.

Outlook

- Extend previous results to include time-varying domains (Stefan problems), spatially varying parameters, explicit ISS criteria
- Further experimental validations for different applications

VI. Observability and High Gain Observer Design for Polynomial Systems

presenter: Klaus Röbenack

Klaus Röbenack and Daniel Gerbet

Istitute of Control Theory, TUD Dresden University of Technology, 01062 Dresden

Observability and High Gain Observer Design for Polynomial Systems

23rd Styrian Workshop on Automatic Control, September 9 –11, 2024,
Schloss Retzhof, Austria

Structure of the Talk

Nonlinear Observability

Nonlinear Observability

Nonlinear state space system

$$\begin{aligned} \dot{x} &= f(x) \quad \text{(system dynamics)} \\ y &= h(x) \quad \text{(measured output)} \end{aligned} \tag{1}$$

defined on $\mathcal{M} \subseteq \mathbb{R}^n$

Usually, the full state x is not measured ($\dim(x) > \dim(y)$), e.g.

- Encoder: measures the angle, but not the angular velocity
- Tachometer: measures the angular velocity, but not the angle

State Observation Problem

Rekonstruct the state x from the measured output y.

Is this possible at all? $\Longrightarrow$ observability

How to do that? $\Longrightarrow$ observer design

Nonlinear Observability

Definition (Indistinguishably)

Two states $x(0), \bar{x}(0) \in \mathcal{M}$ are called indistinguishable on an interval $[0,T]$ with $T > 0$ if

$$\forall t \in [0,T] : \quad h(x(t)) = h(\bar{x}(t)).$$

Otherwise, the states are called distinguishable.

Distinguishable states:

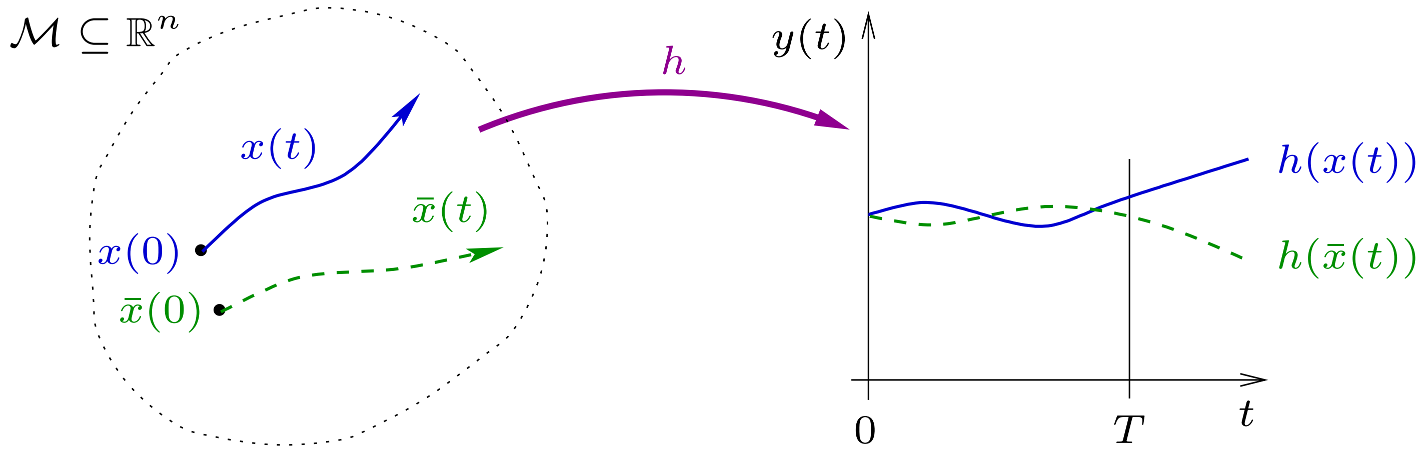

R. Hermann and A. J. Krener. “Nonlinear Controllability and Observability”. In: IEEE Trans. on Automatic Control 22.5 (1977), pp. 728–740. DOI: `10.1109/TAC.1977.1101601`.

Nonlinear Observability
Lie Derivative and Lie Series

- Lie derivative of a function h along the vector field f

$$L_f h(x) = \frac{\partial h}{\partial x}(x) f(x)$$

- Higher order Lie derivatives

$$L_f^{k+1} h(x) = L_f L_f^k h(x)\,, \quad L_f^0 h(x) = h(x)$$

- Series expansion of $y(t) = h(x(t))$ with $\dot{x} = f(x)$ yields Lie series

$$y(t) = h(x(t)) = \sum_{k=0}^{\infty} \frac{t^k}{k!} L_f^k h(x(0))$$

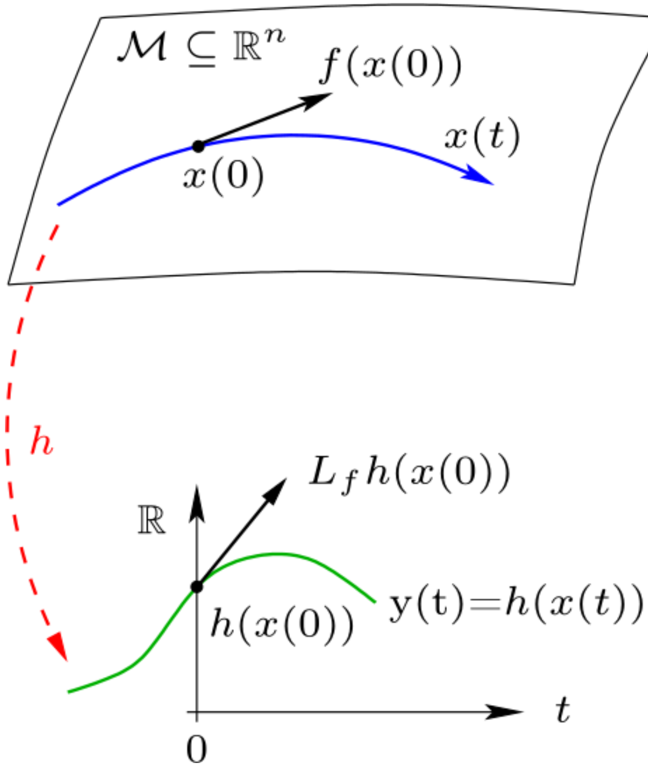

Nonlinear Observability

- Observability map: Taylor coefficients of the output trajectory

$$q_k(x) = \Big(h(x),\ L_f h(x),\ L_f^2 h(x),\ \ldots\ , L_f^{k-1} h(x)\Big)^{\mathrm{T}}$$

- Two states $x, \bar{x} \in \mathcal{M}$ are indistinguishable if the output trajectories are identical

$$q(x) = q(\bar{x})$$

- Set of indistinguishable pairs of states

$$\mathcal{I} = \big\{(x, \bar{x}) \in \mathcal{M}^2 \,|\, q(x) = q(\bar{x})\big\}$$

- Set of identical pairs of states

$$\mathcal{E} = \big\{(x, \bar{x}) \in \mathcal{M}^2 \,|\, x = \bar{x}\big\} \subseteq \mathcal{I}$$

Nonlinear Observability

Definition (Local observability at a point $x_0 \in \mathcal{M}$)

System (1) is called locally observable at a point $x_0 \in \mathcal{M}$, if the observability map is injective in a neighborhood $U_{x_0} \subset \mathcal{M}$ of x_0, i. e.,

$$\forall x, \bar{x} \in U_{x_0} : q(x) = q(\bar{x}) \implies x = \bar{x}$$

or equivalently $\mathcal{I} \cap U_{x_0}^2 = \mathcal{E} \cap U_{x_0}^2$.

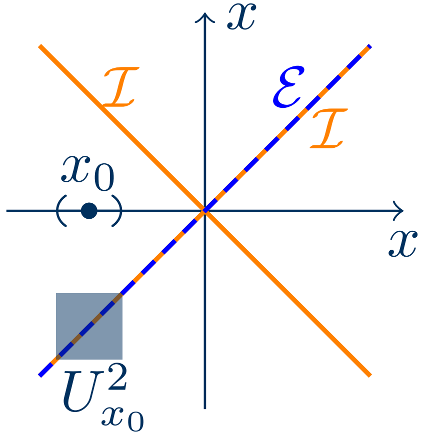

Definition (Local observability)

System (1) is called locally observable if it is locally observable at all $x_0 \in \mathcal{M}$.

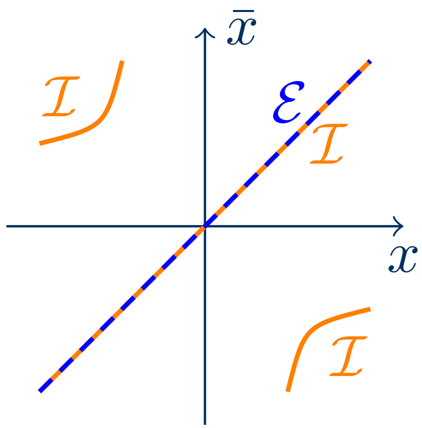

E. D. Sontag. “A concept of local observability”. In: Systems & Control Letters 5 (1984), pp. 41–47.

Nonlinear Observability

Definition (Global observability)

System (1) is called globally observable if

$$\forall x, \bar{x} \in \mathcal{M} : q(x) = q(\bar{x}) \implies x = \bar{x}$$

or equivalently $\mathcal{I} = \mathcal{E}$.

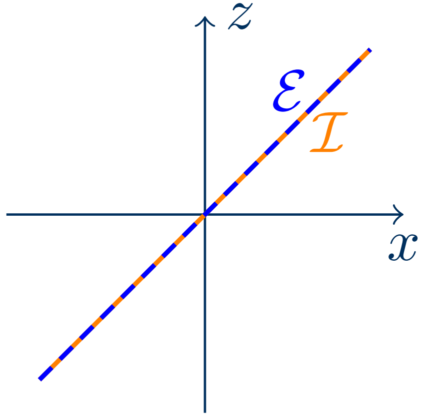

Problem / Question

How many Lie derivatives are needed?

B. Tibken. “Observability of nonlinear systems — an algebraic approach”. In: Proc. IEEE Conf. on Decision and Control (CDC). vol. 5. Nassau, Bahamas, Dec. 2004, pp. 4824–4825. DOI: `10.1109/CDC.2004.1429553`.

Z. Bartosiewicz. “Algebraic criteria of global observability of polynomial systems”. In: Automatica 69 (2016), pp. 210–213.

Polynomials and Varieties

Polynomials and Varieties

Definition (Ideals)

A (polynomial) ideal $I \subseteq \mathbb{R}[x]$, $x = (x_1, \ldots, x_n)$ is a set with

1. $0 \in I$,
2. $a, b \in I \implies a + b \in I$.
3. $a \in I, c \in \mathbb{R}[x] \implies ac \in I$.

Definition (Real varieties)

A real variety $\mathbf{V}(I) \subseteq \mathbb{R}^n$ is the common real zero set of all polynomials in $I \subseteq \mathbb{R}[x]$:

$$\mathbf{V}(I) = \{x \in \mathbb{R}^n \,|\, p(x) = 0 \; \forall p \in I\}.$$

D. A. Cox, J. Little, and D. O'Shea. Ideals, Varieties, and Algorithms. An Introduction to Computational Algebraic Geometry and Commutative Algebra. 4th. Switzerland: Springer International Publishing, 2015.

Polynomials and Varieties

Theorem (Hilbert's Basis Theorem)

For every ideal $I \subseteq \mathbb{R}[x]$ there exists a finite set of polynomials $p_1, \ldots, p_s \in I$ such that

$$I = \{a_1 p_1 + \cdots + a_s p_s \,|\, a_1, \ldots, a_s \in \mathbb{R}[x]\} = \langle p_1, \ldots, p_s \rangle$$

- Different bases can describe the same ideal
- Gröbner bases allow the comparison of ideals
- A reduced Gröbner basis is unique for a given monomial ordering

Polynomials and Varieties

- Every real variety $V \subseteq \mathbb{R}^n$ can be associated with a real ideal

$$\mathbf{I}(V) = \{p \in \mathbb{R}[x] \,|\, p(x) = 0 \; \forall x \in V\}$$

- A real radical of an ideal $I \subseteq \mathbb{R}[x]$ is defined by

$$\sqrt[\mathbb{R}]{I} = \left\{ p \,\middle|\, \exists m \in \mathbb{Z}_{>0} : \exists a \in \sum \mathbb{R}[x]^2 : p^{2m} + a \in I \right\}$$

- There holds the following relation

$$I \subseteq \mathbf{I}(\mathbf{V}(I)) = \sqrt[\mathbb{R}]{I}$$

- Example

$$\mathbb{R}[x] \supset I = \left\langle x^2(1 + x^2) \right\rangle, \quad \mathbf{V}(I) = \{0\} \subset \mathbb{R}, \quad \mathbf{I}(\mathbf{V}(I)) = \langle x \rangle = \sqrt[\mathbb{R}]{I}$$

T. Becker and V. Weispfenning. Gröbner Bases. A Computational Approach to Commutative Algebra. 2nd. New York: Springer-Verlag, 1998.

Polynomials and Varieties
Geometric Operations

	ideals	varieties	
real ideal	$\sqrt[\mathbb{R}]{I} = \mathbf{I}(V)$	$V = \mathbf{V}(I)$	real variety
ideal sum	$I + J$	$\mathbf{V}(I) \cap \mathbf{V}(J)$	intersection
ideal intersection	$I \cap J$	$\mathbf{V}(I) \cup \mathbf{V}(J)$	union
saturation ideal	$I : J^\infty$	$\overline{\mathbf{V}(I) \setminus \mathbf{V}(J)}$	difference
elimination ideal	$I \cap \mathbb{R}[x]$	$\mathrm{proj}_x \mathbf{V}(I)$	projection

Observability Test

Observability Test

sets of zeros (algebraic varieties)	$\Longleftrightarrow$	sets of polynomials (ideals)

indistinguishable states

$$\mathcal{I} = \{(x, \bar{x}) \,|\, q(x) - q(\bar{x}) = 0\}$$

$$\begin{aligned} I &= \langle q(x) - q(\bar{x}) \rangle \\ &= \langle h(x) - h(\bar{x}), \\ &\qquad L_f h(x) - L_f h(\bar{x}), \ldots \rangle \end{aligned}$$

identical states

$$\mathcal{E} = \{(x, \bar{x}) \,|\, x - \bar{x} = 0\} \subseteq \mathcal{I}$$

$$\begin{aligned} E &= \langle x - \bar{x} \rangle \\ &= \langle x_1 - \bar{x}_1, \ldots, x_n - \bar{x}_n \rangle \end{aligned}$$

Remark

The unobservable points can be computed comparing the ideals I, E.

Observability Test
Lie derivative of an ideal

Polynomial system

$$\dot{x} = f(x)$$

Definition

Let $I = \langle g_1, \ldots, g_s \rangle \subseteq \mathbb{R}[x]$ be a polynomial ideal. The Lie derivative of the ideal along a polynomial vector field f is given by

$$L_f^\infty I = \left\{ a_1 L_f^{n_1} g_1 + \cdots + a_s L_f^{n_s} g_s \,\middle|\, n_k \in \mathbb{N}_0,\ g_k \in I,\ a_k \in \mathbb{R}[x] \right\}$$

Properties

- $L_f^\infty I \subseteq \mathbb{R}[x]$ is an ideal, i.e., it a has a finite basis
- $L_f^\infty I$ is closed: $g \in L_f^\infty I \implies L_f g \in L_f^\infty I$

Observability Test
Computation

Computation $L_f^\infty I$ of $I = \langle G \rangle = \langle g_1, \ldots, g_s \rangle$:

1: $G \leftarrow \mathrm{GroebnerBasis}(G)$
2: **for** $g \in G$ **do**
3: $\quad r \leftarrow$ remainder of polynomial division of $L_f g$ w.r.t. G
4: $\quad$ **if** $r \neq 0$ **then**
5: $\quad\quad G \leftarrow G \cup \{r\}$
6: $\quad\quad$ **goto** 1

Remarks

- Algorithm terminates after a finite number of steps (ascending chain condition)
- Finally we obtain $L_f^\infty I = \langle G \rangle$
- Computed basis G depends on the monomial order

Observability Test

- Two instances of the system

$$\left.\begin{aligned}\dot{x} &= f(x)\\ \dot{\bar{x}} &= f(\bar{x})\end{aligned}\right\} \qquad \begin{pmatrix}\dot{x}\\ \dot{\bar{x}}\end{pmatrix} = \begin{pmatrix}f(x)\\ f(\bar{x})\end{pmatrix} = F(x,\bar{x})\,, \qquad (x,\bar{x}) \in \mathcal{M}^2$$

- Output map describes the difference between the outputs

$$r = H(x,\bar{x}) = h(x) - h(\bar{x})$$

- Observability map

$$Q(x,\bar{x}) = \begin{pmatrix} H(x,\bar{x})\\ L_F^1 H(x,\bar{x})\\ \vdots \end{pmatrix} = \begin{pmatrix} h(x) - h(\bar{x})\\ L_f^1 h(x) - L_f^1 h(\bar{x})\\ \vdots \end{pmatrix} = q(x) - q(\bar{x})$$

Observability Test

- Indistinguishable pairs of states $(x, \bar{x}) \in \mathcal{I}$ constitute a real variety

$$q(x) - q(\bar{x}) = Q(x, \bar{x}) = 0 \iff (x, \bar{x}) \in \mathbf{V}\big(\langle H, L_F^1 H, \ldots \rangle\big)$$

- Ideal $\langle H, L_F^1 H, L_F^2 H, \ldots \rangle$ is the stabilized ideal $L_F^\infty \langle H \rangle$ wrt. the differential operator L_F

$$I = \langle H, L_F^1 H, L_F^2 H, \ldots \rangle = L_F^\infty \langle H \rangle$$

Indistinguishable pairs of states

The set of indistinguishable pairs of states is the real variety

$$\mathcal{I} = \mathbf{V}(I) = \mathbf{V}(L_F^\infty \langle H \rangle).$$

Observability Test
Global Observability

Identical pairs of states

The set of identical pairs of states is the real variety

$$\mathcal{E} = \mathbf{V}(E) = \mathbf{V}(\langle x_1 - \bar{x}_1, \ldots, x_n - \bar{x}_n \rangle).$$

Theorem (Global Observability)

The system is globally observable if and only if

$$\mathcal{I} = \mathcal{E} \iff \sqrt[\mathbb{R}]{I} = \sqrt[\mathbb{R}]{E} \iff \sqrt[\mathbb{R}]{L_F^\infty \langle H \rangle} = \langle x_1 - \bar{x}_1, \ldots, x_n - \bar{x}_n \rangle.$$

Observability Test

Example: Van der Pol oscillator

$$\dot{x}_1 = x_2\,, \quad \dot{x}_2 = -x_1 - x_2\big(x_1^2 - 1\big)\,, \quad y = x_2$$

Chain of ideals

$$\begin{aligned}
L_F^0\langle H\rangle &= L_F^0\langle x_2 - \bar{x}_2\rangle = \langle x_2 - \bar{x}_2\rangle \\
L_F^1\langle H\rangle &= \big\langle x_2 - \bar{x}_2, x_1^2\bar{x}_2 - \bar{x}_1^2\bar{x}_2 + x_1 - \bar{x}_1\big\rangle \\
L_F^2\langle H\rangle &= \big\langle x_2 - \bar{x}_2, x_1^2\bar{x}_2 - \bar{x}_1^2\bar{x}_2 + x_1 - \bar{x}_1, \\
&\qquad x_1^2\bar{x}_1 - x_1\bar{x}_1^2 - 2x_1\bar{x}_2^2 + 2\bar{x}_1\bar{x}_2^2 + x_1 - \bar{x}_1, \\
&\qquad x_1\bar{x}_1^2\bar{x}_2 - \bar{x}_1^3\bar{x}_2 + 2x_1\bar{x}_2^3 - 2x_1\bar{x}_2^3 + x_1\bar{x}_1 - \bar{x}_1^2 - x_1\bar{x}_2 + \bar{x}_1\bar{x}_2\big\rangle \\
&\cdots \subsetneq L_F^3\langle H\rangle \subsetneq L_F^4\langle H\rangle = L_F^5\langle H\rangle = L_F^\infty\langle H\rangle = \langle x_1 - \bar{x}_1, x_2 - \bar{x}_2\rangle
\end{aligned}$$

System is globally observable.

Observability Test

Local observability at $x_0 \in \mathcal{M}$

A system is called locally observable at a point x_0 if there exists a neighborhood U_{x_0} of x_0 such that

$$\forall x, \bar{x} \in U_{x_0} : q(x) = q(\bar{x}) \implies x = \bar{x}$$

or equivalently $\mathcal{I} \cap U^2_{x_0} = \mathcal{E} \cap U^2_{x_0}$.

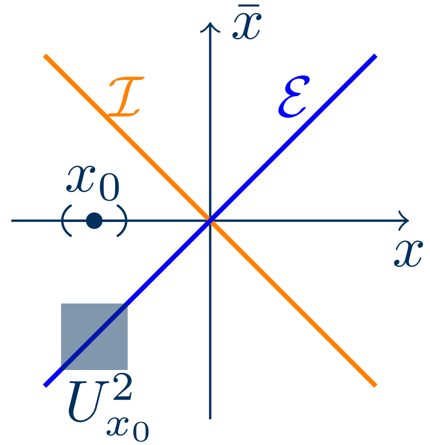

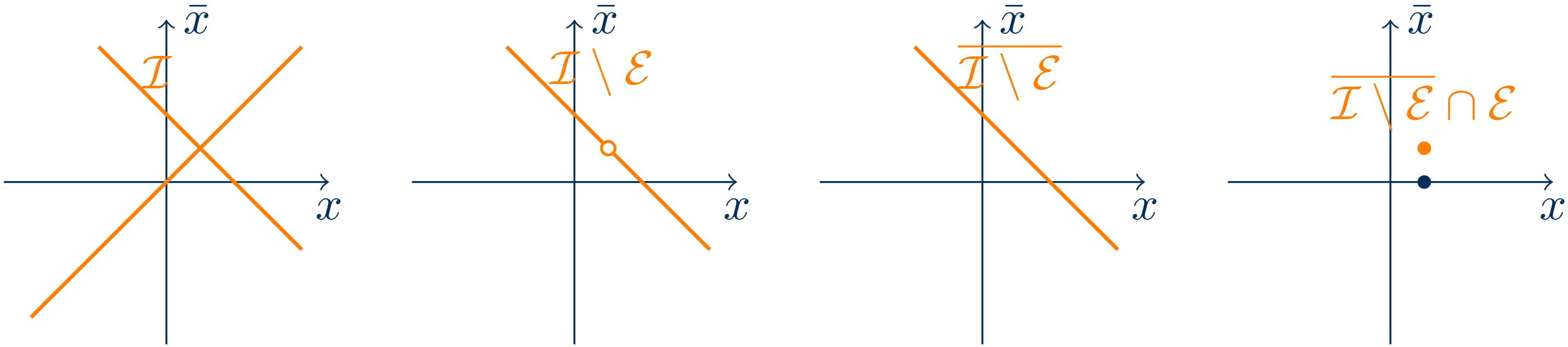

$\sqrt[\mathbb{R}]{I}$ $\qquad$ $\sqrt[\mathbb{R}]{I : E}$ $\qquad$ $\sqrt[\mathbb{R}]{I : E + E}$

Observability Test
Local Observability

Theorem (Local observability)

The points, where the system is not locally observable are given by the real variety

$$\mathrm{proj}_x\left(\overline{\mathcal{I}\setminus\mathcal{E}}\cap\mathcal{E}\right) = \mathbf{V}((I : E^\infty + E)\cap\mathbb{R}[x]).$$

D. Gerbet and K. Röbenack. "On global and local observability of nonlinear polynomial systems: A decidable criterion". In: at-Automatisierungstechnik 68.6 (2020), pp. 395–409. DOI: 10.1515/auto-2020-0027.

Observability Test

Example: Duffing oscillator

$$\dot{x}_1 = x_2\,, \quad \dot{x}_2 = x_1 - x_1^3\,, \quad y = x_2$$

- Stabilized ideal $L_F^4\langle H\rangle = L_F^\infty\langle H\rangle = I$
- Real radical $\implies$ not globally observable

$$\sqrt[\mathbb{R}]{I} = \left\langle x_2 - \bar{x}_2, x_1\bar{x}_2 - \bar{x}_1\bar{x}_2, x_1^3 - \bar{x}_1^3 - x_1 + \bar{x}_1, x_1\bar{x}_1^3 - \bar{x}_1^4 - x_1\bar{x}_1 - \bar{x}_1^2\right\rangle$$

- Saturation ideal

$$\sqrt[\mathbb{R}]{I} : E = \left\langle \bar{x}_2, x_2, x_1^2 + x_1\bar{x}_1 + \bar{x}_1^2 - 1, \bar{x}_1^3 - \bar{x}_1\right\rangle$$

- Ideal sum

$$\sqrt[\mathbb{R}]{I} : E + E = \langle 1\rangle = \mathbb{R}[x, \bar{x}]$$

- System is locally observable

High Gain Observers

High Gain Observers

The observability map

$$q_N : \mathcal{M} \hookrightarrow \mathbb{R}^N \qquad x \mapsto z = q_N(x)$$

embeds system (1) into observability canonical form

$$\left.\begin{array}{lcl} \dot{z}_1 & = & z_2 \\ \dot{z}_2 & = & z_3 \\ & \vdots & \\ \dot{z}_{N-1} & = & z_N \\ \dot{z}_N & = & \alpha(z) \\ y & = & z_1 \end{array}\right\} \qquad \begin{array}{lcl} \dot{z} & = & A\,z + b\,\alpha(z) \\ y & = & c^T z \end{array}$$

with Brunovsky triple (A, b, c^T) and

$$\alpha(z) = L_f^N h(x) \quad \text{with} \quad x = q_N^{-1}(z)$$

Problem

Computation of the inverse q_N^{-1} of the map $q_N : \mathbb{R}^n \to \mathbb{R}^N$ for $N > n$

High Gain Observers

System in observability canonical form

$$\dot{z} = A\,z + b\,\alpha(z), \quad y = c^T x$$

State observer in Luenberger structure with observer gain $l \in \mathbb{R}^n$

$$\dot{\hat{z}} = \underbrace{A\,\hat{z} + b\,\alpha(\hat{z})}_{\text{simulation term}} + \underbrace{l\,(y - c^T\,\hat{z})}_{\text{correction term}}$$

Observation error $e = z - \hat{z}$ is governed by error dynamics

$$\dot{e} = \underbrace{(A - l\,c^T)\,e}_{\text{linear}} + \underbrace{b\,(\alpha(z) - \alpha(\hat{z}))}_{\text{nonlinear}}$$

High gain observer design (Gauthier *et al* 1991, 1992)

Assume that the map α is (locally) Lipschitz continuous. Then, the observer gain l can be chosen such that the equilibrium point $e = 0$ of the error dynamics is (locally) asymptotically stable.

High Gain Observers

Construction of the observability canonical form

$$\underbrace{z_1 = h(x), z_2 = L_f h(x), \ldots, z_N = L_f^{N-1} h(x),}_{\text{coordinates of the canonical form}} \; \underbrace{\dot{z}_N = L_f^N h(x)}_{\text{nonlinearity } \alpha}$$

Formulation as an elimination ideal

$$\begin{aligned} I &= \underbrace{\langle z_1 - h(x), z_2 - L_f h(x), \ldots, \dot{z}_N - L_f^N h(x) \rangle}_{\text{define new coordinates } z_1, \ldots, z_N \text{ and nonlinearity } \dot{z}_N} \cap \underbrace{\mathbb{R}[z_1, \ldots, z_N, \dot{z}_N]}_{\text{eliminate } x} \\ &= \langle p_1, \ldots, p_s \rangle \quad \ldots \quad \text{Gröbner basis} \end{aligned}$$

Collect all polynomials of the form

$$p_i = a\, \dot{z}_N + \cdots \quad \text{with} \quad a \in \mathbb{R}[z_1, \ldots, z_N]$$

Solve linear system $\Longrightarrow \dot{z}_N = \alpha(z_1, \ldots, z_n)$

D. Gerbet and K. Röbenack. "A High-Gain Observer for Embedded Polynomial Dynamical Systems". In: Machines 11.2 (2023). DOI: 10.3390/machines11020190.

High Gain Observers

Example: Globally observable academic system

$$\dot{x} = f(x) = 1, \quad y = h(x) = x^3$$

Embedding with $N = 1$

$$\begin{array}{rcccccc} y & = & z_1 & = & L_f^0 h(x) & = & x^3 \\ \dot{y} & = & \dot{z}_1 & = & L_f^1 h(x) & = & 3x^2 \end{array}$$

Elimination ideal

$$I = \left\langle z_1 - x^3, \dot{z}_1 - 3x^2 \right\rangle \cap \mathbb{R}[z_1, \dot{z}_1] = \left\langle \dot{z}_1^3 - 27 z_1^2 \right\rangle$$

Observability canonical form

$$\dot{z}_1 = 3 z_1^{\frac{2}{3}}$$

with non-Lipschitz nonlinearity ($z_1(0) = 0 \implies z_1(t) = 0$ and $z_1(t) = t^3$)

High Gain Observers

Example: Embedding with $N = 3$

$$\begin{aligned} z_1 &= L_f^0 h(x) &= x^3 \\ z_2 &= L_f^1 h(x) &= 3x^2 \\ z_3 &= L_f^2 h(x) &= 6x \\ \dot{z}_3 &= L_f^3 h(x) &= 6 \end{aligned}$$

Elimination ideal

$$\begin{aligned} I &= \langle z_1 - x^3,\ z_2 - 3x^2,\ z_3 - 6x,\ \dot{z}_3 - 6 \rangle \cap \mathbb{R}[z_1, z_2, z_3, \dot{z}_3] \\ &= \langle \underbrace{\dot{z}_3 - 6}_{\text{nonlinearity}},\ \underbrace{z_3^2 - 12z_2, z_2 z_3 - 18z_1, 3z_1 z_3 - 2z_2^2, z_2^3 - 27z_1^2}_{\text{constraints}} \rangle \end{aligned}$$

Observability canonical form

$$\begin{aligned} \dot{z}_1 &= z_2 \\ \dot{z}_2 &= z_3 \\ \dot{z}_3 &= 6 \end{aligned}$$

High Gain Observers

Example: Rössler Attractor

$$\dot{x}_1 = -x_2 - x_3, \quad \dot{x}_2 = x_1 + \tfrac{1}{5}x_2, \quad \dot{x}_3 = \tfrac{1}{5} + x_3\big(x_1 - \tfrac{57}{10}\big), \qquad y = x_1$$

Embedding with $N = 5$, eliminating state variables x:

$$0 = \dot{z}_5 z_3 - z_4 z_5 - \tfrac{4}{5} z_3 z_5 + \tfrac{3}{5} z_4^2 + \tfrac{3}{25} z_3 z_4 - \tfrac{3}{5} z_2^2 z_4 + \tfrac{4577}{250} z_2 z_4 - \tfrac{61}{250} z_4 - 4 z_3^3 - 2 z_1 z_2 z_3^2 + \cdots$$
$$0 = \dot{z}_5 z_2 - z_4^2 - \tfrac{2}{5} z_3 z_4 - 3 z_2^2 z_4 - \tfrac{7}{25} z_2 z_4 + \tfrac{61}{50} z_4 - 3 z_2 z_3^2 + z_1^2 z_3^2 - \tfrac{53}{5} z_1 z_3^2 + \tfrac{561}{20} z_3^2 - \cdots$$
$$0 = \dot{z}_5 \big(z_1 - \tfrac{59}{10}\big) - z_3 z_4 + \tfrac{1}{5} z_2 z_4 - \tfrac{61}{10} z_4 - 4 z_1 z_3^2 + \tfrac{114}{5} z_3^2 - 3 z_2^2 z_3 - 6 z_1^2 z_2 z_3 + \cdots$$
$$0 = z_2 z_5 - z_3 z_4 - \tfrac{3}{5} z_2 z_4 + z_1 z_3^2 - \tfrac{11}{2} z_3^2 - 3 z_2^2 z_3 - z_1^2 z_2 z_3 + \tfrac{58}{5} z_1 z_2 z_3 - \tfrac{671}{20} z_2 z_3 + \cdots$$
$$0 = z_1 z_5 - \tfrac{59}{10} z_5 - z_3^2 - 3 z_1 z_2 z_3 + \tfrac{173}{10} z_2 z_3 - z_1^3 z_3 + \tfrac{171}{10} z_1^2 z_3 - \tfrac{9747}{100} z_1 z_3 + \tfrac{179101}{1000} z_3 + \cdots$$
$$0 = z_1 z_4 - \tfrac{59}{10} z_4 - z_2 z_3 - z_1^2 z_3 + \tfrac{57}{5} z_1 z_3 - \tfrac{649}{20} z_3 + \tfrac{1}{5} z_2^2 + \tfrac{1}{5} z_1^2 z_2 - \tfrac{58}{25} z_1 z_2 + \tfrac{313}{500} z_2 - \cdots$$

Evaluation of $\dot{z}_5 = \phi(z)$ ill posed at

$$z_1 - \tfrac{59}{10} = 0, \;\; z_2 = 0, \;\; z_3 = 0$$

High Gain Observers

Evaluation of $\dot{z}_5 = \phi(z)$ ill posed at

$$z_1 - \frac{59}{10} = 0, \ z_2 = 0, \ z_3 = 0$$

System can always be solved for $\dot{z}_5$ for $z \in q_5(\mathcal{M})$

$$\begin{aligned} \left(z_1 - \tfrac{59}{10}\right)\dot{z}_5 &= \cdots \\ z_2 \dot{z}_5 &= \cdots \\ z_3 \dot{z}_5 &= \cdots \end{aligned}$$

$$\dot{z}_5 = \frac{1}{\left(z_1 - \frac{59}{10}\right)^2 + z_2^2 + z_3^2} \cdots$$

D. Gerbet and K. Röbenack. “A High-Gain Observer for Embedded Polynomial Dynamical Systems”. In: Machines 11.2 (2023). DOI: 10.3390/machines11020190.

D. Gerbet and K. Röbenack. “An embedding observer for nonlinear dynamical systems with global convergence”. In: Proc. Appl. Math. Mech. 23.4 (2023), e202300099. DOI: 10.1002/pamm.202300099.

Summary

Summary

- Observability of polynomial systems can be decided in a finite number of steps
- The set of unobservable points can be computed
- Analysis dependent on parameters
- Computation of the observability canonical form
- Embedding into high dimension may be advantageous

Acknowledgement

This work has been funded by the Deutsche Forschungsgemeinschaft (DFG, German Research Foundation) –– project number 417698841.

VII. Generalized Hybrid-Integrator-Gain System
presenter: Christoph Weise

Fachgebiet Regelungstechnik

TECHNISCHE UNIVERSITÄT ILMENAU

Generalized Reset Hybrid-Integrator-Gain-System (HIGS)

Christoph Weise*, Kai Wulff*, Johann Reger*

christoph.weise@tu-ilmenau.de

*Control Engineering Group, TU Ilmenau, Germany

10th September 2024

23. Styrian Workshop on Automatic Control, Retzhof

Content

Hybrid-Integrator-Gain-System (HIGS)

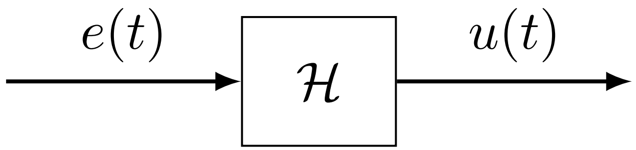

HIGS [Deenen et al., 2021] given by ($k_h > 0$, $\omega_h > 0$)

$$\begin{aligned} \dot{x}(t) &= \omega_h e(t), && (e, \dot{e}, u) \in \mathcal{F}_1 \\ x(t) &= k_h e(t), && (e, \dot{e}, u) \in \mathcal{F}_2 \\ u(t) &= x(t) \end{aligned}$$

$$\mathcal{F}_1 = \left\{ (e, \dot{e}, u) \in \mathbb{R}^3 | eu \geq \frac{1}{k_h} u^2 \wedge (e, \dot{e}, u) \notin \mathcal{F}_2 \right\}$$

$$\mathcal{F}_2 = \left\{ (e, \dot{e}, u) \in \mathbb{R}^3 | u = k_h e \wedge \omega_h e^2 > k_h e \dot{e} \right\}$$

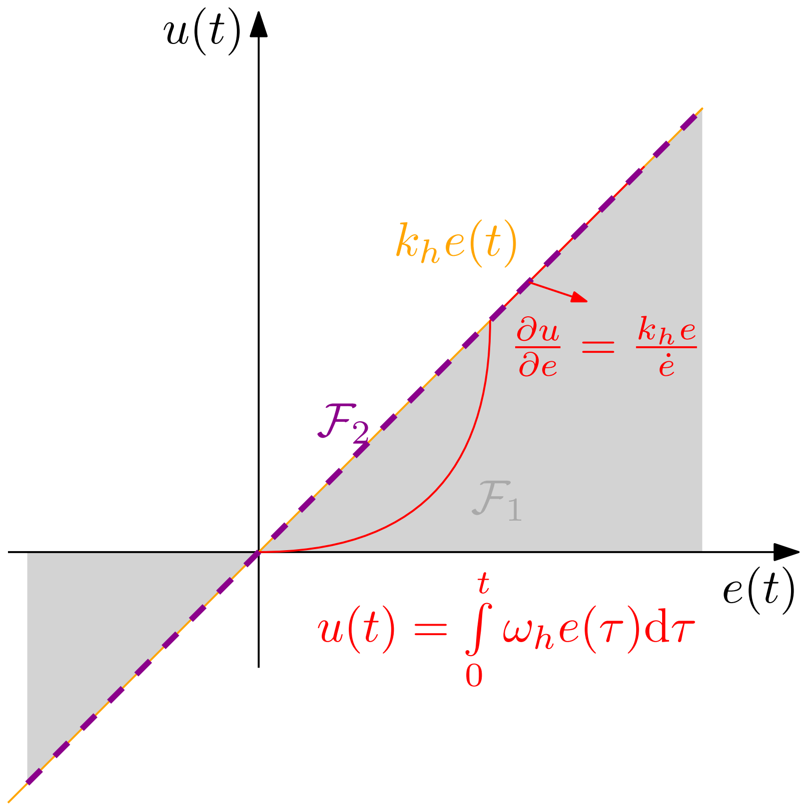

HIGS – Illustration

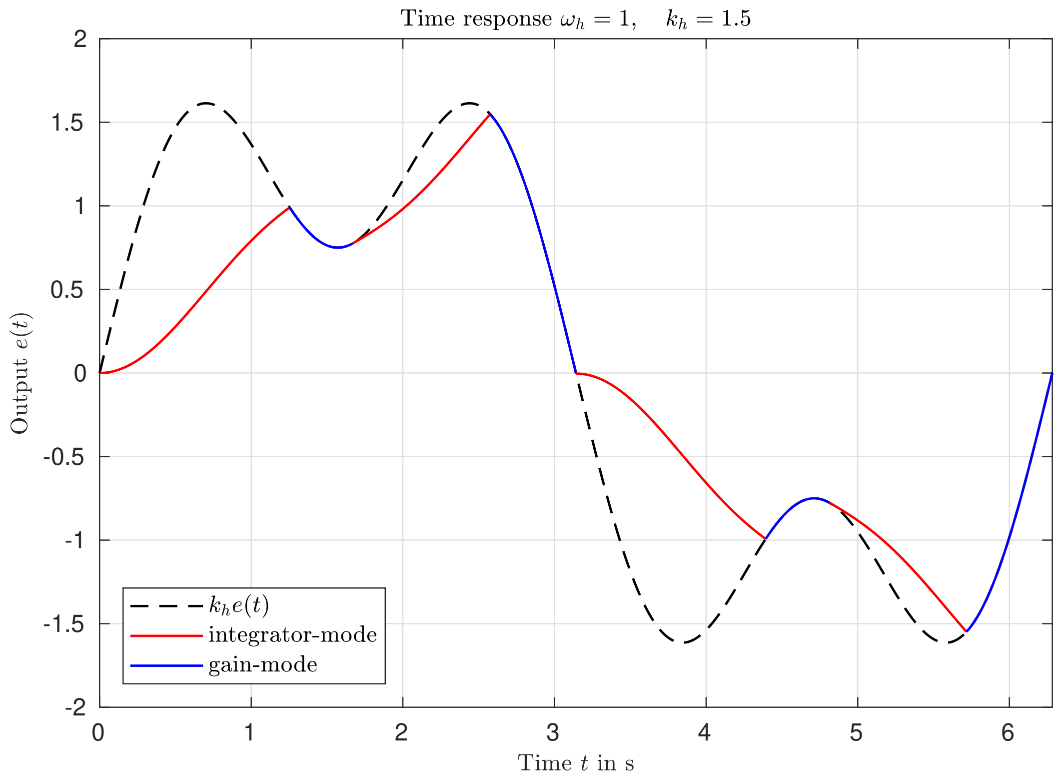

HIGS - Describing function

Sinusoidal input $e(t) = \sin(\omega t)$ to approximate $u(t)$ with the first Fourier coefficients

$$N_A(\mathrm{j}\omega) = b_1 + \mathrm{j}a_1 \quad \text{with} \quad \begin{cases} a_1 = \dfrac{\omega}{\pi}\displaystyle\int_0^{2\pi/\omega} u(t)\cos(\omega t)\mathrm{d}t \\ b_1 = \dfrac{\omega}{\pi}\displaystyle\int_0^{2\pi/\omega} u(t)\sin(\omega t)\mathrm{d}t \end{cases}$$

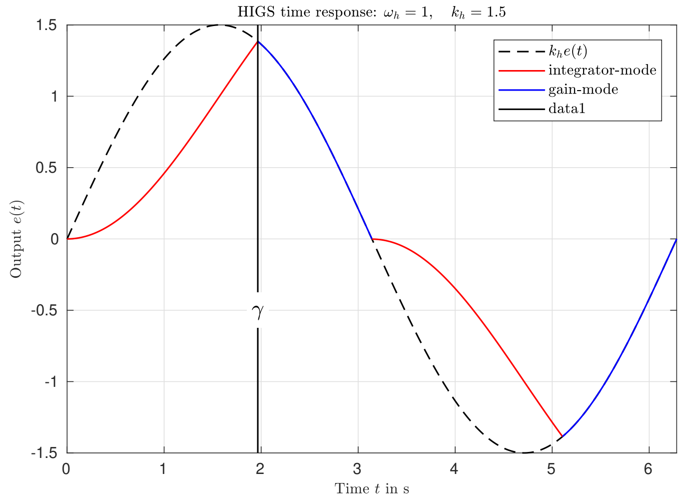

$$e(t) = \begin{cases} \dfrac{\omega_h}{\omega}\left(1 - \cos(\omega t)\right), & t \in \left[0, \dfrac{\gamma(\omega)}{\omega}\right] \\ k_h \sin(\omega t), & t \in \left(\dfrac{\gamma(\omega)}{\omega}, \dfrac{\pi}{\omega}\right] \\ \dfrac{\omega_h}{\omega}\left(-1 - \cos(\omega t)\right), & t \in \left(\dfrac{\pi}{\omega}, \dfrac{\pi+\gamma(\omega)}{\omega}\right] \\ k_h \sin(\omega t), & t \in \left(\dfrac{\pi+\gamma(\omega)}{\omega}, \dfrac{2\pi}{\omega}\right] \end{cases}$$

$$\gamma = 2\arctan\left(k_h \omega {\omega_h}^{-1}\right)$$

HIGS - Describing function

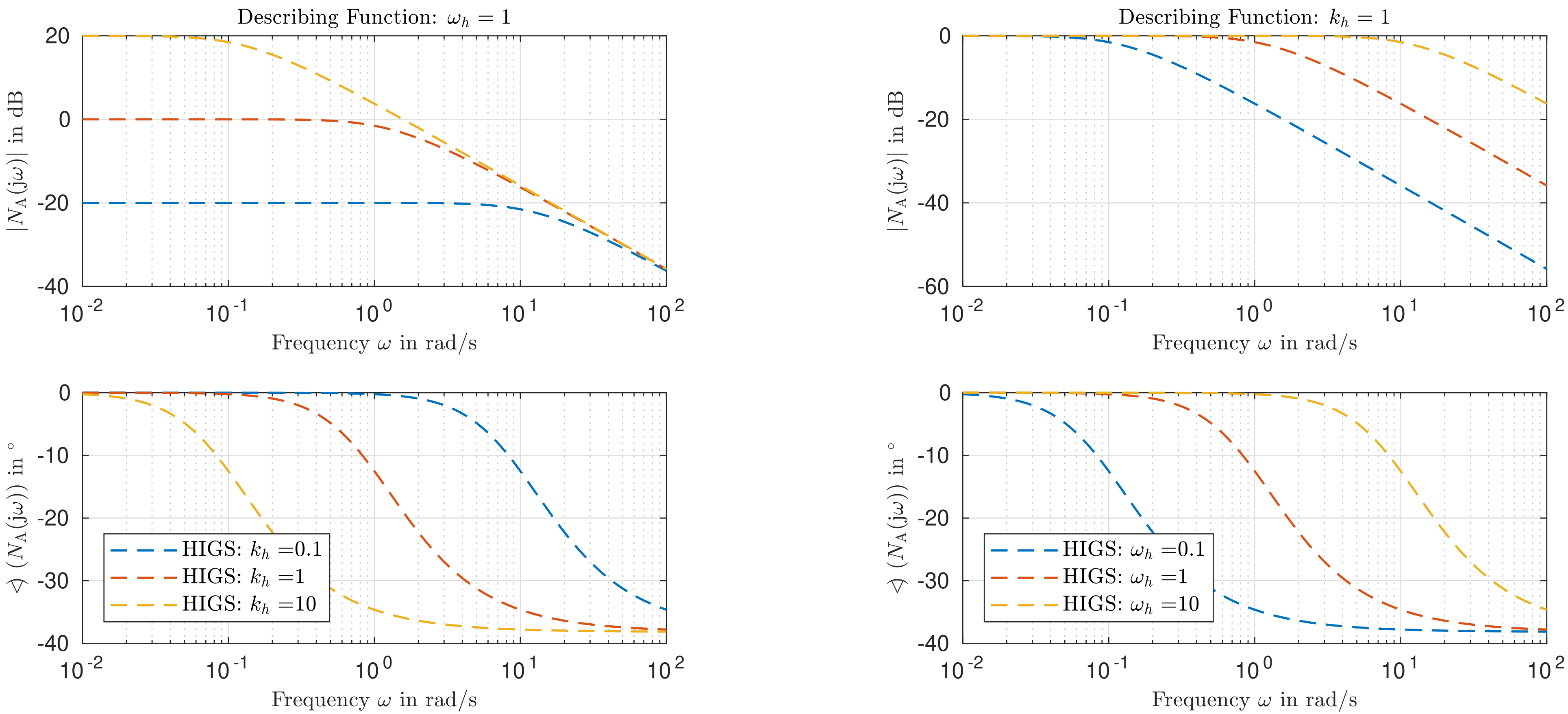

HIGS - Describing function

$$N_A(\mathrm{j}\omega) = \frac{\mathrm{j}\omega_h}{\omega}\left(\frac{\gamma(\omega)}{\pi} + \mathrm{j}\frac{e^{-2\mathrm{j}\gamma(\omega)} - 4e^{-\mathrm{j}\gamma(\omega)} + 3}{2\pi}\right) + k_h\left(\frac{\pi - \gamma(\omega)}{\pi} + \mathrm{j}\frac{e^{-2\mathrm{j}\gamma(\omega)} - 1}{2\pi}\right)$$

- low frequency behavior $\omega \to 0$: $\lim\limits_{\omega\to 0} N_A(\mathrm{j}\omega) = k_h$
- high frequency behavior $\omega \to \infty$:

$$\lim_{\omega\to\infty} N_A(\mathrm{j}\omega) = \frac{\omega_h}{\mathrm{j}\omega}\left(1 + \frac{4\mathrm{j}}{\pi}\right) \Longrightarrow \begin{cases} \lim\limits_{\omega\to\infty} |N_A(\mathrm{j}\omega)| = \dfrac{\omega_h}{\omega}\left|1 + \dfrac{\mathrm{j}}{\pi}\right| \approx 1.62\dfrac{\omega_h}{\omega} \\ \lim\limits_{\omega\to\infty} \arg_s\left(N_A(\mathrm{j}\omega)\right) = \arctan\left(\dfrac{-\pi}{4}\right) \approx -38.15^\circ \end{cases}$$

- cross-over frequency $\omega_c = \left|1 + \frac{4\mathrm{j}}{\pi}\right|\frac{\omega_h}{k_h}$

HIGS - Loop-Shaping

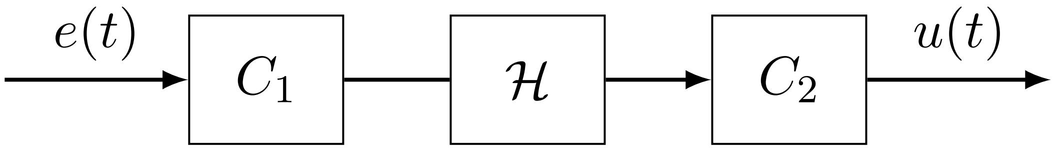

- Precompensator $C_1(s)$ to compensate cross-over frequency and provide $\dot{e}$

$$C_1(s) = \left(\frac{s}{\omega_c} + 1\right)\frac{1}{\tau s + 1}, \qquad \tau > 0$$

- Postcompensator $C_2(s)$ to introduce integrator for low frequencies and damp higher order harmonics

$$C_2(s) = \frac{\omega_i(\tau s + 1)}{s}$$

results in integrating behavior (amplitude response) with phase lead.

HIGS – Stability

Theorem (Passivity [Deenen et al., 2021])

The HIGS is strictly passive in the sense that there exists a positive definite storage function $V(x_h) = \frac{\lambda}{2}x_h^2$ with $\lambda = k/\omega_h$ and $k \in (0,1)$ that satisfies

$$\dot{V} \leq -cx_h^2 + eu, \qquad \textit{with} \qquad c \in (0, k_h)$$

along all solutions with continuous $e \in \mathcal{L}_1^{\mathrm{loc}}$ for almost all times $t \in \mathbb{R}^+$.

Passivity allows for a conservative closed loop stability analysis $\rightarrow$ circle like criterion

Simulation Example

Consider the unstable process to control without overshooting:

$$P(s) = \frac{(s+3)\omega^2}{(s-1)(s^2+2\zeta\omega s+\omega^2)}, \quad \omega = 10\pi, \zeta = \frac{3}{2}$$

and the HIGS ($\omega_h = 0.48, k_h = 0.6$) with $\omega_i = 10, \tau = 0.001$ and compensators

$$C_1(s) = \frac{s+\omega_c}{\omega_c(\tau s+1)}, \quad C_2(s) = \frac{\omega_i(\tau s+1)}{s}$$

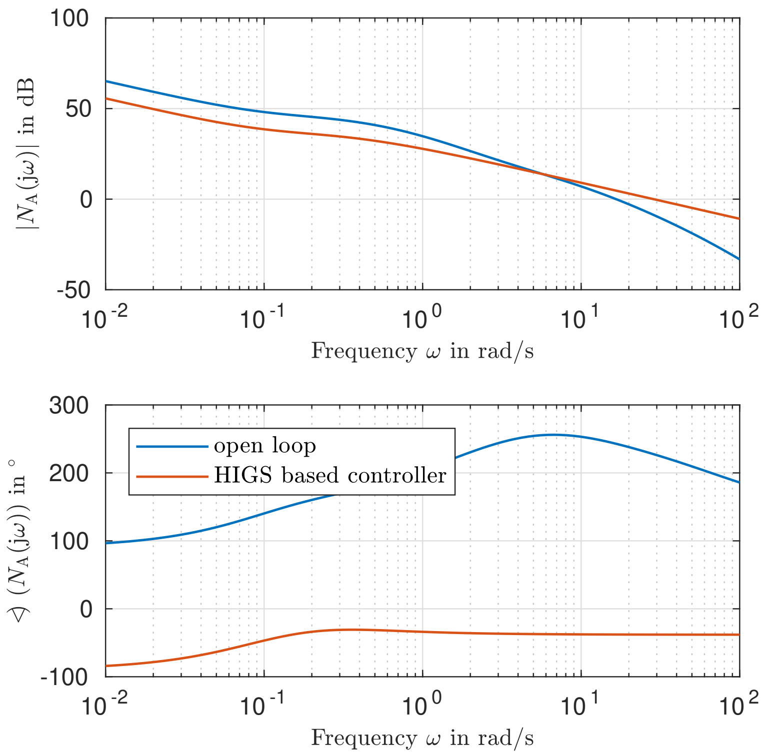

Simulation Results

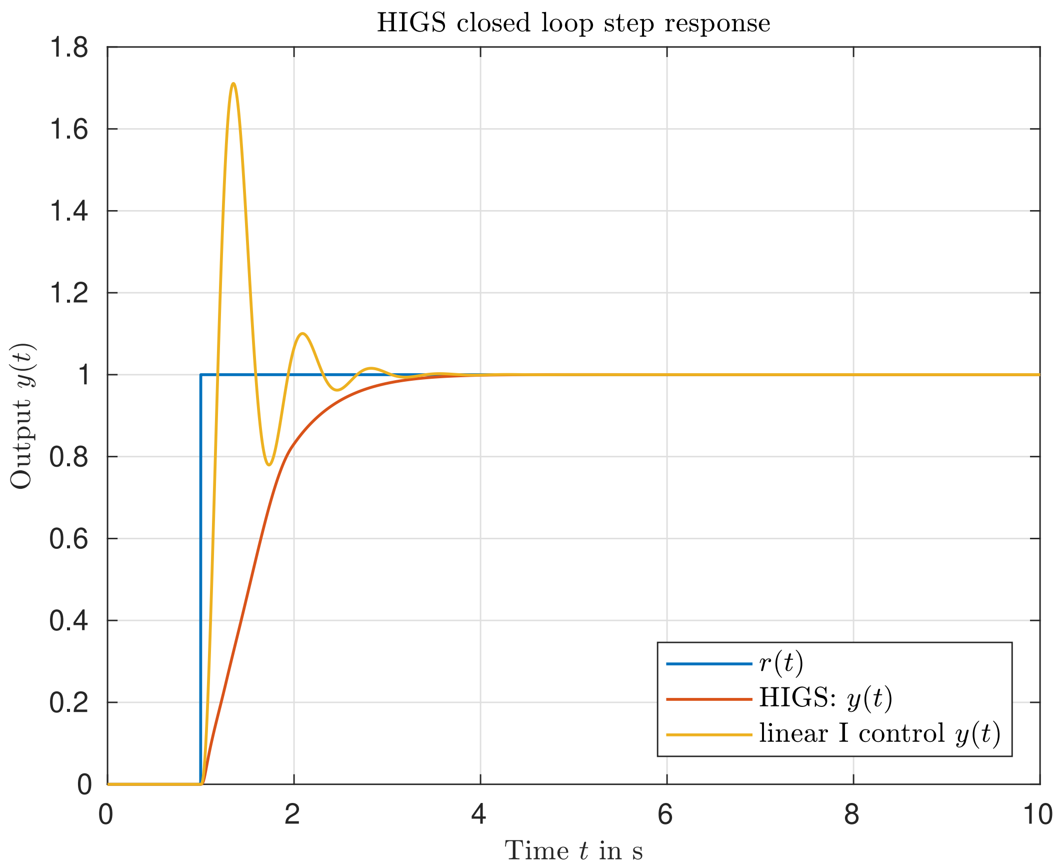

Fractional-Order HIGS

Fractional-order HIGS [Hosseini et al., 2022] applies Caputo's Operator:

$$\begin{aligned} {}_0\mathcal{D}_t^\alpha x(t) &= \omega_h e(t), && (e,\dot e,u)\in\mathcal{F}_1 && k_h \geq 0 \\ x(t) &= k_h e(t), && (e,\dot e,u)\in\mathcal{F}_2 && \omega_h \geq 0 \\ x(t) &= 0, && (e,\dot e,u)\in\mathcal{F}_3 && \alpha \in (0,1) \\ u(t) &= x(t) \end{aligned}$$

$$\mathcal{F} = \left\{(e,\dot e,u)\in\mathbb{R}^3 | eu \geq \frac{1}{k_h}u^2\right\} \qquad \mathcal{F}_1 = \mathcal{F}\backslash(\mathcal{F}_2\cup\mathcal{F}_3)$$

$$\begin{aligned} \mathcal{F}_2 = \{(e,\dot e,u)\in\mathcal{F}|u = k_h e \wedge (\omega_h e\, {}_0\mathcal{D}_t^\alpha e > k_h \dot e e \vee e\, {}_0\mathcal{D}_t^\alpha e < 0 \vee \\ \left(e = 0 \wedge \omega_h \dot e\, {}_0\mathcal{D}_t^{1-\alpha} e > k_k \dot e^2\right)\} \end{aligned}$$

$$\mathcal{F}_3 = \left\{(e,\dot e,u)\in\mathcal{F}|u = 0 \wedge \omega_h e^2 > k_h e\dot e\right\}$$

Generalized HIGS

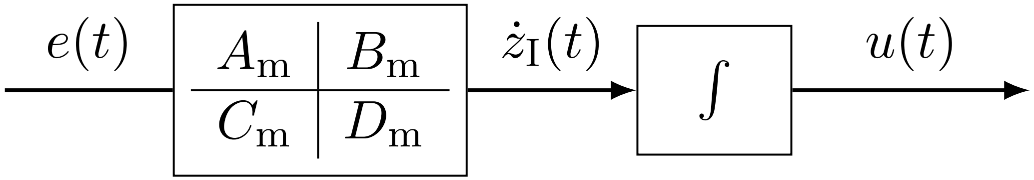

$$
\begin{aligned}
\dot{z}(t) &= A_z z(t) + B_z e(t), && (e, \dot{e}, u, z_\mathrm{m}) \in \bar{\mathcal{F}}_1 \quad \text{(I-Mode)}\\
z(t) &= \begin{pmatrix} 0 & k_h e(t) \end{pmatrix}^\top && (e, \dot{e}, u, z_\mathrm{m}) \in \bar{\mathcal{F}}_2 \quad \text{(P-Mode)}\\
z(t) &= 0 && (e, \dot{e}, u, z_\mathrm{m}) \in \bar{\mathcal{F}}_3 \quad \text{(0-Mode)}\\
u(t) &= \begin{pmatrix} 0 & 1 \end{pmatrix} z(t) && z = \begin{pmatrix} z_\mathrm{m} & z_\mathrm{I} \end{pmatrix}^\top
\end{aligned}
$$

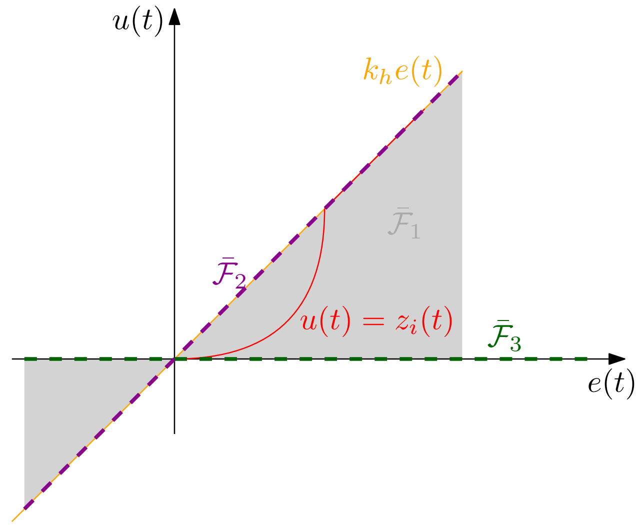

$$
\begin{aligned}
\bar{\mathcal{F}}_1 &= \left\{ (e, \dot{e}, u, z_\mathrm{m}) \in \mathbb{R}^q \middle| eu \geq \frac{1}{k_h} u^2 \wedge (e, \dot{e}, u, z_\mathrm{m}) \notin (\bar{\mathcal{F}}_2 \cup \bar{\mathcal{F}}_3) \right\}\\
\bar{\mathcal{F}}_2 &= \{ (e, \dot{e}, u, z_\mathrm{m}) \in \mathbb{R}^q | u = k_h e \wedge (C_\mathrm{m} z_\mathrm{m} + D_\mathrm{m} e) e > k_h e \dot{e} \},\\
\bar{\mathcal{F}}_3 &= \{ (e, \dot{e}, u, z_\mathrm{m}) \in \mathbb{R}^q | u = 0 \wedge e \neq 0 \wedge (C_\mathrm{m} z_\mathrm{m} + D_\mathrm{m} e) e < 0 \}.
\end{aligned}
$$

G-HIGS – Describing Function Computation

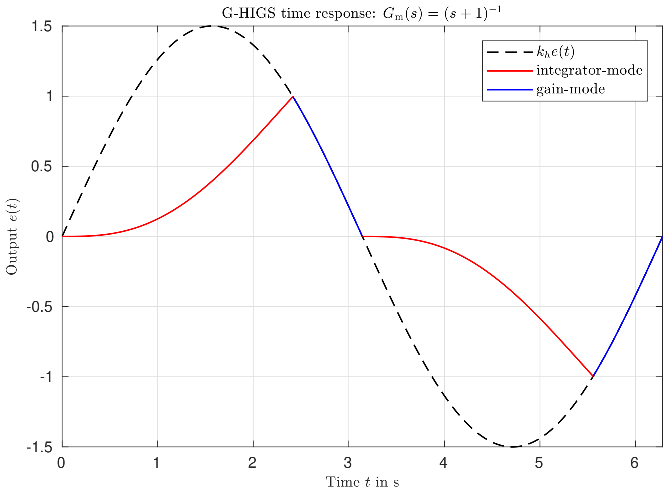

$$e(t) = \begin{cases} \int_0^t \exp(A_z(t-\tau))B_z \sin(\omega\tau)\mathrm{d}\tau, & t \in [0, T^\star], \\ k_h \sin(\omega t), & t \in \left(T^\star, \frac{\pi}{\omega}\right] \\ \int_{\pi/\omega}^t \exp(A_z(t-\tau))B_z \sin(\omega\tau)\mathrm{d}\tau, & t \in \left(\frac{\pi}{\omega}, \frac{\pi}{\omega} + T^\star\right] \\ k_h \sin(\omega t), & t \in \left(\frac{\pi}{\omega} + T^\star, \frac{2\pi}{\omega}\right] \end{cases}$$

Tasks:

- Find an analytic expression without integral for the output in the first time interval $t \in [0, T^\star)$.
- Solve the integrals to derive the Fourier coefficients and the describing function.

Describing Functions - Computation - II

Sinusoidal input is the output of an integer-order generator system:

$$\dot{x}_s = \begin{pmatrix} 0 & -\omega \\ \omega & 0 \end{pmatrix} x_s = A_\omega x_s, \qquad x_s(0) = \begin{pmatrix} 0 \\ -1 \end{pmatrix}$$
$$y_s = \begin{pmatrix} 1 & 0 \end{pmatrix} x_s = C_\omega x_s = \sin(\omega t)$$

With the extended System

$$\begin{pmatrix} \dot{z} \\ \dot{x}_s \end{pmatrix} = \begin{pmatrix} A_z & B_z C_\omega \\ 0 & A_\omega \end{pmatrix} \begin{pmatrix} z \\ x_s \end{pmatrix} = \bar{A}\bar{z}, \quad \bar{z}(0) = \begin{pmatrix} z(0) \\ x_s(0) \end{pmatrix} = \begin{pmatrix} 0 \\ x_s(0) \end{pmatrix}$$

the output can be determined in terms of Matrix Exponential functions

$$u(t) = \begin{pmatrix} e_1^\top & 0 \end{pmatrix} \exp\left(\bar{A}t\right) \bar{z}(0) = \bar{C} \exp\left(\bar{A}t\right) \bar{z}(0), \qquad t \in [0, T^\star]$$

Fourier Coefficients – I

$$b_1 = \frac{\omega}{\pi}\int_0^{2\pi/\omega} u(t)\sin(\omega t)\mathrm{d}t = \underbrace{\frac{2\omega}{\pi}\int_0^{T^\star} u(t)\sin(\omega t)\mathrm{d}t}_{B_1} + \underbrace{\frac{2\omega}{\pi}\int_{T^\star}^{\pi/\omega} u(t)\sin(\omega t)\mathrm{d}t}_{B_2}$$

Note: B_2 can be solved analytically as $u(t) = k_h \sin(\omega t)$ Idea: reshape multiplication in the integral B_1 to a suitable convolution $\varphi = -\omega T^\star$:

$$B_1 = \int_0^{T^\star} u(\tau)\sin(\omega\tau)\mathrm{d}\tau = -\int_0^{T^\star} \sin(\omega(T^\star - \tau) + \varphi)u(\tau)\mathrm{d}\tau$$

Hence u can be interpreted as the input to the generator system

$$\dot{\zeta} = \begin{pmatrix} 0 & -\omega \\ \omega & 0 \end{pmatrix}\zeta + \begin{pmatrix} \sin(\omega T^\star) \\ \cos(\omega T^\star) \end{pmatrix} u = A_\omega \zeta + B_\omega u, \qquad \zeta(0) = 0$$

Fourier Coefficients – II

$$\begin{pmatrix} B_1 \\ A_1 \end{pmatrix} = -\begin{pmatrix} 1 & 0 \\ 0 & 1 \end{pmatrix} \int_0^{T^\star} \exp\left(A_\omega (T^\star - \tau)\right) B_\omega y(\tau) \mathrm{d}\tau$$

Note that the $\cos$-term $a_1 = A_1 + A_2$ can also be incorporated. The analysis of higher-order harmonics is also possible with the second generator system, i.e. $A_{2\omega}$

$$\begin{pmatrix} \dot{\zeta} \\ \dot{\bar{z}} \end{pmatrix} = \underbrace{\begin{pmatrix} A_\omega & B_\omega \bar{C} \\ 0 & \bar{A} \end{pmatrix}}_{\bar{A}_e} \begin{pmatrix} \zeta \\ \bar{z} \end{pmatrix}$$

$$\begin{pmatrix} B_1 \\ A_1 \end{pmatrix} = \begin{pmatrix} I & 0 \end{pmatrix} \begin{pmatrix} \zeta \\ \bar{z} \end{pmatrix}$$

Also the Fourier coefficients can be expressed in terms of matrix exponentials.

Fourier Coefficients – II

The Fourier coefficients can be expressed in terms of matrix exponentials and only the intersection time $T^\star$ has to be found numerically:

$$\begin{pmatrix} B_1 \\ A_1 \end{pmatrix} = \begin{pmatrix} I & 0 & 0 \end{pmatrix} \exp\left(\bar{A}_e(T^\star)\right) \begin{pmatrix} 0 \\ \bar{z}(0) \end{pmatrix}$$

The remaining terms are given by:

$$\begin{aligned} B_2 &= k_h \left[\frac{t}{2} - \frac{1}{4\omega}\sin(2\omega t)\right]_{t=T^\star}^{t=\frac{\pi}{\omega}} &&= k_h \left[\frac{\pi}{2\omega} - \frac{T^\star}{2} + \frac{1}{4\omega}\sin(2\omega T^\star)\right] \\ A_2 &= k_h \left[\frac{1}{2\omega}\sin^2(\omega t)\right]_{t=T^\star}^{t=\frac{\pi}{\omega}} &&= -\frac{k_h}{2\omega}\sin^2(\omega T^\star) \end{aligned}$$

Describing function - Single Pole

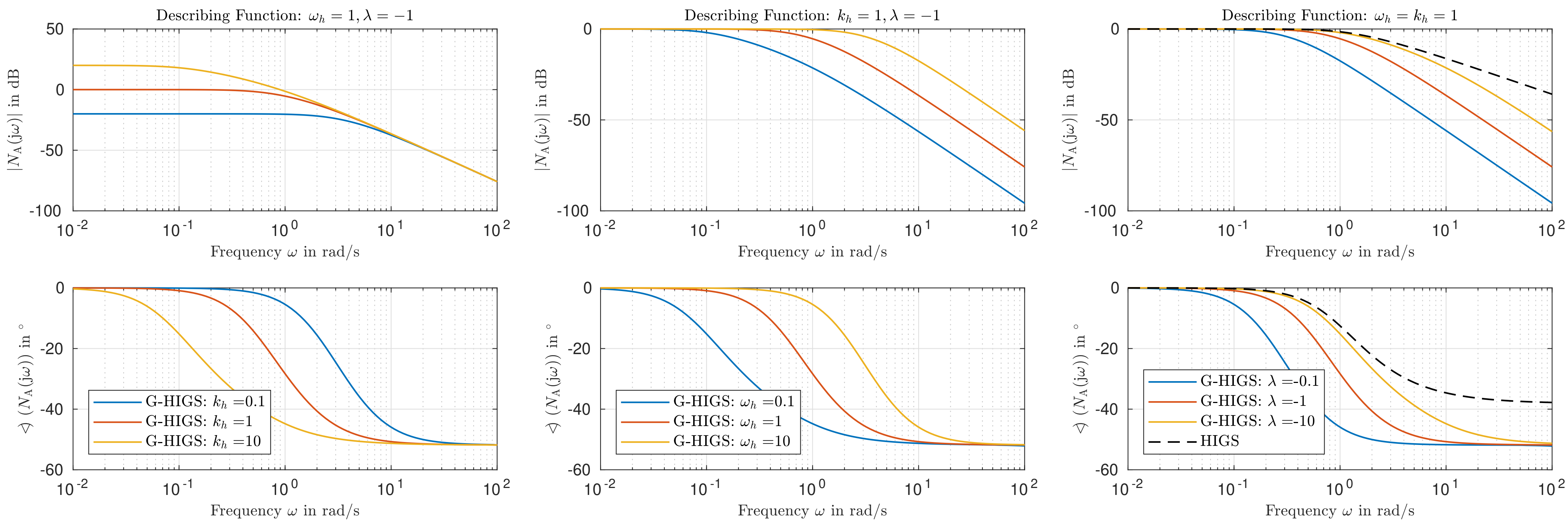

Describing function - Pole-Zero Pair

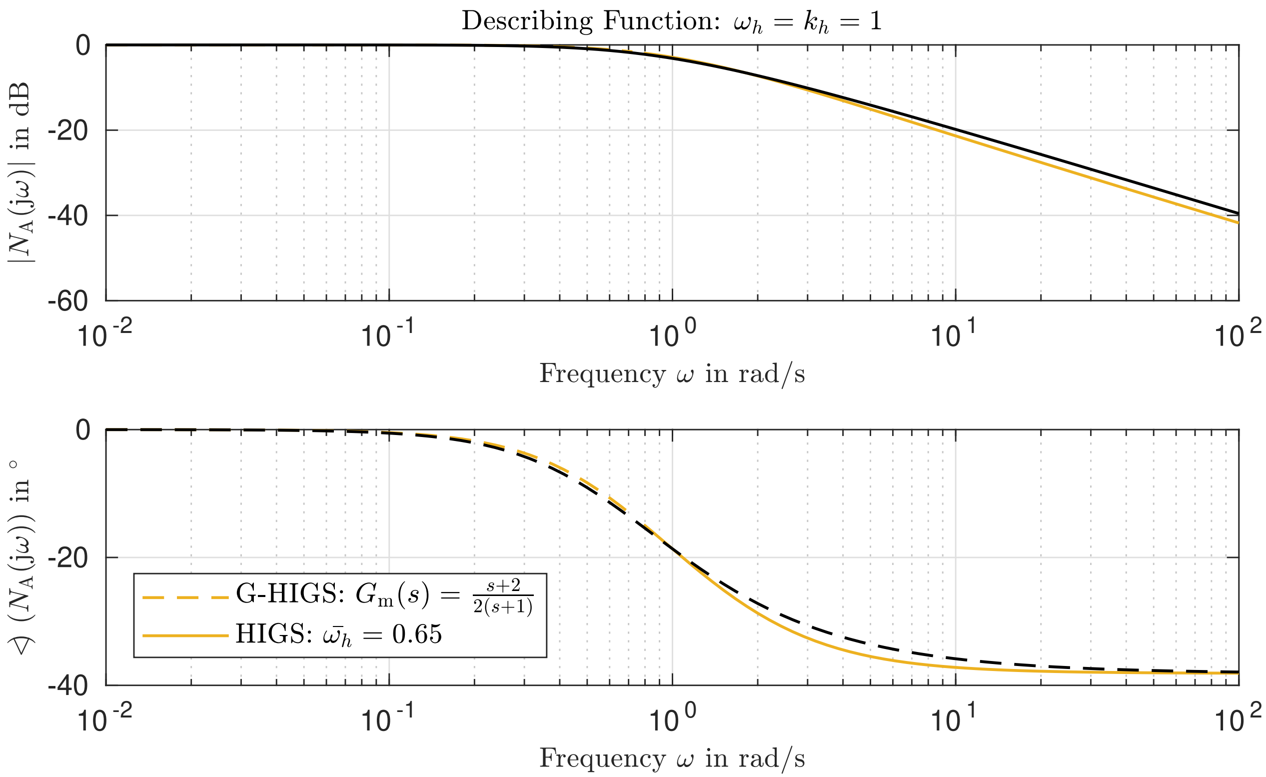

Simulation Example

Consider the unstable process to control without overshooting:

$$P(s) = \frac{(s+3)\omega^2}{(s-1)(s^2+2\zeta\omega s+\omega^2)}, \quad \omega = 10\pi, \zeta = \frac{3}{2}$$

and the HIGS ($\omega_h = 0.48, k_h = 0.6$) with $\omega_i = 10, \tau = 0.001$ and compensators

$$C_1(s) = \frac{s+\omega_c}{\omega_c(\tau s+1)}, \quad C_2(s) = \frac{\omega_i(\tau s+1)}{s(s+3)}$$

and the G-HIGS ($\omega_h = 0.48, k_h = 0.6, G_{\mathrm{m}}(s) = (s+3)^{-1}$) with $\omega_i = 10, \tau = 0.001$ and compensators

$$C_1(s) = \frac{s+\omega_c}{\omega_c(\tau s+1)}, \quad \tilde{C}_2(s) = \frac{1.25\omega_i(\tau s+1)}{s}$$

Simulation Example

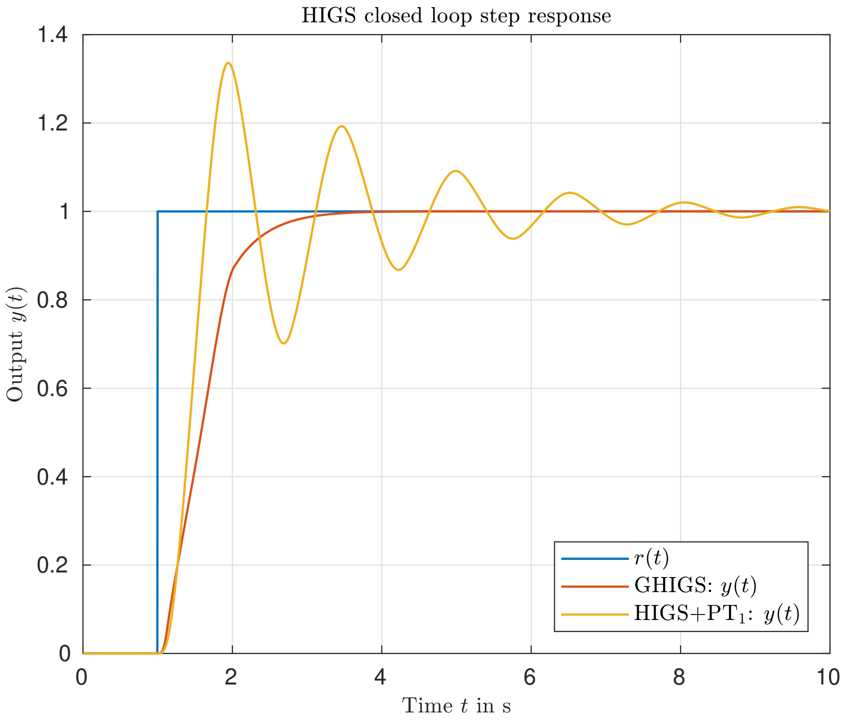

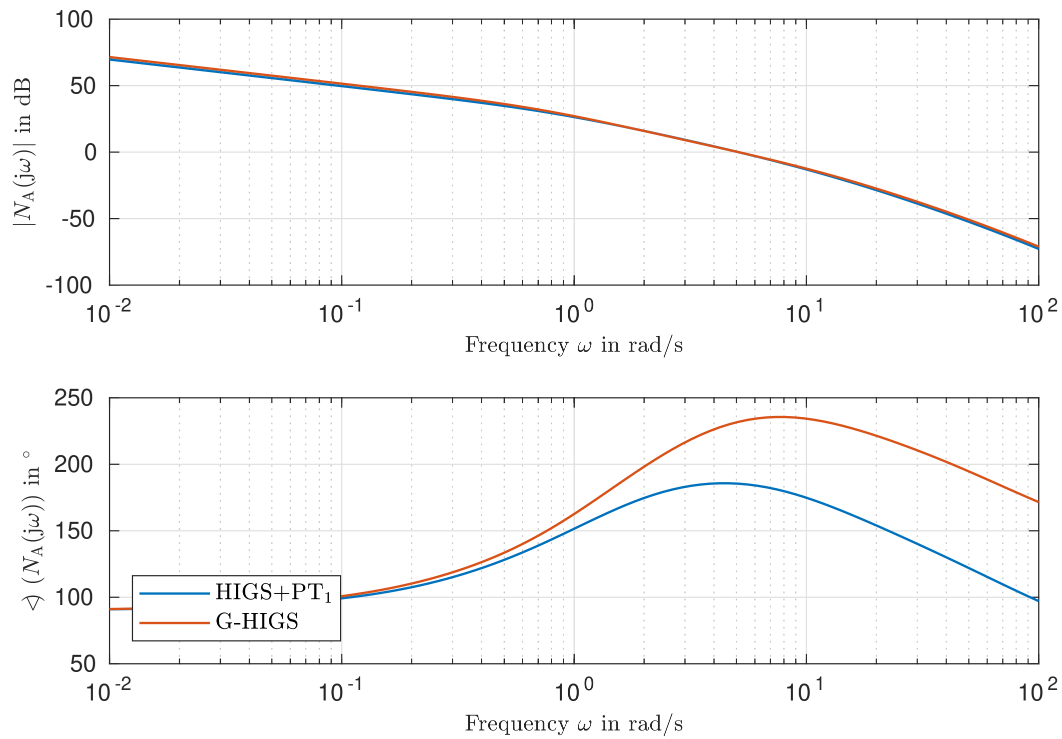

Conclusions and Future Work

Conclusions

- Additional reset system in combination with the integrator maintains the pahse advangate of the HIGS but adds damping for higher frequencies.
- Higher order harmonics are not dominant for the G-HIGS.

Outlock

- Improve describing function computation for lower frequency range.
- Include time regularization to avoid zeno behaviour.
- Improve stability analysis for less conservative results
- Show passivitiy for $D_{\mathrm{m}} = 0$.
- Include not BIBO stable memory systems (double HIGS).

Thank you!

\end{presentation}

\begin{questions}

Thank you!

\end{presentation}

\begin{questions}

Literature

Deenen, D. A., Sharif, B., van den Eijnden, S., Nijmeijer, H., Heemels, M., and Heertjes, M. (2021).
Projection-based integrators for improved motion control: Formalization, well-posedness and stability of hybrid integrator-gain systems.
Automatica, 133:109830.
tex.ids= Deenen21a.

Hosseini, S. A., Tavazoei, M. S., and HosseinNia, S. H. (2022).
Generalizing Hybrid Integrator-Gain Systems Using Fractional Calculus.
arXiv:2204.13544 [cs, eess].
arXiv: 2204.13544.

VIII. Efficient operation of pharmaceutical processes via model based approaches

presenter: Jakob Rehrl

Efficient operation of pharmaceutical processes via model based approaches

Selma Celikovic[1,2], Katrina Wilfling[1], Atabak Azimi[1,2], Jakob Rehrl[1,3]

[1]Research Center Pharmaceutical Engineering
[2]Institute of Automation and Control, Graz University of Technology
[3]Salzburg University of Applied Sciences, Department for Information Technologies and Digitalisation

10.9.2024

Salzburg University of Applied Sciences

Motivation

Effort spent in transition from **batch** to continuous manufacturing in previous years.

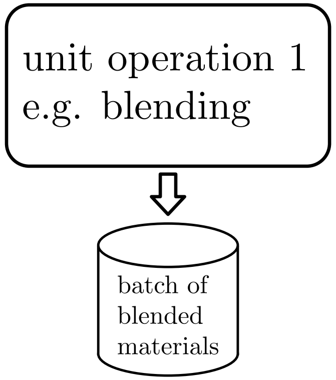

Motivation

Effort spent in transition from **batch** to continuous manufacturing in previous years.

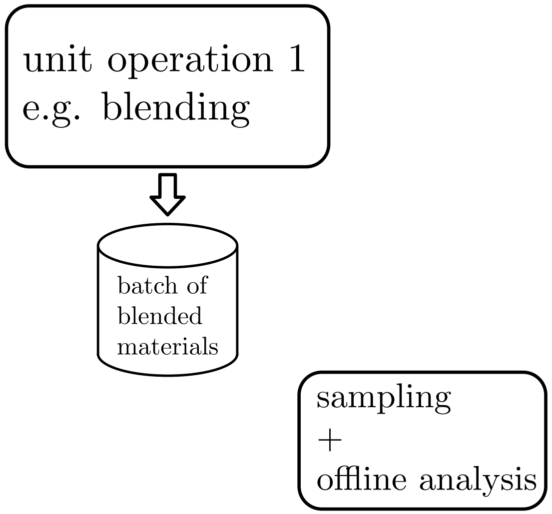

Motivation

Effort spent in transition from **batch** to continuous manufacturing in previous years.

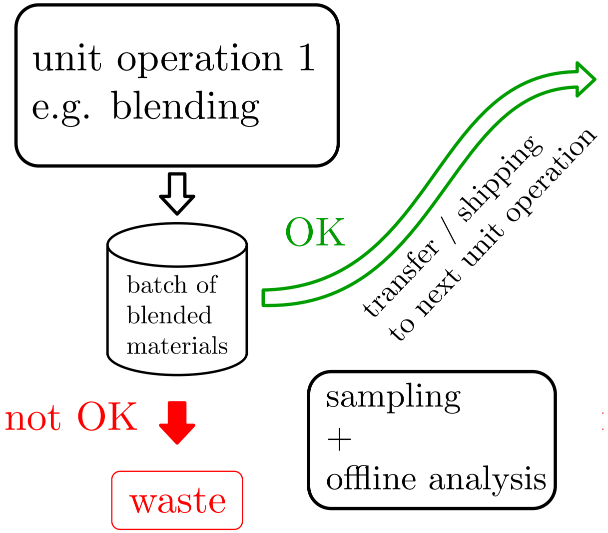

Motivation

Effort spent in transition from **batch** to continuous manufacturing in previous years.

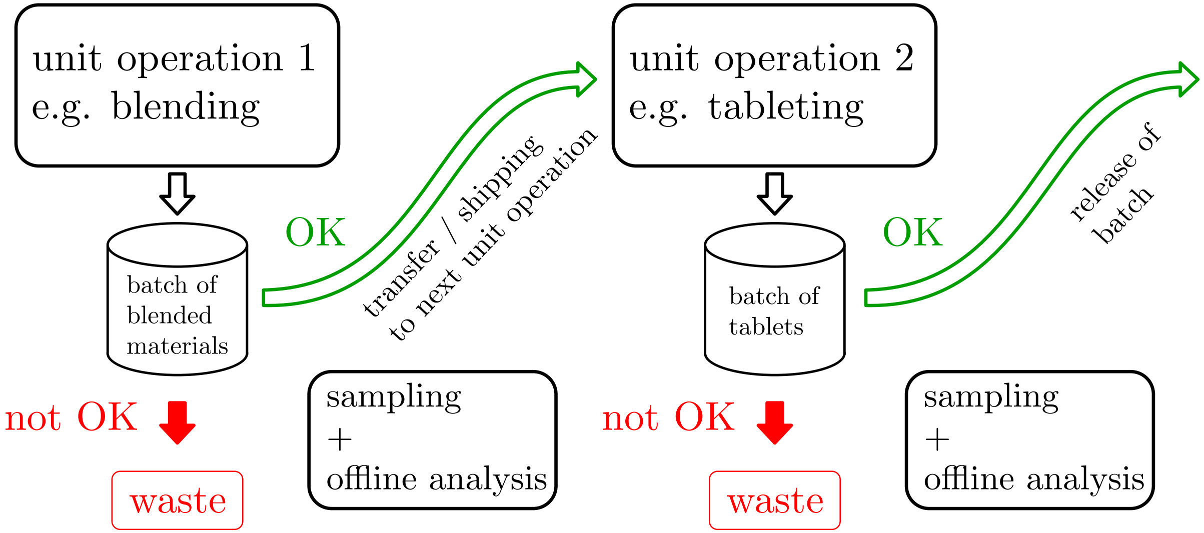

Motivation

Effort spent in transition from batch to **continuous** manufacturing in previous years.

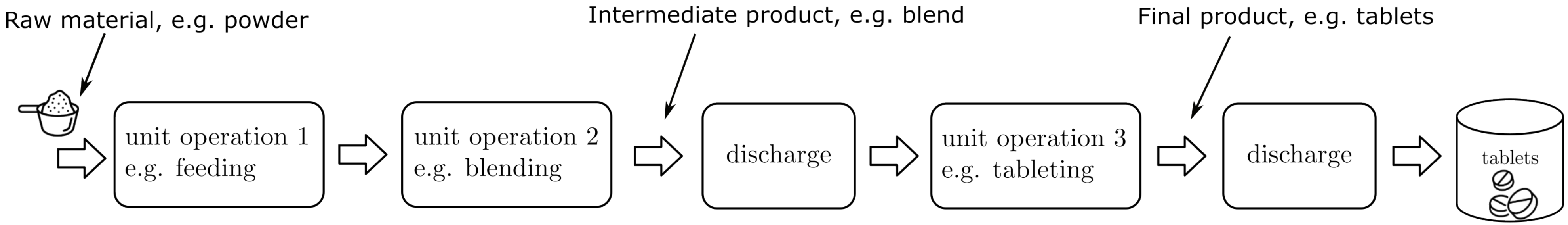

Motivation

Effort spent in transition from batch to **continuous** manufacturing in previous years.

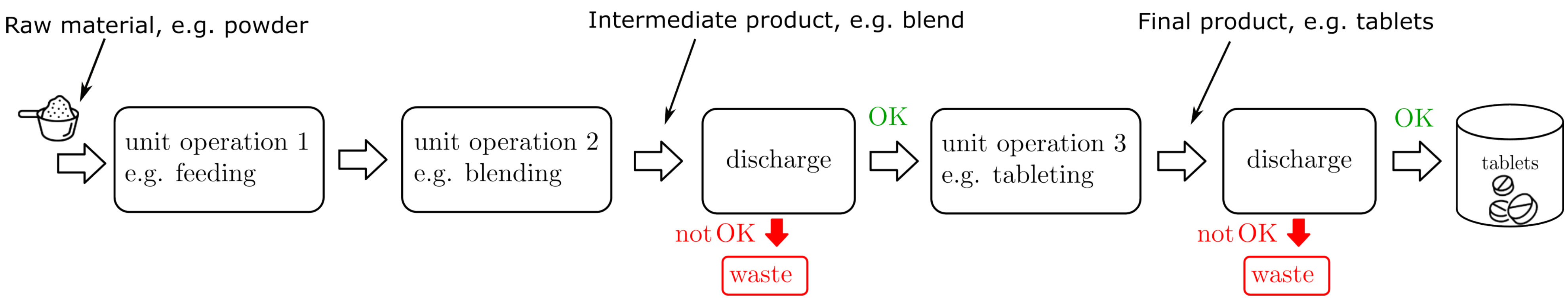

Motivation

Effort spent in transition from batch to **continuous** manufacturing in previous years.

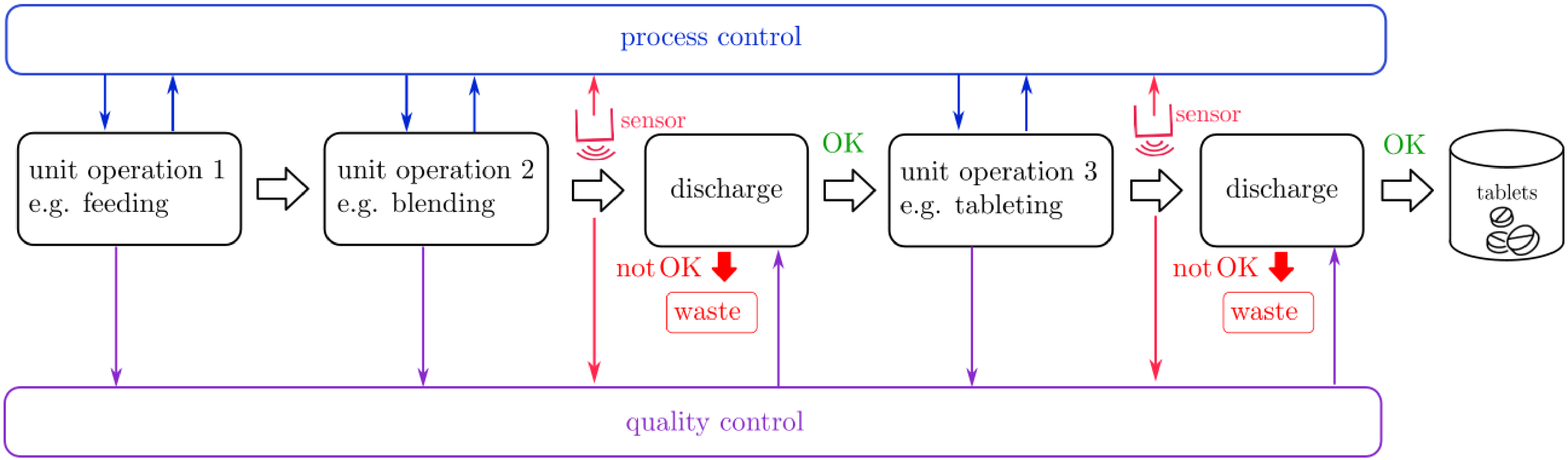

Motivation

Effort spent in transition from batch to **continuous** manufacturing in previous years

- to reduce production costs (small footprint of continuous manufacturing line vs. multiple batch processing units / sites),

Motivation

Effort spent in transition from batch to **continuous** manufacturing in previous years

- to reduce production costs (small footprint of continuous manufacturing line vs. multiple batch processing units / sites),
- to reduce production time (all unit operations at one site, no shipping),

Motivation

Effort spent in transition from batch to **continuous** manufacturing in previous years

- to reduce production costs (small footprint of continuous manufacturing line vs. multiple batch processing units / sites),
- to reduce production time (all unit operations at one site, no shipping),
- to enable alternative quality control concepts (real-time monitoring of process parameters and quality attributes, real-time release testing).

Example 1 - Primary manufacturing

Production of active pharmaceutical ingredients (APIs):

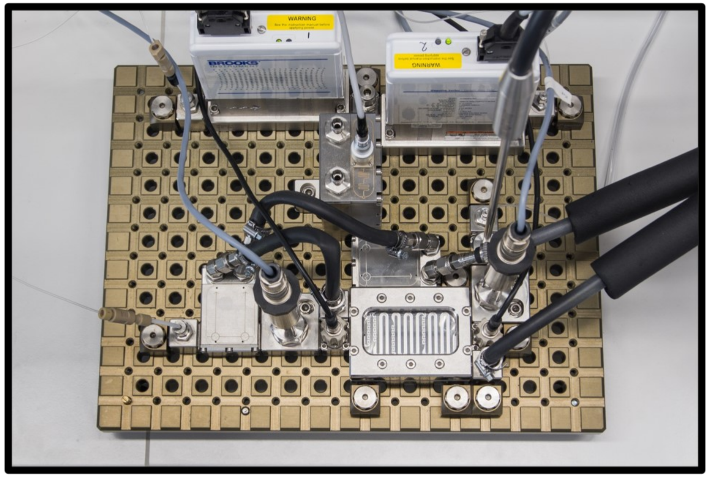

- Continuous chemical reaction

Example 1 - Primary manufacturing

Production of active pharmaceutical ingredients (APIs):

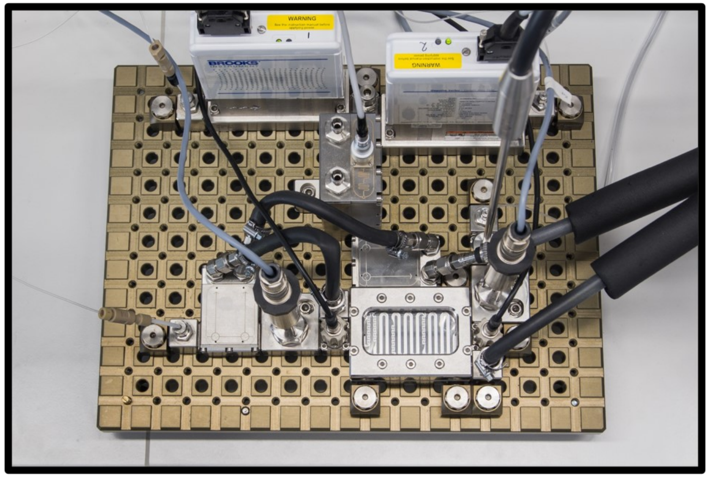

- Continuous chemical reaction
- Reduced production risks (small potentially explosive material in the process at a time)

Example 1 - Primary manufacturing

Production of active pharmaceutical ingredients (APIs):

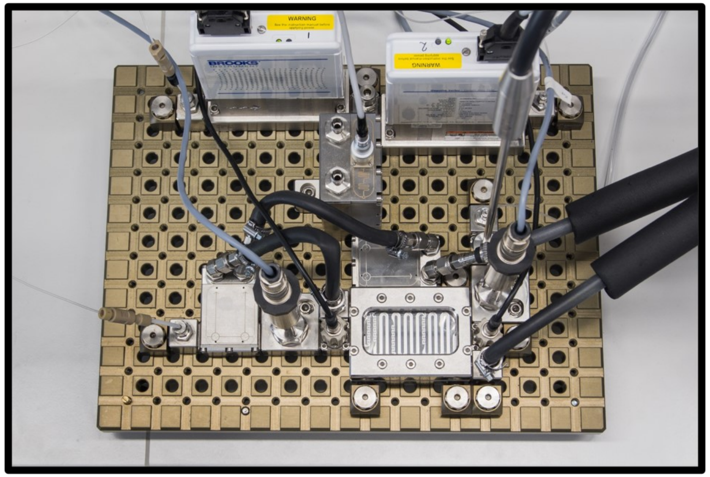

- Continuous chemical reaction
- Reduced production risks (small potentially explosive material in the process at a time)
- Enable exothermic reactions (good heat transfer in continuous reactors)

Production of active pharmaceutical ingredients (APIs):

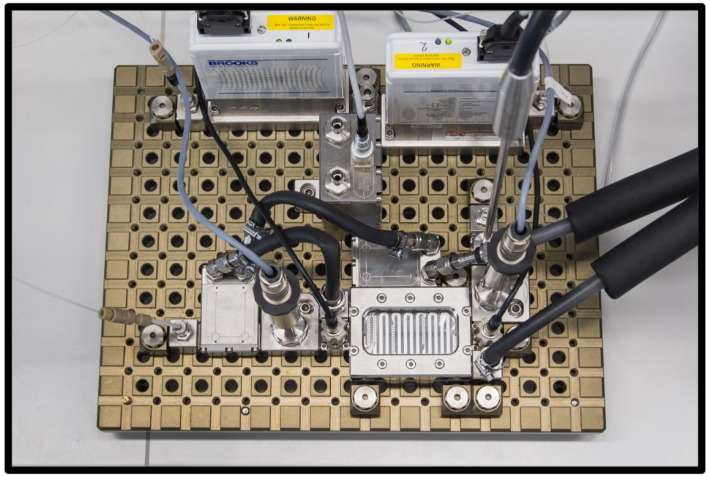

- Continuous chemical reaction
- Reduced production risks (small potentially explosive material in the process at a time)
- Enable exothermic reactions (good heat transfer in continuous reactors)
- Drive process settings / quality attributes to their optimal values in real-time

Example 2 - Secondary manufacturing

- Control of API concentration after the granulation unit

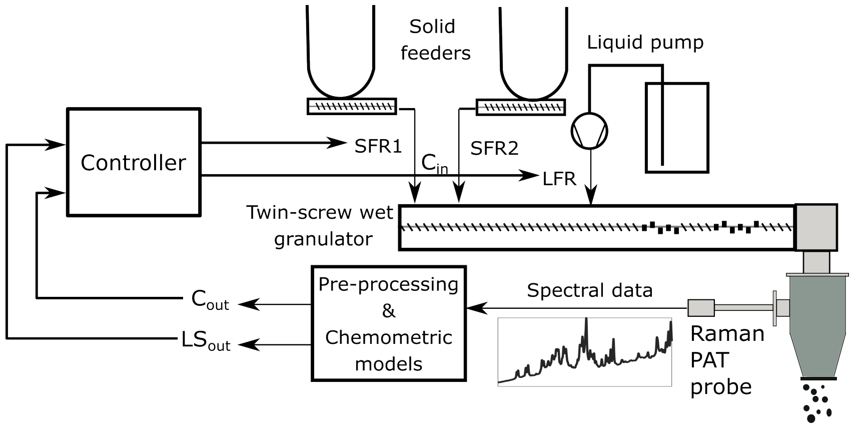

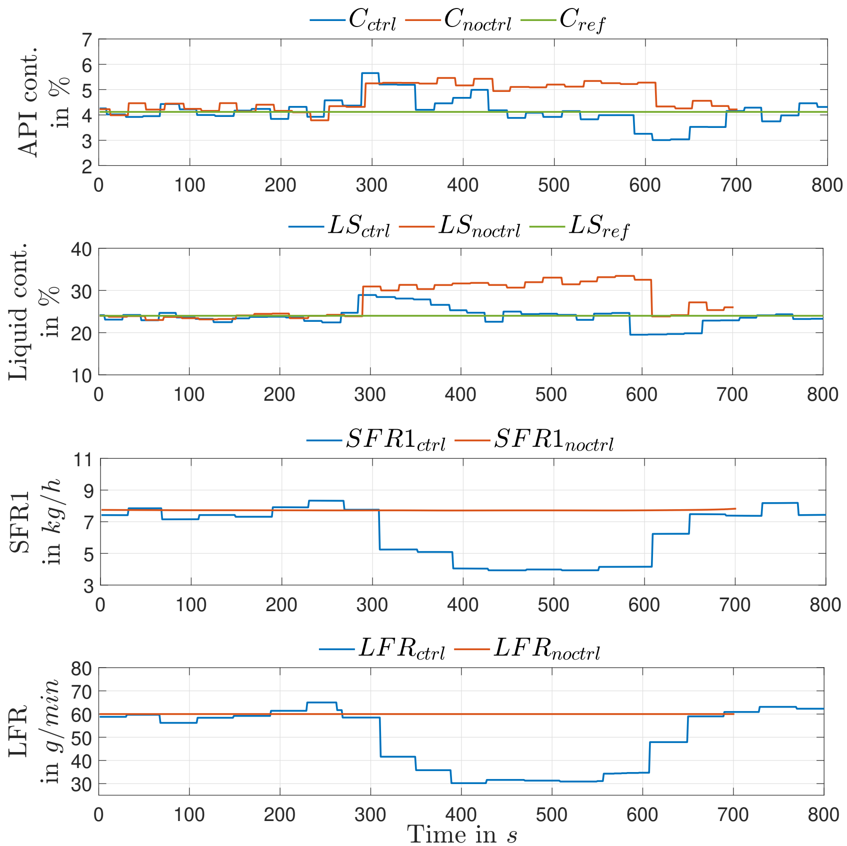

Selma Celikovic et al. "Development and Application of Control Concepts for Twin-Screw Wet Granulation in the ConsiGmaTM-25: Part 1 Granule Composition." In: *International Journal of Pharmaceutics* 657 (2024), p. 124124. ISSN: 0378-5173. DOI: https://doi.org/10.1016/j.ijpharm.2024.124124. URL: https://www.sciencedirect.com/science/article/pii/S0378517324003582

Example 2 - Secondary manufacturing

- Diversion of out-of-specification material

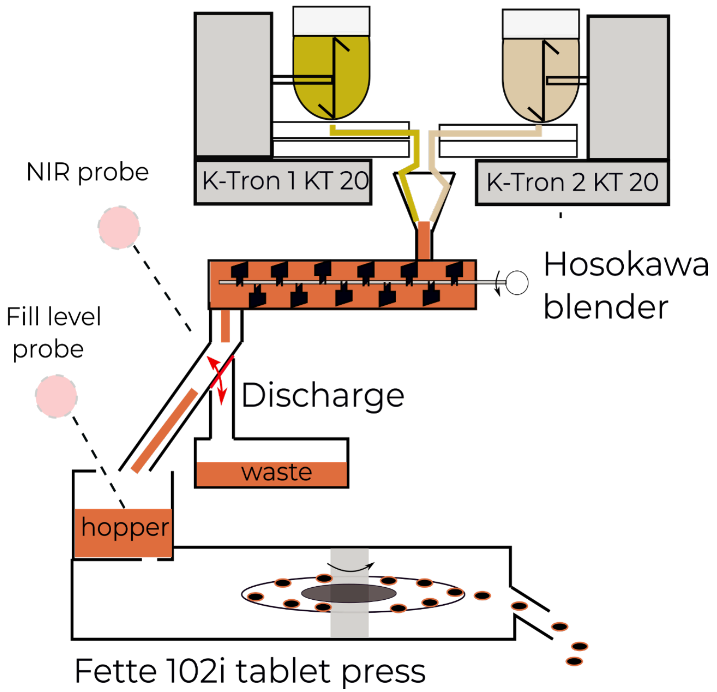

Example 2 - Secondary manufacturing

- Diversion of out-of-specification material

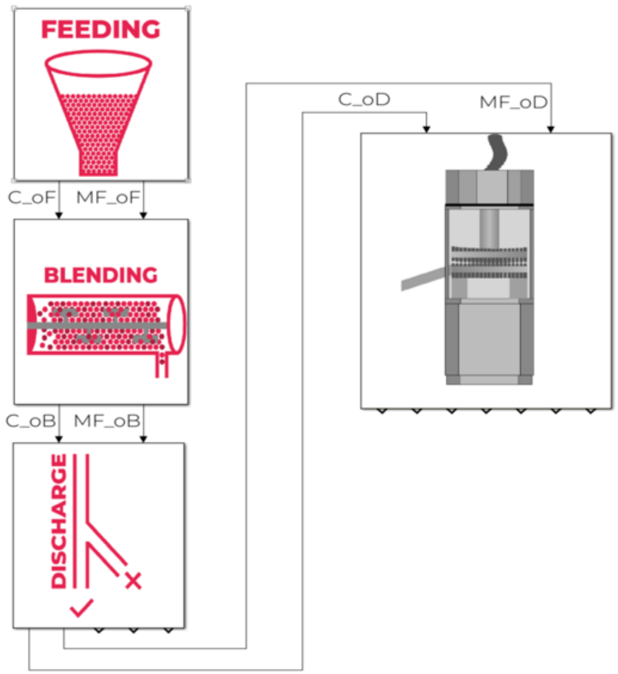

Example 2 - Secondary manufacturing

- Diversion of out-of-specification material

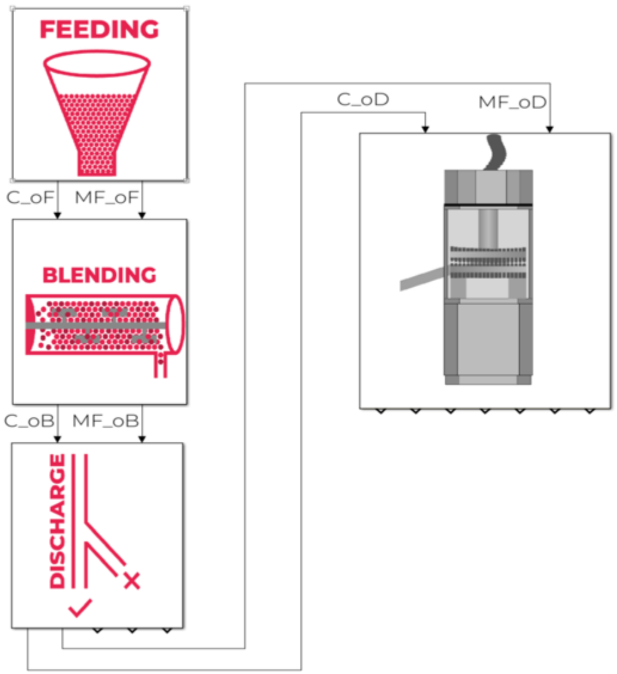

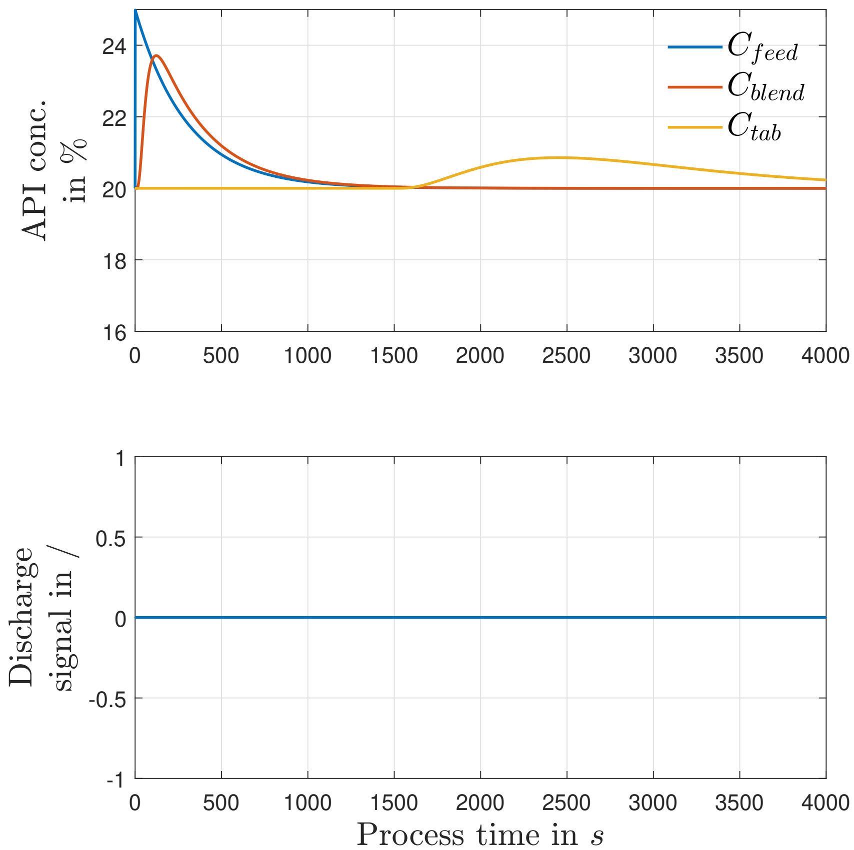

Example 2 - Secondary manufacturing

- Diversion of out-of-specification material

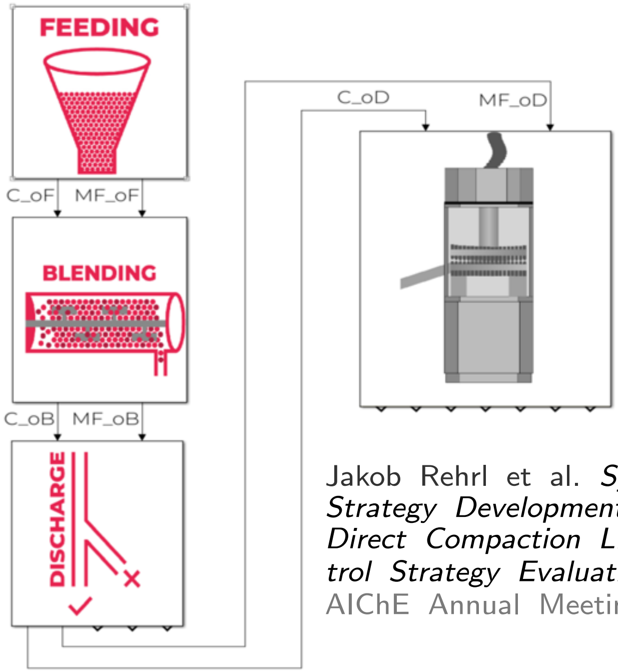

Jakob Rehrl et al. *Systematic Control Strategy Development for a Continuous Direct Compaction Line Via the Control Strategy Evaluation Tool (CET).* AIChE Annual Meeting 2022. 2022

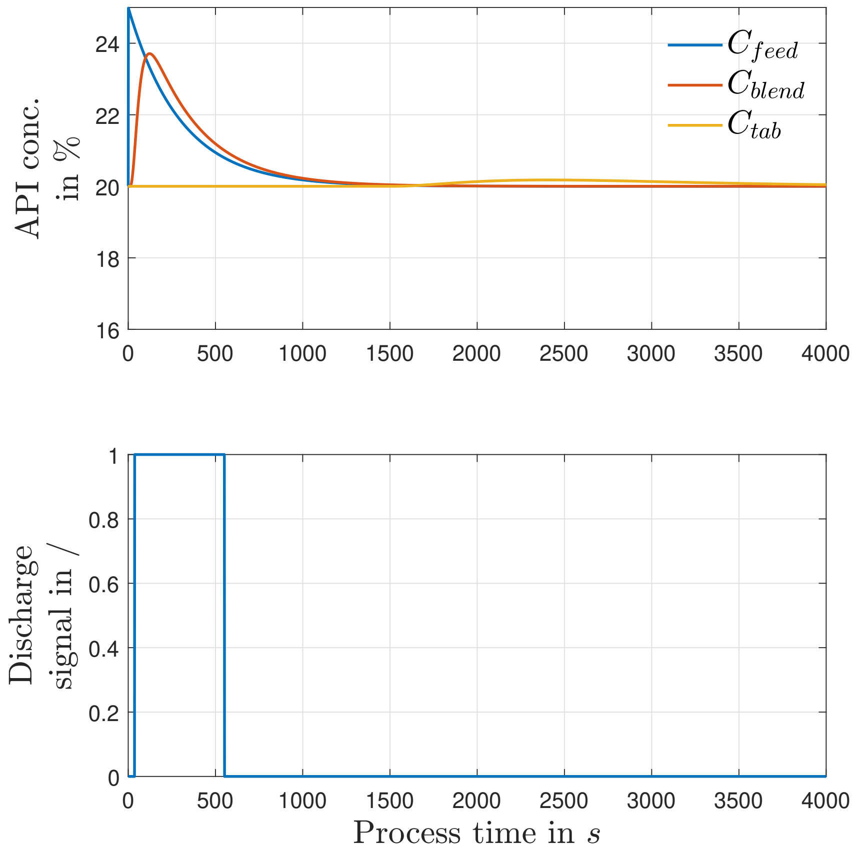

Example 2 - Secondary manufacturing

- Estimation of granule moisture in the dryer (soft-sensor)

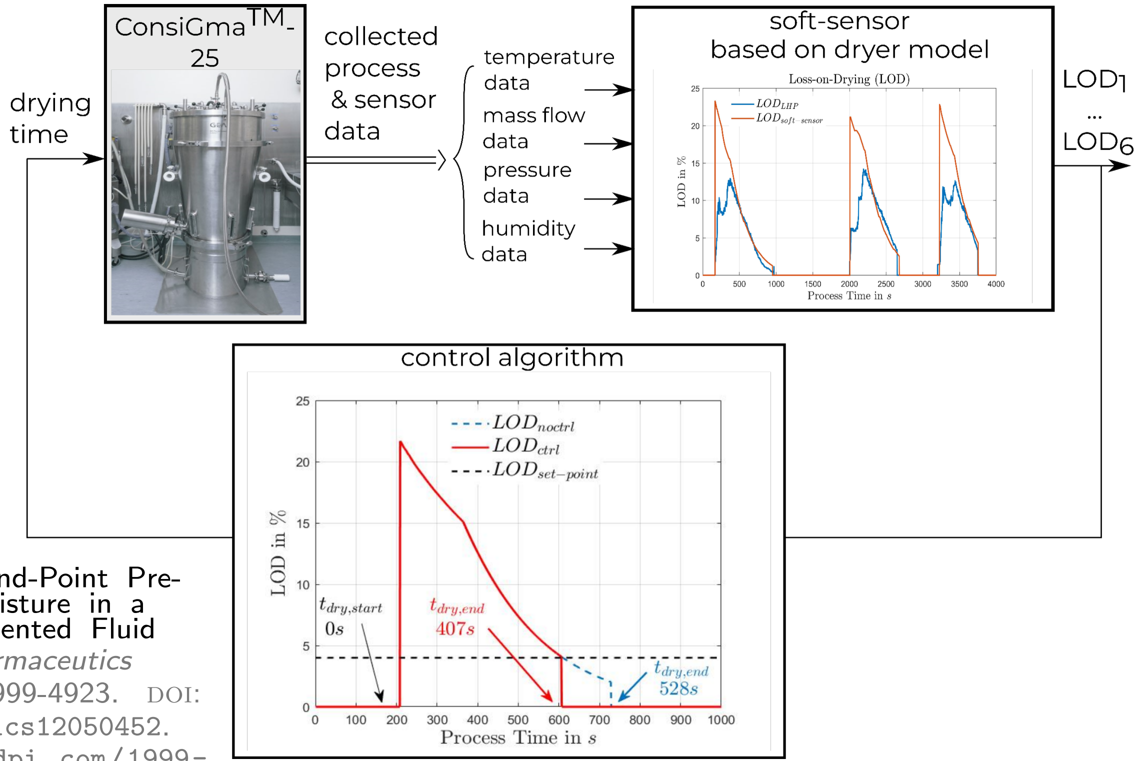

Jakob Rehrl et al. "End-Point Prediction of Granule Moisture in a ConsiGmaTM-25 Segmented Fluid Bed Dryer." In: *Pharmaceutics* 12.5 (2020). ISSN: 1999-4923. DOI: 10.3390/pharmaceutics12050452. URL: https://www.mdpi.com/1999-4923/12/5/452

Motivation

- Benefits of control strategies implemented in continuous processes are evident

Motivation

- Benefits of control strategies implemented in continuous processes are evident
- However, some processes are still operated in batch, e.g., *bioprocesses* used to produce biopharmaceuticals, e.g. insulin, mRNA
- What is the potential of applying model-based control strategies to batch-bioprocesses?

Investigated Process

E. coli (HMS174 (DE3)) (Novagen, Germany)

- Production of a protein (recombinant human superoxide dismutase)

Investigated Process

E. coli (HMS174 (DE3)) (Novagen, Germany)

- Production of a protein (recombinant human superoxide dismutase)
- Isopropyl-β-D-thiogalactopyranosid (IPTG) as inductor

Investigated Process

E. coli (HMS174 (DE3)) (Novagen, Germany)

- Production of a protein (recombinant human superoxide dismutase)
- Isopropyl-β-D-thiogalactopyranosid (IPTG) as inductor
- Processing takes place in a 20L batch reactor

Investigated Process

E. coli (HMS174 (DE3)) (Novagen, Germany)

- Production of a protein (recombinant human superoxide dismutase)
- Isopropyl-β-D-thiogalactopyranosid (IPTG) as inductor
- Processing takes place in a 20L batch reactor
- Typical approach: pre-defined process input profiles, obtained from Design of Expriments (DoE)

Investigated Process

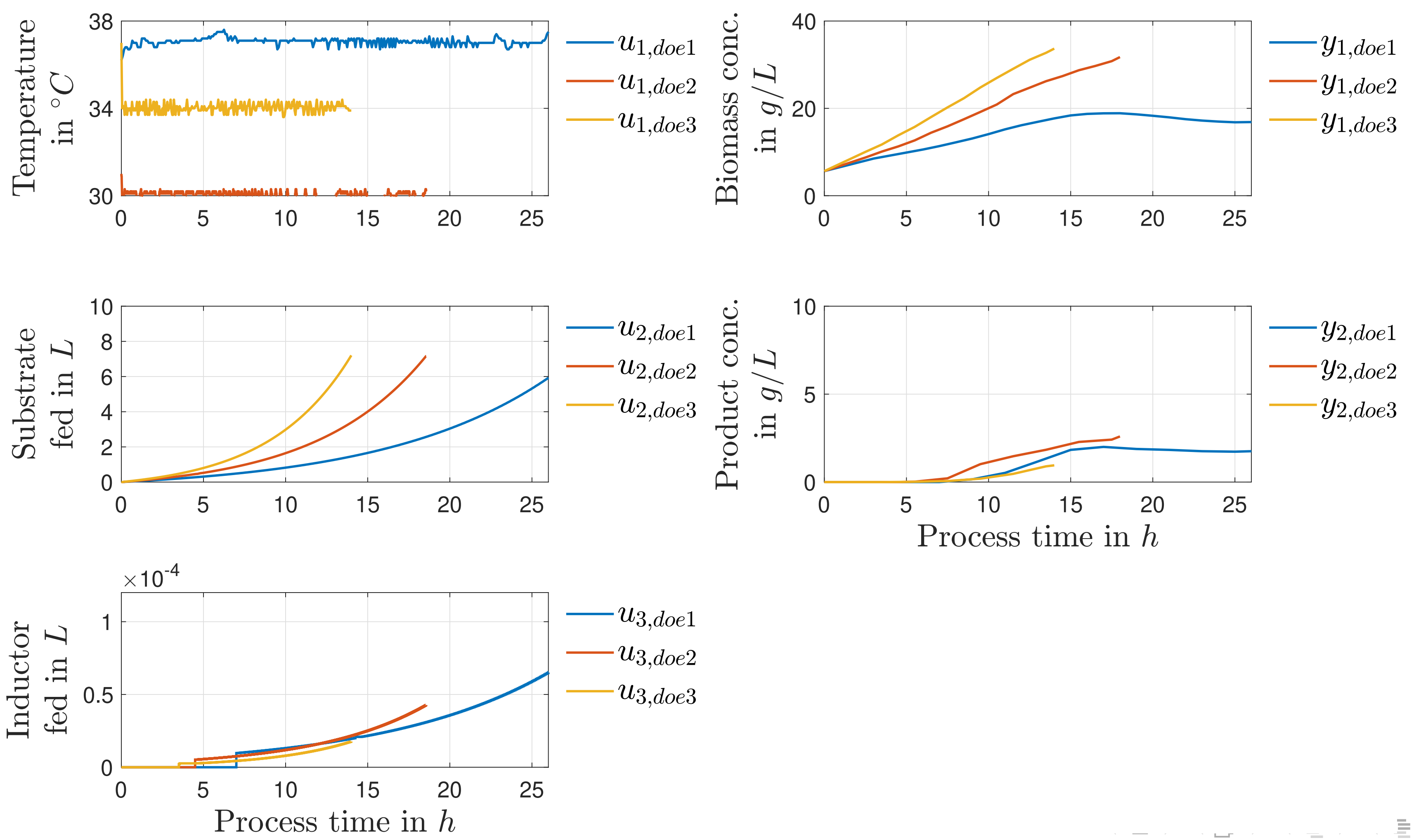

Investigated Process

Preparation + two phases:

- Preparation of 4 L medium containing 22.5 g of cell dry mass (CDM), i.e., biomass concentration $y_{1,0} = 5.625\, g/L$
- Phase 1:
  - Biomass growth to double the initial biomass concentration $y_{1,0}$
- Phase 2:
  - Production of desired substance (product), i.e., product concentration y_2

Investigated Process

Preparation + two phases:

- Preparation of 4 L medium containing 22.5 g of cell dry mass (CDM), i.e., biomass concentration $y_{1,0} = 5.625\, g/L$
- Phase 1:
  - Biomass growth to double the initial biomass concentration $y_{1,0}$
  - Process inputs: Temperature u_1, fed amount of glucose u_2
- Phase 2:
  - Production of desired substance (product), i.e., product concentration y_2
  - Process inputs: Temperature u_1, fed amount of glucose u_2, fed amount of inductor u_3

Typical Batch Profile

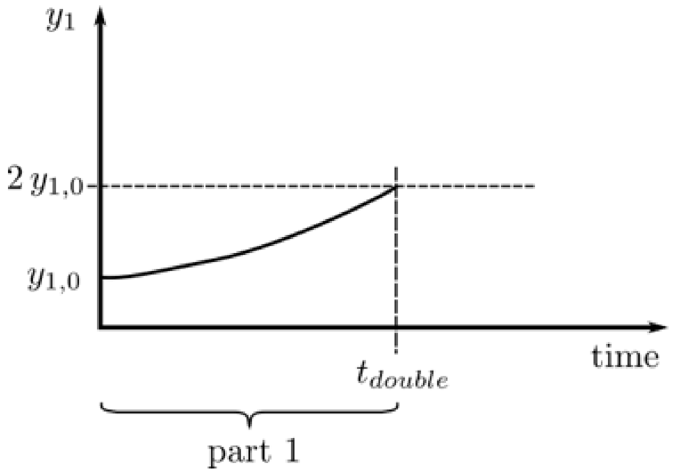

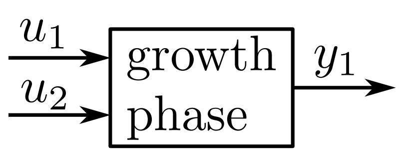

$$u_1(t) = \text{const.}$$

$$u_2(t) = y_{1,0}\,K_1\;(e^{\mu\,t} - 1)$$

$\mu \ldots$ growth rate in h^{-1}

Typical Batch Profile

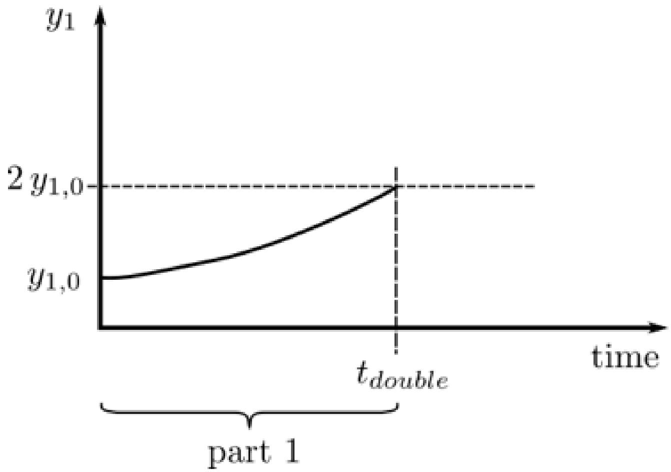

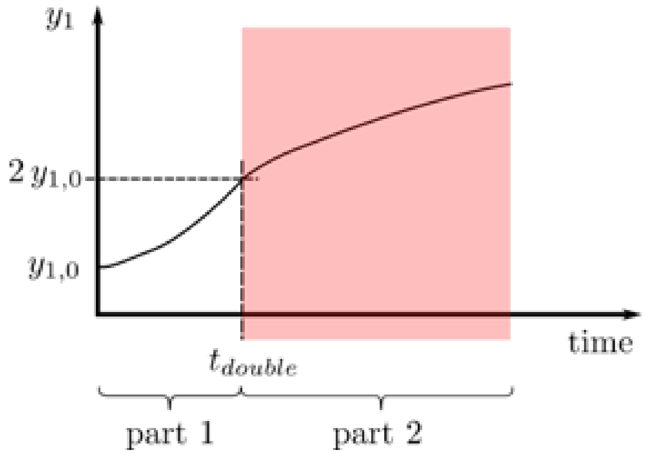

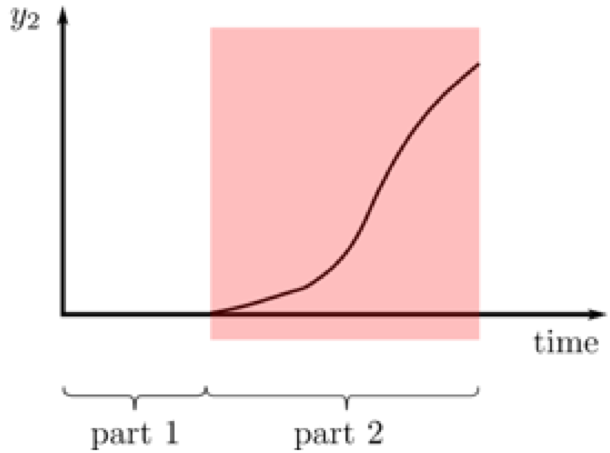

$u_1(t) = \text{const.}$

$u_2(t) = y_{1,0}\, K_1\ (e^{\mu\, t} - 1)$

$\mu \ldots$ growth rate in h^{-1}

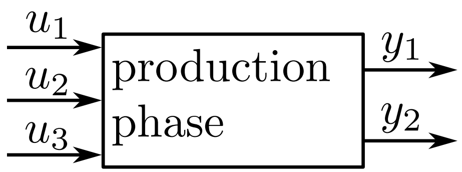

$u_1(t) = \text{const.}$

$u_2(t) = y_{1,0}\, K_1\ (e^{\mu\, t} - 1)$

$u_3(t) = y_{1,0}\, K_2\, e^{\mu\, t}\, k_{ind}$

$k_{ind} \ldots$ induction strength in μmol IPTG / g CDM

Typical Batch Profile

Traditional approach

- Test different settings of u_1, μ and k_{ind}, e.g., systematically via a DoE
- Select the best one (e.g., maximum product concentration after feeding 8L of glucose
- Run batch at the obtained u_1, $u_2 = f(\mu, t)$, $u_3 = f(\mu, k_{ind}, t)$

$$u_1(t) = \text{const.}$$

$$u_2(t) = y_{1,0}\, K_1\ (e^{\mu\, t} - 1)$$

$\mu \ldots$ growth rate in h^{-1}

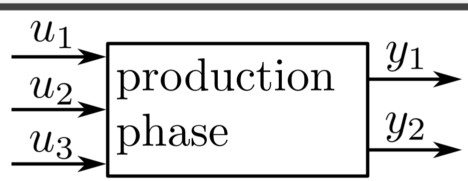

$$u_1(t) = \text{const.}$$

$$u_2(t) = y_{1,0}\, K_1\ (e^{\mu\, t} - 1)$$

$$u_3(t) = y_{1,0}\, K_2\, e^{\mu\, t}\, k_{ind}$$

$k_{ind} \ldots$ induction strength in μmol IPTG / g CDM

Typical Batch Profile

Traditional approach

- Test different settings of u_1, μ and k_{ind}, e.g., systematically via a DoE
- Select the best one (e.g., maximum product concentration after feeding 8L of glucose
- Run batch at the obtained u_1, $u_2 = f(\mu, t)$, $u_3 = f(\mu, k_{ind}, t)$

Questions

- Can variations of process inputs during batch processing yield better performance?
- What is an appropriate performance measure?
- What approach is useful to find the corresponding (input) profile?
- How can real-time process control be incorporated?

Can variations of process inputs during batch processing yield better performance?

- Recap: DoE is traditionally performed for u_1, μ, k_{ind}
- Three process inputs $\rightarrow$ 27 combinations for full-factorial with 3 levels each
- Experimental test of potential changes of any input during batch is practically infeasible
- Idea:
  - Develop process model (experimental data from DoE is available already)
  - Use process model to perform test runs / compute optimal input profile

What is an appropriate performance measure?

Potential targets:

- Minimize time to reach a certain amount of product y_2
- Maximize amount of product y_2 at a certain time / after 8L of glucose feed

Process model

- Mechanistic model is not available / difficult to develop
- Purely data driven model requires a lot of identification data (goal: available DoE data should allow model creation)
- **Hybrid model** of the fermentation will be used

Process model

- Mechanistic model is not available / difficult to develop
- Purely data driven model requires a lot of identification data (goal: available DoE data should allow model creation)
- **Hybrid model** of the fermentation will be used

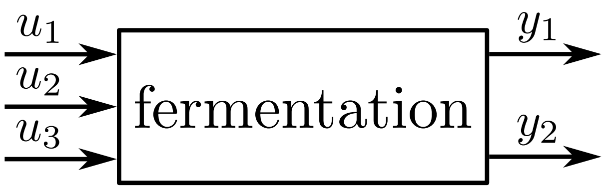

y_1	...	biomass concentration
y_2	...	product concentration
u_1	...	reactor temperature
u_2	...	fed glucose
u_3	...	fed inductor

Process Model

Model equations [BSD20]:

- Biomass concentration:
  $\frac{dy_1}{dt} = \mu\, y_1 - D\, y_1$

- Product concentration:
  $\frac{dy_2}{dt} = \vartheta\, y_1\, I_{y/n} - D\, y_2$

[BSD20] . . . Benjamin Bayer, Gerald Striedner, and Mark Duerkop. "Hybrid Modeling and Intensified DoE: An Approach to Accelerate Upstream Process Characterization." In: *Biotechnology Journal* 15.9 (2020-06). ISSN: 1860-7314. DOI: 10.1002/biot.202000121

Process Model

Model equations [BSD20]:

- Biomass concentration:
  $\frac{dy_1}{dt} = \mu\, y_1 - D\, y_1$
- Product concentration:
  $\frac{dy_2}{dt} = \vartheta\, y_1\, I_{y/n} - D\, y_2$

D	...	dilution (feeding rate / reactor volume)
μ	...	biomass growth rate
ϑ	...	product growth rate
$I_{y/n}$	...	1 inductor present, 0 no inductor present

[BSD20] ... Benjamin Bayer, Gerald Striedner, and Mark Duerkop. "Hybrid Modeling and Intensified DoE: An Approach to Accelerate Upstream Process Characterization." In: *Biotechnology Journal* 15.9 (2020-06). ISSN: 1860-7314. DOI: 10.1002/biot.202000121

Process Model

Model equations [BSD20]:

- Biomass concentration:
  $\frac{dy_1}{dt} = \mu\, y_1 - D\, y_1$ ⟵ mechanistic

D	...	dilution (feeding rate / reactor volume)
μ	...	biomass growth rate
ϑ	...	product growth rate
$I_{y/n}$	...	1 inductor present, 0 no inductor present

- Product concentration:
  $\frac{dy_2}{dt} = \vartheta\, y_1\, I_{y/n} - D\, y_2$ ⟵ mechanistic

[BSD20] ... Benjamin Bayer, Gerald Striedner, and Mark Duerkop. "Hybrid Modeling and Intensified DoE: An Approach to Accelerate Upstream Process Characterization." In: *Biotechnology Journal* 15.9 (2020-06). ISSN: 1860-7314. DOI: 10.1002/biot.202000121

Process Model

Model equations [BSD20]:

- Biomass concentration:
  $\frac{dy_1}{dt} = \mu\, y_1 - D\, y_1$ ⟵ mechanistic

  $\mu(u_1, u_2, u_3, y_1, y_2)$

D	...	dilution (feeding rate / reactor volume)
μ	...	biomass growth rate
ϑ	...	product growth rate
$I_{y/n}$	...	1 inductor present, 0 no inductor present

- Product concentration:
  $\frac{dy_2}{dt} = \vartheta\, y_1\, I_{y/n} - D\, y_2$ ⟵ mechanistic

  $\vartheta(u_1, u_2, u_3, y_1, y_2)$

[BSD20] ... Benjamin Bayer, Gerald Striedner, and Mark Duerkop. "Hybrid Modeling and Intensified DoE: An Approach to Accelerate Upstream Process Characterization." In: *Biotechnology Journal* 15.9 (2020-06). ISSN: 1860-7314. DOI: 10.1002/biot.202000121

Process Model

Model equations [BSD20]:

- Biomass concentration:
  $\frac{dy_1}{dt} = \mu\, y_1 - D\, y_1$
  mechanistic
  $\mu(u_1, u_2, u_3, y_1, y_2)$

D	...	dilution (feeding rate / reactor volume)
μ	...	biomass growth rate
ϑ	...	product growth rate
$I_{y/n}$	...	1 inductor present, 0 no inductor present

- Product concentration:
  $\frac{dy_2}{dt} = \vartheta\, y_1\, I_{y/n} - D\, y_2$
  mechanistic
  $\vartheta(u_1, u_2, u_3, y_1, y_2)$

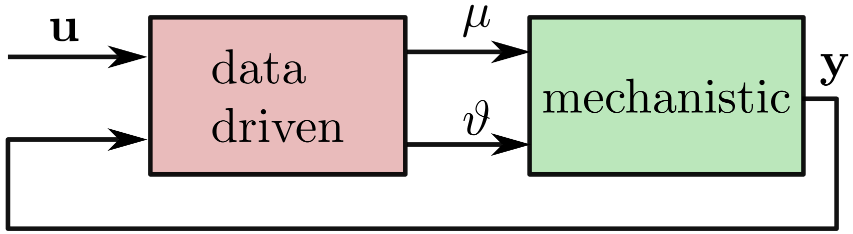

[BSD20] ... Benjamin Bayer, Gerald Striedner, and Mark Duerkop. "Hybrid Modeling and Intensified DoE: An Approach to Accelerate Upstream Process Characterization." In: *Biotechnology Journal* 15.9 (2020-06). ISSN: 1860-7314. DOI: 10.1002/biot.202000121

Process Model

Discrete time implementation of the model + parametrization via [Nov]:

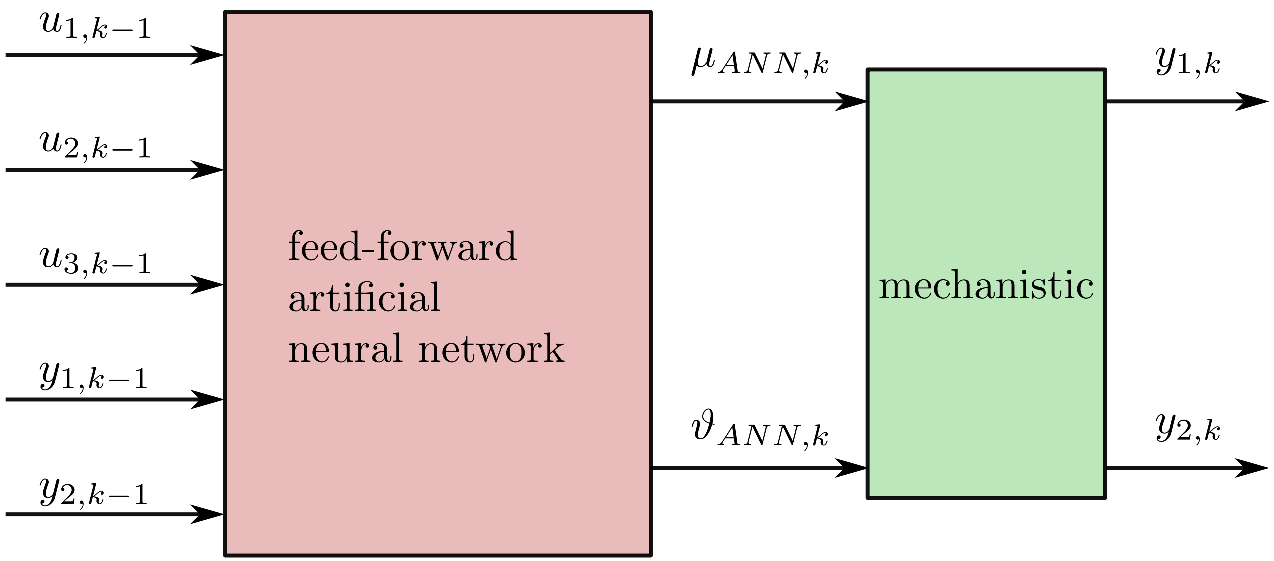

[Nov] . . . Novasign. *Hybrid Modeling Toolbox*. URL: `https://docs.novasign.at/toolbox/index.html` (visited on 08/14/2024)

Identification Data - Training

- Design of experiments of 32 batches
  $T = \{30, 34, 37\}$, $\mu = \{0.1, 0.15, 0.2\}$,
  $k_{ind} = \{0.2, 0.5, 0.9\} \rightarrow 27 + 5$ replicates

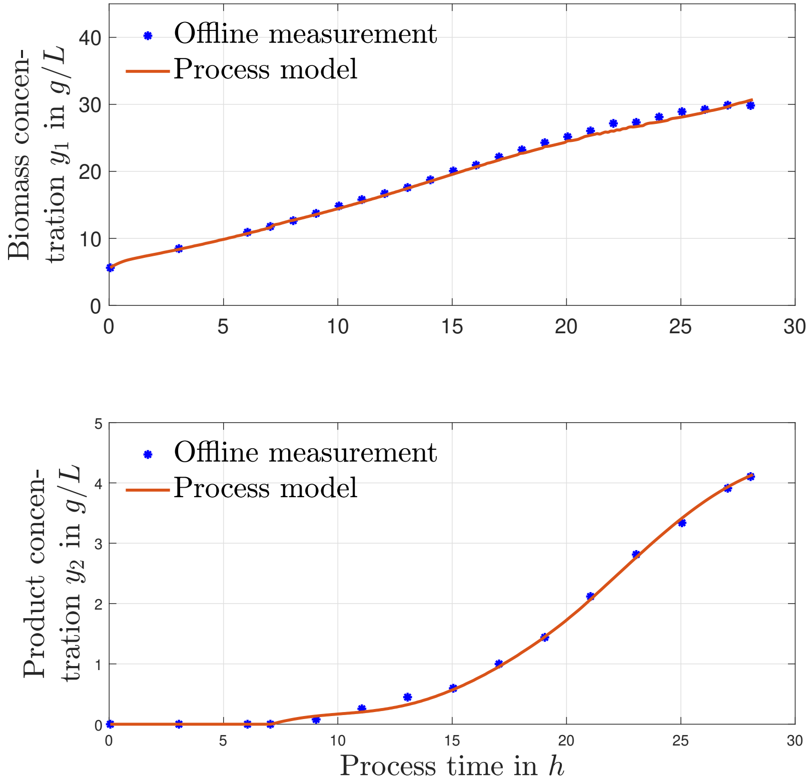

Identification Data - Training

- Design of experiments of 32 batches
  $T = \{30, 34, 37\}$, $\mu = \{0.1, 0.15, 0.2\}$,
  $k_{ind} = \{0.2, 0.5, 0.9\} \rightarrow 27 + 5$ replicates
- Training of an ANN [Nov]

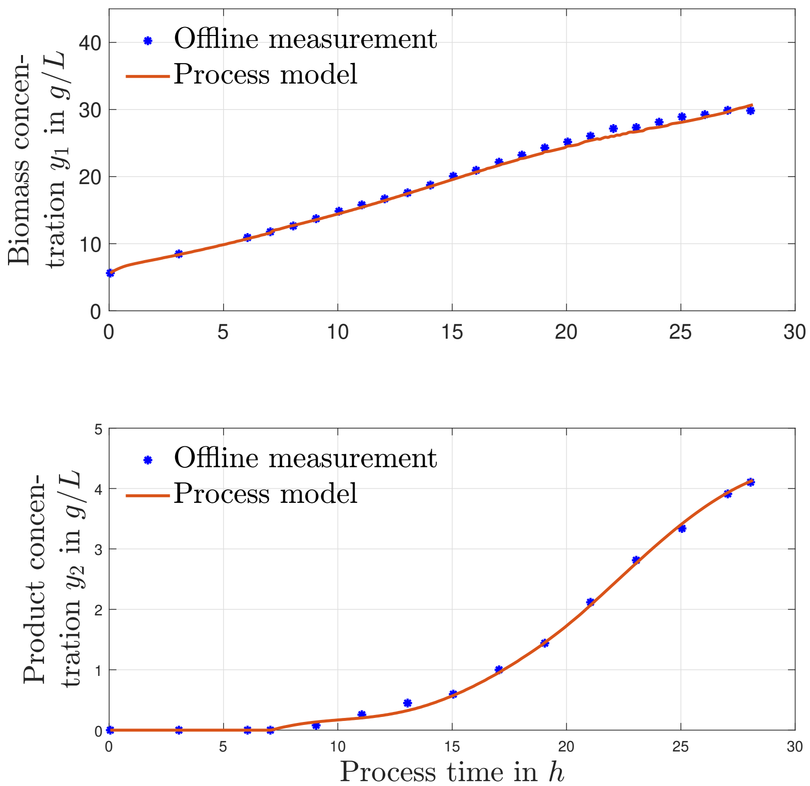

Identification Data - Test

- Design of experiments of 32 batches
  $T = \{30, 34, 37\}$, $\mu = \{0.1, 0.15, 0.2\}$,
  $k_{ind} = \{0.2, 0.5, 0.9\} \to 27 + 5$ replicates
- Training of an ANN [Nov]

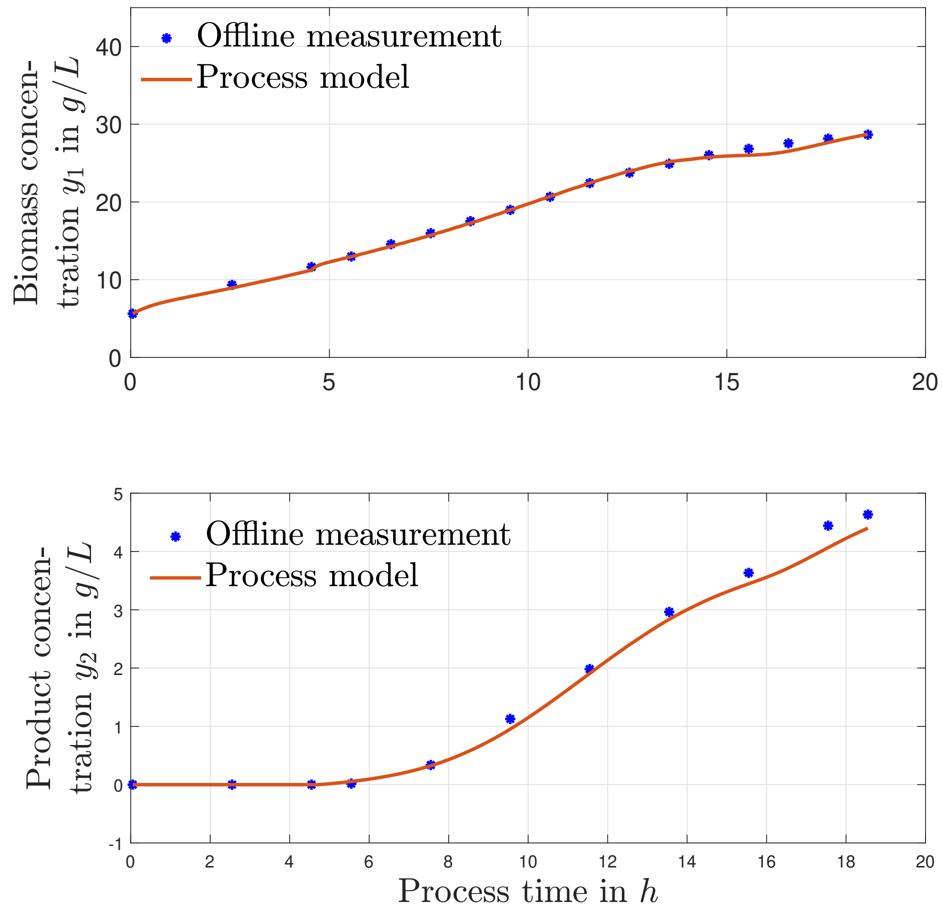

Optimal trajectory

- Goal: maximize amount of product y_2 at a certain time / after 8L of glucose feed

Optimal trajectory

- Goal: maximize amount of product y_2 at a certain time / after 8L of glucose feed
- Recall: two phases $\rightarrow$ considered separately

Optimal trajectory

- Goal: maximize amount of product y_2 at a certain time / after 8L of glucose feed
- Recall: two phases $\rightarrow$ considered separately
- Phase 1: minimize time to double biomass concentration:

$$\begin{aligned}
&min_{u_1,u_2} t_{phase1}\\
&\text{s.t. } y_1(t_{phase1}) \geq 2\, y_{1,0}\\
&\mathbf{u} \in \text{“DoE”}
\end{aligned}$$

Optimal trajectory

- Phase 2: maximize amount of product y_2 at a certain time / after 8L of glucose feed

Optimal trajectory

- Phase 2: maximize amount of product y_2 at a certain time / after 8L of glucose feed
- $$\begin{aligned} & min_{u_1,u_2,u_3} \quad -y_2(t_{end}) \\ \text{s.t.} \;\; & u_2(t_{end}) \leq 8 \\ & t_{end} \leq t_{max} \\ & \mathbf{u} \in \text{``DoE''} \end{aligned}$$

Optimal trajectory

- Phase 2: maximize amount of product y_2 at a certain time / after 8L of glucose feed
- $$\begin{aligned} & min_{u_1,u_2,u_3} \quad -y_2(t_{end}) \\ \text{s.t.} \quad & u_2(t_{end}) \leq 8 \\ & t_{end} \leq t_{max} \\ & \mathbf{u} \in \text{“DoE”} \end{aligned}$$
- Remark 1: $t_{max} = 350 \rightarrow > 1000$ optimization variables + nonlinear constraints "DoE"

Optimal trajectory

- Phase 2: maximize amount of product y_2 at a certain time / after 8L of glucose feed
- $$\begin{aligned} & min_{u_1,u_2,u_3} \quad -y_2(t_{end}) \\ & \text{s.t. } u_2(t_{end}) \leq 8 \\ & \qquad t_{end} \leq t_{max} \\ & \qquad \mathbf{u} \in \text{“DoE”} \end{aligned}$$
- Remark 1: $t_{max} = 350 \rightarrow > 1000$ optimization variables + nonlinear constraints "DoE"
- Remark 2: possibly, re-computation of optimal trajectories during batch required

Optimal trajectory - setup of the optimization problem

- Recall DoE during phase 2
  - $u_2(t) = y_{1,0}\left(e^{\mu\, t} - 1\right)$
  - $u_3(t) = y_{1,0}e^{\mu\, t}k_{ind}$

Optimal trajectory - setup of the optimization problem

- Recall DoE during phase 2
  - $u_2(t) = y_{1,0}\,(e^{\mu\,t} - 1)$
  - $u_3(t) = y_{1,0}e^{\mu\,t}k_{ind}$
- Idea: split phase 2 into sections,
  - Choose μ and k_{ind} for each section, i.e., $\mu(t) = \mu_1, k_{ind}(t) = k_1 \quad \text{for} \quad t_{start} \leq t < t_1,$ $\mu(t) = \mu_2, k_{ind}(t) = k_2 \quad \text{for} \quad t_1 \leq t < t_2, \ldots$

Optimal trajectory - setup of the optimization problem

- Recall DoE during phase 2
  - $u_2(t) = y_{1,0}\,(e^{\mu\, t} - 1)$
  - $u_3(t) = y_{1,0}e^{\mu\, t}k_{ind}$
- Idea: split phase 2 into sections,
  - Choose μ and k_{ind} for each section, i.e., $\mu(t) = \mu_1, k_{ind}(t) = k_1 \quad \text{for} \quad t_{start} \leq t < t_1$, $\mu(t) = \mu_2, k_{ind}(t) = k_2 \quad \text{for} \quad t_1 \leq t < t_2, \ldots$
  - Similar approach for u_1, linear interpolation between points $(\tilde{t}, T_1)$ and $(\tilde{t}_2, T_2)$ etc.

Optimal trajectory - setup of the optimization problem

- Recall DoE during phase 2
  - $u_2(t) = y_{1,0}\,(e^{\mu\, t} - 1)$
  - $u_3(t) = y_{1,0} e^{\mu\, t} k_{ind}$
- Idea: split phase 2 into sections,
  - Choose μ and k_{ind} for each section, i.e., $\mu(t) = \mu_1, k_{ind}(t) = k_1 \quad \text{for} \quad t_{start} \le t < t_1,$ $\mu(t) = \mu_2, k_{ind}(t) = k_2 \quad \text{for} \quad t_1 \le t < t_2, \ldots$
  - Similar approach for u_1, linear interpolation between points $(\tilde{t}, T_1)$ and $(\tilde{t}_2, T_2)$ etc.
  - Find optimal time points + values, i.e., $\mathbf{x} = [\tilde{t}_1, \ldots, \tilde{t}_{nT+1}, T_1, \ldots, T_{nT}, t_1, \ldots t_{nP}, \mu_1, \ldots \mu_{nP+1}, k_1, \ldots, k_{nP+1}]$

Optimal trajectory - setup of the optimization problem

- Recall DoE during phase 2
  - $u_2(t) = y_{1,0}\,(e^{\mu\,t} - 1)$
  - $u_3(t) = y_{1,0}e^{\mu\,t}k_{ind}$
- Idea: split phase 2 into sections,
  - Choose μ and k_{ind} for each section, i.e., $\mu(t) = \mu_1, k_{ind}(t) = k_1 \quad \text{for} \quad t_{start} \leq t < t_1$, $\mu(t) = \mu_2, k_{ind}(t) = k_2 \quad \text{for} \quad t_1 \leq t < t_2, \ldots$
  - Similar approach for u_1, linear interpolation between points $(\tilde{t}, T_1)$ and $(\tilde{t}_2, T_2)$ etc.
  - Find optimal time points + values, i.e., $\mathbf{x} = [\tilde{t}_1, \ldots, \tilde{t}_{nT+1}, T_1, \ldots, T_{nT}, t_1, \ldots t_{nP}, \mu_1, \ldots \mu_{nP+1}, k_1, \ldots, k_{nP+1}]$

$$
\begin{aligned}
min_{\mathbf{x}} \quad & -y_2(t_{end}) + \text{“}biopenalty\text{''} \\
\text{s.t.} \quad & u_2(t_{end}) \leq 8 \\
& t_{end} \leq t_{max} \\
& \mathbf{x}_{min} \leq \mathbf{x} \leq \mathbf{x_{max}}
\end{aligned}
$$

Optimal trajectory - example $n_T = 3,\ n_P = 2$

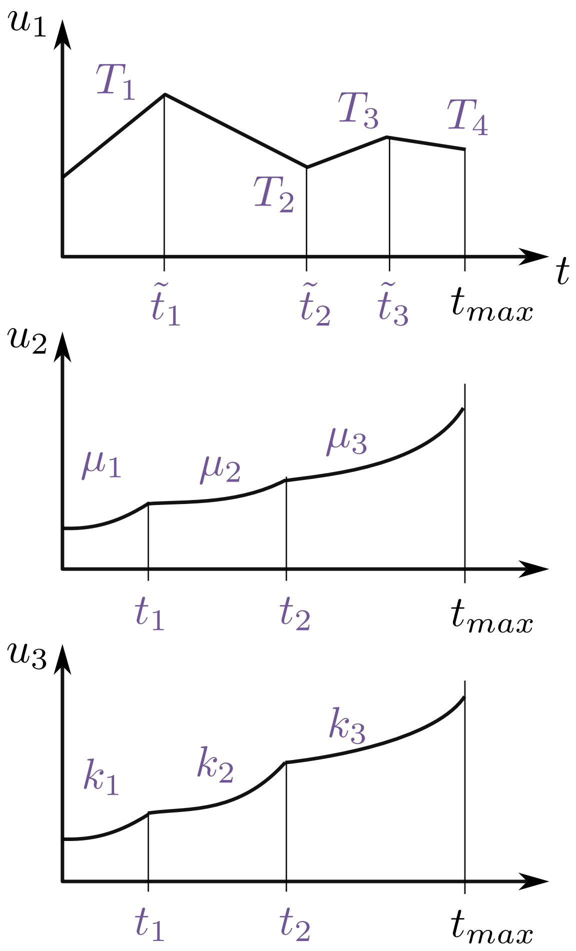

$$\mathbf{x} = \begin{bmatrix} \tilde{t}_1 \\ \tilde{t}_2 \\ \tilde{t}_3 \\ T_1 \\ T_2 \\ T_3 \\ T_4 \\ t_1 \\ t_2 \\ \mu_1 \\ \mu_2 \\ \mu_3 \\ k_1 \\ k_2 \\ k_3 \end{bmatrix} \rightarrow 15 \text{ vs. } \underbrace{350}_{\textit{samples}} \cdot \underbrace{3}_{\textit{inputs}} = 1050 \text{ elements}$$

Offline trajectory - result

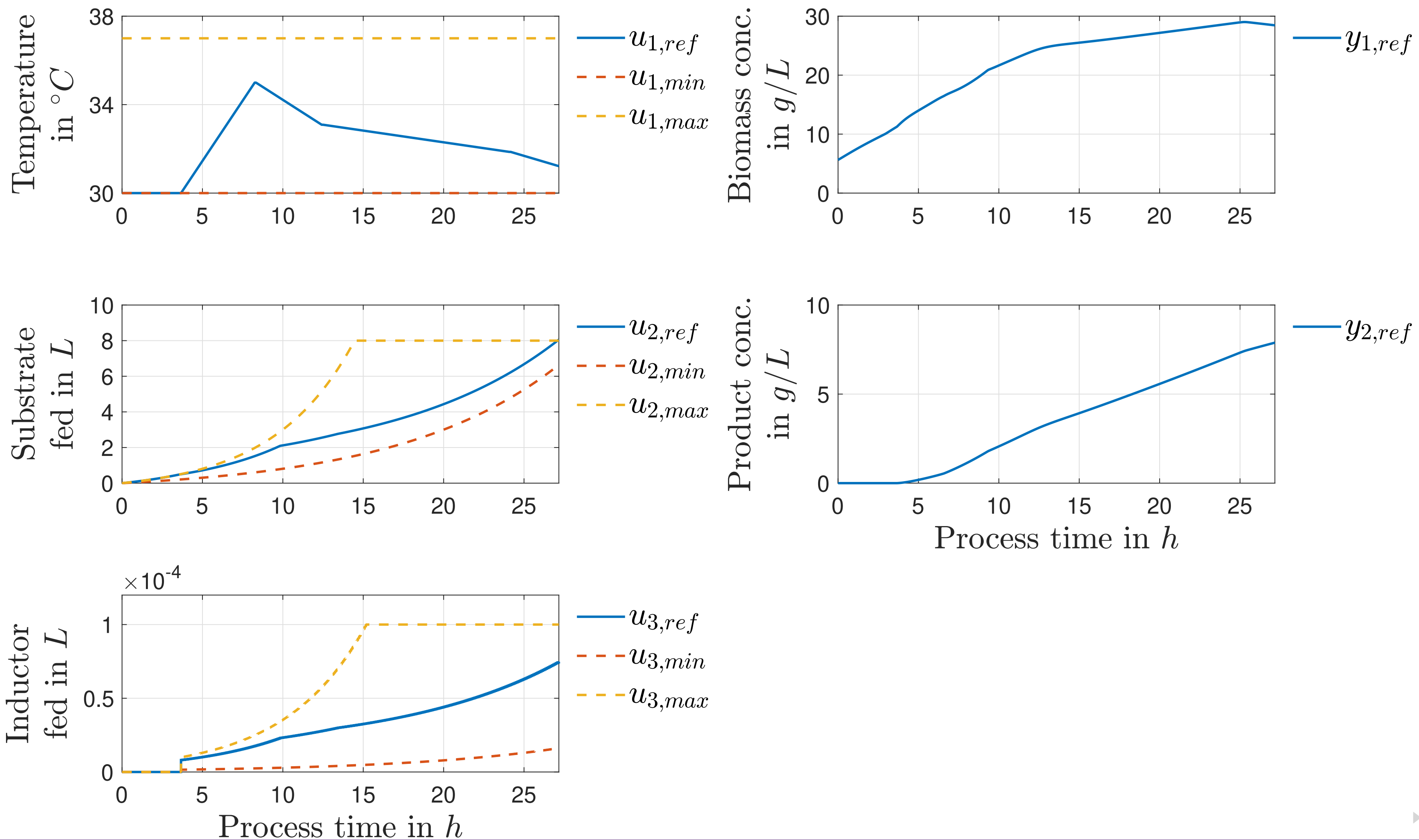

Tracking of the trajectories

Tracking control via MPC. Two test scenarios:

- No disturbance

Tracking of the trajectories

Tracking control via MPC. Two test scenarios:

- No disturbance
- Input disturbance (temperature deviations and pump faults)

Tracking of the trajectories

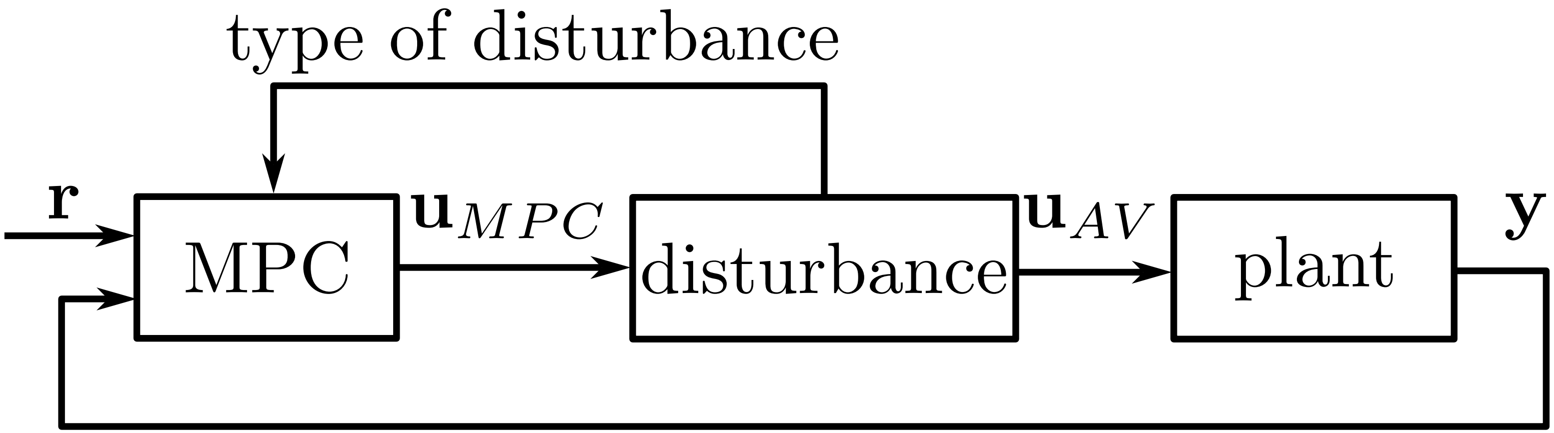

Tracking control via MPC. Two test scenarios:

- No disturbance
- Input disturbance (temperature deviations and pump faults)

Formulation of the MPC problem

- First idea:

$$\min_{\mathbf{u}_{k+i}} \sum_{j=1}^{n_p} (\mathbf{y}_{ref,k+j} - \mathbf{y}_{k+j})^T \mathbf{Q} (\mathbf{y}_{ref,k+j} - \mathbf{y}_{k+j}) + \sum_{i=0}^{n_c} (\mathbf{u}_{ref,k+i} - \mathbf{u}_{k+i})^T \mathbf{R} (\mathbf{u}_{ref,k+i} - \mathbf{u}_{k+i}) + \mathbf{\Delta u}_{k+i}^T \mathbf{R}_{\mathbf{\Delta}} \mathbf{\Delta u}_{k+i}$$

$$s.t. \quad \mathbf{u} \in \text{“DoE”}$$

Formulation of the MPC problem

- First idea:

nonlinear objective

$$\min_{\mathbf{u}_{k+i}} \sum_{j=1}^{n_p} (\mathbf{y}_{ref,k+j} - \mathbf{y}_{k+j})^T \mathbf{Q} (\mathbf{y}_{ref,k+j} - \mathbf{y}_{k+j})$$
$$+ \sum_{i=0}^{n_c} (\mathbf{u}_{ref,k+i} - \mathbf{u}_{k+i})^T \mathbf{R} (\mathbf{u}_{ref,k+i} - \mathbf{u}_{k+i}) + \boldsymbol{\Delta}\mathbf{u}_{k+i}^T \mathbf{R}_{\boldsymbol{\Delta}} \boldsymbol{\Delta}\mathbf{u}_{k+i}$$
$$s.t. \quad \mathbf{u} \in \text{“DoE”}$$

Formulation of the MPC problem

- First idea:

nonlinear objective

$$\min_{\mathbf{u}_{k+i}} \sum_{j=1}^{n_p} (\mathbf{y}_{ref,k+j} - \mathbf{y}_{k+j})^T \mathbf{Q} (\mathbf{y}_{ref,k+j} - \mathbf{y}_{k+j})$$

$$+ \sum_{i=0}^{n_c} (\mathbf{u}_{ref,k+i} - \mathbf{u}_{k+i})^T \mathbf{R} (\mathbf{u}_{ref,k+i} - \mathbf{u}_{k+i}) + \boldsymbol{\Delta}\mathbf{u}_{k+i}^T \mathbf{R}_{\boldsymbol{\Delta}} \boldsymbol{\Delta}\mathbf{u}_{k+i}$$

$$s.t. \quad \mathbf{u} \in \text{"DoE"}$$

nonlinear value and rate constraints

No disturbance without ($\mathbf{R} = \mathbf{0}$) / with offline input reference ($\mathbf{R} \neq \mathbf{0}$)

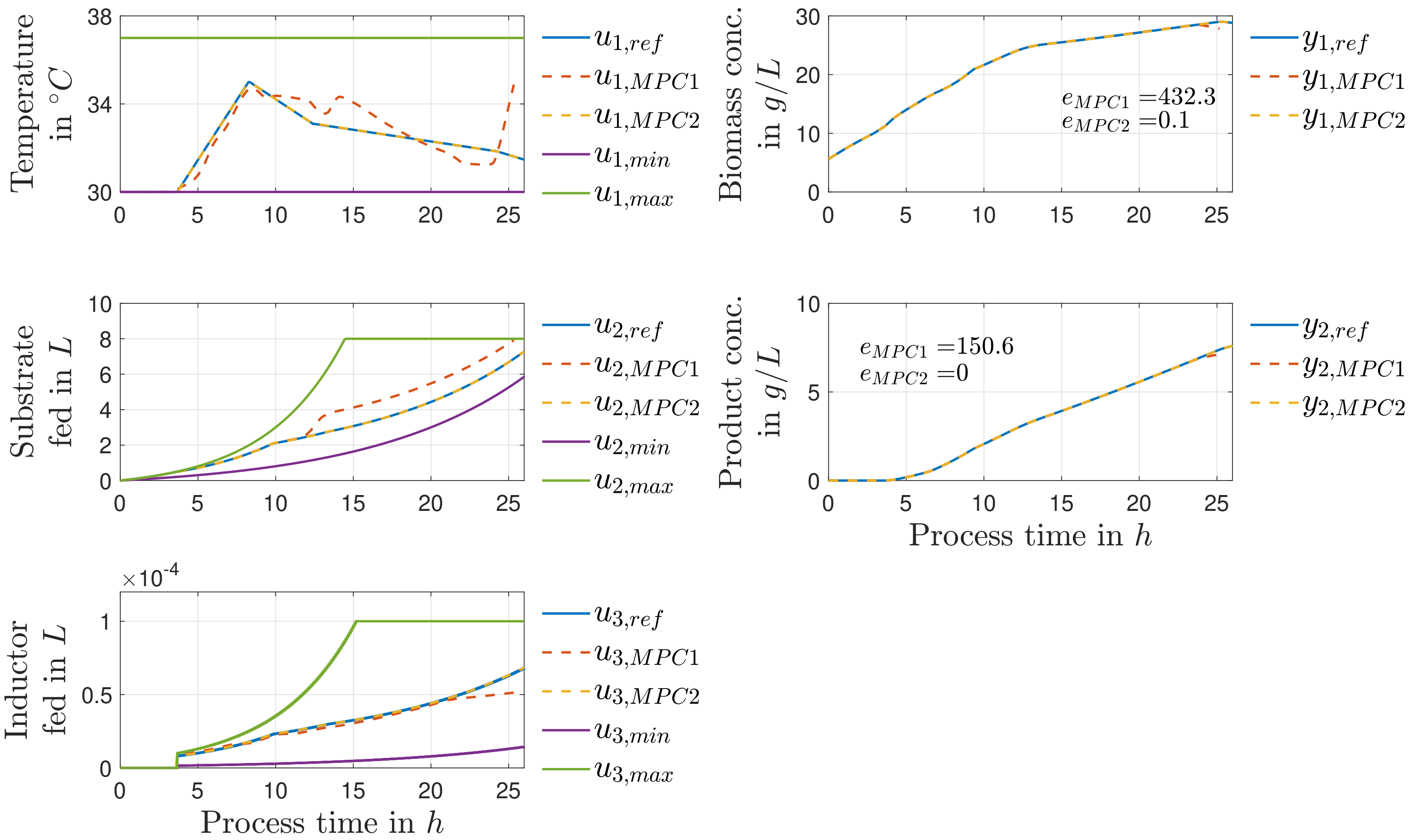

Temperature disturbance until ≈ 14h

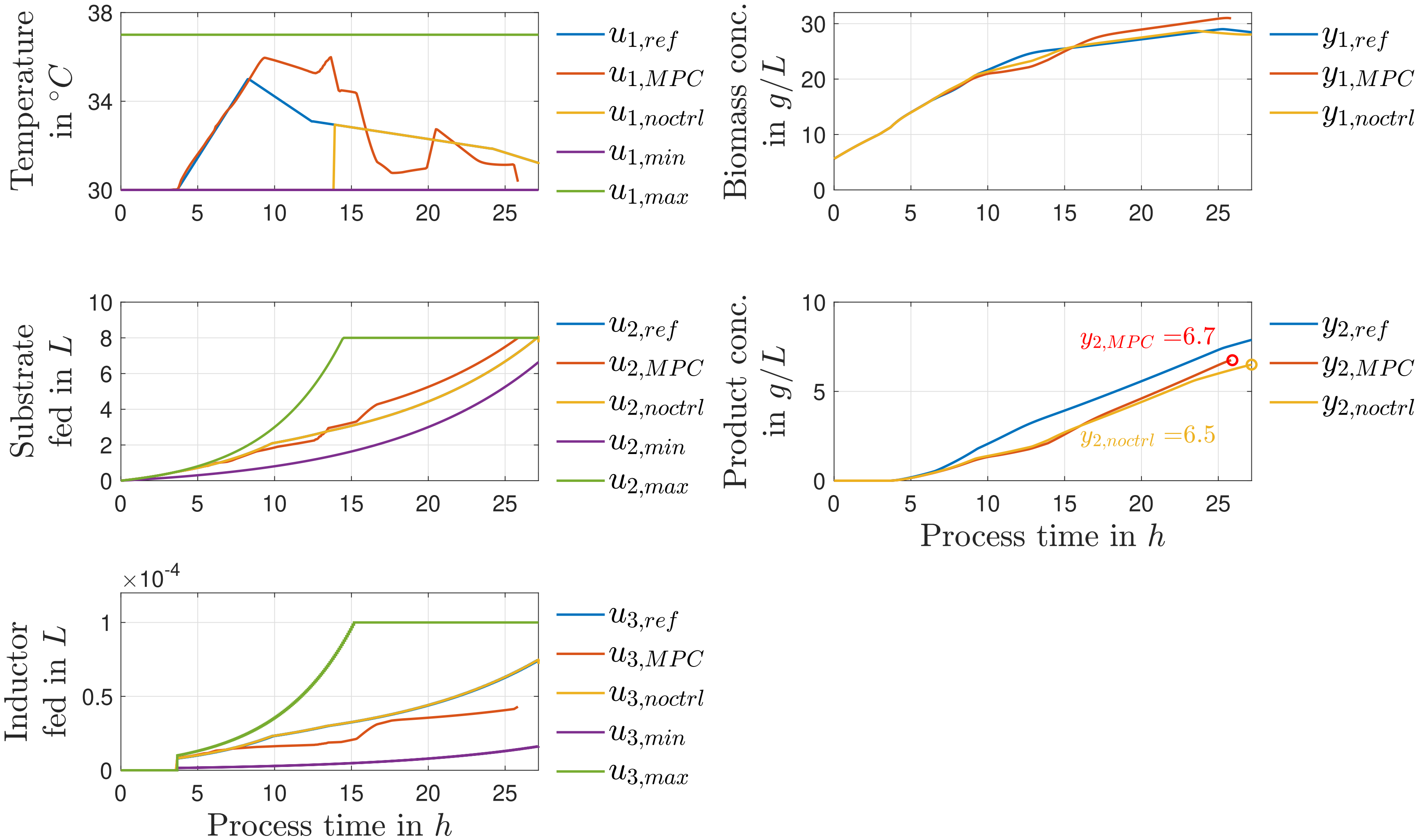

Glucose pump failure at 5h30 for approx. 1 hour

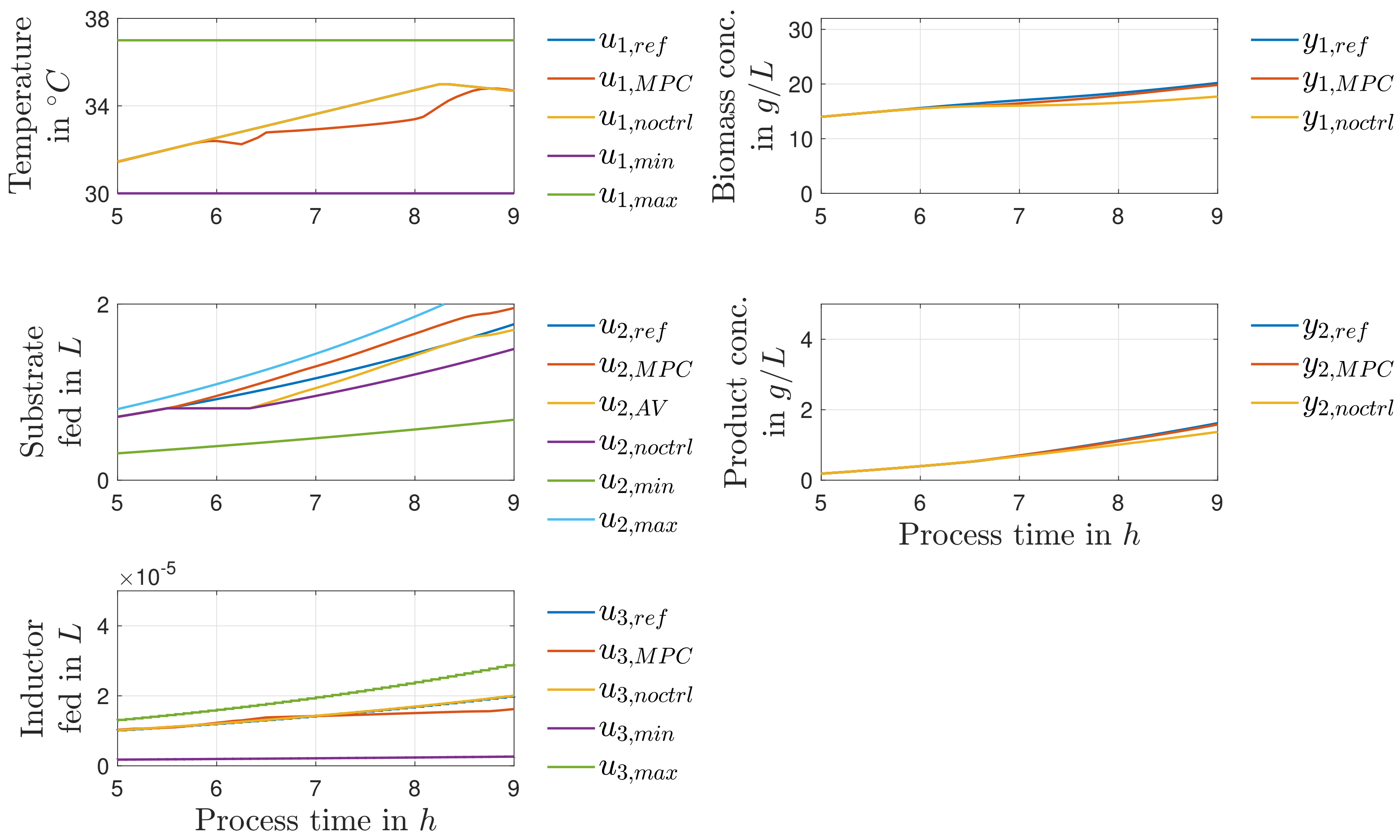

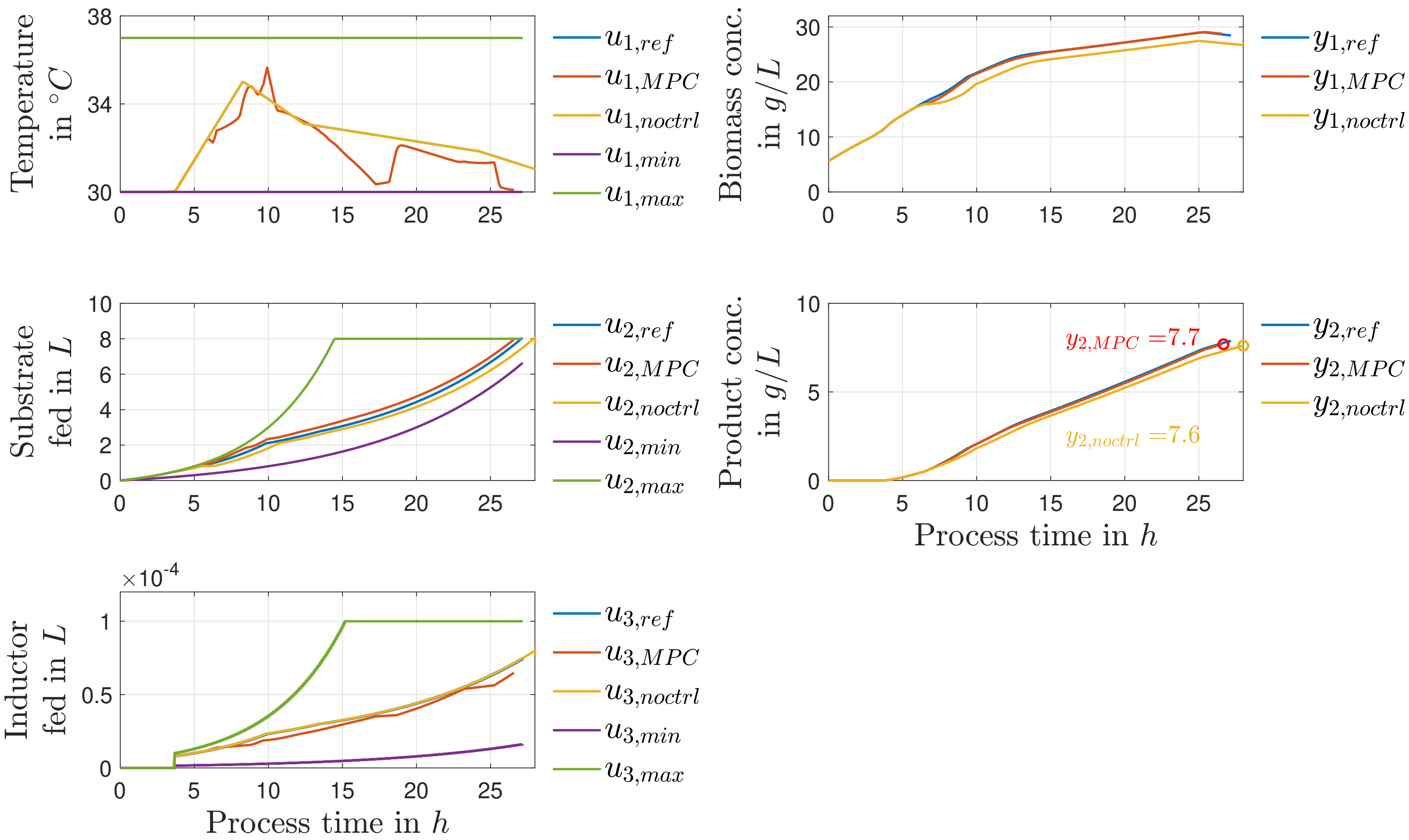

Temperature in °C
$u_{1,ref}$
$u_{1,MPC}$
$u_{1,noctrl}$
$u_{1,min}$
$u_{1,max}$
Biomass conc. in g/L
$y_{1,ref}$
$y_{1,MPC}$
$y_{1,noctrl}$
Substrate fed in L
$u_{2,ref}$
$u_{2,MPC}$
$u_{2,noctrl}$
$u_{2,min}$
$u_{2,max}$
Product conc. in g/L
$y_{2,MPC}$ =7.7
$y_{2,noctrl}$ =7.6
$y_{2,ref}$
$y_{2,MPC}$
$y_{2,noctrl}$
Process time in h
Inductor fed in L
$\times 10^{-4}$
$u_{3,ref}$
$u_{3,MPC}$
$u_{3,noctrl}$
$u_{3,min}$
$u_{3,max}$
Process time in h

Conclusion and Outlook

- 2-step approach:
  - Model based computation of optimal input and output trajectories (6.5g/L of "best" DoE point vs. 7.9 g/L after optimization)

Conclusion and Outlook

- 2-step approach:
  - Model based computation of optimal input and output trajectories (6.5g/L of "best" DoE point vs. 7.9 g/L after optimization)
  - Tracking of trajectories via model predictive control

Conclusion and Outlook

- 2-step approach:
  - Model based computation of optimal input and output trajectories (6.5g/L of "best" DoE point vs. 7.9 g/L after optimization)
  - Tracking of trajectories via model predictive control
- (Timely limited) actuator faults are well compensated by the controller

Conclusion and Outlook

- 2-step approach:
  - Model based computation of optimal input and output trajectories (6.5g/L of "best" DoE point vs. 7.9 g/L after optimization)
  - Tracking of trajectories via model predictive control
- (Timely limited) actuator faults are well compensated by the controller
  - Knowledge on faults improves performance → fault detection and isolation will be developed

Conclusion and Outlook

- 2-step approach:
  - Model based computation of optimal input and output trajectories (6.5g/L of “best” DoE point vs. 7.9 g/L after optimization)
  - Tracking of trajectories via model predictive control
- (Timely limited) actuator faults are well compensated by the controller
  - Knowledge on faults improves performance → fault detection and isolation will be developed
  - Until know: optimal references are computed once in advance. Performance gain expected by re-computation of offline-trajectories after a fault was recovered

Conclusion and Outlook

- 2-step approach:
  - Model based computation of optimal input and output trajectories (6.5g/L of “best” DoE point vs. 7.9 g/L after optimization)
  - Tracking of trajectories via model predictive control
- (Timely limited) actuator faults are well compensated by the controller
  - Knowledge on faults improves performance $\rightarrow$ fault detection and isolation will be developed
  - Until know: optimal references are computed once in advance. Performance gain expected by re-computation of offline-trajectories after a fault was recovered
- Next Steps:
  - Implementation of above points

Conclusion and Outlook

- 2-step approach:
  - Model based computation of optimal input and output trajectories (6.5g/L of "best" DoE point vs. 7.9 g/L after optimization)
  - Tracking of trajectories via model predictive control
- (Timely limited) actuator faults are well compensated by the controller
  - Knowledge on faults improves performance $\rightarrow$ fault detection and isolation will be developed
  - Until know: optimal references are computed once in advance. Performance gain expected by re-computation of offline-trajectories after a fault was recovered
- Next Steps:
  - Implementation of above points
  - Verification of the concept on a real bioreactor

Conclusion and Outlook

- 2-step approach:
  - Model based computation of optimal input and output trajectories (6.5g/L of "best" DoE point vs. 7.9 g/L after optimization)
  - Tracking of trajectories via model predictive control
- (Timely limited) actuator faults are well compensated by the controller
  - Knowledge on faults improves performance → fault detection and isolation will be developed
  - Until know: optimal references are computed once in advance. Performance gain expected by re-computation of offline-trajectories after a fault was recovered
- Next Steps:
  - Implementation of above points
  - Verification of the concept on a real bioreactor
    - Process model development (different process)

Conclusion and Outlook

- 2-step approach:
  - Model based computation of optimal input and output trajectories (6.5g/L of "best" DoE point vs. 7.9 g/L after optimization)
  - Tracking of trajectories via model predictive control
- (Timely limited) actuator faults are well compensated by the controller
  - Knowledge on faults improves performance $\rightarrow$ fault detection and isolation will be developed
  - Until know: optimal references are computed once in advance. Performance gain expected by re-computation of offline-trajectories after a fault was recovered
- Next Steps:
  - Implementation of above points
  - Verification of the concept on a real bioreactor
    - Process model development (different process)
    - Implementation of suitable process analytical technology (PAT) to measure biomass and product

Thank you for listening

Acknowledgement:
This work was funded through the Austrian Research Promotion Agency (FFG) as part of the "BIOPTI" project (project number FO999902671) within the "Digitale Technologien" program.

Bibliography I

[BSD20] Benjamin Bayer, Gerald Striedner, and Mark Duerkop. "Hybrid Modeling and Intensified DoE: An Approach to Accelerate Upstream Process Characterization." In: *Biotechnology Journal* 15.9 (2020-06). ISSN: 1860-7314. DOI: 10.1002/biot.202000121.

[Cel+24] Selma Celikovic et al. "Development and Application of Control Concepts for Twin-Screw Wet Granulation in the ConsiGmaTM-25: Part 1 Granule Composition." In: *International Journal of Pharmaceutics* 657 (2024), p. 124124. ISSN: 0378-5173. DOI: https://doi.org/10.1016/j.ijpharm.2024.124124. URL: https://www.sciencedirect.com/science/article/pii/S0378517324003582.

[Nov] Novasign. *Hybrid Modeling Toolbox*. URL: https://docs.novasign.at/toolbox/index.html (visited on 08/14/2024).

[Reh+20] Jakob Rehrl et al. "End-Point Prediction of Granule Moisture in a ConsiGmaTM-25 Segmented Fluid Bed Dryer." In: *Pharmaceutics* 12.5 (2020). ISSN: 1999-4923. DOI: 10.3390/pharmaceutics12050452. URL: https://www.mdpi.com/1999-4923/12/5/452.

[Reh+22] Jakob Rehrl et al. *Systematic Control Strategy Development for a Continuous Direct Compaction Line Via the Control Strategy Evaluation Tool (CET)*. AIChE Annual Meeting 2022. 2022.

IX. Event-triggered control approach for time-critical dynamic systems

presenter: Andrej Sarjas

Event-triggered control approach for time-critical dynamic systems

Andrej Sarjaš, Dušan Gleich
andrej.sarjas@um.si

Faculty of Electrical Engineering and Computer Science,
University of Maribor, Slovenia

9-11th September 2024
23. Styrian Workshop on Automatic Control

Outline:

- Time-critical feedback dynamic systems
- Event-Triggering (ET) control
- Desing of the Sliding mode ET control system (static-dynamic triggering law)
- Practical example, algorithm comparisons and validations

Time-critical feedback dynamic systems

The time-critical feedback dynamics systems require accurate and incessant monitoring to ensure proper behavior. The stability becomes critical due to the tight constraints on reaction time. Many time-critical systems are driven by complex embedded systems with scheduled tasks, advanced power management over the network, distributed systems, etc... All the significant priorities can be assigned as a Deadline-driven performance, which means that the system operates within strict time limitations.

Most control algorithms are designed to produce the output in an adequate time sequence, known as a sampling time. Such strict time conditions ensure the stability and desired performance of the time-critical systems. On the other hand, the excessive usage of resources can lead to the lowered performance of the whole system and the required demand for systems with higher speed or a tendency to use high-performance communications networks.

Event-triggering approach

An event-triggered feedback control strategy is an alternative to the classic time-triggered approach. Regard to the time-triggered technique, the event-triggered plan is executed upon the prescribed triggering rule. The controller output remains unchanged until the next triggered event.

Event-triggering control is an approach used in control systems to optimize the utilization of resources and reduce communication or computation overhead by triggering control actions only when necessary.

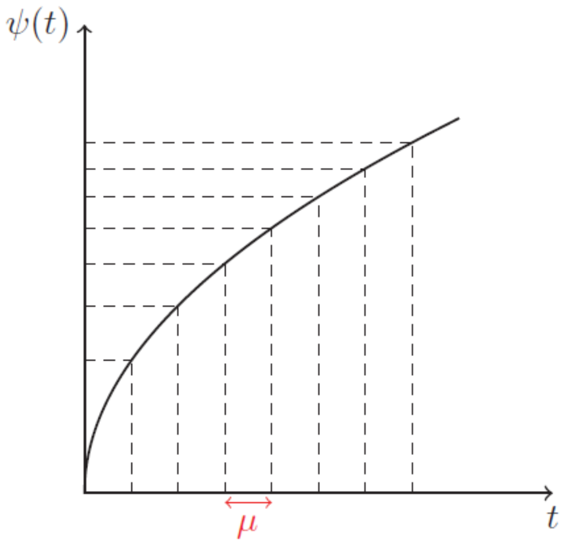

Time-triggered strategy. Riemann sampling technique.

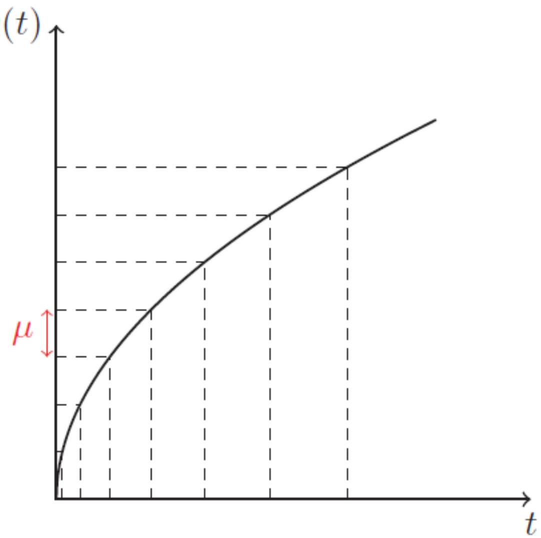

Event-triggered strategy. Lebesque sampling technique.

Sliding Mode Control

Sliding Mode Control (SMC) was first proposed and elaborated in the early 1950s by Emelyanov and several researchers such as Utkins and Itkis. SMC can be applied to nonlinear systems, (MIMO) systems, discrete-time models, and large-scale systems. The most significant feature of SMC is that it is completely insensitive to parametric uncertainty and external disturbances during sliding mode.

SMC control law has two parts:

- **Equivalent Control:** maintains the system on a sliding surface in the ideal condition.
- **Switching Control:** discontinuous control action drives the system trajectory to the sliding surface and rejects the disturbance and system uncertainty.

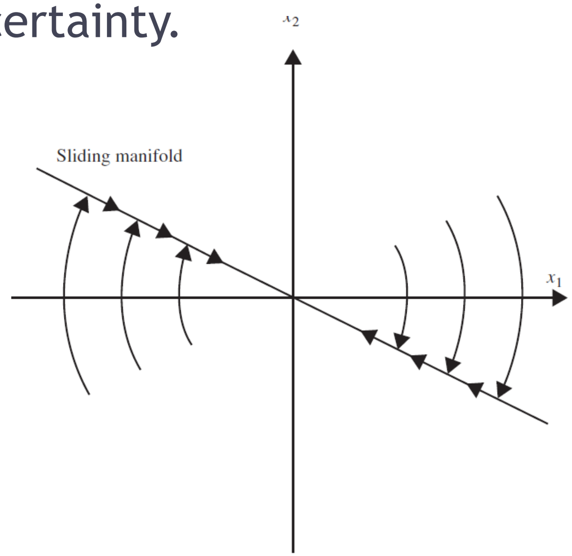

SMC advantage:

- Robustness,
- Effective in nonlinear system,
- Simple design, and implementation

SMC disadvantage

- Chattering (High-frequency oscillations)

Event-triggered - Sliding Mode Control

Event triggering control is introduced with triggering sequence:

$$t_0, t_1, t_2, \ldots, t_i, \quad i \in \mathbb{Z}^{0+}$$

Where $\{t_i\}_{i=0}^{\infty}$ is an event-triggering instant satisfying the conditions $t_{i+1} > t_i$ with $t_0 \geq 0$ being the initial sampling instant.The event-triggering instants are not uniformly distributed and constant:

$$t \in [t_i, t_{i+1}) \qquad t_{i+1} = t_i + \eta, \quad \eta > 0$$

The controller u is updated at the instance t_i and holds the last value until the next triggering event occurs t_{i+1}. The inter-event time is defined as:

$$T_i = \{t_{i+1} - t_i\}_{i=0}^{\infty}, \quad T_i > 0$$

Among update instance the error is defined:

$$e(t) = x(t) - x(t_i) \qquad \text{and holds:} \qquad e(t) = x(t_i) - x(t_i) = 0$$

Event-triggered - Sliding Mode Control

Consider the following single-input, single-output nonlinear system of the following class,

$$\dot{x}_1(t) = f_1(x_1) + x_2(t),$$
$$\dot{x}_2(t) = f_2(x_1, x_2) + g\left(u(t) + d(t)\right),$$

$$\dot{x}(t) = f(x) + G\left(u(t) + d(t)\right), \quad x(0) = x_0, x = [x_1; x_2] \in \mathbb{R}^n$$
$$f(x) = [f_1(x_1)\ f_2(x_1, x_2)]^T \in \mathbb{R}^n$$
$$G = [0\ g]^T \in \mathbb{R}^n, \quad |d| \le \delta_d < \infty$$

where $x_1 \in \mathbb{R}^{n-1}$ and $x_2 \in \mathbb{R}$ are the system states, u , d and g are the control input, external disturbance, and input gain function, respectively. $f_1(x_1)$ and $f_2(x_1, x_2)$ are nonlinear functions with unique equilibrium point and function are bounded $\|f_1(x_1)\| \le F_1$ and $\|f_2(x_1, x_2)\| \le F_2$, where $F_1 \ge 0$, $F_2 \ge 0$ are known constants.

Design the sliding manifold as :

$$S \in \left\{x \in \mathbb{R}^n \,\middle|\, s = cx = 0\right\}, \qquad c = [c_1\ \ 1], x = [x_1\ \ x_2]^T$$

where is:

$$s(t) = cx(t)$$
$$\dot{s}(t) = c\dot{x}(t)$$
$$= c\left(f(x) + G\left(u(t) + d(t)\right)\right) \quad \Rightarrow \boxed{u(t) = -G^{-1}\left(f(x) + \rho sign(s)\right)}$$

First order SMC

$$\rho > |G|\delta_d$$

ET First Order - Sliding Mode Control (ET-FSMC)

Regarding the ET paradigm, the controller u(t) is:

$$u(t_i) = -G^{-1}\left(f\left(x(t_i)\right) + \rho sign\left(s(t_i)\right)\right)$$

where are the last updated values: $u(t_i) = u_i, x(t_i) = x_i$, $s(t_i) = s_i$

The stability is tested based on Lyapunov candidate $V = \frac{1}{2}s^2$ with its derivative,

$$\dot{V} = s\dot{s} = sc\left(f(x(t)) + G\left(-G^{-1}\left(f\left(x(t_i)\right) + \rho sign\left(s_i\right)\right) + d(t)\right)\right)$$

$$\leq -s\rho sign\left(s_i\right) + c|s||G|\delta_d + c|s|\left\|f(x) - f(x_i)\right\|$$

$$\left\|f(x) - f(x_i)\right\| \leq L\left\|x - x_i\right\| = L\left\|e\right\|, \quad L > 0$$

$$\leq -s\rho sign\left(s_i\right) + c|s||G|\delta_d + cL|s|\left\|e\right\|$$

Case1: $sign(s) = sign(s_i)$:

$$\dot{V} \leq -\rho|s| + c|s||G|\delta_d + cL|s|\left\|e\right\|$$

$$\boxed{L\left\|c\right\|\left\|e\right\| \leq \beta, \quad \beta > 0}$$

Triggering law

$$\leq -\rho|s| + c|s||G|\delta_d + |s|\beta$$

$$\leq \left(-\rho + c|G|\delta_d + \beta\right)|s|$$

Stability condition

$$\rho > c\left(|G|\delta_d + c^{-1}\beta\right)$$

Case 2: $sign(s) \neq sign(s_i)$:

$$\left|s(t) - s(t_i)\right| = \left|cx - cx_i\right| =$$

$$\leq \left\|c\right\|\left\|e\right\|$$

$$\leq L^{-1}\beta$$

Admissible minimum inter-event time T_i for ET-FSMC

The inter-event time T_i is the time between two successive updates. The T_i is not fixed, and varies according to the system trajectory evolution and the preselected triggering boundary. To avoid the Zeno-phenomena T_i has to be positively lower bounded.

$$\begin{aligned}\frac{d}{dt}\|e(t)\| &\le \left\|\frac{d}{dt}e(t)\right\| = \left\|\frac{d}{dt}(x - x_i)\right\| \\ &= \left\|\frac{d}{dt}x\right\| = \|f(x) - f(x_i) + \rho sign(s_i) + Gd(t)\| \\ &\le L\|e\| + \rho + |G|\delta_d\end{aligned}$$

where the solution is:

$$\|e(t)\| \le \frac{\rho + |G|\delta_d}{L}\left(e^{LT_i} - 1\right)$$

$$\frac{\beta}{L\|c\|} = \|e(t)\| \le \frac{\rho + |G|\delta_d}{L}\left(e^{LT_i} - 1\right)$$

$$\boxed{T_i \ge \ln\left(1 + \frac{\beta}{\|c\|\left(\rho + |G|\delta_d\right)}\right)}$$

T_i is lower bounded

ET Super-Twisting Controller/Algorithm (ET-STA)

For the given system the Super-Twisting controller is given as,

System:

$$\dot{x}(t) = f(x) + G\big(u(t) + d(t)\big),$$

Super-Twisting Controller:

$$u(t) = (cG)^{-1}\Big(-cf(x) - k_1 |s(t)|^{1/2} sign\big(s(t)\big) + v(t)\Big)$$

$$\dot{v}(t) = -k_2 sign\big(s(t)\big)$$

ET Super-Twisting Controller:

$$u(t) = (cG)^{-1}\Big(-cf(x_i) - k_1 |s_i|^{1/2} sign(s_i) + v_i\Big)$$

$$\dot{v}(t) = -k_2 sign(s_i)$$

Closed-loop system with ET-STA:

$$\dot{x} = f(x) - (c)^{-1}\Big(cf(x_i) - k_1 |s_i|^{1/2} sign(s_i) + v_i\Big) + Gd,$$

$$\dot{v}(t) = -k_2 sign(s_i).$$

Selected sliding variable:

$$s = cx, \quad c > 0$$

ET Super-Twisting Controller/Algorithm (ET-STA)

Derivative of the sliding variable s,

$$\dot{s} = c\dot{x},$$
$$\dot{s} = c\left(f(x) - f(x_i)\right) - k_1 \left|s_i\right|^{1/2} sign\left(s_i\right) + v_i,$$
$$\dot{v}\left(t\right) = -k_2 sign\left(s_i\right) + G\dot{d}.$$

Introducing new variable:

$$\zeta = \left[\zeta_1 \quad \zeta_2\right]^T = \left[\left|s\right|^{1/2} sign\left(s\right) \quad v\right]^T,$$

And rewritten system: $\left|\zeta_1\right| = \left|s\right|^{1/2}$

$$\dot{\zeta}_1 = \frac{1}{2\left|\zeta_1\right|}\left(c\left(f(x) - f(x_i)\right) - k_1 \left|s_i\right|^{1/2} sign\left(s_i\right) + v_i\right),$$
$$\dot{\zeta}_2 = -k_2 sign\left(s_i\right) + G\dot{d},$$

The compact form of the rewritten system:

$$\dot{\zeta} = \frac{1}{\left|\zeta_1\right|}\left(A\begin{bmatrix}\zeta_{1i} \\ \zeta_2\end{bmatrix} + B\right),$$

where A and B are,

$$A = \frac{1}{2}\begin{bmatrix}k_1 & 1 \\ 0 & 0\end{bmatrix} \qquad B = \begin{bmatrix}\frac{1}{2}c\left(f(x) - f(x_i)\right) \\ \left|\zeta_1\right|\left(-k_2 sign\left(s_i\right) + G\dot{d}\right)\end{bmatrix}.$$

ET Super-Twisting Controller/Algorithm (ET-STA)

The stability is checked with the Lyapunov function,

$$V(s) = \zeta^T \begin{bmatrix} 4k_2 + k_1^2 & -k_1 \\ -k_1 & 1 \end{bmatrix} \zeta$$

The derivative is:

$$\dot{V}(s) = \dot{\zeta}^T P\zeta + \zeta^T P\dot{\zeta}$$

$$\dot{V}(s) = \frac{1}{\|\zeta_1\|}\left(\zeta^T PA\begin{bmatrix} \zeta_{1i} \\ \zeta_2 \end{bmatrix} + \begin{bmatrix} \zeta_{1i} & \zeta_2 \end{bmatrix} A^T P\zeta + 2\zeta^T PB\right)$$

$$\vdots$$

$$\dot{V}(s) \le \frac{1}{\|\zeta_1\|}\begin{pmatrix} -\left(4k_1k_2 + k_1^3\right)\|\zeta_{1i}\|\|\zeta_1\| + k_1^2\|\zeta_{1i}\|\|\zeta_2\| + \left(k_1^2 + 2k_2 + 2G\xi_d\right)\|\zeta_1\|\|\zeta_2\| \\ +2\left(k_1k_2 - k_1G\xi_d\right)\|\zeta_1\|^2 - k_1\|\zeta_2\|^2 + \\ +2c\left(4k_2 + k_1^2\right)\underline{L\|(x - x_i)\|}\|\zeta_1\| \\ -2ck_1L\|(x - x_i)\|\|\zeta_2\| \end{pmatrix}$$

Introducing the triggering law:

$$\|s\| = \left\| s_i + c\underbrace{\left(x - x_i\right)}_{e} \right\|$$

$$\|s\| \le \|s_i\| + \|c\|\|e\|$$

$$\le \|s\| + \boxed{\|c\|\beta}$$

$$\|\bar{\zeta}_1\| \le \|\zeta_1\| + \tilde{\beta}, \quad \tilde{\beta} = \beta^{\frac{1}{2}}$$

ET Super-Twisting Controller/Algorithm (ET-STA)

The final value of the derivative,

$$\dot{V}(s) \le -\frac{1}{\|\zeta_1\|}\begin{bmatrix}\|\zeta_1\| & \|\zeta_2\|\end{bmatrix} Q \begin{bmatrix}\|\zeta_1\| \\ \|\zeta_2\|\end{bmatrix} + \frac{1}{\|\zeta_1\|}\Upsilon \begin{bmatrix}\|\zeta_1\| \\ \|\zeta_2\|\end{bmatrix}$$
$$\le \frac{1}{\|\zeta_1\|}\left(-Z^T Q Z + \Upsilon Z\right)$$

where Q and ϒ are:

$$Q = \begin{bmatrix} \left(2k_1k_2 + 2k_1 G\xi_d + k_1^3\right) & -\left(\frac{k_1^2}{2} + k_2 + G\xi_d\right) \\ -\left(\frac{k_1^2}{2} + k_2 + G\xi_d\right) & k_1 \end{bmatrix}$$

$$\Upsilon = \begin{bmatrix} \left(8k_2L\beta + 2k_1^2L\beta - 4k_1k_2\tilde{\beta} - k_1^3\tilde{\beta}\right) & -\left(2k_1L\beta - k_1^2\tilde{\beta}\right) \end{bmatrix}$$

Parameters conditions:

$$k_1 > \sqrt{\frac{3}{2}\left(k_2 + G\xi_d\right) + \eta}$$
$$k_2 \ge \frac{7}{3} + G\xi_d + \eta$$

Attracted region: $\Omega = \left\{ \zeta \in \mathbb{R}^n \mid \|\zeta\| \ge \frac{\Upsilon}{\lambda_{\min}(Q)} \right\}$

$$Z \ge \frac{\Upsilon}{\lambda_{\min}(Q)} \Rightarrow \|s\| \to \frac{\Upsilon^2}{\lambda_{\min}(Q)^2}$$

Admissible minimum inter-event time T_i for ET-STA

The inter-event time is derived as,

$$\frac{d}{dt}\left\|e(t)\right\| \le \left\|\frac{d}{dt}e(t)\right\| = \left\|\frac{d}{dt}(x - x_i)\right\|$$

$$= \left\| f(x) - \left(f(\bar{x}) - ck_1\left|s_i\right|^{1/2} sign(s_i) - ck_2\int_{t_i}^{t} sign(s_i)dt \right) + Gd \right\|$$

$$\le L\left\|e(t)\right\| \underbrace{+k_1\left\|c\right\|\left\|s_i\right\|^{1/2} + k_2\left\|c\right\|T_i + \left\|G\right\|\Delta_d}_{\kappa}$$

$$\le L\left\|e\right\| + \kappa$$

The solution $e(t)$ is,

$$\left\|e(t)\right\| \le \frac{\kappa}{L}\left(e^{LT_i} - 1\right) = \frac{k_1\left\|c\right\|\left\|s_i\right\|^{1/2} + \left\|G\right\|\Delta_d + +k_2\left\|c\right\|T_i}{L}\left(e^{LT_i} - 1\right)$$

Triggering condition,

$$\frac{k_1\left\|c\right\|\left\|s_i\right\|^{1/2} + \left\|G\right\|\Delta_d + +k_2\left\|c\right\|T_i}{L}\left(e^{LT_i} - 1\right) = \beta$$

$$\frac{k_1\left\|c\right\|\left\|s_i\right\|^{1/2} + \left\|G\right\|\Delta_d + +k_2\left\|c\right\|T_i}{L}\left(e^{LT_i} - 1\right) - \beta = 0$$

$\Rightarrow$ T_i is positively lower bounded

$$T_i \ge T_{i\,\min} > 0$$

Dynamic Event-Triggering approach (DET)

Dynamic Event-Triggering control introduces the triggering rule, which does not involve a fixed triggering boundary but is dynamically generated regarding the system state conditions. The dynamic triggering bound is generated with the internal dynamic system.

The dynamic event-triggered law is,

$$\|e\| \geq \eta + \beta, \qquad \beta > 0, \eta > 0$$

Internal dynamic system is given as,

$$\boxed{\dot{\eta} = -\alpha\eta + \Theta\left(\beta - \|e\|\right),} \quad \eta(0) = \eta_0, \ \eta_0, \Theta, \alpha \in \mathbb{R}_0^+$$

If not triggering occurred,

$$\|e\| < \eta + \beta$$

$$-\eta \leq \beta - \|e\|$$

Leads to,

$$\dot{\eta} = -\alpha\eta + \Theta\left(\beta - \|e\|\right),$$

$$\dot{\eta} = -\alpha\eta - \Theta\eta = -\left(\alpha + \Theta\right)\eta$$

Dynamic Event-Triggering approach (DET)

The stability of DET-FSMC is,

$$V = V_{ET-FSMC} + \eta$$
$$\dot{V} = \dot{V}_{ET-FSMC} + \dot{\eta}$$

DET

$$\dot{V} = \left(-\rho + c\left|G\right|\delta_d + \beta\right)\left|s\right| \boxed{-(\alpha + \Theta)\eta}$$

The stability of DET-STA is,

$$V = V_{ET-STA} + \eta$$
$$\dot{V} = \dot{V}_{ET-STA} + \dot{\eta}$$

DET

$$\dot{V} = \frac{1}{\|\zeta_1\|}\left(-Z^T QZ + \Upsilon Z\right) \boxed{-(\alpha + \Theta)\eta}$$

Inter event time T_{i-DET} of,

$$T_{i_{DET-FSMC}} \geq \ln\left(1 + \frac{\beta + \eta}{\|c\|\left(\rho + \left|G\right|\delta_d\right)}\right)$$

$$\boxed{T_{i_{DET-FSMC}} \geq T_i}$$

Inter event time T_{i-DET} of,

$$\frac{k_1\|c\|\|s_i\|^{1/2} + \|G\|\Delta_d + +k_2\|c\|T_i}{L}\left(e^{LT_i} - 1\right) - (\beta + \eta) = 0$$

$$\boxed{T_{i_{DET-STA}} \geq T_i}$$

NETWORKED CONTROL SYSTEM STRUCTURE FOR AIR LEVITATION SYSTEM FOR ET-FSCM and ET-STA

NCS network architecture:

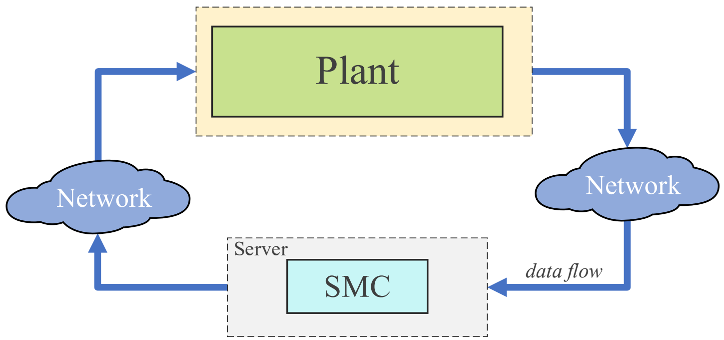

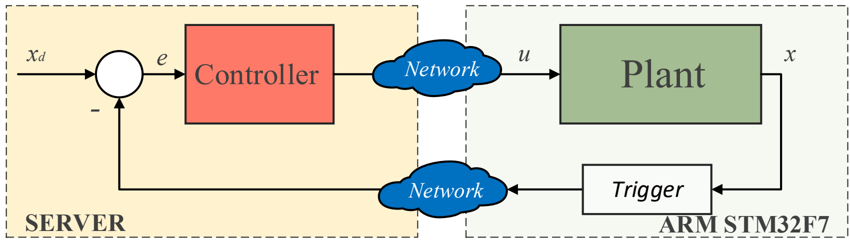

Hardware:

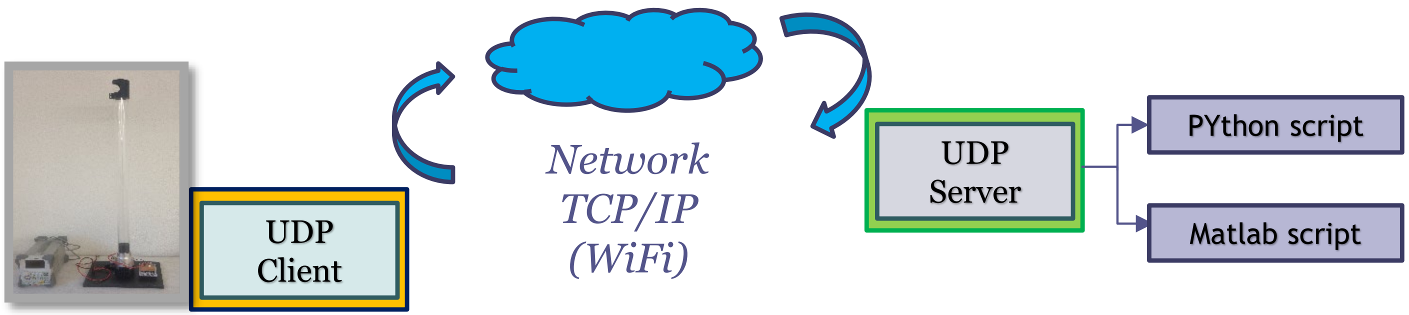

STM32F7, LwIP stack

- Estimated latency for fixed data length of 200Bytes < 3ms
- Data transmission with time-badges for Network-delay estimation
- CRC data encoding

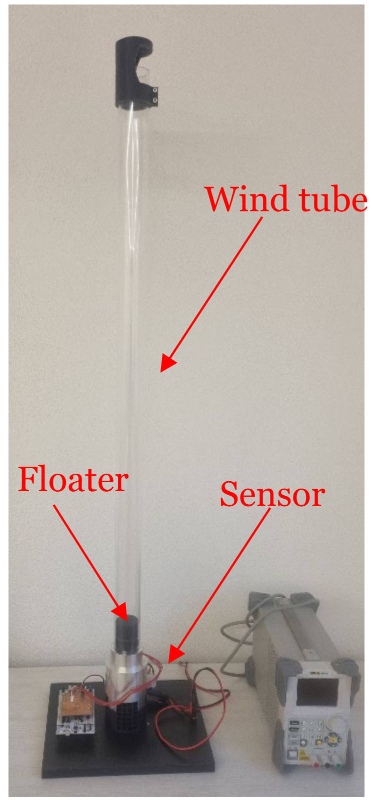

Modeling of the system

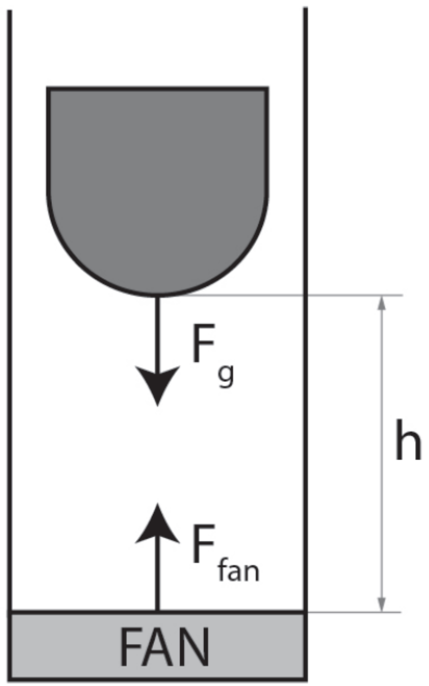

Second Newton law of motion:

$$m\ddot{h} = -mg + F_{fan}$$

Second order differential equation:

$$\ddot{h} = -g + \frac{1}{m}F_{fan}$$

State space representation:

$$x_1 = x_2,$$

$$\dot{x_2} = -g + \frac{1}{m}F_{fan}$$

where is $F_{fan} \approx \frac{1}{2}\varrho v_1^2 S$

ρ-air density, v- air velocity, S-cross surface

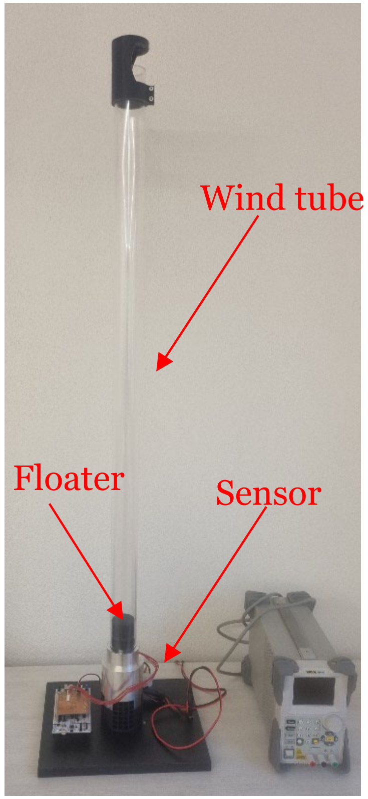

Controller design

Introducing new variable:

$$x_1 = x_2 \qquad \tilde{x}_1 = x_{d1} - x_1 \qquad \tilde{x}_1 = \tilde{x}_2$$

$$x_2 = -g + \frac{1}{m}F_{fan} + d \qquad \tilde{x}_2 = \dot{x}_{d1} - x_2 \qquad \tilde{x}_2 = g - \frac{1}{m}F_{fan} + \ddot{x}_{d1} - d$$

$$\delta_d = 9$$

Sliding variable:

$$s = \tilde{x}_2 + c\tilde{x}_1, \qquad c = 12.3$$

ET- FSMC:

$$F_{fan\_FSMC} = m\left(g + c\tilde{x}_2 + \rho sign(s) + \ddot{x}_{d1}\right), \ \ \rho = 14.3$$

$$\rho = 14.3, m = 57g$$

ET- STA:

$$F_{fan-STA} = m\left(g + c\tilde{x}_2 + k_1 |s|^{1/2} sign(s_i) + v + \ddot{x}_{d1}\right)$$

$$\dot{v} = k_2 sign(s)$$

$$k_1 = 15.3, \ \ k_2 = 7.771$$

Triggering law

$$\beta = 0.234$$

DET- FSMC/STA

$$\dot{\eta} = -\alpha\eta + \Theta\left(\beta - \|e\|\right), \quad \alpha = 21, \Theta = 0.95, \eta_0 = \frac{|x_d(0)|}{2}$$

Experimental results of the FSMC

Comparison of the TT-FSMC (Time-Triggered), ET-FSMC (Event-Triggered), and DET-FSMC (Dynamic Event-Triggered) controllers.

Tracking performance:

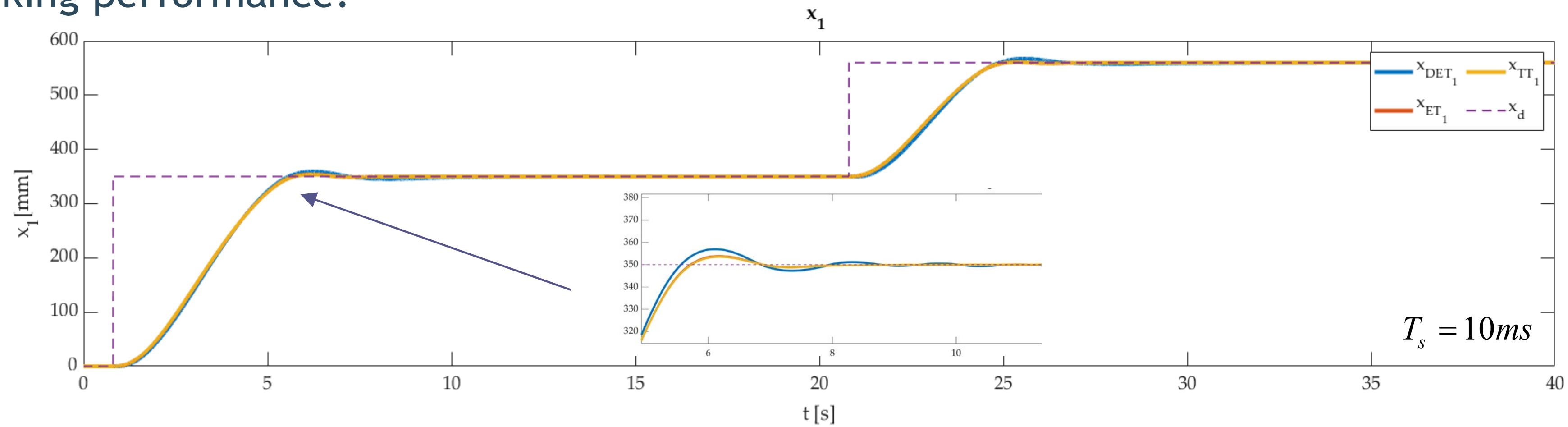

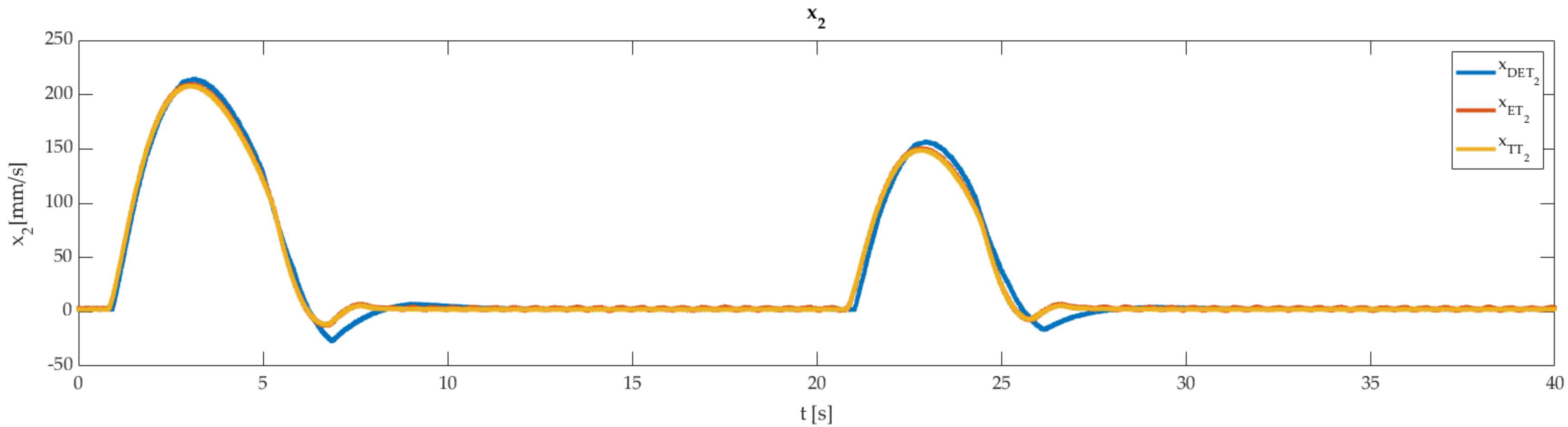

Experimental results of the FSMC

Controller output u_{FSMC} and sliding variable s_{FSMC} :

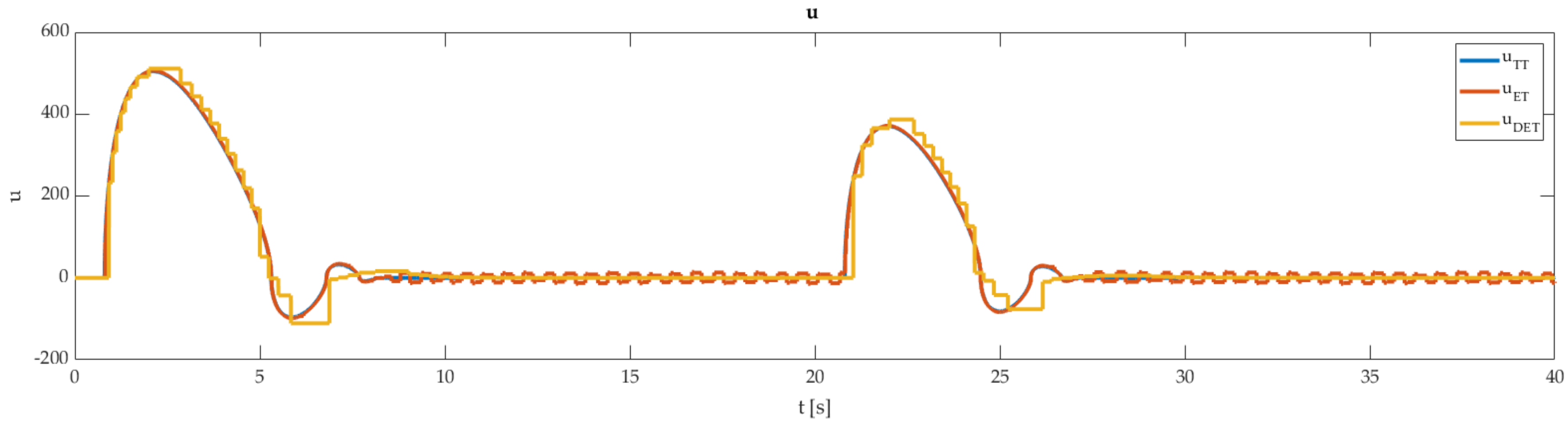

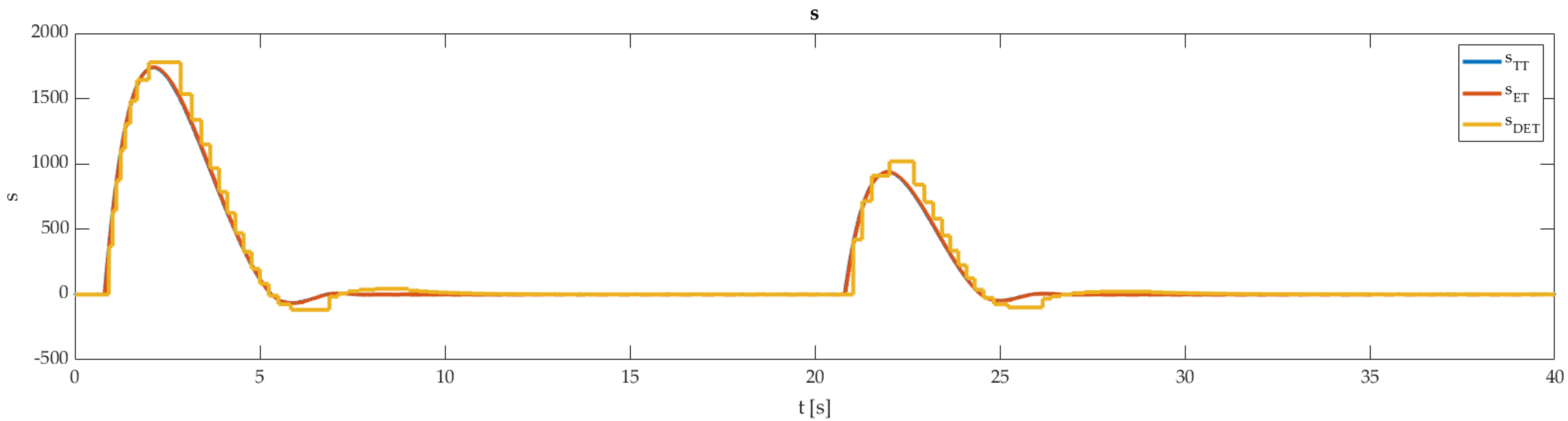

Experimental results of the FSMC

Error functions and triggering events:

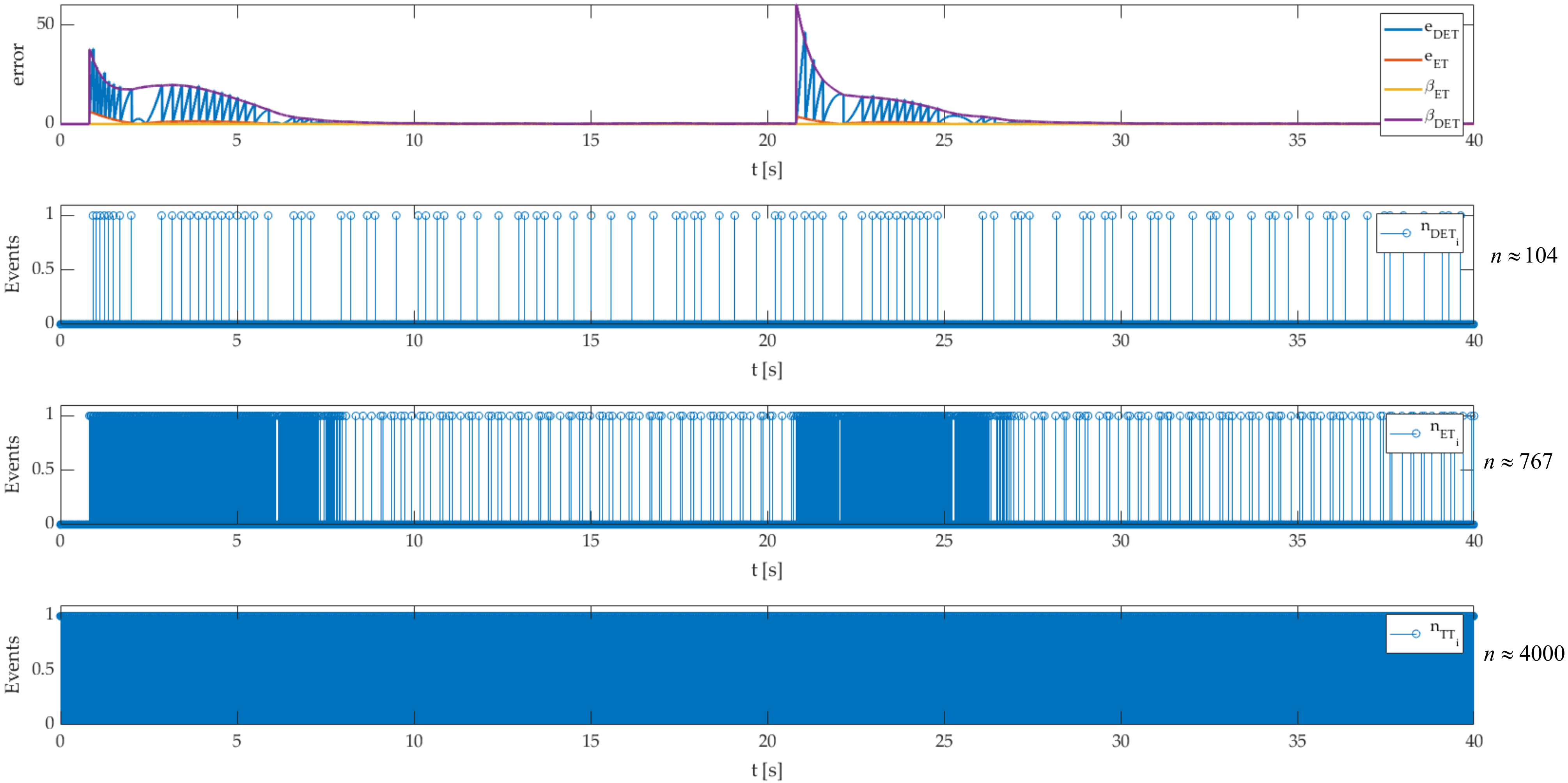

Experimental results of the STA

Comparison of the TT-STA (Time-Triggered), ET-STA (Event-Triggered), and DET-STA (Dynamic Event-Triggered) controllers.

Tracking performance:

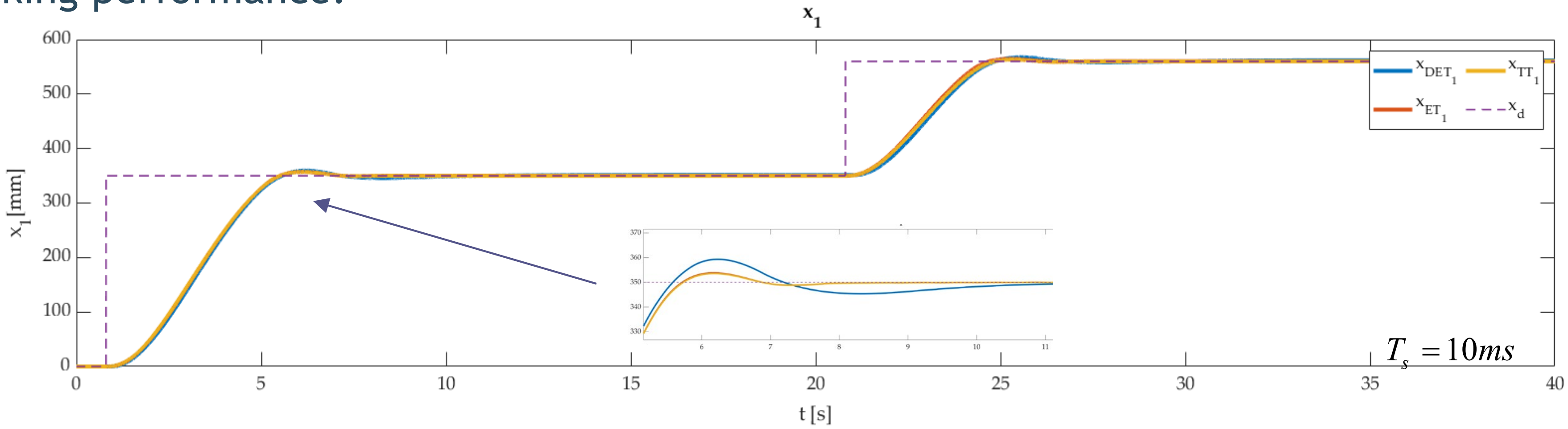

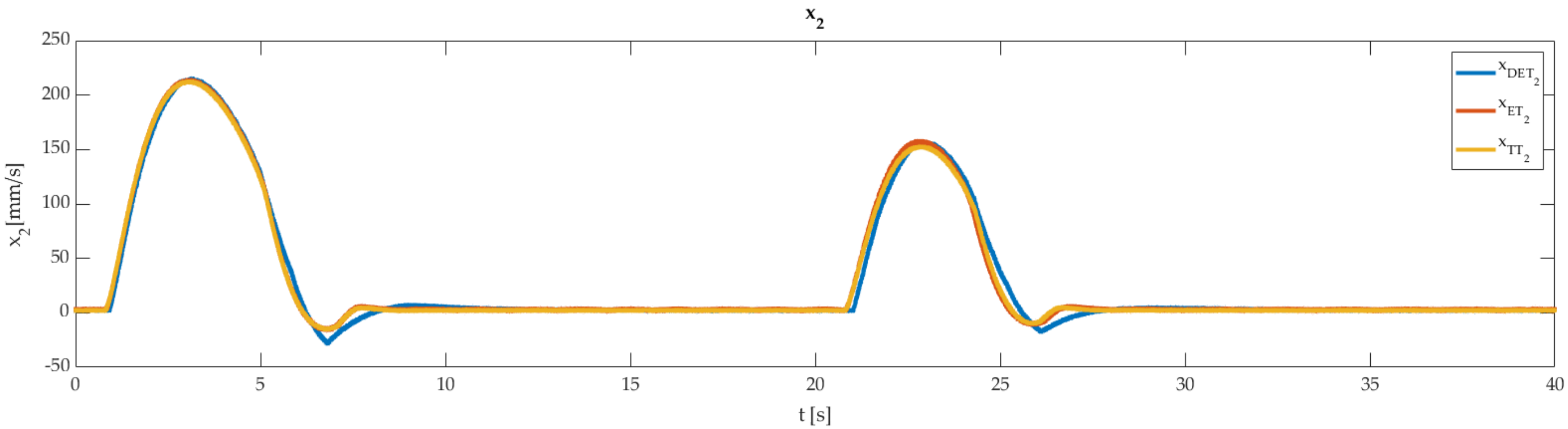

Experimental results of the STA

Controller output u_{STA} and sliding variable s_{STA} :

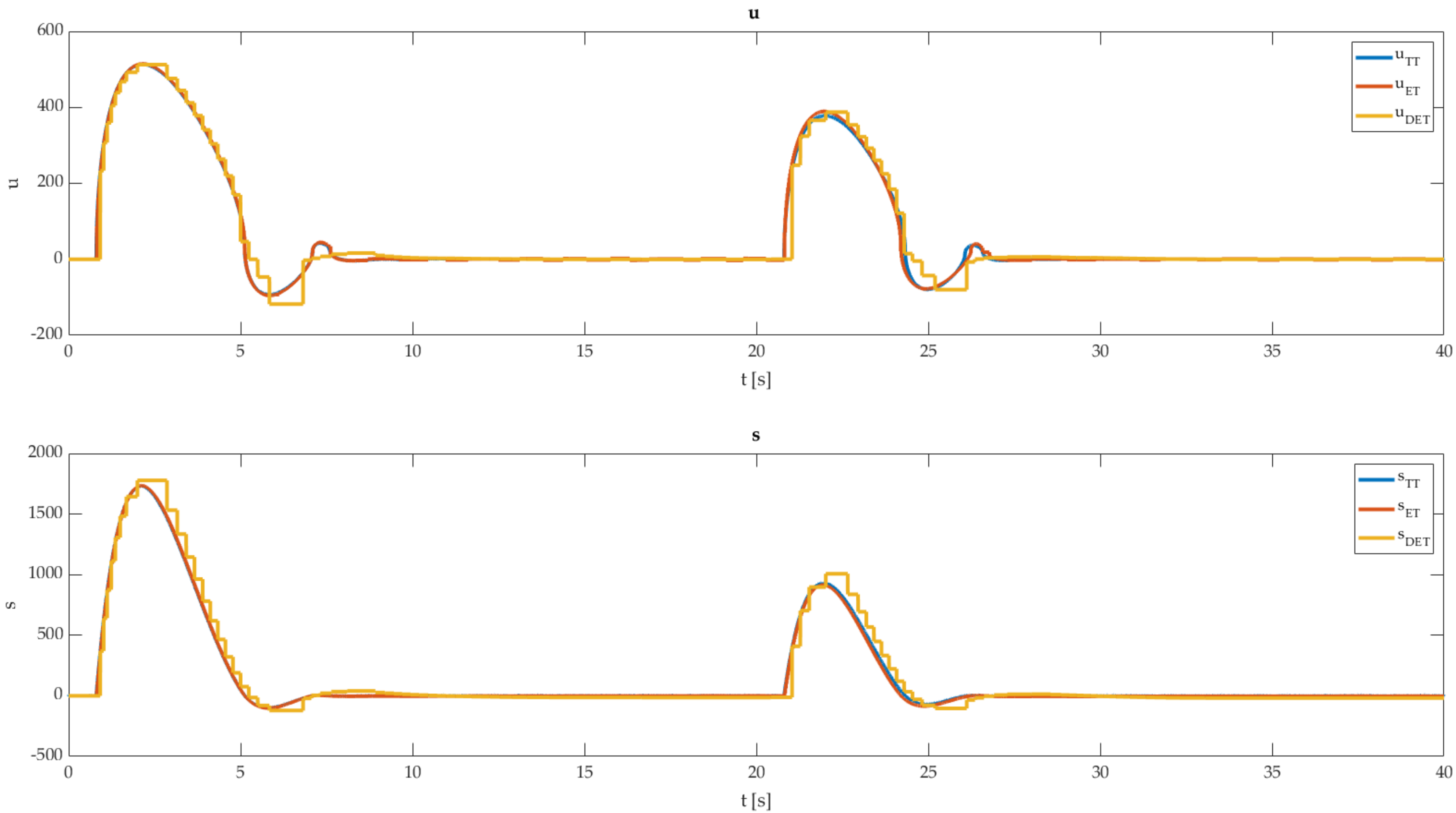

Experimental results of the STA

Error functions and triggering events:

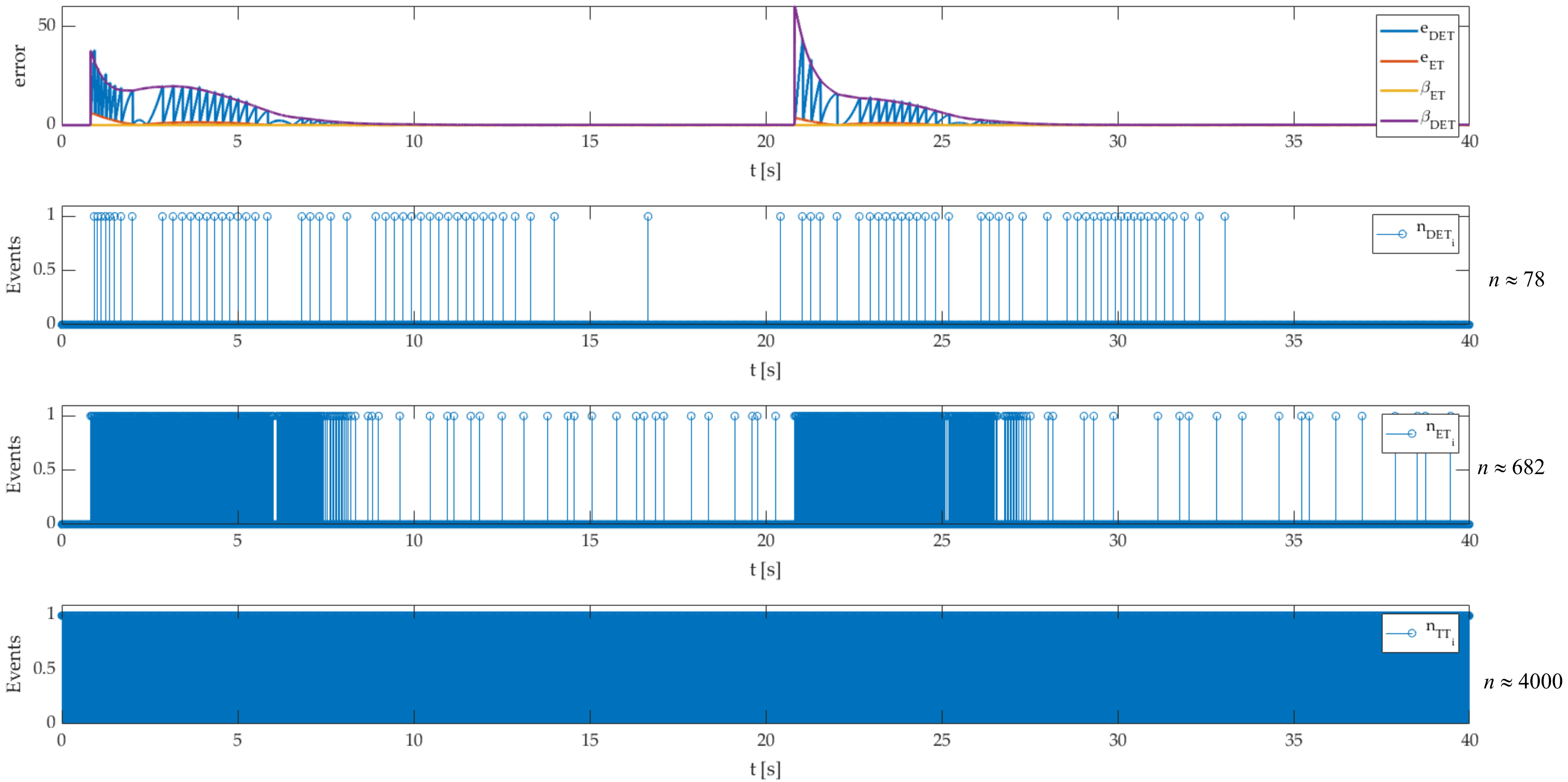

Events comparisons FSMC/STA

Event-triggering FSMC/STA:

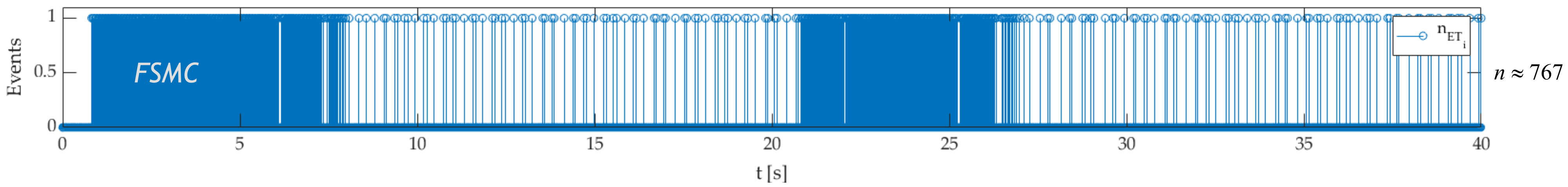

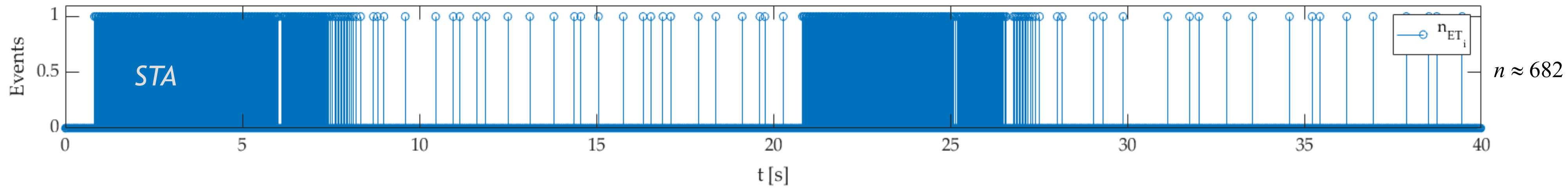

Dynamic Event-triggering FSMC/STA:

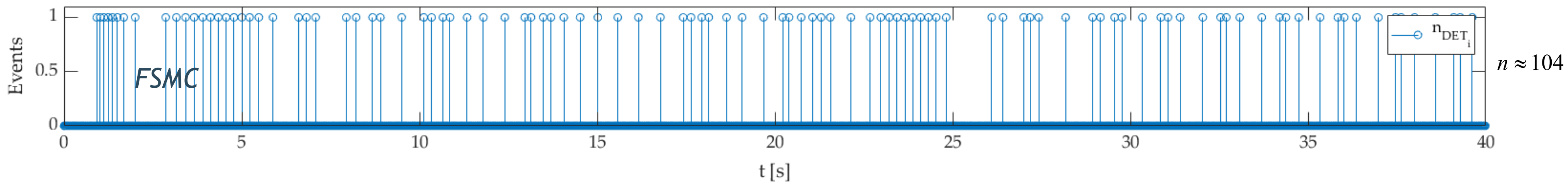

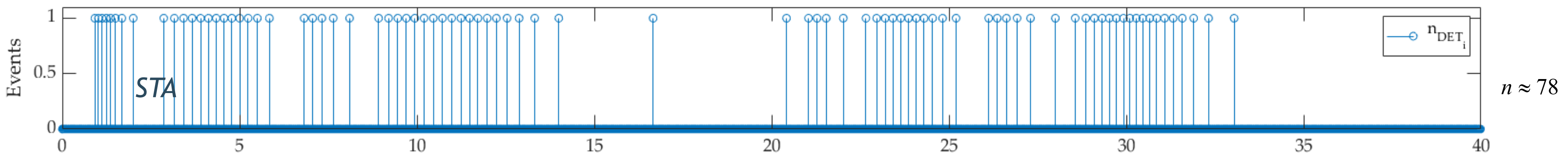

Thank you for your attention!

X. A Lyapunov Function-Based Control Concept for Networked Systems

presenter: Katarina Stanojevic

A Lyapunov Function-Based Control Concept for Networked Systems

Katarina Stanojevic

Institute of Automation and Control
Graz University of Technology
Graz, Austria

11.09.2024

Control System

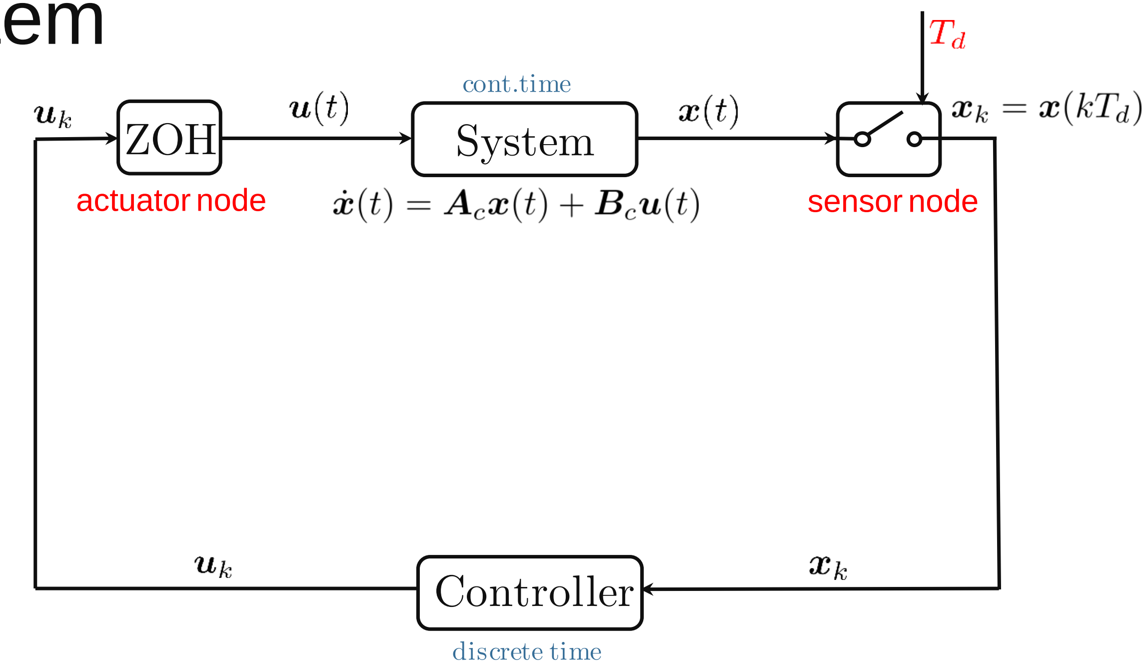

Networked Control System

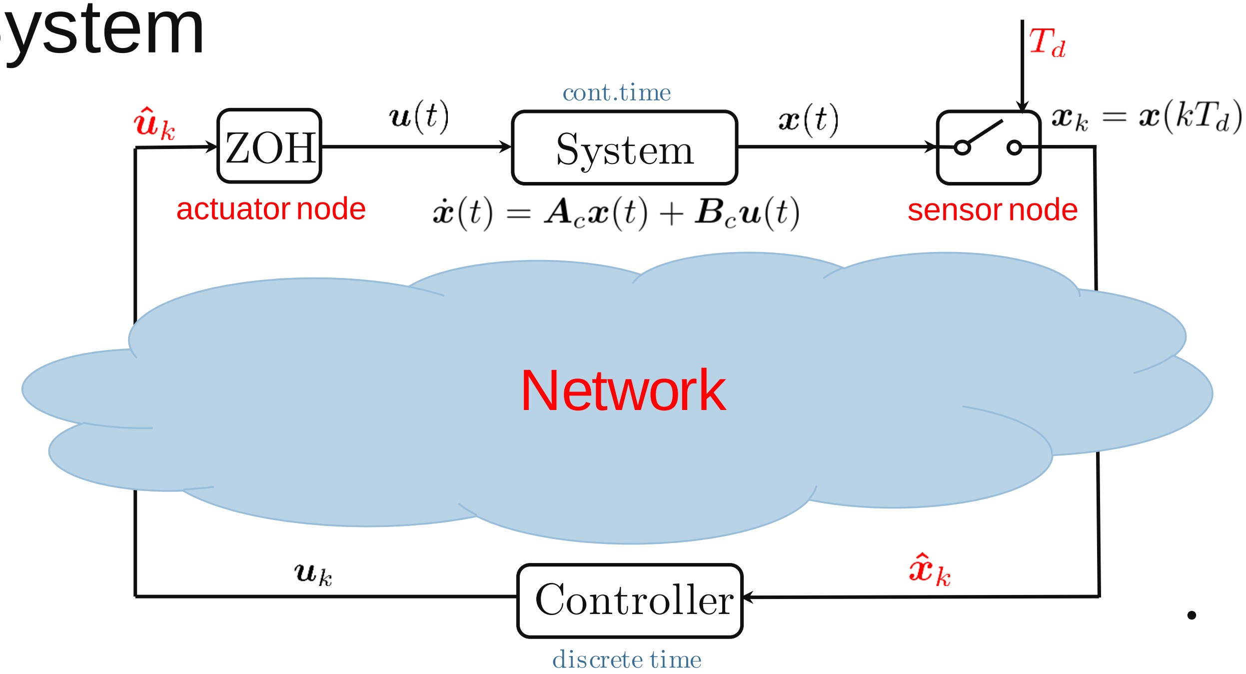

Advantages:
- Flexibility
- Adaptability
- Low installation and maintenance cost

Disadvantages:
- Imperfections of the network
  - Time-varying delays
  - Data loss

Design of State Feedback Controller for Networked Control Systems affected by unknown time-varying delays and data loss

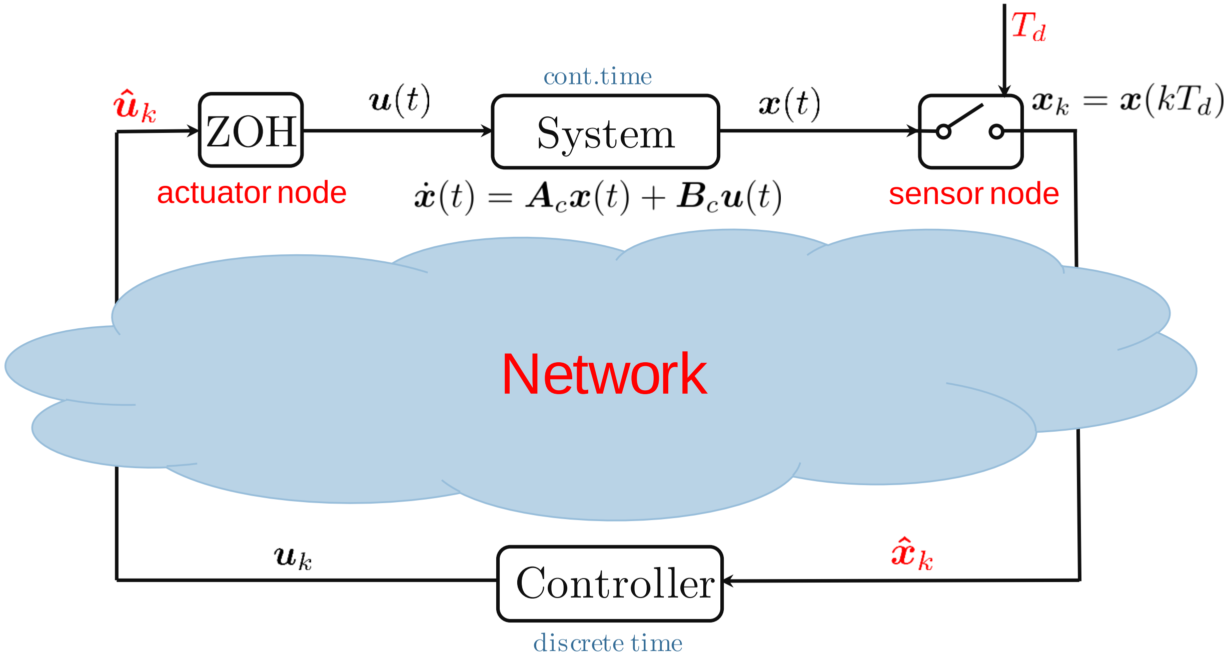

How to keep computational effort low?

Networked Control System

$\boldsymbol{x}(t) \in \mathbb{R}^n, \boldsymbol{u}^*(t) \in \mathbb{R}^m$

$$\dot{\boldsymbol{x}}(t) = \boldsymbol{A}_c \boldsymbol{x}(t) + \boldsymbol{B}_c \boldsymbol{u}^*(t)$$

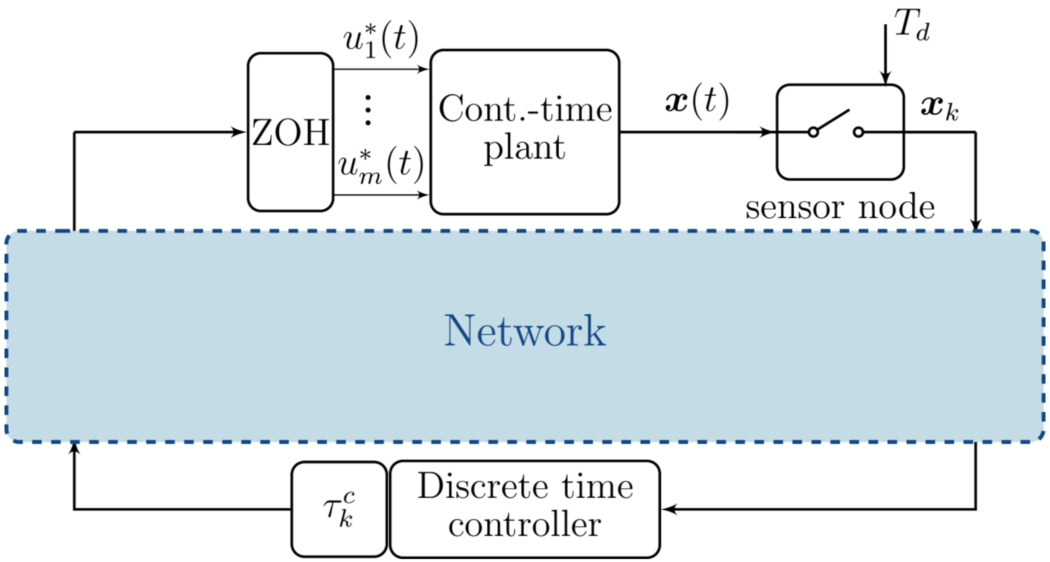

Networked Control System

$\boldsymbol{x}(t) \in \mathbb{R}^n, \boldsymbol{u}^*(t) \in \mathbb{R}^m$

$$\dot{\boldsymbol{x}}(t) = \boldsymbol{A}_c \boldsymbol{x}(t) + \boldsymbol{B}_c \boldsymbol{u}^*(t)$$

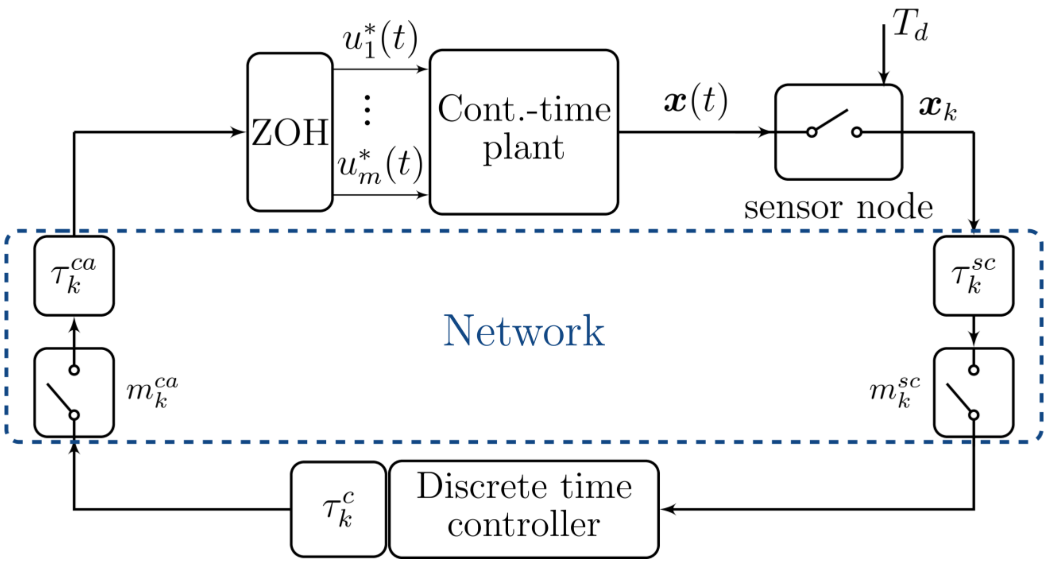

Network imperfections:

- limited transmission speed - delays
- unreliability of the communication channel – data loss

Time-varying and unknown!

Networked Control System

$\boldsymbol{x}(t) \in \mathbb{R}^n, \boldsymbol{u}^*(t) \in \mathbb{R}^m$

$$\dot{\boldsymbol{x}}(t) = \boldsymbol{A}_c \boldsymbol{x}(t) + \boldsymbol{B}_c \boldsymbol{u}^*(t)$$

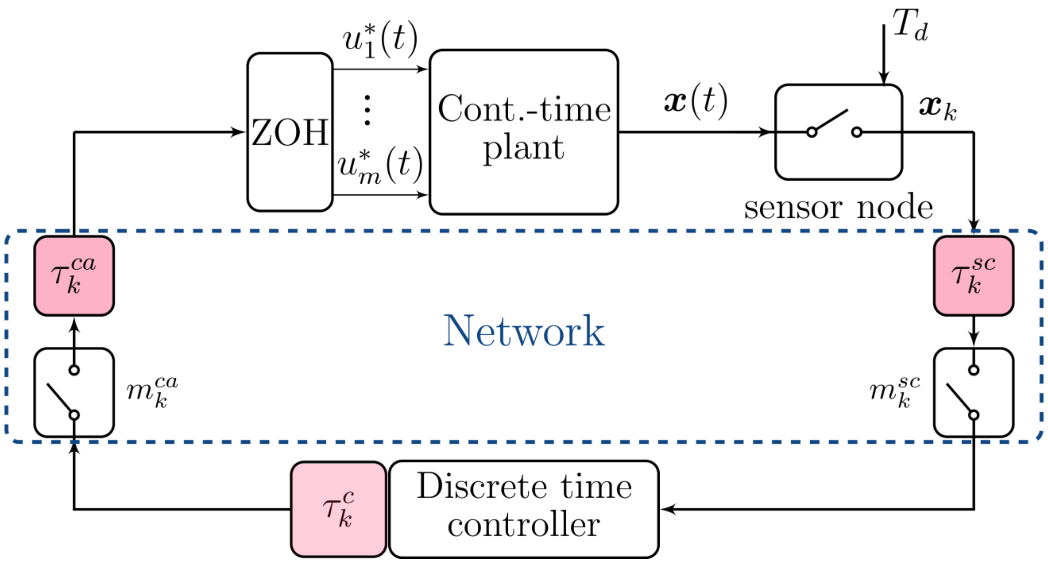

Network imperfections:

- limited transmission speed - delays
- unreliability of the communication channel – data loss

Time-varying and unknown!

delays

$0 \leq \tau_k^{SC} \leq \bar{\tau}^{SC}$

$0 \leq \tau_k^{C} \leq \bar{\tau}^{C}$

$0 \leq \tau_k^{CA} \leq \bar{\tau}^{CA}$

Networked Control System

$\boldsymbol{x}(t) \in \mathbb{R}^n, \boldsymbol{u}^*(t) \in \mathbb{R}^m$

$$\dot{\boldsymbol{x}}(t) = \boldsymbol{A}_c\boldsymbol{x}(t) + \boldsymbol{B}_c\boldsymbol{u}^*(t)$$

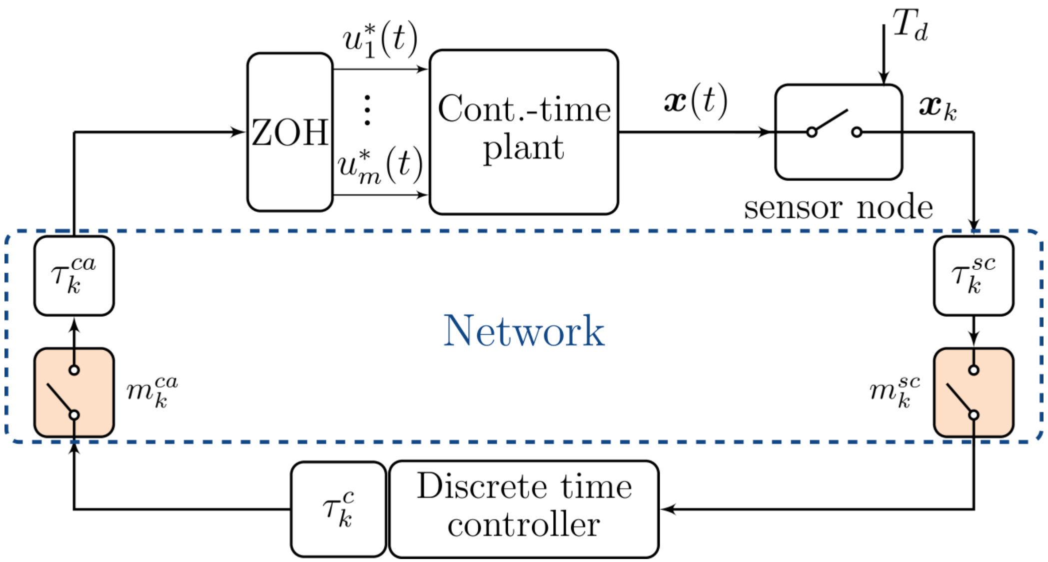

Network imperfections:

- limited transmission speed - delays
- unreliability of the communication channel – data loss

Time-varying and unknown!

delays

$$0 \le \tau_k^{SC} \le \bar{\tau}^{SC}$$
$$0 \le \tau_k^{C} \le \bar{\tau}^{C}$$
$$0 \le \tau_k^{CA} \le \bar{\tau}^{CA}$$

data loss

$$m_k^* = \begin{cases} 1, & \text{data packet is lost} \\ 0, & \text{data packet is received} \end{cases}$$

$$0 \le m_k^{SC} \le \bar{m}^{SC} \qquad 0 \le m_k^{CA} \le \bar{m}^{CA}$$

Model of a Networked Control System

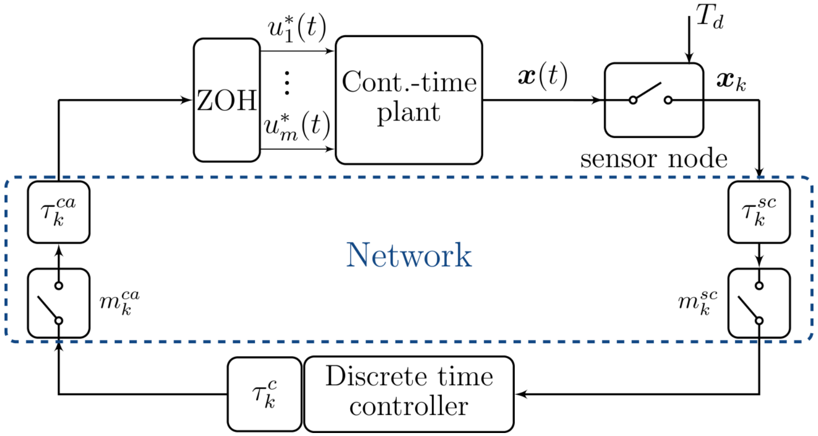

Model of a Networked Control System

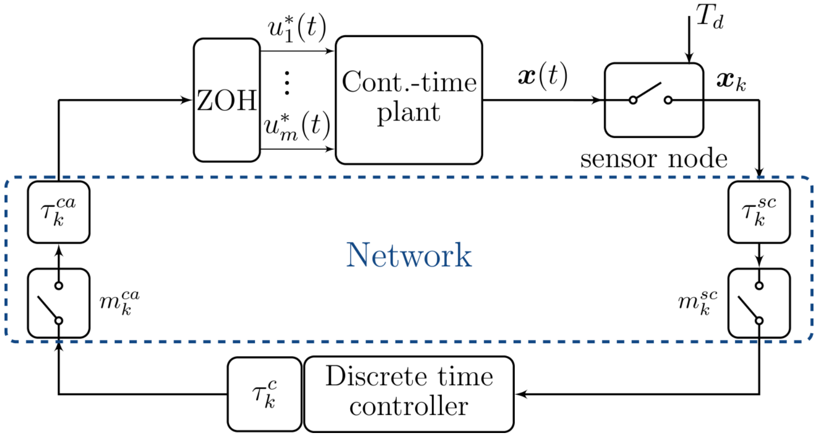

Static
feedback controller

$$\boldsymbol{u}_k = -\boldsymbol{K}\boldsymbol{x}_k$$

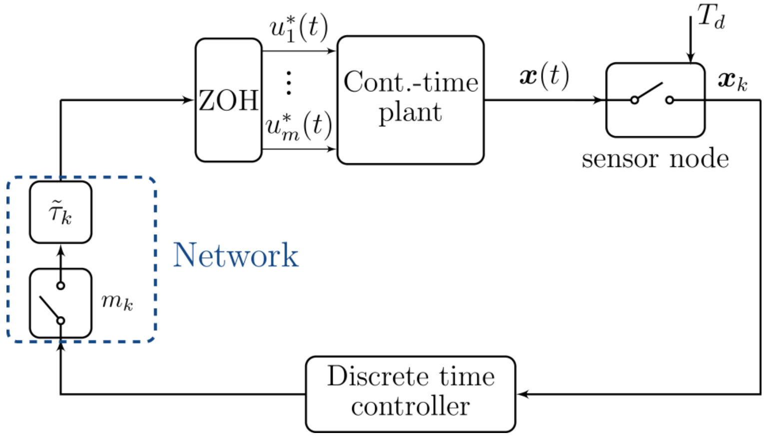

$$\tilde{\tau}_k = \tau_k^{SC} + \tau_k^{C} + \tau_k^{CA} \leq \bar{d}T_d \quad \bar{d} \in \mathbb{N}^+$$

$$m_k = \max\{m_k^{sc}, m_k^{ca}\}$$

$$\sum_{i=k-\bar{p}}^{k} m_i \leq \bar{p} \quad \forall k, \quad \bar{p} \in \mathbb{N}^+$$

$$\bar{\delta} = \bar{d} + \bar{p}$$

$$\dot{\boldsymbol{x}}(t) = \boldsymbol{A}_c\boldsymbol{x}(t) + \boldsymbol{B}_c\boldsymbol{u}^*(t)$$

$$\boldsymbol{u}^*(t) = \boldsymbol{u}_{k+j-\bar{\delta}}$$

$$kT_d + t_k^j \leq t < kT_d + t_k^{j+1}$$

Model of a Networked Control System

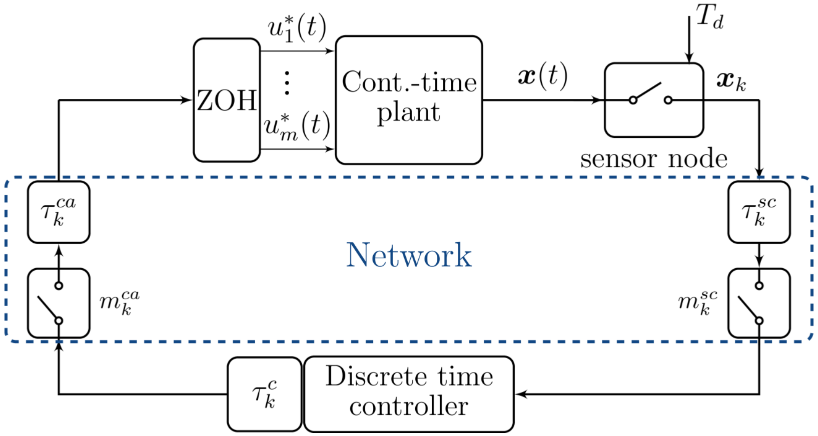

Static feedback controller

$$\boldsymbol{u}_k = -\boldsymbol{K}\boldsymbol{x}_k$$

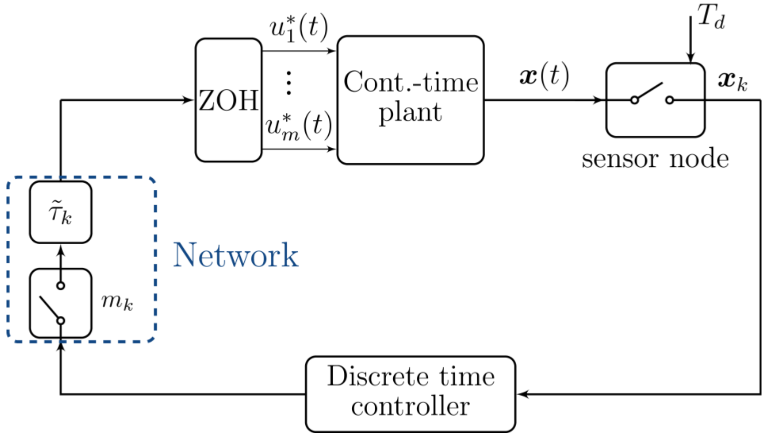

$$\tilde{\tau}_k = \tau_k^{SC} + \tau_k^{C} + \tau_k^{CA} \le \bar{d}T_d \quad \bar{d} \in \mathbb{N}^+$$

$$m_k = \max\{m_k^{sc}, m_k^{ca}\}$$

$$\sum_{i=k-\bar{p}}^{k} m_i \le \bar{p} \quad \forall k, \quad \bar{p} \in \mathbb{N}^+$$

$$\bar{\delta} = \bar{d} + \bar{p}$$

$$\dot{\boldsymbol{x}}(t) = \boldsymbol{A}_c\boldsymbol{x}(t) + \boldsymbol{B}_c\boldsymbol{u}^*(t)$$

$$\boldsymbol{u}^*(t) = \boldsymbol{u}_{k+j-\bar{\delta}}$$

$$kT_d + t_k^j \le t < kT_d + t_k^{j+1}$$

$$\boldsymbol{x}_{k+1} = \boldsymbol{A}_d\boldsymbol{x}_k + \sum_{j=0}^{\bar{\delta}} \boldsymbol{B}_j(t_k^j, t_k^{j+1})\boldsymbol{u}_{k+j-\bar{\delta}}$$

$$\boldsymbol{B}_j(t_k^j, t_k^{j+1}) = \int_{t_k^j}^{t_k^{j+1}} e^{\boldsymbol{A}_c(T_d-s)}\boldsymbol{B}_c\,ds$$

Existing Work

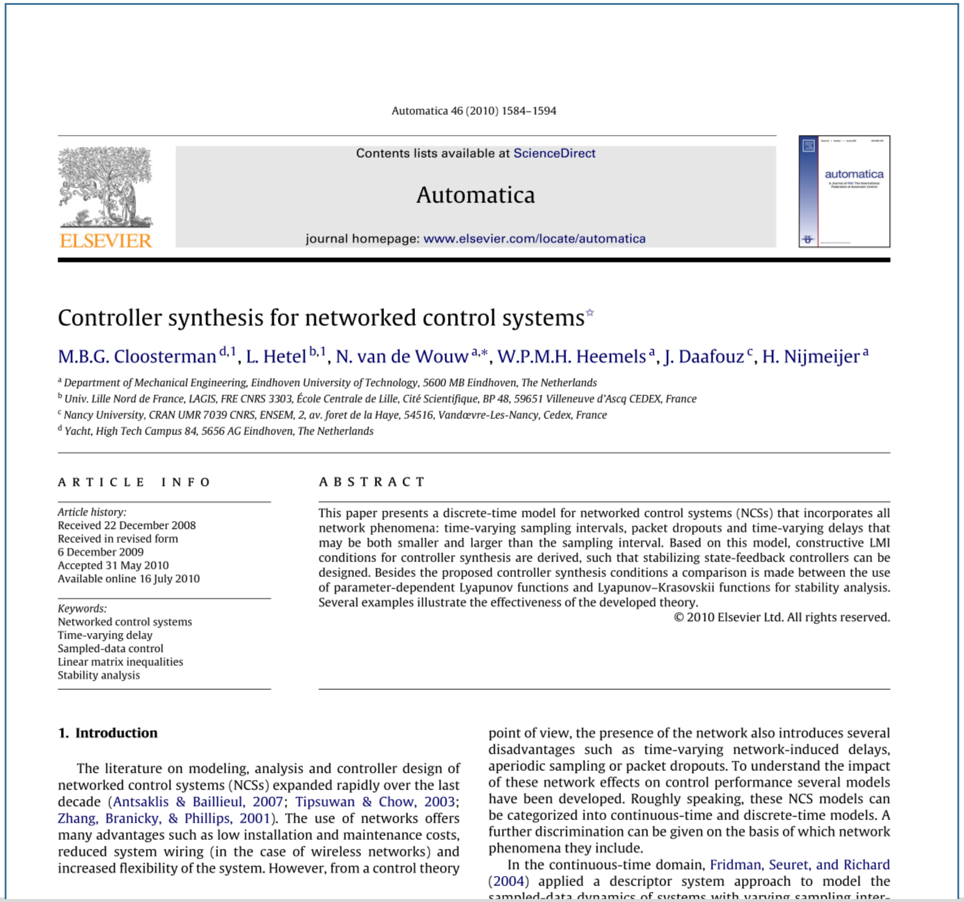

Automatica 46 (2010) 1584–1594

Contents lists available at ScienceDirect

Automatica

journal homepage: www.elsevier.com/locate/automatica

ELSEVIER

Controller synthesis for networked control systems☆

M.B.G. Cloosterman[d,1], L. Hetel[b,1], N. van de Wouw[a,*], W.P.M.H. Heemels[a], J. Daafouz[c], H. Nijmeijer[a]

[a] Department of Mechanical Engineering, Eindhoven University of Technology, 5600 MB Eindhoven, The Netherlands
[b] Univ. Lille Nord de France, LAGIS, FRE CNRS 3303, École Centrale de Lille, Cité Scientifique, BP 48, 59651 Villeneuve d'Ascq CEDEX, France
[c] Nancy University, CRAN UMR 7039 CNRS, ENSEM, 2, av. foret de la Haye, 54516, Vandœvre-Les-Nancy, Cedex, France
[d] Yacht, High Tech Campus 84, 5656 AG Eindhoven, The Netherlands

ARTICLE INFO

Article history:
Received 22 December 2008
Received in revised form
6 December 2009
Accepted 31 May 2010
Available online 16 July 2010

Keywords:
Networked control systems
Time-varying delay
Sampled-data control
Linear matrix inequalities
Stability analysis

ABSTRACT

This paper presents a discrete-time model for networked control systems (NCSs) that incorporates all network phenomena: time-varying sampling intervals, packet dropouts and time-varying delays that may be both smaller and larger than the sampling interval. Based on this model, constructive LMI conditions for controller synthesis are derived, such that stabilizing state-feedback controllers can be designed. Besides the proposed controller synthesis conditions a comparison is made between the use of parameter-dependent Lyapunov functions and Lyapunov–Krasovskii functions for stability analysis. Several examples illustrate the effectiveness of the developed theory.

1. Introduction

The literature on modeling, analysis and controller design of networked control systems (NCSs) expanded rapidly over the last decade (Antsaklis & Baillieul, 2007; Tipsuwan & Chow, 2003; Zhang, Branicky, & Phillips, 2001). The use of networks offers many advantages such as low installation and maintenance costs, reduced system wiring (in the case of wireless networks) and increased flexibility of the system. However, from a control theory point of view, the presence of the network also introduces several disadvantages such as time-varying network-induced delays, aperiodic sampling or packet dropouts. To understand the impact of these network effects on control performance several models have been developed. Roughly speaking, these NCS models can be categorized into continuous-time and discrete-time models. A further discrimination can be given on the basis of which network phenomena they include.

In the continuous-time domain, Fridman, Seuret, and Richard (2004) applied a descriptor system approach to model the sampled-data dynamics of systems with varying sampling inter-

Control design

- Linear Matrix Inequality based approach
- ensures stability for any network imperfection inside defined bounds

- convex over-approximation is necessary (e.g. Jordan Form)
- Nr of LMIs depends not only on the network imperfections but on the system to be controlled as well
- Only 1 degree of freedom

Existing Work

Automatica 46 (2010) 1584–1594

Contents lists available at ScienceDirect

Automatica

journal homepage: www.elsevier.com/locate/automatica

ELSEVIER

Controller synthesis for networked control systems☆

M.B.G. Cloosterman[d,1], L. Hetel[b,1], N. van de Wouw[a,*], W.P.M.H. Heemels[a], J. Daafouz[c], H. Nijmeijer[a]

Network imperfections

Nr of inputs

Nr of states

E

$\bar{\delta}=3$, $m=1$, $n=2$	$\#\text{LMIs}=4096$, $\#\text{opt.var}=1926$	$\bar{\delta}=4$, $m=1$, $n=2$	$\#\text{LMIs}=65536$, $\#\text{opt.var}=11526$
$\bar{\delta}=5$, $m=1$, $n=2$	$\#\text{LMIs}=1048576$, $\#\text{opt.var}=64518$	$\bar{\delta}=6$, $m=1$, $n=2$	$\#\text{LMIs}=16777216$, $\#\text{opt.var}=344070$

Control design

- Linear Matrix Inequality based approach
- ensures stability for any network imperfection inside defined bounds
- convex over-approximation is necessary (e.g. Jordan Form)
- Nr of LMIs depends not only on the network imperfections but on the system to be controlled as well
- Only 1 degree of freedom

Existing Work

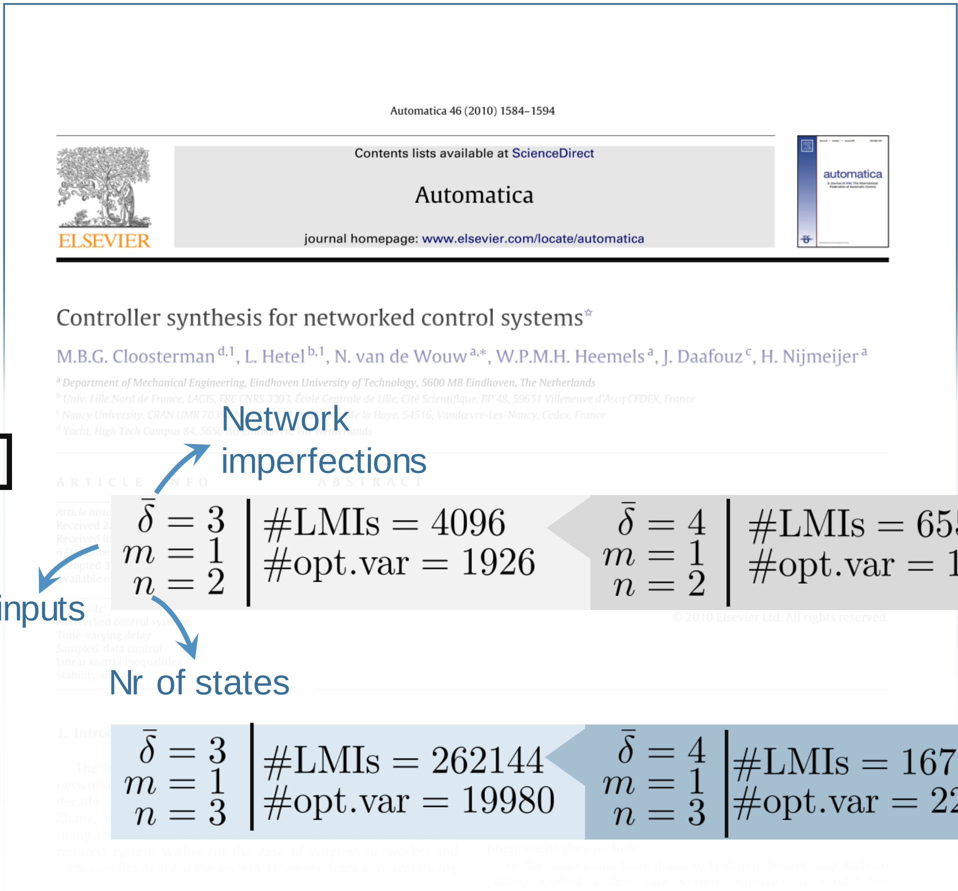
Automatica 46 (2010) 1584–1594

Contents lists available at ScienceDirect

Automatica

journal homepage: www.elsevier.com/locate/automatica

Controller synthesis for networked control systems

M.B.G. Cloosterman[d,1], L. Hetel[b,1], N. van de Wouw[a,*], W.P.M.H. Heemels[a], J. Daafouz[c], H. Nijmeijer[a]

Control design

- Linear Matrix Inequality based approach
- ensures stability for any network imperfection inside defined bounds
- convex over-approximation is necessary (e.g. Jordan Form)
- Nr of LMIs depends not only on the network imperfections but on the system to be controlled as well
- Only 1 degree of freedom

E

Network imperfections

Nr of inputs

Nr of states

$\bar{\delta}=3,\ m=1,\ n=2$	$\#\text{LMIs}=4096$, $\#\text{opt.var}=1926$
$\bar{\delta}=4,\ m=1,\ n=2$	$\#\text{LMIs}=65536$, $\#\text{opt.var}=11526$
$\bar{\delta}=5,\ m=1,\ n=2$	$\#\text{LMIs}=1048576$, $\#\text{opt.var}=64518$
$\bar{\delta}=6,\ m=1,\ n=2$	$\#\text{LMIs}=16777216$, $\#\text{opt.var}=344070$

$\bar{\delta}=3,\ m=1,\ n=3$	$\#\text{LMIs}=262144$, $\#\text{opt.var}=19980$
$\bar{\delta}=4,\ m=1,\ n=3$	$\#\text{LMIs}=16777216$, $\#\text{opt.var}=229388$

$\ldots$

Existing Work

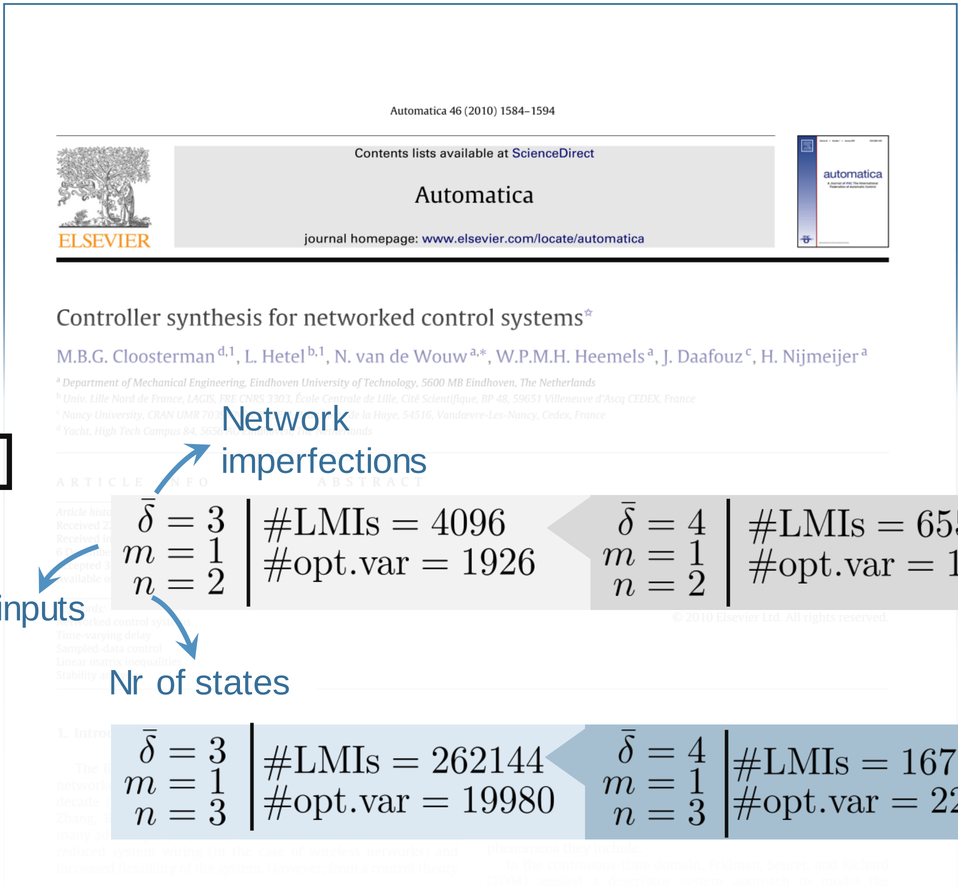
Automatica 46 (2010) 1584–1594

Contents lists available at ScienceDirect

Automatica

journal homepage: www.elsevier.com/locate/automatica

Controller synthesis for networked control systems

M.B.G. Cloosterman[d,1], L. Hetel[b,1], N. van de Wouw[a,*], W.P.M.H. Heemels[a], J. Daafouz[c], H. Nijmeijer[a]

Control design

- Linear Matrix Inequality based approach
- ensures stability for any network imperfection inside defined bounds
- convex over-approximation is necessary (e.g. Jordan Form)
- Nr of LMIs depends not only on the network imperfections but on the system to be controlled as well
- Only 1 degree of freedom

E

Network imperfections

Nr of inputs

Nr of states

$\bar{\delta} = 3$, $m = 1$, $n = 2$	$\#\text{LMIs} = 4096$, $\#\text{opt.var} = 1926$
$\bar{\delta} = 4$, $m = 1$, $n = 2$	$\#\text{LMIs} = 65536$, $\#\text{opt.var} = 11526$
$\bar{\delta} = 5$, $m = 1$, $n = 2$	$\#\text{LMIs} = 1048576$, $\#\text{opt.var} = 64518$
$\bar{\delta} = 6$, $m = 1$, $n = 2$	$\#\text{LMIs} = 16777216$, $\#\text{opt.var} = 344070$

$\bar{\delta} = 3$, $m = 1$, $n = 3$	$\#\text{LMIs} = 262144$, $\#\text{opt.var} = 19980$
$\bar{\delta} = 4$, $m = 1$, $n = 3$	$\#\text{LMIs} = 16777216$, $\#\text{opt.var} = 229388$

$\dots$

Effects of the network

- It is unknown which signal will arrive
- It is unknown for how long the signal will be active

Switched Lyapunov Function-Based Controller Synthesis

1. Buffering Mechanism [1]
2. Control Design [2]

[1] K. Stanojevic, M. Steinberger and M. Horn, "Robust Control of Networked Systems: Buffering, Control Design and Application," 2022 IEEE Conference on Control Technology and Applications (CCTA), Trieste, Italy, 2022, pp. 1068-1073

[2] K. Stanojevic, M. Steinberger and M. Horn, "Switched Lyapunov Function-Based Controller Synthesis for Networked Control Systems: A Computationally Inexpensive Approach," in IEEE Control Systems Letters, vol. 7, pp. 2023-2028, 2023

Buffering Mechanism

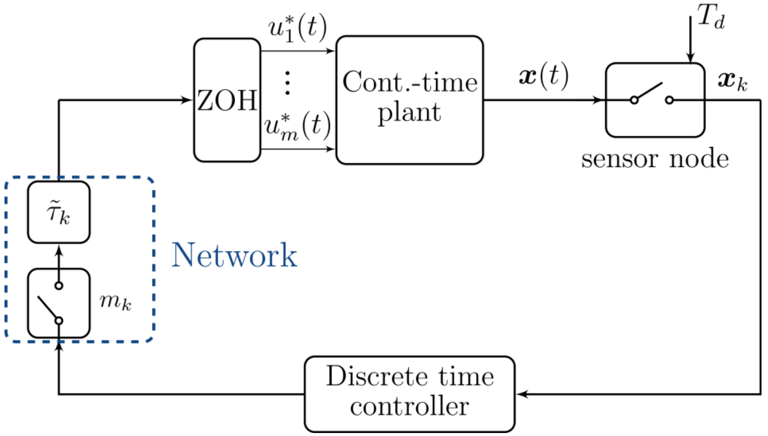

Buffering Mechanism

RTT: $\tau_k = \tilde{\tau}_k + \tau_k^B \quad \tau_k = \left\lceil \frac{\tilde{\tau}_k}{T_d} \right\rceil \cdot T_d = q_k T_d \quad q_k \in \{1, 2, \ldots, \bar{\delta}\}$

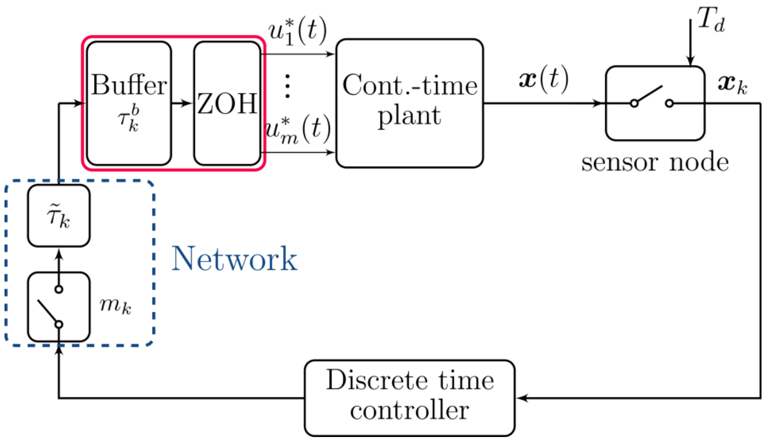

Buffering Mechanism

RTT: $\tau_k = \tilde{\tau}_k + \tau_k^B \qquad \tau_k = \left\lceil \frac{\tilde{\tau}_k}{T_d} \right\rceil \cdot T_d = q_k T_d \qquad q_k \in \{1, 2, \ldots, \bar{\delta}\}$

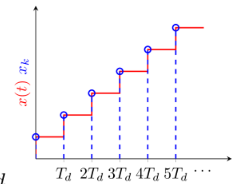

$x_k = k + 1$

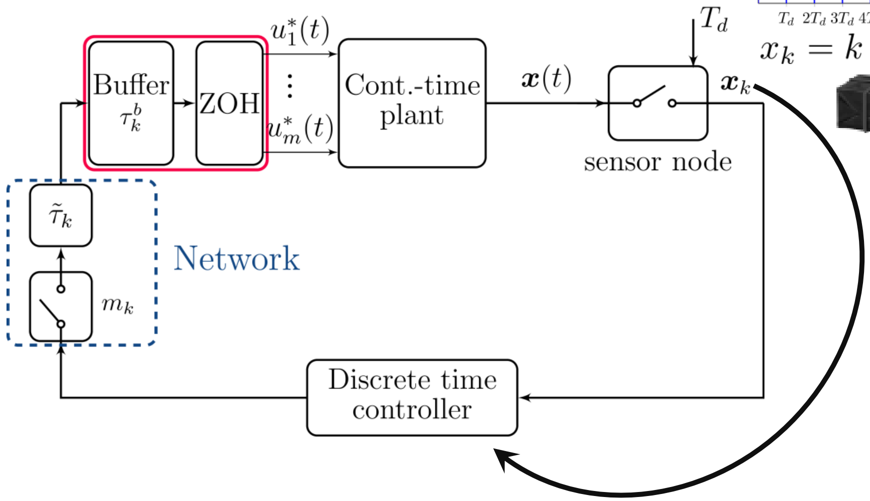

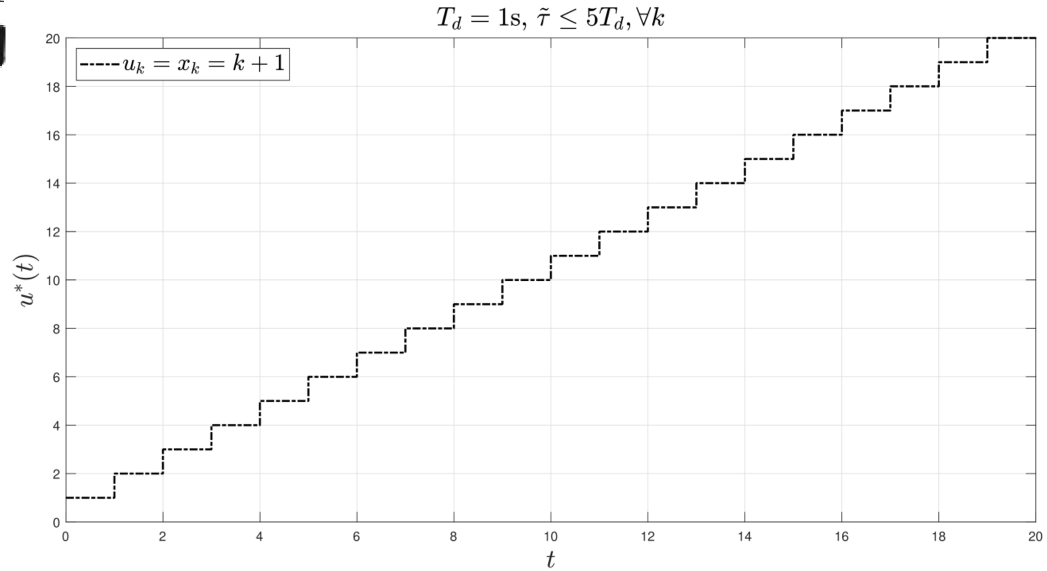

Buffering Mechanism

$$\text{RTT: } \tau_k = \tilde{\tau}_k + \tau_k^B \qquad \tau_k = \left\lceil \frac{\tilde{\tau}_k}{T_d} \right\rceil \cdot T_d = q_k T_d \qquad q_k \in \{1, 2, \dots, \bar{\delta}\}$$

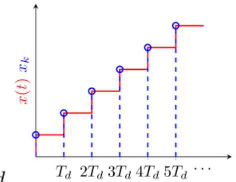

$$x_k = k + 1$$

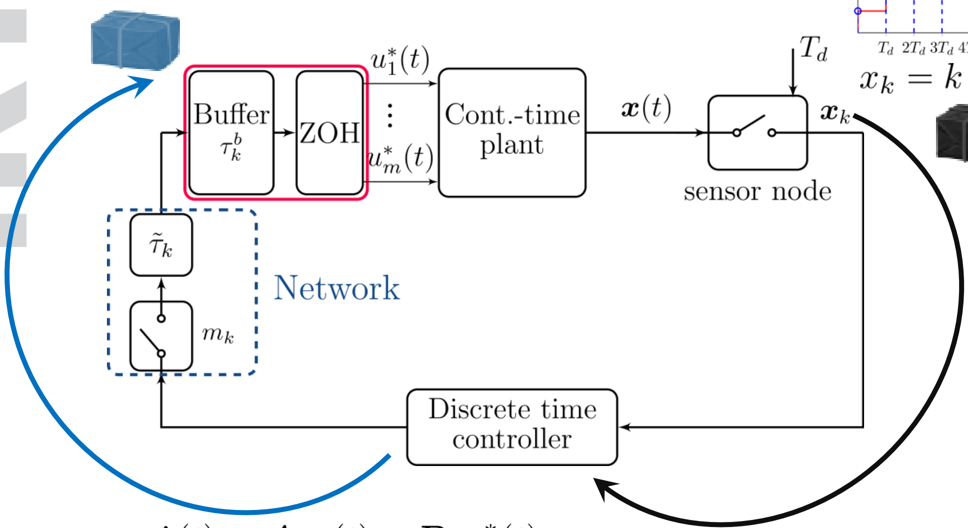

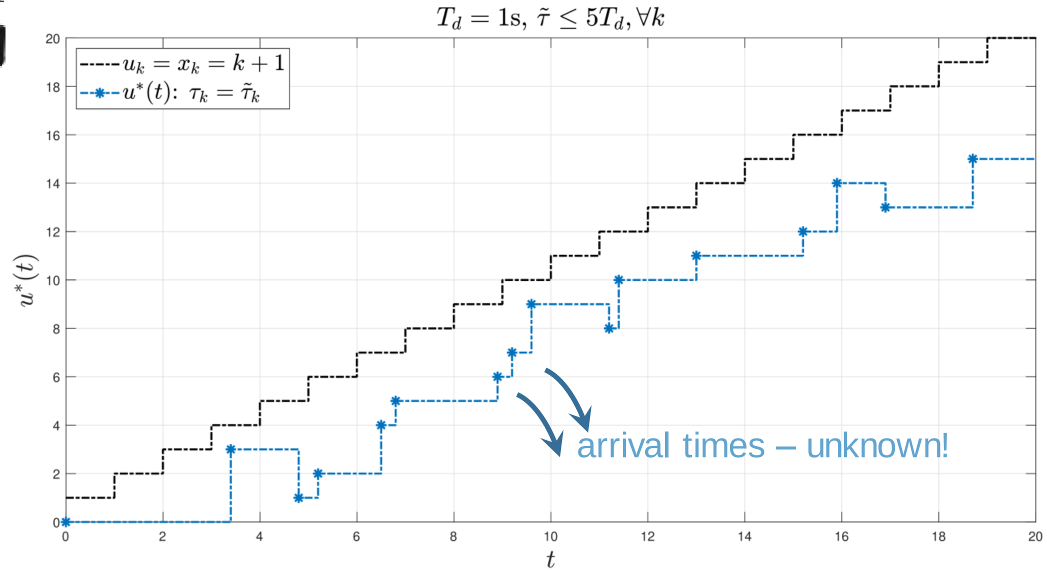

$$\dot{\boldsymbol{x}}(t) = \boldsymbol{A}_c \boldsymbol{x}(t) + \boldsymbol{B}_c \boldsymbol{u}^*(t)$$

$$\boldsymbol{u}^*(t) = \boldsymbol{u}_{k+j-\bar{\delta}}$$

$$kT_d + t_k^j \leq t < kT_d + t_k^{k+1}$$

$$\boxed{\begin{aligned} \boldsymbol{x}_{k+1} &= \boldsymbol{A}_d \boldsymbol{x}_k + \sum_{j=0}^{\bar{\delta}} \boldsymbol{B}_j(t_k^j, t_k^{j+1}) \boldsymbol{u}_{k+j-\bar{\delta}} \\ \boldsymbol{B}_j(t_k^j, t_k^{j+1}) &= \int_{t_k^j}^{t_k^{j+1}} e^{\boldsymbol{A}_c(T_d - s)} \boldsymbol{B}_c ds \end{aligned}}$$

Buffering Mechanism

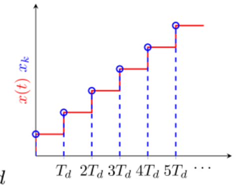

$x_k = k+1$

RTT: $\tau_k = \tilde{\tau}_k + \tau_k^B \qquad \tau_k = \left\lceil \frac{\tilde{\tau}_k}{T_d} \right\rceil \cdot T_d = q_k T_d \qquad q_k \in \{1, 2, \ldots, \bar{\delta}\}$

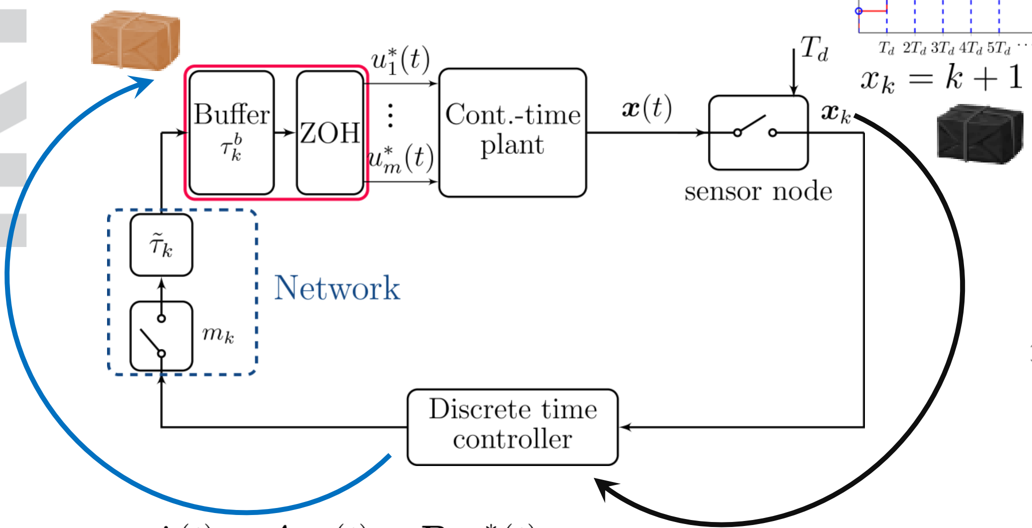

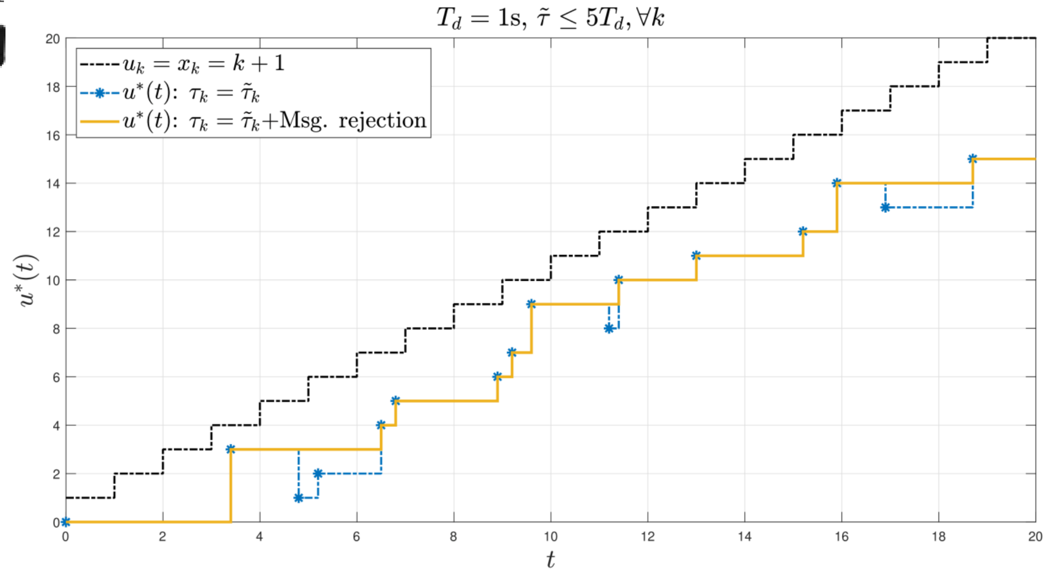

$$\dot{\boldsymbol{x}}(t) = \boldsymbol{A}_c \boldsymbol{x}(t) + \boldsymbol{B}_c \boldsymbol{u}^*(t)$$

$$\boldsymbol{u}^*(t) = \boldsymbol{u}_{k+j-\bar{\delta}}$$

$$kT_d + t_k^j \leq t < kT_d + t_k^{k+1}$$

$$\boldsymbol{x}_{k+1} = \boldsymbol{A}_d \boldsymbol{x}_k + \sum_{j=0}^{\bar{\delta}} \boldsymbol{B}_j(t_k^j, t_k^{j+1}) \boldsymbol{u}_{k+j-\bar{\delta}}$$

$$\boldsymbol{B}_j(t_k^j, t_k^{j+1}) = \int_{t_k^j}^{t_k^{j+1}} e^{\boldsymbol{A}_c(T_d - s)} \boldsymbol{B}_c ds$$

Buffering Mechanism

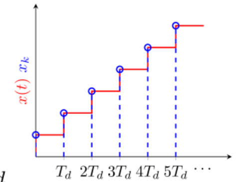

$x_k = k + 1$

RTT: $\tau_k = \tilde{\tau}_k + \tau_k^B \qquad \tau_k = \left\lceil \frac{\tilde{\tau}_k}{T_d} \right\rceil \cdot T_d = q_k T_d \qquad q_k \in \{1, 2, \ldots, \bar{\delta}\}$

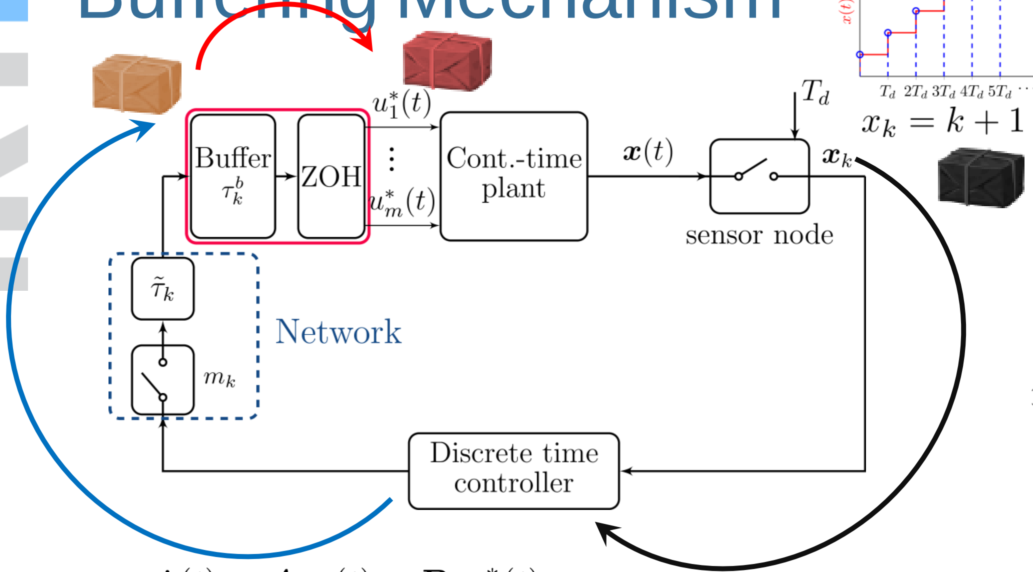

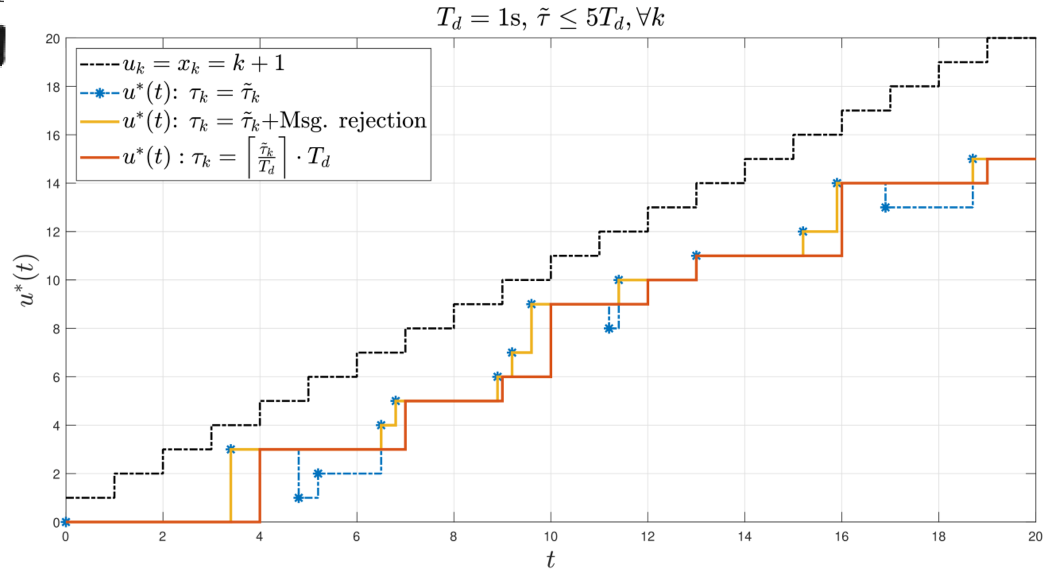

$$\dot{\boldsymbol{x}}(t) = \boldsymbol{A}_c \boldsymbol{x}(t) + \boldsymbol{B}_c \boldsymbol{u}^*(t)$$

$$\boldsymbol{u}^*(t) = \boldsymbol{u}_{k+j-\bar{\delta}}$$

$$kT_d + t_k^j \le t < kT_d + t_k^{k+1}$$

$$\boldsymbol{x}_{k+1} = \boldsymbol{A}_d \boldsymbol{x}_k + \sum_{j=0}^{\bar{\delta}} \boldsymbol{B}_j(t_k^j, t_k^{j+1}) \boldsymbol{u}_{k+j-\bar{\delta}}$$

$$\boldsymbol{B}_j(t_k^j, t_k^{j+1}) = \int_{t_k^j}^{t_k^{j+1}} e^{\boldsymbol{A}_c(T_d - s)} \boldsymbol{B}_c ds$$

$\longrightarrow$

$$\boldsymbol{x}_{k+1} = \boldsymbol{A}_d \boldsymbol{x}_k + \boldsymbol{B}_d \boldsymbol{u}_{k-q_k} \qquad q_k \in \{1, 2, \ldots, \bar{\delta}\}$$

$$\boldsymbol{B}_d = \int_0^{T_d} e^{\boldsymbol{A}_c(T_d - s)} \boldsymbol{B}_c ds$$

Control Design for Buffered Networked Control Systems

$$\boldsymbol{x}_{k+1} = \boldsymbol{A}_d \boldsymbol{x}_k + \boldsymbol{B}_d \boldsymbol{u}_{k-q_k}$$

$$q_k \in \{1, 2, \ldots, \bar{\delta}\}$$

$$\boldsymbol{\xi}_k = \begin{bmatrix} \boldsymbol{x}_k \\ \boldsymbol{u}_{k-1} \\ \boldsymbol{u}_{k-2} \\ \vdots \\ \boldsymbol{u}_{k-\bar{\delta}} \end{bmatrix} \qquad \boldsymbol{\xi}_{k+1} = \hat{\boldsymbol{A}}(\boldsymbol{\alpha}_k)\boldsymbol{\xi}_k + \hat{\boldsymbol{B}}\boldsymbol{u}_k$$

$\boldsymbol{u}_{k-1}$ is active for $kT_d \leq (k+1)T_d$

$$\boldsymbol{\xi}_{k+1} = \begin{bmatrix} \boldsymbol{A}_d & \boldsymbol{B}_d & \mathbf{0} & \ldots & \mathbf{0} & \mathbf{0} \\ \mathbf{0} & \mathbf{0} & \mathbf{0} & \ldots & \mathbf{0} & \mathbf{0} \\ \mathbf{0} & \boldsymbol{I} & \mathbf{0} & \ldots & \mathbf{0} & \mathbf{0} \\ \mathbf{0} & \mathbf{0} & \boldsymbol{I} & \ldots & \mathbf{0} & \mathbf{0} \\ & & & \ddots & & \\ \mathbf{0} & \mathbf{0} & \mathbf{0} & \ldots & \boldsymbol{I} & \mathbf{0} \end{bmatrix} \boldsymbol{\xi}_k + \begin{bmatrix} \mathbf{0} \\ \boldsymbol{I} \\ \mathbf{0} \\ \mathbf{0} \\ \vdots \\ \mathbf{0} \end{bmatrix} \boldsymbol{u}_k$$

Control Design for Buffered Networked Control Systems

$$\boldsymbol{x}_{k+1} = \boldsymbol{A}_d \boldsymbol{x}_k + \boldsymbol{B}_d \boldsymbol{u}_{k-q_k}$$

$$q_k \in \{1, 2, \dots, \bar{\delta}\}$$

$$\boldsymbol{\xi}_k = \begin{bmatrix} \boldsymbol{x}_k \\ \boldsymbol{u}_{k-1} \\ \boldsymbol{u}_{k-2} \\ \vdots \\ \boldsymbol{u}_{k-\bar{\delta}} \end{bmatrix} \qquad \boldsymbol{\xi}_{k+1} = \hat{\boldsymbol{A}}(\boldsymbol{\alpha}_k)\boldsymbol{\xi}_k + \hat{\boldsymbol{B}}\boldsymbol{u}_k$$

$\boldsymbol{u}_{k-2}$ is active for $kT_d \leq (k+1)T_d$

$$\boldsymbol{\xi}_{k+1} = \begin{bmatrix} \boldsymbol{A}_d & \boldsymbol{0} & \boldsymbol{B}_d & \dots & \boldsymbol{0} & \boldsymbol{0} \\ \boldsymbol{0} & \boldsymbol{0} & \boldsymbol{0} & \dots & \boldsymbol{0} & \boldsymbol{0} \\ \boldsymbol{0} & \boldsymbol{I} & \boldsymbol{0} & \dots & \boldsymbol{0} & \boldsymbol{0} \\ \boldsymbol{0} & \boldsymbol{0} & \boldsymbol{I} & \dots & \boldsymbol{0} & \boldsymbol{0} \\ & & & \ddots & & \\ \boldsymbol{0} & \boldsymbol{0} & \boldsymbol{0} & \dots & \boldsymbol{I} & \boldsymbol{0} \end{bmatrix} \boldsymbol{\xi}_k + \begin{bmatrix} \boldsymbol{0} \\ \boldsymbol{I} \\ \boldsymbol{0} \\ \boldsymbol{0} \\ \vdots \\ \boldsymbol{0} \end{bmatrix} \boldsymbol{u}_k$$

Control Design for Buffered Networked Control Systems

$$\boldsymbol{x}_{k+1} = \boldsymbol{A}_d \boldsymbol{x}_k + \boldsymbol{B}_d \boldsymbol{u}_{k-q_k}$$

$$q_k \in \{1, 2, \dots, \bar{\delta}\}$$

$$\boldsymbol{\xi}_k = \begin{bmatrix} \boldsymbol{x}_k \\ \boldsymbol{u}_{k-1} \\ \boldsymbol{u}_{k-2} \\ \vdots \\ \boldsymbol{u}_{k-\bar{\delta}} \end{bmatrix} \qquad \boldsymbol{\xi}_{k+1} = \hat{\boldsymbol{A}}(\boldsymbol{\alpha}_k)\boldsymbol{\xi}_k + \hat{\boldsymbol{B}}\boldsymbol{u}_k$$

$\boldsymbol{u}_{k-\boxed{(\bar{\delta}-1)}}$ is active for $kT_d \leq (k+1)T_d$

$$\boldsymbol{\xi}_{k+1} = \begin{bmatrix} \boldsymbol{A}_d & \boldsymbol{0} & \boldsymbol{0} & \dots & \boldsymbol{B}_d & \boldsymbol{0} \\ \boldsymbol{0} & \boldsymbol{0} & \boldsymbol{0} & \dots & \boldsymbol{0} & \boldsymbol{0} \\ \boldsymbol{0} & \boldsymbol{I} & \boldsymbol{0} & \dots & \boldsymbol{0} & \boldsymbol{0} \\ \boldsymbol{0} & \boldsymbol{0} & \boldsymbol{I} & \dots & \boldsymbol{0} & \boldsymbol{0} \\ & & & \ddots & & \\ \boldsymbol{0} & \boldsymbol{0} & \boldsymbol{0} & \dots & \boldsymbol{I} & \boldsymbol{0} \end{bmatrix} \boldsymbol{\xi}_k + \begin{bmatrix} \boldsymbol{0} \\ \boldsymbol{I} \\ \boldsymbol{0} \\ \boldsymbol{0} \\ \vdots \\ \boldsymbol{0} \end{bmatrix} \boldsymbol{u}_k$$

Control Design for Buffered Networked Control Systems

$$\boldsymbol{x}_{k+1} = \boldsymbol{A}_d \boldsymbol{x}_k + \boldsymbol{B}_d \boldsymbol{u}_{k-q_k}$$

$$q_k \in \{1, 2, \dots, \bar{\delta}\}$$

$$\boldsymbol{\xi}_k = \begin{bmatrix} \boldsymbol{x}_k \\ \boldsymbol{u}_{k-1} \\ \boldsymbol{u}_{k-2} \\ \vdots \\ \boldsymbol{u}_{k-\bar{\delta}} \end{bmatrix} \qquad \boldsymbol{\xi}_{k+1} = \hat{\boldsymbol{A}}(\boldsymbol{\alpha}_k)\boldsymbol{\xi}_k + \hat{\boldsymbol{B}}\boldsymbol{u}_k$$

$\boldsymbol{u}_{k-\boxed{\bar{\delta}}}$ is active for $kT_d \leq (k+1)T_d$

$$\boldsymbol{\xi}_{k+1} = \begin{bmatrix} \boldsymbol{A_d} & \boldsymbol{0} & \boldsymbol{0} & \dots & \boldsymbol{0} & \boldsymbol{B}_d \\ \boldsymbol{0} & \boldsymbol{0} & \boldsymbol{0} & \dots & \boldsymbol{0} & \boldsymbol{0} \\ \boldsymbol{0} & \boldsymbol{I} & \boldsymbol{0} & \dots & \boldsymbol{0} & \boldsymbol{0} \\ \boldsymbol{0} & \boldsymbol{0} & \boldsymbol{I} & \dots & \boldsymbol{0} & \boldsymbol{0} \\ & & & \ddots & & \\ \boldsymbol{0} & \boldsymbol{0} & \boldsymbol{0} & \dots & \boldsymbol{I} & \boldsymbol{0} \end{bmatrix} \boldsymbol{\xi}_k + \begin{bmatrix} \boldsymbol{0} \\ \boldsymbol{I} \\ \boldsymbol{0} \\ \boldsymbol{0} \\ \vdots \\ \boldsymbol{0} \end{bmatrix} \boldsymbol{u}_k$$

$$\hat{\boldsymbol{A}}(\boldsymbol{\alpha}_k) = \begin{bmatrix} \boldsymbol{A_d} & \alpha_{1,k}\boldsymbol{B}_d \; \dots \; \alpha_{\bar{\delta}-1,k}\boldsymbol{B}_d & \alpha_{\bar{\delta},k}\boldsymbol{B}_d \\ \boldsymbol{0}_{m\times n} & \boldsymbol{0}_m \; \dots \; \boldsymbol{0}_m & \boldsymbol{0}_m \\ \boldsymbol{0}_{(\bar{\delta}-1)m\times n} & \boldsymbol{I}_{(\bar{\delta}-1)m} & \boldsymbol{0}_{(\bar{\delta}-1)m\times m} \end{bmatrix}$$

$$\hat{\boldsymbol{B}} = \begin{bmatrix} \boldsymbol{0}_{n\times m} \\ \boldsymbol{I}_{m\times m} \\ \boldsymbol{0}_{(\bar{\delta}-1)m\times m} \end{bmatrix}$$

Control Design for Buffered Networked Control Systems

$$\boldsymbol{x}_{k+1} = \boldsymbol{A}_d \boldsymbol{x}_k + \boldsymbol{B}_d \boldsymbol{u}_{k-q_k}$$

$$q_k \in \{1, 2, \dots, \bar{\delta}\}$$

$$\boldsymbol{\xi}_k = \begin{bmatrix} \boldsymbol{x}_k \\ \boldsymbol{u}_{k-1} \\ \boldsymbol{u}_{k-2} \\ \vdots \\ \boldsymbol{u}_{k-\bar{\delta}} \end{bmatrix} \qquad \boldsymbol{\xi}_{k+1} = \hat{\boldsymbol{A}}(\boldsymbol{\alpha}_k)\boldsymbol{\xi}_k + \hat{\boldsymbol{B}}\boldsymbol{u}_k$$

$\boldsymbol{u}_{k-\boxed{\bar{\delta}}}$ is active for $kT_d \leq (k+1)T_d$

$$\boldsymbol{\xi}_{k+1} = \begin{bmatrix} \boldsymbol{A_d} & \boldsymbol{0} & \boldsymbol{0} & \dots & \boldsymbol{0} & \boldsymbol{B}_d \\ \boldsymbol{0} & \boldsymbol{0} & \boldsymbol{0} & \dots & \boldsymbol{0} & \boldsymbol{0} \\ \boldsymbol{0} & \boldsymbol{I} & \boldsymbol{0} & \dots & \boldsymbol{0} & \boldsymbol{0} \\ \boldsymbol{0} & \boldsymbol{0} & \boldsymbol{I} & \dots & \boldsymbol{0} & \boldsymbol{0} \\ & & & \ddots & & \\ \boldsymbol{0} & \boldsymbol{0} & \boldsymbol{0} & \dots & \boldsymbol{I} & \boldsymbol{0} \end{bmatrix} \boldsymbol{\xi}_k + \begin{bmatrix} \boldsymbol{0} \\ \boldsymbol{I} \\ \boldsymbol{0} \\ \boldsymbol{0} \\ \vdots \\ \boldsymbol{0} \end{bmatrix} \boldsymbol{u}_k$$

$$\hat{\boldsymbol{A}}(\boldsymbol{\alpha}_k) = \begin{bmatrix} \boldsymbol{A_d} & \alpha_{1,k}\boldsymbol{B}_d \ \dots \ \alpha_{\bar{\delta}-1,k}\boldsymbol{B}_d & \alpha_{\bar{\delta},k}\boldsymbol{B}_d \\ \boldsymbol{0}_{m\times n} & \boldsymbol{0}_m \ \dots \ \boldsymbol{0}_m & \boldsymbol{0}_m \\ \boldsymbol{0}_{(\bar{\delta}-1)m\times n} & \boldsymbol{I}_{(\bar{\delta}-1)m} & \boldsymbol{0}_{(\bar{\delta}-1)m\times m} \end{bmatrix}$$

$$\hat{\boldsymbol{B}} = \begin{bmatrix} \boldsymbol{0}_{n\times m} \\ \boldsymbol{I}_{m\times m} \\ \boldsymbol{0}_{(\bar{\delta}-1)m\times m} \end{bmatrix}$$

Switching function

$$\alpha_{i,k} = \begin{cases} 1, & \boldsymbol{u}_{k-i} \text{ is active for } kT_d \leq t < (k+1)T_d \\ 0, & \text{otherwise} \end{cases}$$

- Network uncertainties are completely embedded in the switching function
- Complex overapproximation is not needed!

LMI based Controller for Switched NCS

Theorem 1

If there exist symmetric positive definite matrices $\boldsymbol{Y}_i \in \mathbb{R}^{(n+\bar{\delta}m)\times(n+\bar{\delta}m)}$, a matrix $\boldsymbol{Z} \in \mathbb{R}^{m\times n}$, matrices $\boldsymbol{X}_i = \begin{bmatrix} \boldsymbol{X}_1 & \boldsymbol{0}_{n\times\bar{\delta}m} \\ \boldsymbol{X}_{2,i} & \boldsymbol{X}_{3,i} \end{bmatrix}$ with $\boldsymbol{X}_1 \in \mathbb{R}^{n\times n}$, $\boldsymbol{X}_{2,i} \in \mathbb{R}^{\bar{\delta}m\times n}$, $\boldsymbol{X}_{3,i} \in \mathbb{R}^{\bar{\delta}m\times\delta m}$ for $i \in \{0, 1 \ldots, \bar{\delta}\}$ and a scalar $0 \leq \gamma < 1$ such that

$$\begin{bmatrix} \boldsymbol{X}_i + \boldsymbol{X}_i^T - \boldsymbol{Y}_i & \boldsymbol{X}_i^T \hat{\boldsymbol{A}}_i^T - \hat{\boldsymbol{Z}}^T \hat{\boldsymbol{B}}^{\boldsymbol{T}} \\ \hat{\boldsymbol{A}}_i \boldsymbol{X}_i - \hat{\boldsymbol{B}}\hat{\boldsymbol{Z}} & (1-\gamma)\boldsymbol{Y}_j \end{bmatrix} > \boldsymbol{0}$$

with $\hat{\boldsymbol{Z}} = \begin{bmatrix} \boldsymbol{Z} & \boldsymbol{0}_{m\times\bar{\delta}} \end{bmatrix}$ is satisfied for $\forall i, j \in \{1, 2, \ldots, \bar{\delta}\}$, then the buffered NCS affected by unknown time-varying network delays and dropouts is asymptotically stable.

- The state feedback gain matrix

  $\boldsymbol{K}_x = \boldsymbol{Z}\boldsymbol{X}_1^{-1}$
- Lyapunov function

  $V(\boldsymbol{\xi}_k, \boldsymbol{\alpha}_k) = \boldsymbol{\xi}_k^T \hat{\boldsymbol{P}}(\boldsymbol{\alpha}_k)\boldsymbol{\xi}_k$
- Parameter dependent Lyapunov matrix

  $\hat{\boldsymbol{P}}(\boldsymbol{\alpha}_k) = \sum_{i=1}^{\bar{\delta}} \alpha_{i,k}\boldsymbol{P}_i$

  $\boldsymbol{P}_i = \boldsymbol{Y}_i^{-1}$

LMI based Controller for Switched NCS

Theorem 1

If there exist symmetric positive definite matrices $\boldsymbol{Y}_i \in \mathbb{R}^{(n+\bar{\delta}m)\times(n+\bar{\delta}m)}$, a matrix $\boldsymbol{Z} \in \mathbb{R}^{m\times n}$, matrices $\boldsymbol{X}_i = \begin{bmatrix} \boldsymbol{X}_1 & \boldsymbol{0}_{n\times\bar{\delta}m} \\ \boldsymbol{X}_{2,i} & \boldsymbol{X}_{3,i} \end{bmatrix}$ with $\boldsymbol{X}_1 \in \mathbb{R}^{n\times n}$, $\boldsymbol{X}_{2,i} \in \mathbb{R}^{\bar{\delta}m\times n}$, $\boldsymbol{X}_{3,i} \in \mathbb{R}^{\bar{\delta}m\times\bar{\delta}m}$ for $i \in \{0, 1\ldots, \bar{\delta}\}$ and a scalar $0 \le \gamma < 1$ such that

$$\begin{bmatrix} \boldsymbol{X}_i + \boldsymbol{X}_i^T - \boldsymbol{Y}_i & \boldsymbol{X}_i^T\hat{\boldsymbol{A}}_i^T - \hat{\boldsymbol{Z}}^T\hat{\boldsymbol{B}}^T \\ \hat{\boldsymbol{A}}_i\boldsymbol{X}_i - \hat{\boldsymbol{B}}\hat{\boldsymbol{Z}} & (1-\gamma)\boldsymbol{Y}_j \end{bmatrix} > \boldsymbol{0}$$

with $\hat{\boldsymbol{Z}} = \begin{bmatrix} \boldsymbol{Z} & \boldsymbol{0}_{m\times\bar{\delta}} \end{bmatrix}$ is satisfied for $\forall i, j \in \{1, 2, \ldots, \boxed{\bar{\delta}}\}$, then the buffered NCS affected by unknown time-varying network delays and dropouts is asymptotically stable.

- The state feedback gain matrix $\boldsymbol{K}_x = \boldsymbol{Z}\boldsymbol{X}_1^{-1}$
- Lyapunov function $V(\boldsymbol{\xi}_k, \boldsymbol{\alpha}_k) = \boldsymbol{\xi}_k^T\hat{\boldsymbol{P}}(\boldsymbol{\alpha}_k)\boldsymbol{\xi}_k$
- Parameter dependent Lyapunov matrix $\hat{\boldsymbol{P}}(\boldsymbol{\alpha}_k) = \sum_{i=1}^{\bar{\delta}} \alpha_{i,k}\boldsymbol{P}_i$, $\boldsymbol{P}_i = \boldsymbol{Y}_i^{-1}$
- Nr of LMIs to be solved: $\bar{\delta}^2$

E

$\bar{\delta}=3$, $m=1$, $n=2$	#LMIs = 4096, #opt.var = 1926	$\bar{\delta}=4$, $m=1$, $n=2$	#LMIs = 65536, #opt.var = 11526	$\bar{\delta}=5$, $m=1$, $n=2$	#LMIs = 1048576, #opt.var = 64518	$\bar{\delta}=6$, $m=1$, $n=2$	#LMIs = 16777216, #opt.var = 344070

$\bar{\delta}=3$, $m=1$, $n=3$	#LMIs = 262144, #opt.var = 19980	$\bar{\delta}=4$, $m=1$, $n=3$	#LMIs = 16777216, #opt.var = 229388	…

LMI based Controller for Switched NCS

Theorem 1

If there exist symmetric positive definite matrices $\boldsymbol{Y}_i \in \mathbb{R}^{(n+\bar{\delta}m)\times(n+\bar{\delta}m)}$, a matrix $\boldsymbol{Z} \in \mathbb{R}^{m\times n}$, matrices $\boldsymbol{X}_i = \begin{bmatrix} \boldsymbol{X}_1 & \boldsymbol{0}_{n\times\bar{\delta}m} \\ \boldsymbol{X}_{2,i} & \boldsymbol{X}_{3,i} \end{bmatrix}$ with $\boldsymbol{X}_1 \in \mathbb{R}^{n\times n}$, $\boldsymbol{X}_{2,i} \in \mathbb{R}^{\bar{\delta}m\times n}$, $\boldsymbol{X}_{3,i} \in \mathbb{R}^{\bar{\delta}m\times\delta m}$ for $i \in \{0, 1\ldots, \bar{\delta}\}$ and a scalar $0 \leq \gamma < 1$ such that

$$\begin{bmatrix} \boldsymbol{X}_i + \boldsymbol{X}_i^T - \boldsymbol{Y}_i & \boldsymbol{X}_i^T \hat{\boldsymbol{A}}_i^T - \hat{\boldsymbol{Z}}^T \hat{\boldsymbol{B}}^T \\ \hat{\boldsymbol{A}}_i \boldsymbol{X}_i - \hat{\boldsymbol{B}}\hat{\boldsymbol{Z}} & (1-\gamma)\boldsymbol{Y}_j \end{bmatrix} > \boldsymbol{0}$$

with $\hat{\boldsymbol{Z}} = \begin{bmatrix} \boldsymbol{Z} & \boldsymbol{0}_{m\times\bar{\delta}} \end{bmatrix}$ is satisfied for $\forall i, j \in \{1, 2, \ldots, \boxed{\bar{\delta}}\}$, then the buffered NCS affected by unknown time-varying network delays and dropouts is asymptotically stable.

- The state feedback gain matrix

  $\boldsymbol{K}_x = \boldsymbol{Z}\boldsymbol{X}_1^{-1}$
- Lyapunov function

  $V(\boldsymbol{\xi}_k, \boldsymbol{\alpha}_k) = \boldsymbol{\xi}_k^T \hat{\boldsymbol{P}}(\boldsymbol{\alpha}_k)\boldsymbol{\xi}_k$
- Parameter dependent Lyapunov matrix

  $\hat{\boldsymbol{P}}(\boldsymbol{\alpha}_k) = \sum_{i=1}^{\bar{\delta}} \alpha_{i,k}\boldsymbol{P}_i$

  $\boldsymbol{P}_i = \boldsymbol{Y}_i^{-1}$
- Nr of LMIs to be solved: $\bar{\delta}^2$

E

$\bar{\delta}=3$, $m=1$, $n=2$	#LMIs = ~~4096~~ 9 #opt.var = ~~1926~~ 96	$\bar{\delta}=4$, $m=1$, $n=2$	#LMIs = ~~65536~~ 16 #opt.var = ~~11526~~ 186	$\bar{\delta}=5$, $m=1$, $n=2$	#LMIs = ~~1048576~~ 25 #opt.var = ~~64518~~ 321	$\bar{\delta}=6$, $m=1$, $n=2$	#LMIs = ~~16777216~~ 36 #opt.var = ~~344070~~ 510

$\bar{\delta}=3$, $m=1$, $n=3$	#LMIs = ~~262144~~ 9 #opt.var = ~~19980~~ 129	$\bar{\delta}=4$, $m=1$, $n=3$	#LMIs = ~~16777216~~ 16 #opt.var = ~~229388~~ 236

...

#LMIs independent of the system to be controlled!

Example: DC Motor

$$\dot{\boldsymbol{x}} = \begin{bmatrix} 0 & 1 \\ 0 & -\left(\frac{k_G^2 k_M^2}{RJ} + \frac{k_R}{J}\right) \end{bmatrix} \boldsymbol{x} + \begin{bmatrix} 0 \\ \frac{k_G k_M}{RJ} \end{bmatrix} u^*$$

$$\boldsymbol{x}_{k+1} = \begin{bmatrix} 1 & 0.0106 \\ 0 & 0.2347 \end{bmatrix} \boldsymbol{x}_k + \begin{bmatrix} 0.0098 \\ 0.7953 \end{bmatrix} u_{k-q_k}$$

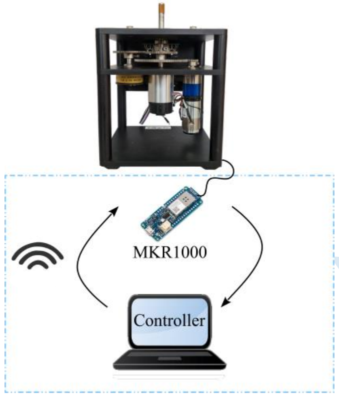

$$0 \leq \tau_k^{SC} < 2T_d$$

$$\tau_k^C = 0$$

$$0 \leq \tau_k^{CS} < 2T_d, \forall k$$

$$m_k^{sc} = m_k^{ca} = 0, \forall k$$

$$\bar{d} = 4, \bar{p} = 0$$

$$\bar{\delta} = 4$$

Example: DC Motor

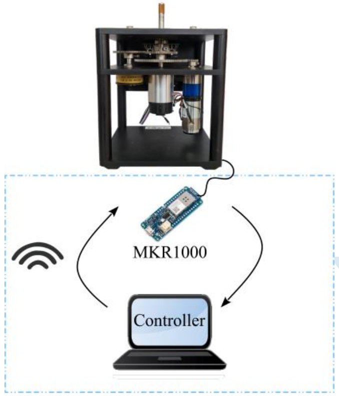

$0 \leq \tau_k^{SC} < 2T_d$

$\tau_k^{C} = 0$

$0 \leq \tau_k^{CS} < 2T_d, \forall k$

$m_k^{sc} = m_k^{ca} = 0, \forall k$

$\bar{d} = 4, \bar{p} = 0$

$\bar{\delta} = 4$

$$\dot{\boldsymbol{x}} = \begin{bmatrix} 0 & 1 \\ 0 & -\left(\frac{k_G^2 k_M^2}{RJ} + \frac{k_R}{J}\right) \end{bmatrix} \boldsymbol{x} + \begin{bmatrix} 0 \\ \frac{k_G k_M}{RJ} \end{bmatrix} u^*$$

$$\boldsymbol{x}_{k+1} = \begin{bmatrix} 1 & 0.0106 \\ 0 & 0.2347 \end{bmatrix} \boldsymbol{x}_k + \begin{bmatrix} 0.0098 \\ 0.7953 \end{bmatrix} u_{k-q_k}$$

Control Law		γ	opt.var. / LMIs	Time in s
[1]	$\boldsymbol{u}_k = -\begin{bmatrix} \boldsymbol{K}_x & \boldsymbol{0} \end{bmatrix} \xi_k$ $\boldsymbol{K}_x = \begin{bmatrix} 2.62 & 0.04 \end{bmatrix}$	0.075	11526 65536	4648.7
Th 1	$\boldsymbol{u}_k = -\begin{bmatrix} \boldsymbol{K}_x & \boldsymbol{0} \end{bmatrix} \xi_k$ $\boldsymbol{K}_x = \begin{bmatrix} 2.73 & 0.034 \end{bmatrix}$	0.089	186 16	0.39

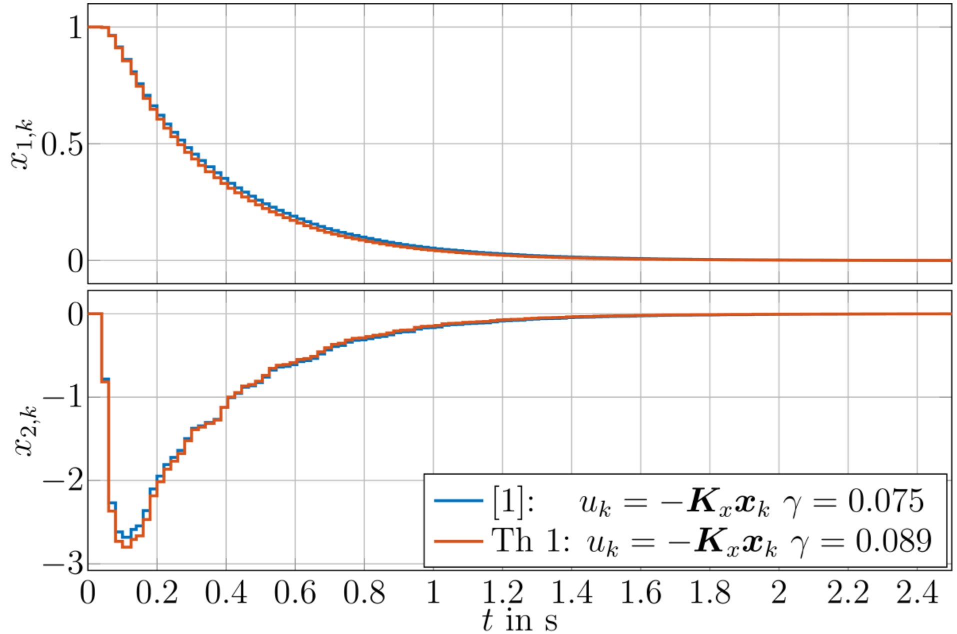

[1] M. Cloosterman, L. Hetel, N. van de Wouw, W. Heemels, J. Daafouz, and H. Nijmeijer, ``Controller synthesis for networked control systems," Automatica, vol. 46, no. 10, pp. 1584 – 1594, 2010.

Extensions and the Flexibility of the Control Design

Theorem 2: Switched State Feedback Control Law $\boldsymbol{u}_k = -\boldsymbol{K}_{x,i}\boldsymbol{x}_k = -\hat{\boldsymbol{K}}_i\boldsymbol{\xi}_k = -\begin{bmatrix}\boldsymbol{K}_{x,i} & \boldsymbol{0}\end{bmatrix}\boldsymbol{\xi}_k$

Theorem 3: Extended State Feedback Control Law $\boldsymbol{u}_k = -\hat{\boldsymbol{K}}\boldsymbol{\xi}_k = -\begin{bmatrix}\boldsymbol{K}_x & \boldsymbol{K}_u\end{bmatrix}\boldsymbol{\xi}_k$

Theorem 4: Additional Influence on the Transient Performance

$$\begin{bmatrix} \boldsymbol{X}_i + \boldsymbol{X}_i^T - \boldsymbol{Y}_i & \boldsymbol{X}_i^T\hat{\boldsymbol{A}}_i^T - \hat{\boldsymbol{Z}}^T\hat{\boldsymbol{B}}^{\boldsymbol{T}} \\ \hat{\boldsymbol{A}}_i\boldsymbol{X}_i - \hat{\boldsymbol{B}}\hat{\boldsymbol{Z}} & (1-\gamma_{\boldsymbol{i}})\boldsymbol{Y}_j \end{bmatrix} > \boldsymbol{0} \qquad \boldsymbol{\gamma} = \begin{bmatrix} \gamma_1 \\ \gamma_2 \\ \vdots \\ \gamma_{\bar{\delta}} \end{bmatrix}$$

Extensions and the Flexibility of the Control Design

Theorem 2: Switched State Feedback Control Law $\boldsymbol{u}_k = -\boldsymbol{K}_{x,i}\boldsymbol{x}_k = -\hat{\boldsymbol{K}}_i\boldsymbol{\xi}_k = -\begin{bmatrix}\boldsymbol{K}_{x,i} & \boldsymbol{0}\end{bmatrix}\boldsymbol{\xi}_k$

Theorem 3: Extended State Feedback Control Law $\boldsymbol{u}_k = -\hat{\boldsymbol{K}}\boldsymbol{\xi}_k = -\begin{bmatrix}\boldsymbol{K}_x & \boldsymbol{K}_u\end{bmatrix}\boldsymbol{\xi}_k$

Theorem 4: Additional Influence on the Transient Performance

$$\begin{bmatrix}\boldsymbol{X}_i + \boldsymbol{X}_i^T - \boldsymbol{Y}_i & \boldsymbol{X}_i^T\hat{\boldsymbol{A}}_i^T - \hat{\boldsymbol{Z}}^T\hat{\boldsymbol{B}}^{\boldsymbol{T}} \\ \hat{\boldsymbol{A}}_i\boldsymbol{X}_i - \hat{\boldsymbol{B}}\hat{\boldsymbol{Z}} & (1-\gamma_{\boldsymbol{i}})\boldsymbol{Y}_j\end{bmatrix} > \boldsymbol{0} \qquad \boldsymbol{\gamma} = \begin{bmatrix}\gamma_1 \\ \gamma_2 \\ \vdots \\ \gamma_{\bar{\delta}}\end{bmatrix}$$

$$\begin{bmatrix}\hat{\boldsymbol{P}} & \left(\hat{\boldsymbol{A}}(\boldsymbol{\alpha}_k) - \hat{\boldsymbol{B}}\hat{\boldsymbol{K}}\right)^T\hat{\boldsymbol{P}}^+ \\ \hat{\boldsymbol{P}}^+\left(\hat{\boldsymbol{A}}(\boldsymbol{\alpha}_k) - \hat{\boldsymbol{B}}\hat{\boldsymbol{K}}\right) & \left(1-\sum_{i=1}^{\bar{\delta}}\alpha_{i,k}\gamma_i\right)\hat{\boldsymbol{P}}^+\end{bmatrix} > 0 \longrightarrow -\Delta V(\boldsymbol{\xi}_k,\boldsymbol{\alpha}_k) = \hat{\boldsymbol{P}} - \left(\hat{\boldsymbol{A}}(\boldsymbol{\alpha}_k) - \hat{\boldsymbol{B}}\hat{\boldsymbol{K}}\right)^T\hat{\boldsymbol{P}}^+\left(\hat{\boldsymbol{A}}(\boldsymbol{\alpha}_k) - \hat{\boldsymbol{B}}\hat{\boldsymbol{K}}\right) > \sum_{i=1}^{\bar{\delta}}\alpha_{i,k}\gamma_i\hat{\boldsymbol{P}}$$

Additional Influence on the Transient Performance

Control Law		γ	opt.var. / LMIs	Time in s
[1]	$\boldsymbol{u}_k = -\begin{bmatrix}\boldsymbol{K}_x & \boldsymbol{0}\end{bmatrix}\xi_k$ $\boldsymbol{K}_x = \begin{bmatrix}2.62 & 0.04\end{bmatrix}$	0.075	11526 65536	4648.7
Th 4	$\boldsymbol{u}_k = -\begin{bmatrix}\boldsymbol{K}_x & \boldsymbol{0}\end{bmatrix}\xi_k$ $\boldsymbol{K}_x = \begin{bmatrix}4.93 & 0.09\end{bmatrix}$	$\begin{bmatrix}0.19\\0\\0\\0\end{bmatrix}$	186 16	0.32
Th 4 switched control law	$\boldsymbol{u}_k = -\begin{bmatrix}\boldsymbol{K}_{x,i} & \boldsymbol{0}\end{bmatrix}\xi_k$ $\boldsymbol{K}_{x,1} = \begin{bmatrix}5.56 & 0.086\end{bmatrix}$ $\boldsymbol{K}_{x,2} = \begin{bmatrix}5.6 & 0.08\end{bmatrix}$ $\boldsymbol{K}_{x,3} = \begin{bmatrix}5.87 & 0.08\end{bmatrix}$ $\boldsymbol{K}_{x,4} = \begin{bmatrix}6.09 & 0.096\end{bmatrix}$	$\begin{bmatrix}0.225\\0\\0\\0\end{bmatrix}$	204 16	0.24

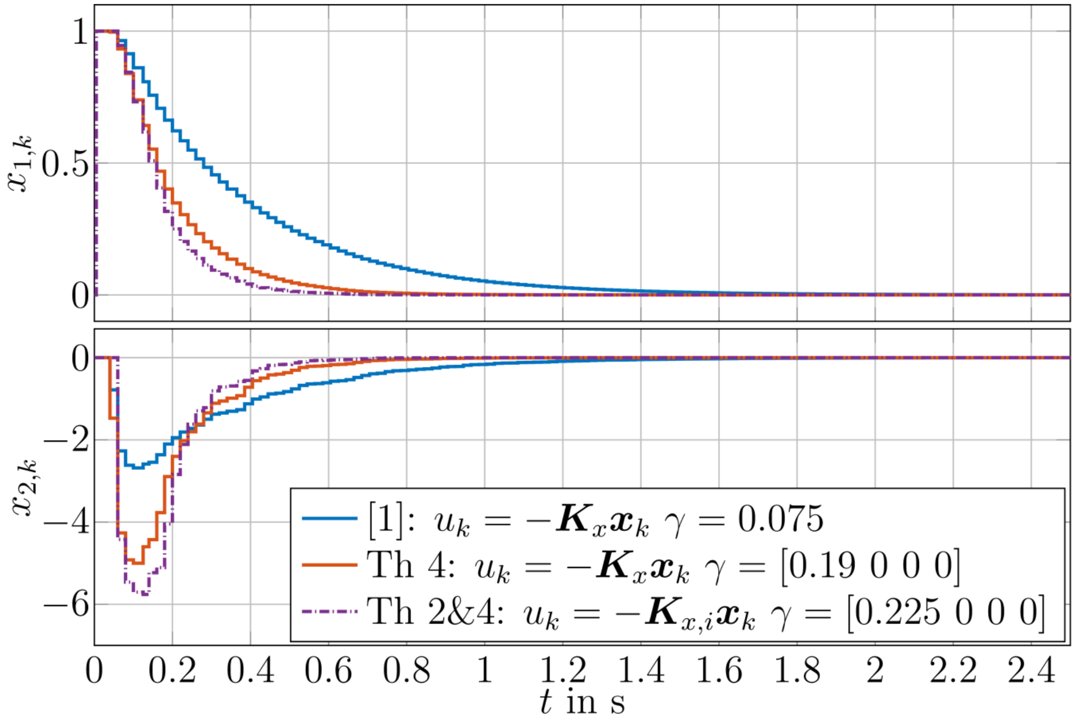

[1] M. Cloosterman, L. Hetel, N. van de Wouw, W. Heemels, J. Daafouz, and H. Nijmeijer, ``Controller synthesis for networked control systems," Automatica, vol. 46, no. 10, pp. 1584 – 1594, 2010.

Limitations through the system?

$$\dot{\boldsymbol{x}}(t) = \begin{bmatrix} 0 & 1 & 0 \\ -\frac{c}{m} & -\frac{v}{m} & \frac{c}{m} \\ 0 & 0 & 0 \end{bmatrix} \boldsymbol{x}(t) + \begin{bmatrix} 0 \\ 0 \\ b \end{bmatrix} \boldsymbol{u}^*(t)$$

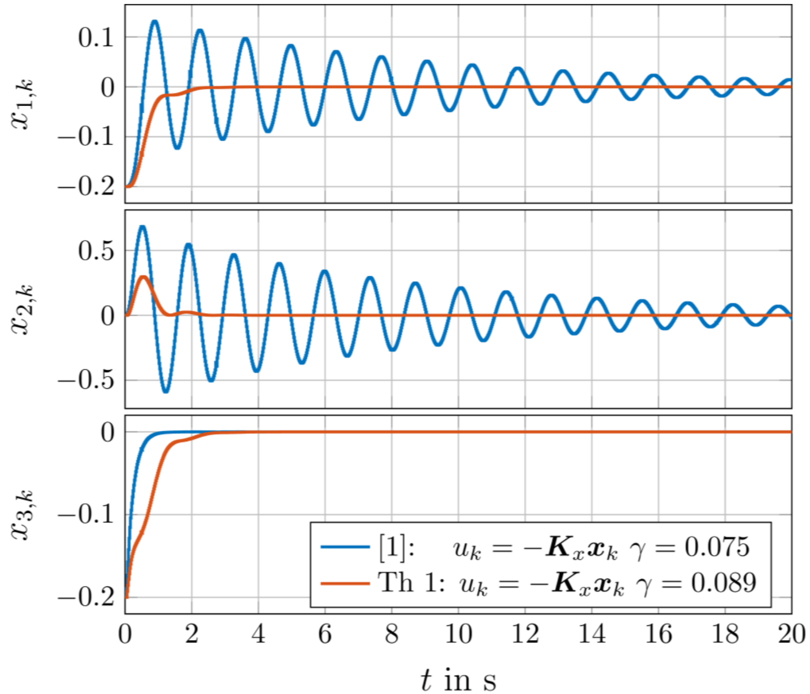

$\bar{\delta} = 3$	Control Law	γ	LMIs / opt.var.
[1]	$\boldsymbol{u}_k = -\begin{bmatrix}\boldsymbol{K}_x & \boldsymbol{0}\end{bmatrix} \xi_k$ $\boldsymbol{K}_x = \begin{bmatrix}-0.0002 & -0.008 & 46.52\end{bmatrix}$	0.12	262144 19980
Th 1	$\boldsymbol{u}_k = -\begin{bmatrix}\boldsymbol{K}_x & \boldsymbol{0}\end{bmatrix} \xi_k$ $\boldsymbol{K}_x = \begin{bmatrix}-32.30 & 3.05 & 53.42\end{bmatrix}$	0.052	9 129

Limitations through the system?

[1] no feasible solution found!

$$\dot{\boldsymbol{x}}(t) = \begin{bmatrix} 0 & 1 & 0 \\ -\frac{c}{m} & -\frac{v}{m} & \frac{c}{m} \\ 0 & 0 & 0 \end{bmatrix} \boldsymbol{x}(t) + \begin{bmatrix} 0 \\ 0 \\ b \end{bmatrix} \boldsymbol{u}^*(t)$$

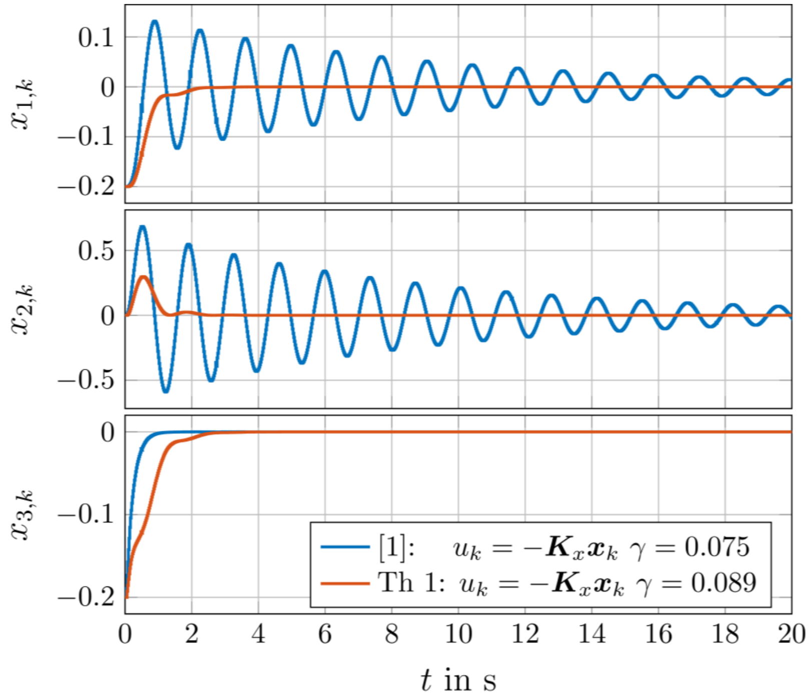

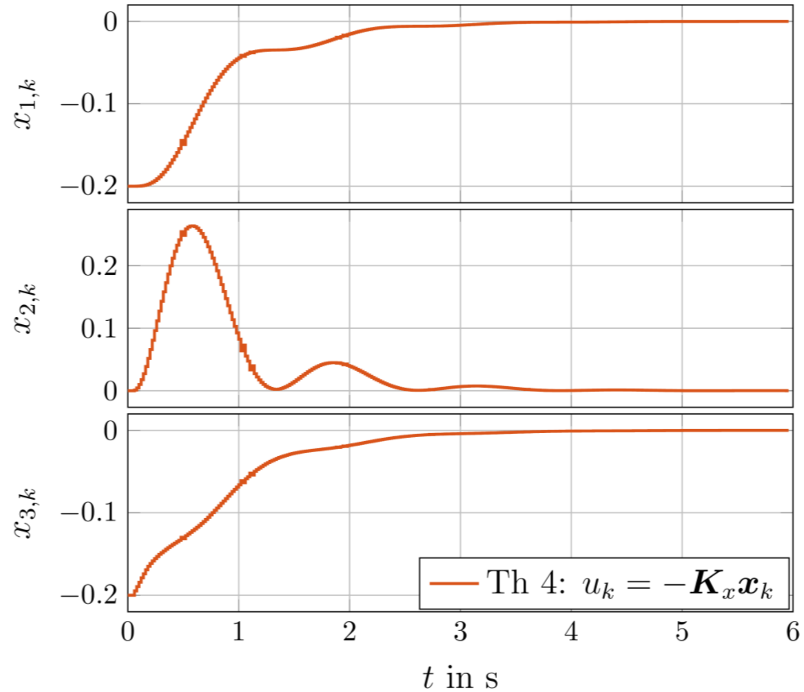

$\bar{\delta} = 3$	Control Law	γ	LMIs / opt.var.
[1]	$\boldsymbol{u}_k = -\begin{bmatrix}\boldsymbol{K}_x & \boldsymbol{0}\end{bmatrix} \xi_k$ $\boldsymbol{K}_x = \begin{bmatrix}-0.0002 & -0.008 & 46.52\end{bmatrix}$	0.12	262144 19980
Th 1	$\boldsymbol{u}_k = -\begin{bmatrix}\boldsymbol{K}_x & \boldsymbol{0}\end{bmatrix} \xi_k$ $\boldsymbol{K}_x = \begin{bmatrix}-32.30 & 3.05 & 53.42\end{bmatrix}$	0.052	9 129

$\bar{\delta} = 4$	Control Law	γ	LMIs / opt.var.
Th 4	$\boldsymbol{u}_k = -\begin{bmatrix}\boldsymbol{K}_x & \boldsymbol{0}\end{bmatrix} \xi_k$ $\boldsymbol{K}_x = \begin{bmatrix}24.65 & 1.76 & 39.98\end{bmatrix}$	$\begin{bmatrix}0.045 \\ 0 \\ 0 \\ 0\end{bmatrix}$	16 236

Further Improvement of the Buffer

Buffer updates the control signal p times for

$$kT_d \leq t < (k+1)T_d$$

$$\boldsymbol{x}_{k+1} = \boldsymbol{A}_d \boldsymbol{x}_k + \sum_{l=1}^{p} \boldsymbol{B}_l u^*_{k-q_{k,l}}$$

$$\boldsymbol{B}_l = \int_{(l-1)\frac{T_d}{p}}^{l\frac{T_d}{p}} e^{\boldsymbol{A}_c(T_d-s)} \boldsymbol{b}_c ds.$$

$$q_{k,l} \in \{0, 1, 2, \ldots, \bar{\delta}\}$$

#LMIs: $\binom{\bar{\delta}+p}{\bar{\delta}}^2$

	$\bar{\delta}=1$	$\bar{\delta}=2$	$\bar{\delta}=3$	$\bar{\delta}=4$
$p=1$	1	4	9	16
$p=2$	9	36	100	225
$p=3$	16	100	400	1225
$p=4$	25	225	1225	4900

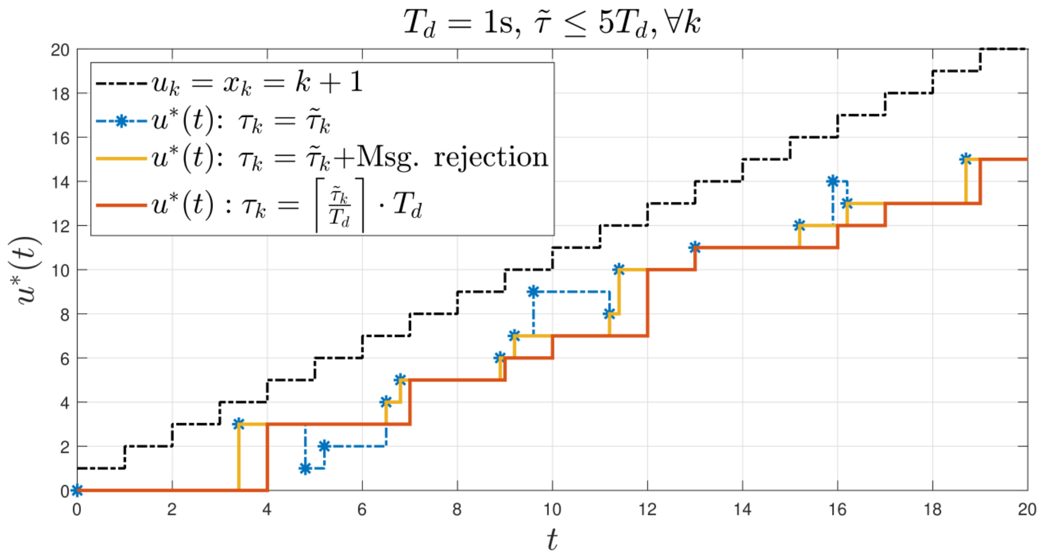

Further Improvement of the Buffer

Buffer updates the control signal p times for

$$kT_d \leq t < (k+1)T_d$$

$$\boldsymbol{x}_{k+1} = \boldsymbol{A}_d \boldsymbol{x}_k + \sum_{l=1}^{p} \boldsymbol{B}_l u^*_{k-q_{k,l}}$$

$$\boldsymbol{B}_l = \int_{(l-1)\frac{T_d}{p}}^{l\frac{T_d}{p}} e^{\boldsymbol{A}_c(T_d-s)} \boldsymbol{b}_c ds.$$

$$q_{k,l} \in \{0, 1, 2, \ldots, \bar{\delta}\}$$

#LMIs: $\binom{\bar{\delta}+p}{\bar{\delta}}^2$

	$\bar{\delta}=1$	$\bar{\delta}=2$	$\bar{\delta}=3$	$\bar{\delta}=4$
$p=1$	1	4	9	16
$p=2$	9	36	100	225
$p=3$	16	100	400	1225
$p=4$	25	225	1225	4900

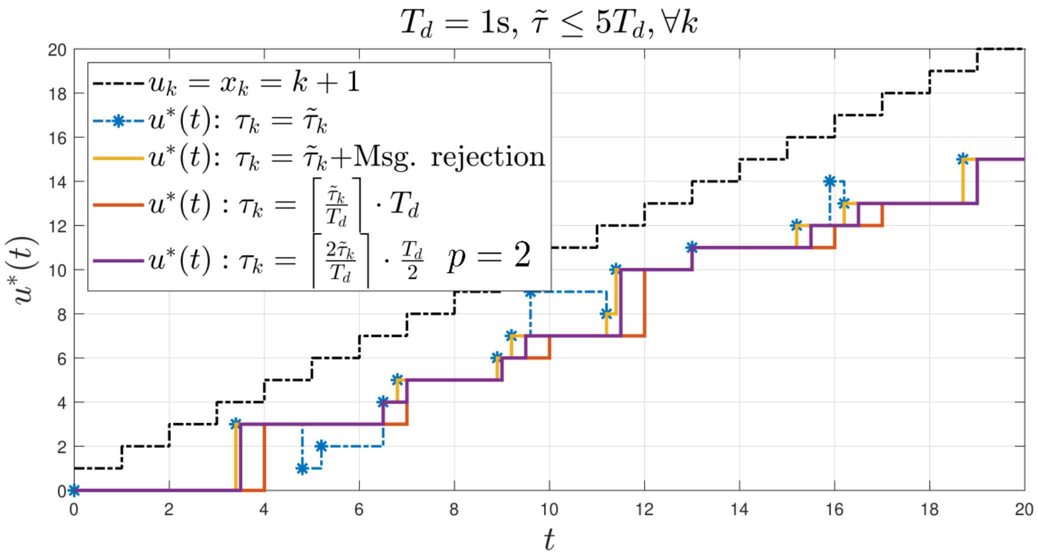

Further Improvement of the Buffer

Buffer updates the control signal p times for

$$kT_d \leq t < (k+1)T_d$$

$$\boldsymbol{x}_{k+1} = \boldsymbol{A}_d \boldsymbol{x}_k + \sum_{l=1}^{p} \boldsymbol{B}_l u^*_{k-q_{k,l}}$$

$$\boldsymbol{B}_l = \int_{(l-1)\frac{T_d}{p}}^{l\frac{T_d}{p}} e^{\boldsymbol{A}_c(T_d - s)} \boldsymbol{b}_c ds.$$

$$q_{k,l} \in \{0, 1, 2, \ldots, \bar{\delta}\}$$

#LMIs: $\binom{\bar{\delta}+p}{\bar{\delta}}^2$

	$\bar{\delta}=1$	$\bar{\delta}=2$	$\bar{\delta}=3$	$\bar{\delta}=4$
$p=1$	1	4	9	16
$p=2$	9	36	100	225
$p=3$	16	100	400	1225
$p=4$	25	225	1225	4900

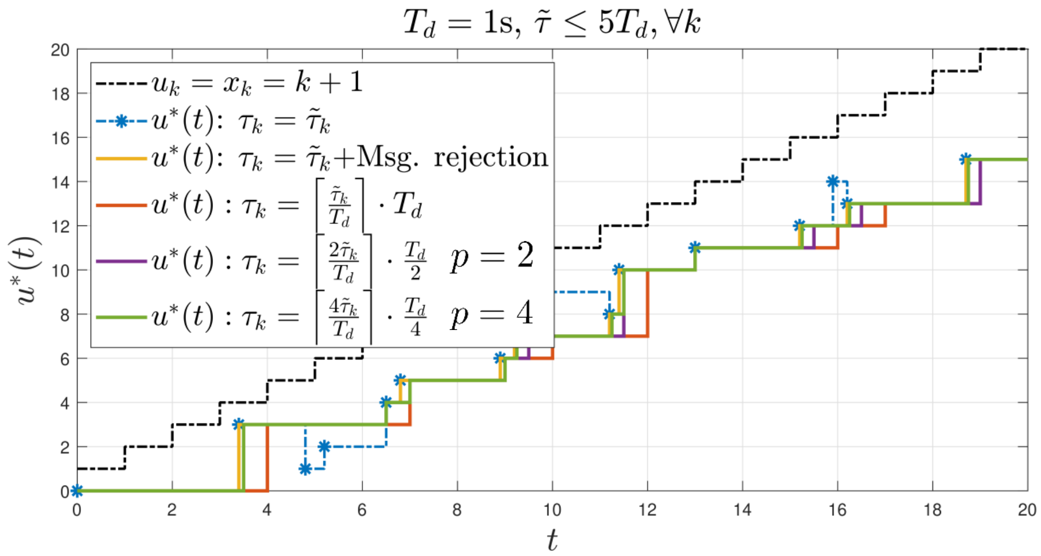

State Estimation in Networked Control Systems with Time-Varying Delays: A Simple yet Powerful Observer Framework

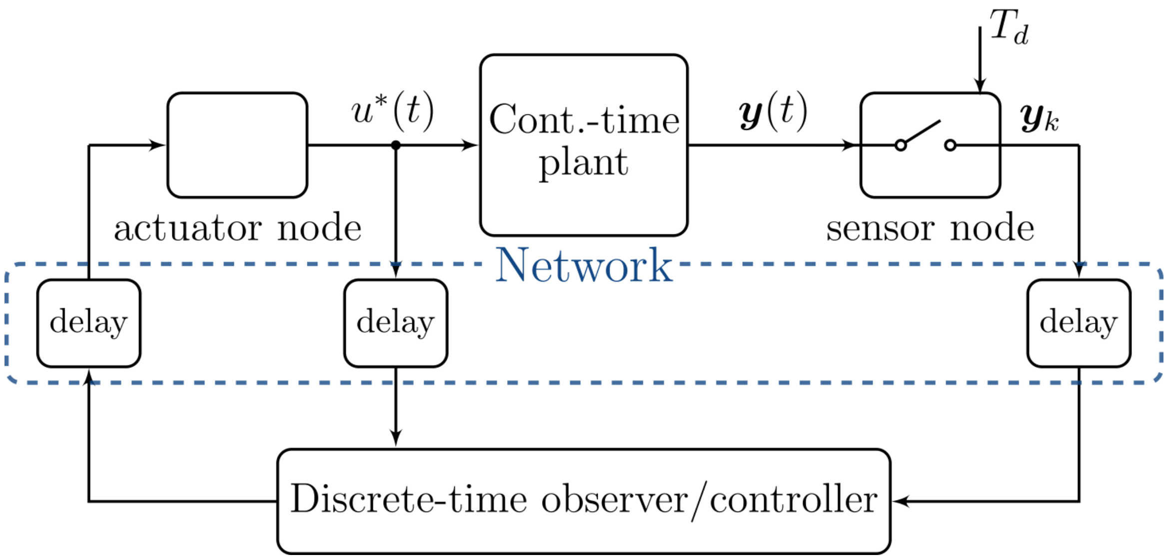

State Estimation in Networked Control Systems with Time-Varying Delays: A Simple yet Powerful Observer Framework

Challenges:

1. Out-of-order arrival of data packets
2. Unpredictable and asynchronous availability of input/output data at the observer
3. separation principle?

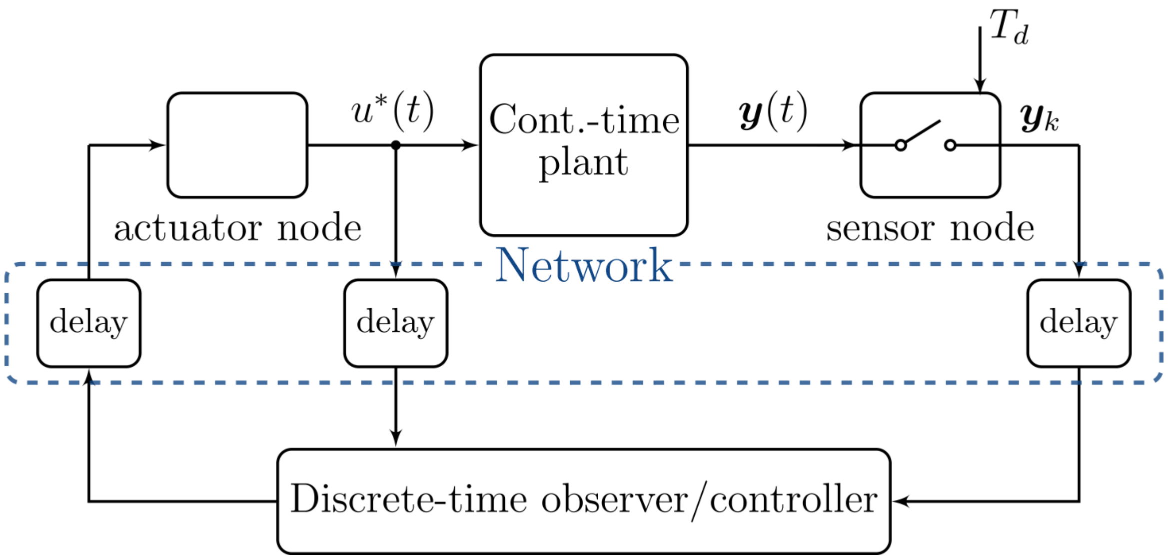

[3] K. Stanojevic, M. Steinberger and M. Horn, "State Estimation in Networked Control Systems with Time-Varying Delays: A Simple yet Powerful Observer Framework," 2024 IEEE 63th Conference on Decision and Control (CDC) (accepted)

Mathematical description using packet notation

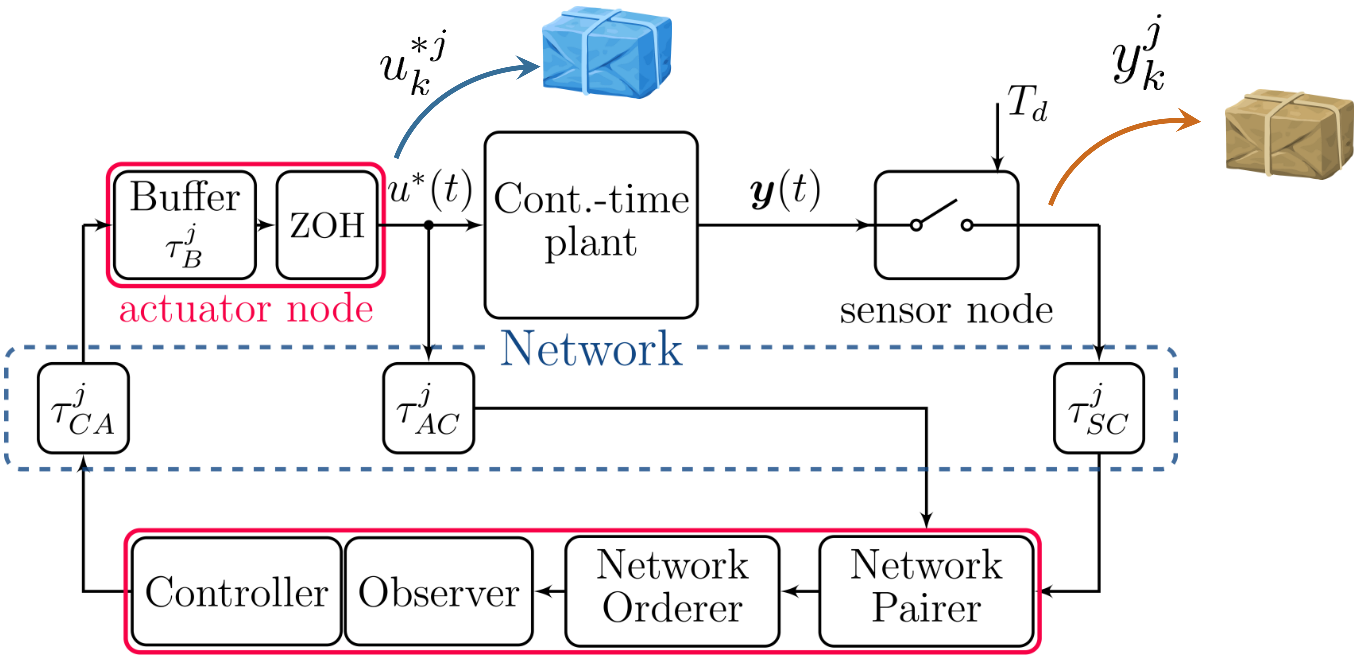

Mathematical description using packet notation

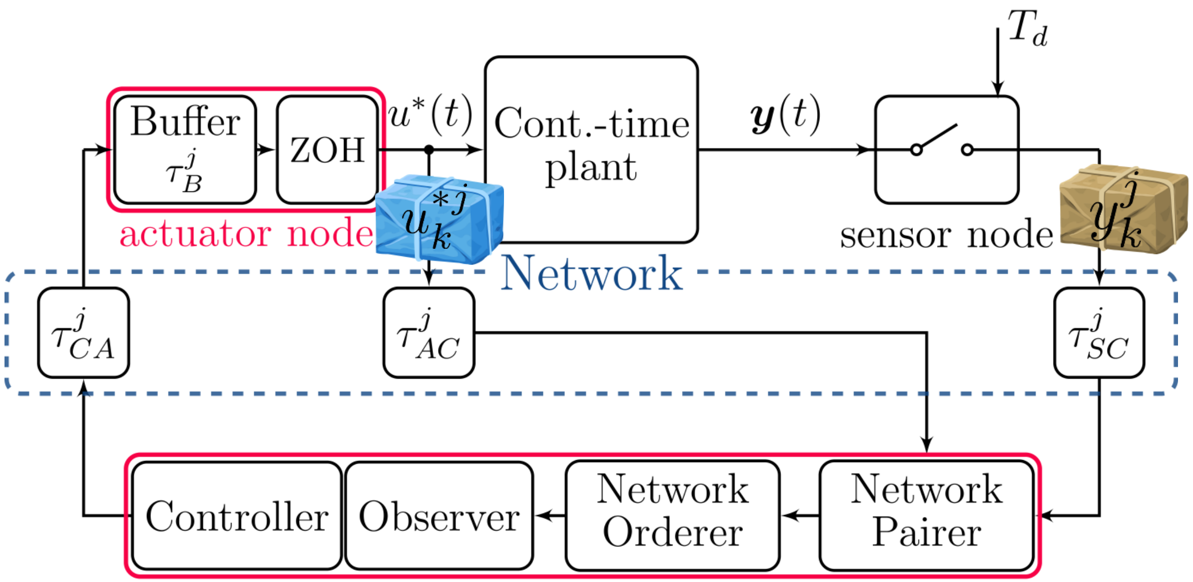

Mathematical description using packet notation

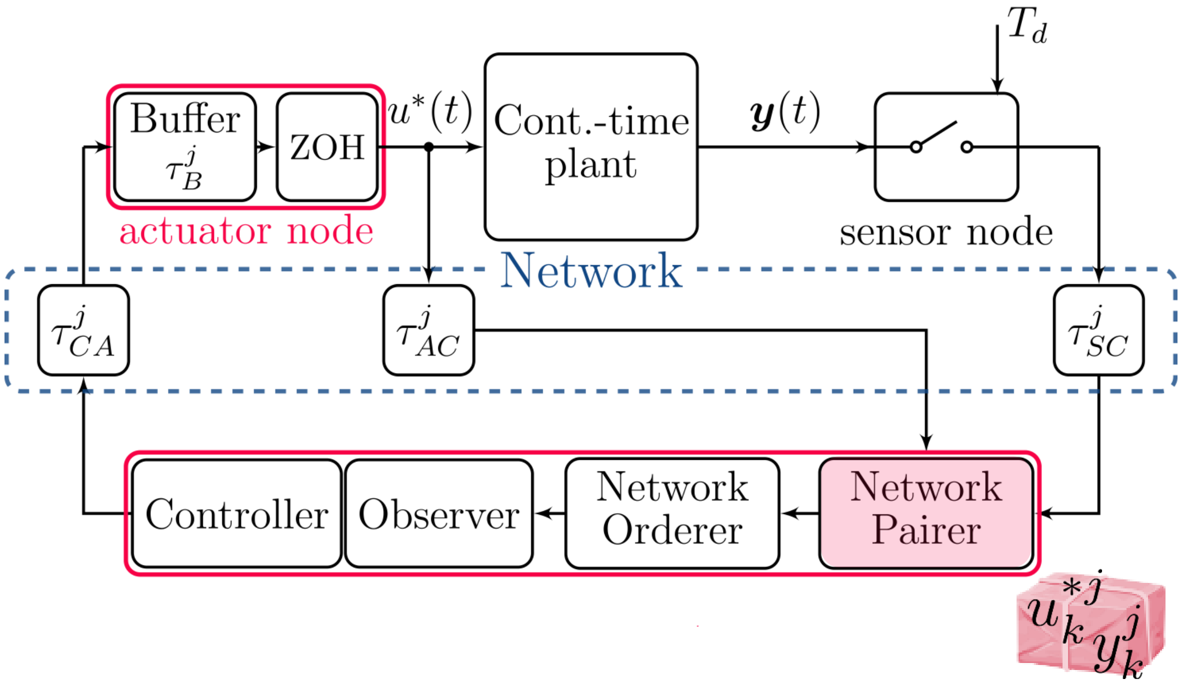

Mathematical description using packet notation

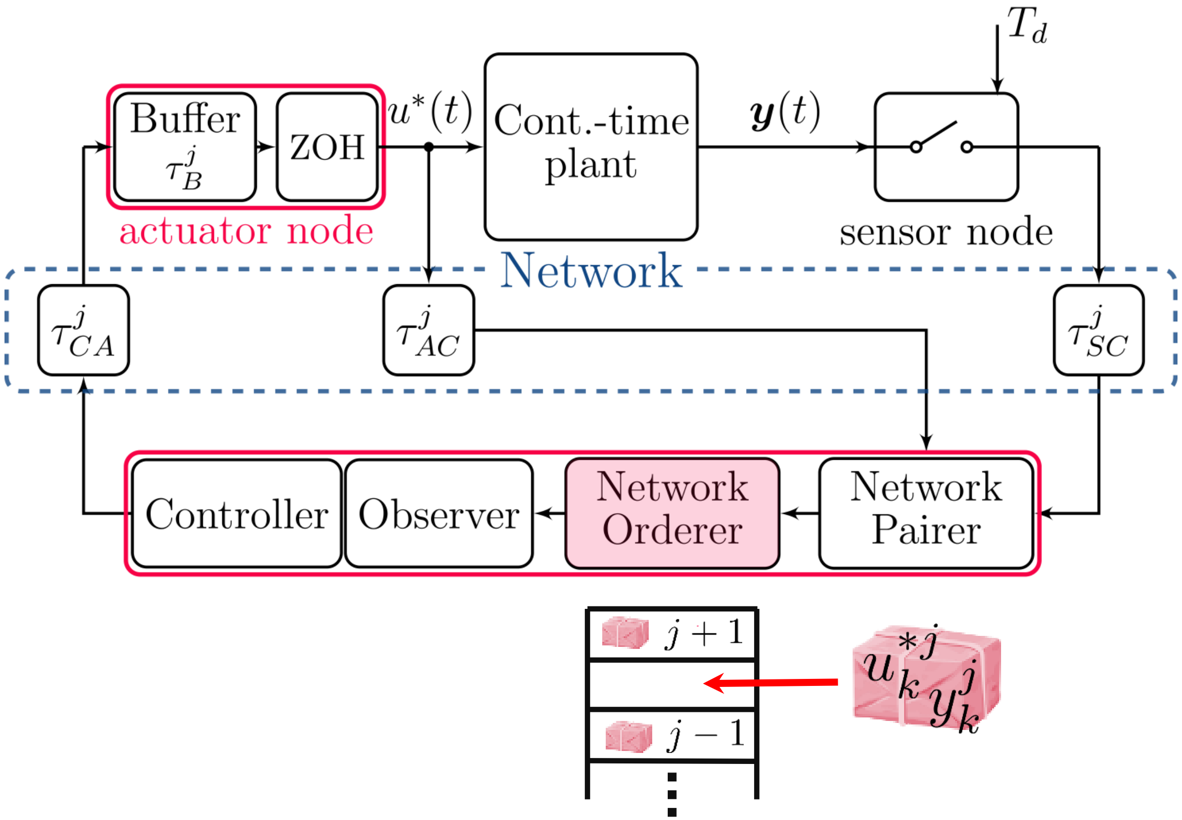

Mathematical description using packet notation

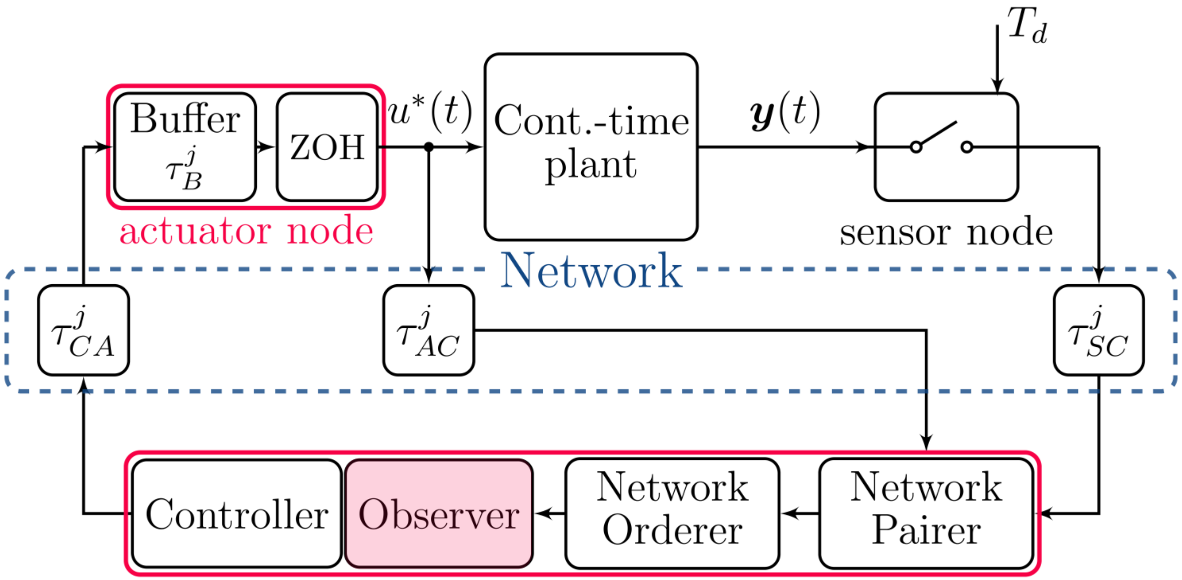

asynchronous
Luenberger observer

sends future estimation

Mathematical description using packet notation

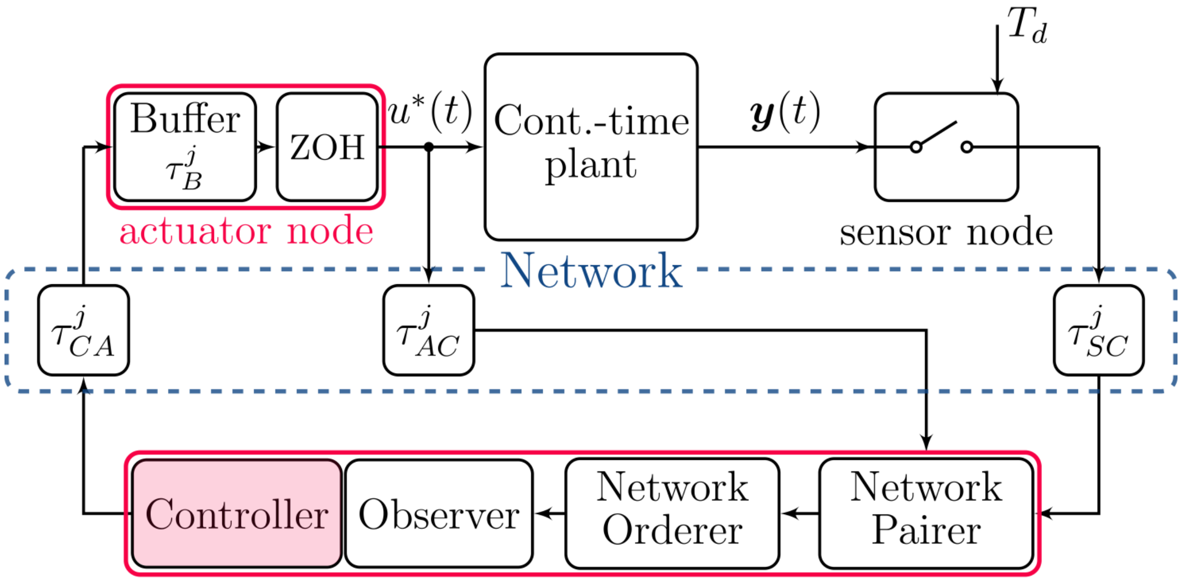

Switched Lyapunov Function-Based Controller for $\bar{\delta} - 1$

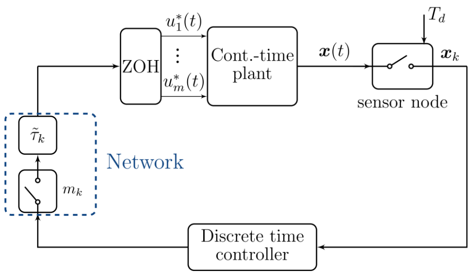

asynchronous Luenberger observer

sends future estimation

Example: DC Motor

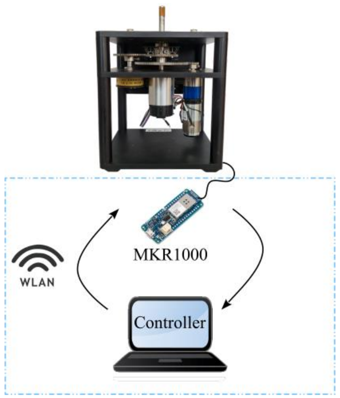

$\bar{\delta} = 4$

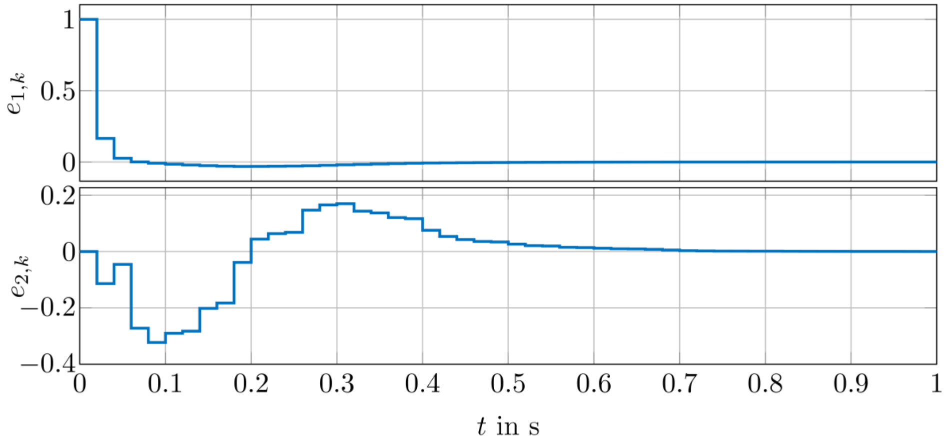

Example: DC Motor

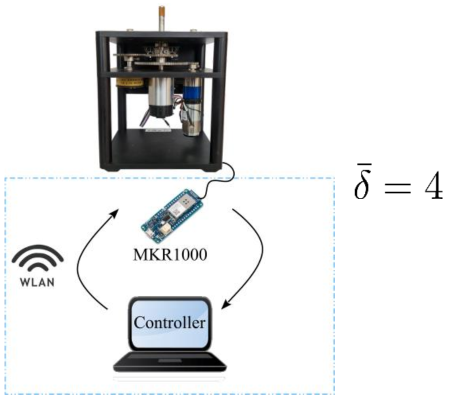

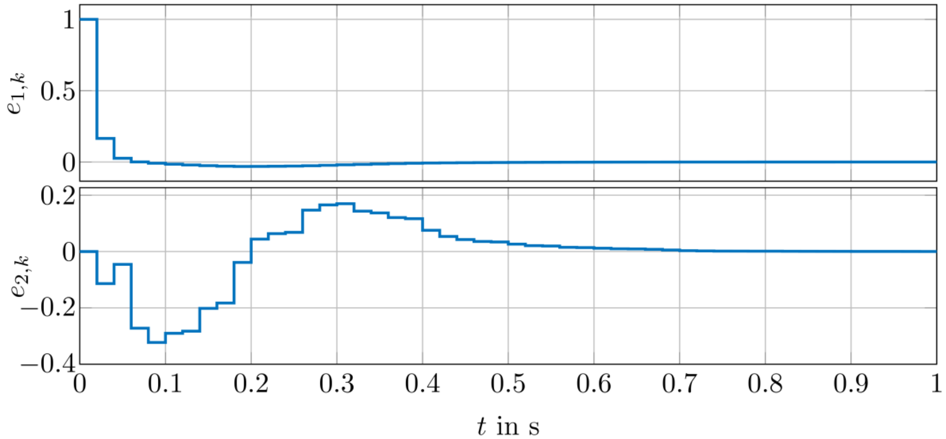

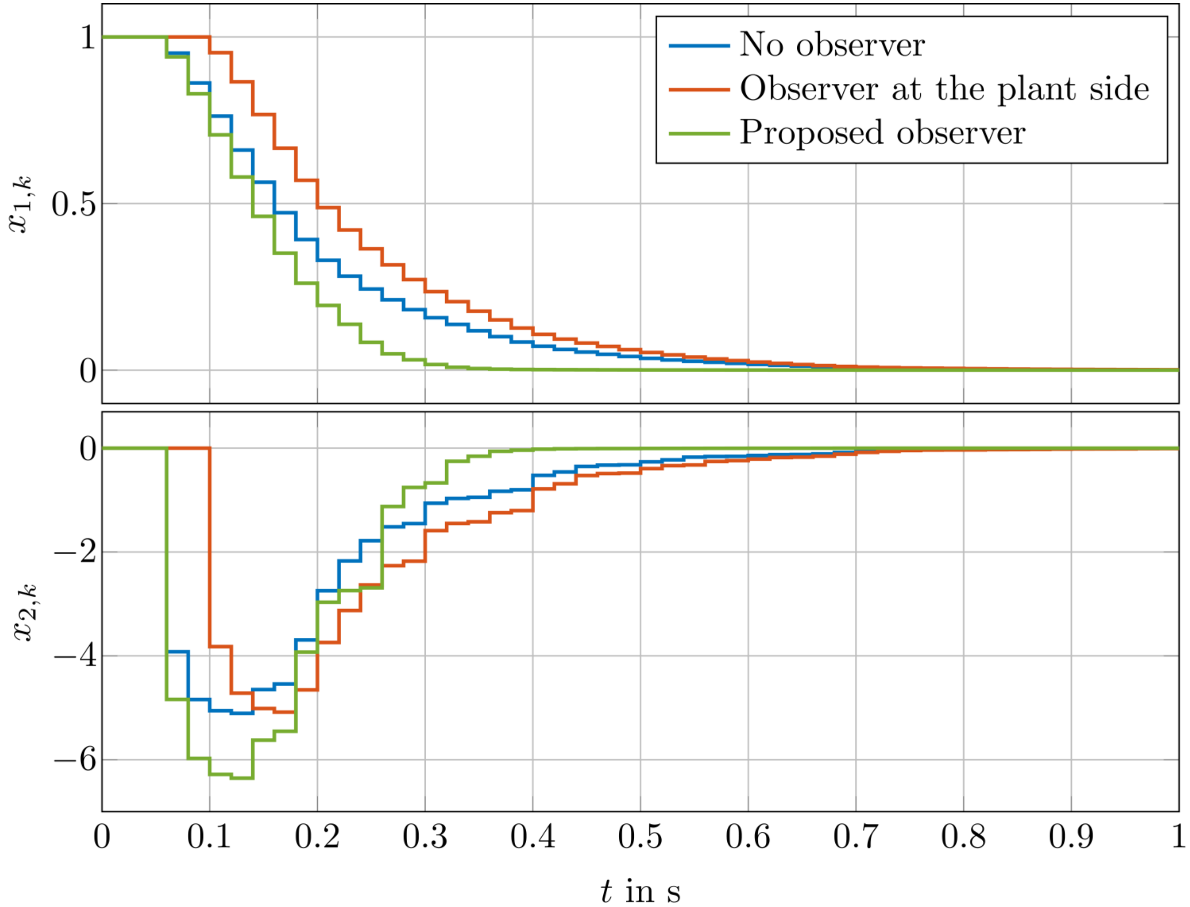

Summary

Switched Lyapunov Function-Based Controller

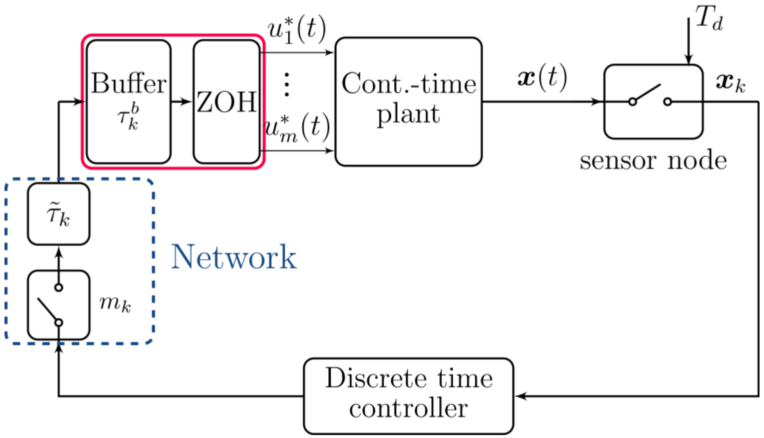

- The necessity for convex over-approximation is circumvented
- The significant reduction in the number of LMIs and optimization variables.
- additional degrees of freedom that influence the transient behavior of the closed-loop system

Summary

Switched Lyapunov Function-Based Controller

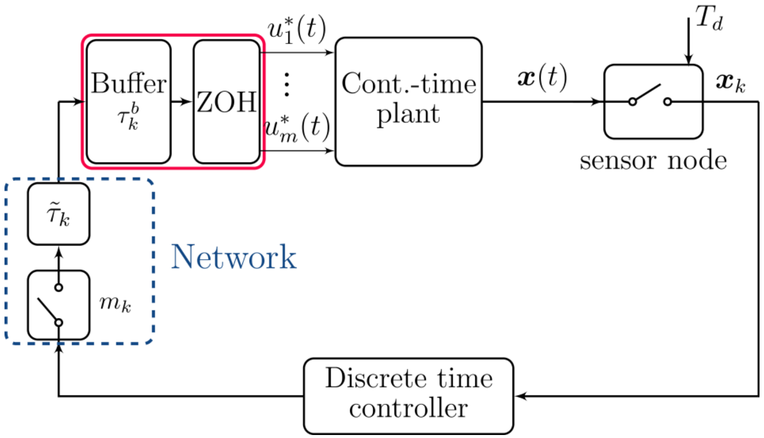

- The necessity for convex over-approximation is circumvented
- The significant reduction in the number of LMIs and optimization variables.
- additional degrees of freedom that influence the transient behavior of the closed-loop system

Observer Strategies for Buffered NCS

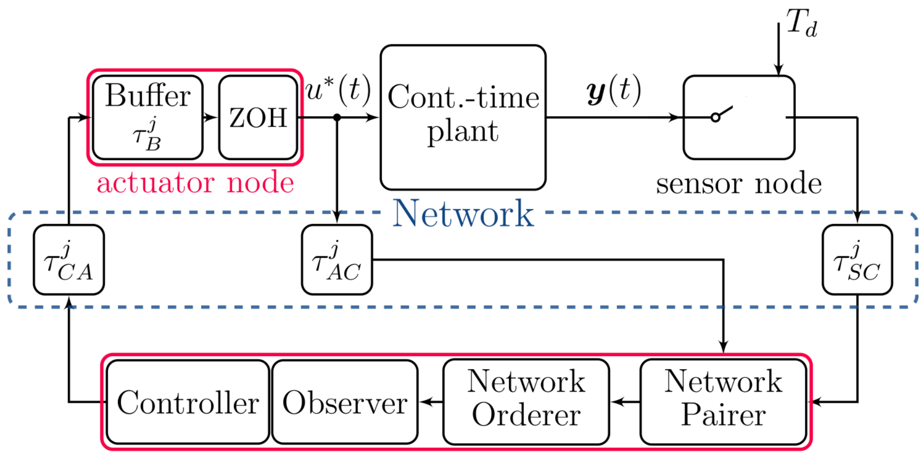

- The asynchronous Luenberger-type observer designed entirely independent from the network
- The stability is ensured through the separate design of
  1. the observer for the delay free case and
  2. the controller for NCS with measurable states
- Strategy mitigates network delay by reducing it by Td.

XI. Local stability analysis of sliding-mode control approaches within the model-following control architecture

presenter: Niclas Tietze

Local stability analysis of sliding-mode control approaches within the model-following control architecture

Niclas Tietze, Kai Wulff, and Johann Reger

niclas.tietze@tu-ilmenau.de

Control Engineering Group, TU Ilmenau, Germany

11th September 2024

23rd Styrian Workshop on Automatic Control

Schloss Retzhof, Austria

Outlook

Control problem: local stabilisation of perturbed systems in Brunovský form

- Time- and state-dependent perturbations

Model-following control (MFC)

- 2-DOF architecture: track solution of stabilised process model
- Sliding-mode control of the error dynamics
- Estimate region of attraction using positively invariant sets

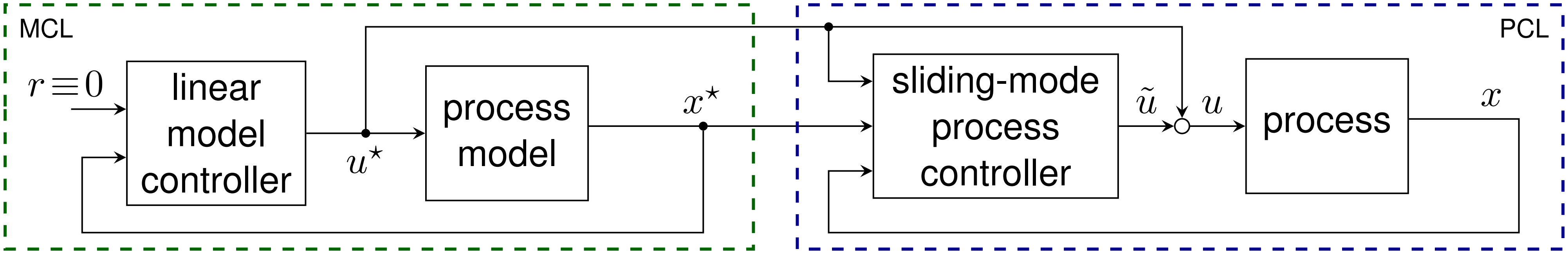

Problem definition

Process dynamics: $\dot{x} = A\,x + B\big(u + \Delta(x,t)\big), \quad x(t) \in \mathbb{R}^n$

$$A = \begin{bmatrix} 0 & 1 & 0 & \dots & 0 \\ \vdots & \ddots & \ddots & \ddots & \vdots \\ \vdots & & \ddots & \ddots & 0 \\ \vdots & \dots & \dots & \ddots & 1 \\ 0 & \dots & \dots & \dots & 0 \end{bmatrix} \in \mathbb{R}^{n\times n}, \qquad B = \begin{bmatrix} 0 \\ \vdots \\ 0 \\ 0 \\ 1 \end{bmatrix} \in \mathbb{R}^n$$

- Unknown perturbation $\Delta : \mathbb{R}^n \times \mathbb{R} \mapsto \mathbb{R}$ bounded on $\mathcal{D} \subset \mathbb{R}^n$

$$\max_{x\in\mathcal{D}, t\geq 0} \left|\Delta(x,t)\right| \leq \delta$$

Goal:

- Local stabilisation of $x = 0$ using sliding-mode control
- Estimate of the region of attraction $\left\{ x_0 \,\middle|\, \lim_{t\to\infty} x(t) = 0 \right\}$

Motivating example

Process dynamics: $$\dot{x} = A\,x + B\,\big(u + \Delta(x,t)\big)$$

$$A = \begin{bmatrix} 0 & 1 \\ 0 & 0 \end{bmatrix}, \quad B = \begin{bmatrix} 0 \\ 1 \end{bmatrix}$$

Local stabilisation: $\lim_{t\to\infty} x(t) = 0$ with $x(t) \in \mathcal{D}$ for all $t \geq 0$

$$\mathcal{D} = \left\{ \begin{bmatrix} x_1 \\ x_2 \end{bmatrix} \,\middle|\, |x_1| \leq 1 \,\wedge\, |x_2| \leq 1 \right\}, \qquad \delta = \max_{x\in\mathcal{D}, t\geq 0} \big|\Delta(x,t)\big|$$

Sliding-mode control (SMC): $u = -m\,x_2 - \rho\,\mathrm{sgn}(s(x))$

$$s(x) = m\,x_1 + x_2, \quad m > 0, \quad \rho > \delta$$

Motivating example - first order SMC

Control law:

$$u = -m\,x_2 - \rho\,\mathrm{sgn}(s(x))$$

Closed loop

- Invariant sets: $c \geq 0, c_\mathrm{z} \geq \frac{c}{m}$

$$\Gamma_{c,c_\mathrm{z}} = \left\{ \begin{bmatrix} x_1 \\ x_2 \end{bmatrix} \,\middle|\, \left|s(x)\right| \leq c \wedge \left|x_1\right| \leq c_\mathrm{z} \right\}$$

Estimate of region of attraction

$$\Psi_\mathrm{sl} = \bigcup_{\substack{c \geq 0, c_\mathrm{z} \geq \frac{c}{m} \\ \text{s.t. } \Gamma_{c,c_\mathrm{z}} \subseteq \mathcal{D}}} \Gamma_{c,c_\mathrm{z}}$$

x_1-x_2-planes

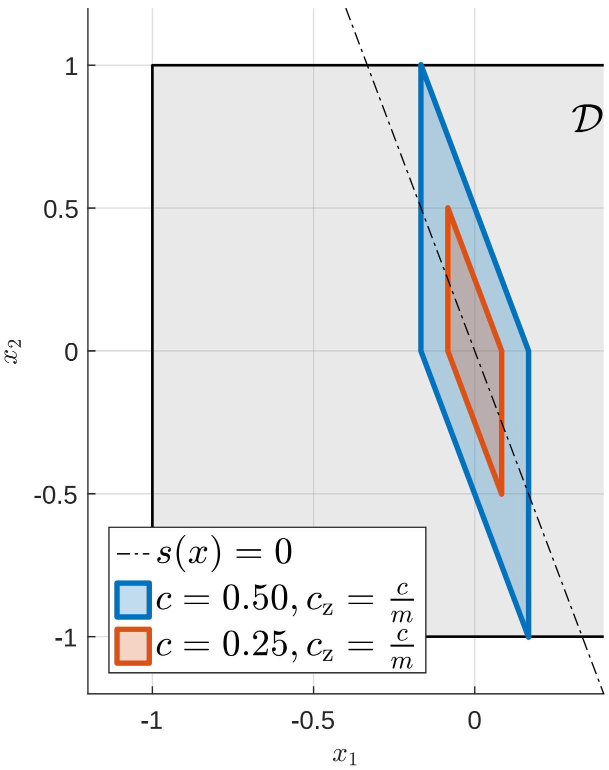

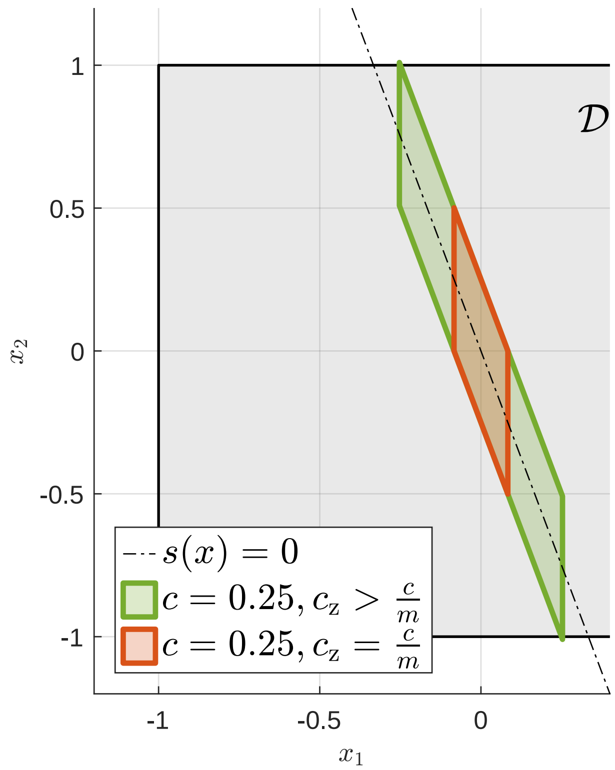

Motivating example - first order SMC

Control law:

$$u = -m\,x_2 - \rho\,\mathrm{sgn}(s(x))$$

Closed loop

- Invariant sets: $c \geq 0, c_\mathrm{z} \geq \frac{c}{m}$

$$\Gamma_{c,c_\mathrm{z}} = \left\{ \begin{bmatrix} x_1 \\ x_2 \end{bmatrix} \;\middle|\; |s(x)| \leq c \wedge |x_1| \leq c_\mathrm{z} \right\}$$

Estimate of region of attraction

$$\Psi_\mathrm{sl} = \bigcup_{\substack{c \geq 0, c_\mathrm{z} \geq \frac{c}{m} \\ \text{s.t. } \Gamma_{c,c_\mathrm{z}} \subseteq \mathcal{D}}} \Gamma_{c,c_\mathrm{z}}$$

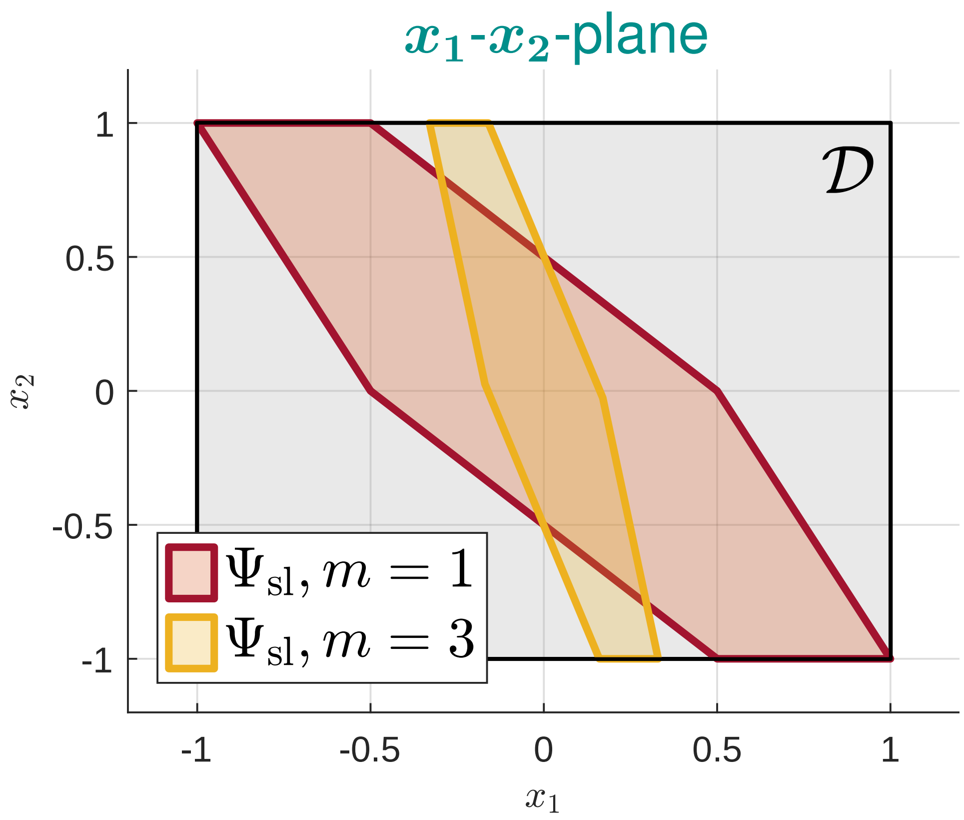

Motivating example - MFC

Sliding-mode MFC: $u = k^{\star\top} x^\star \;-\; \big(m\,(x_2 - x_2^\star) + \rho\,\mathrm{sgn}(s(x - x^\star))\big)\;, \quad k^\star = -\big[1, 2\big]^\top$

Model: $\dot{x}^\star = \big(A + B\,k^{\star\top}\big)\,x^\star, \;\; x^\star(0) = x(0)$

Closed loop: exact model tracking

$x \equiv x^\star$ whenever $x^\star(t) \in \mathcal{D}$ for all $t \geq 0$

- Estimate of region of attraction

$$\Lambda_0 = \left\{x_0^\star \,\middle|\, x^\star(t) \in \mathcal{D} \text{ for all } t \geq 0\right\}$$
$$= \left\{x_0^\star \,\middle|\, e^{(A + B\,k^{\star\top})\,t} x_0^\star \in \mathcal{D} \text{ for all } t \geq 0\right\}$$

  - Largest invariant set in $\mathcal{D}$ is computable

N. Athanasopoulos, G. Bitsoris, and M. Lazar, "Construction of invariant polytopic sets with specified complexity," *International Journal of Control*, vol. 87, no. 8, pp. 1681–1693, 2014

L. Schäfer, F. Gruber, and M. Althoff, "Scalable computation of robust control invariant sets of nonlinear systems," *IEEE Transactions on Automatic Control*, vol. 69, no. 2, pp. 755–770, 2024

x_1-x_2-plane

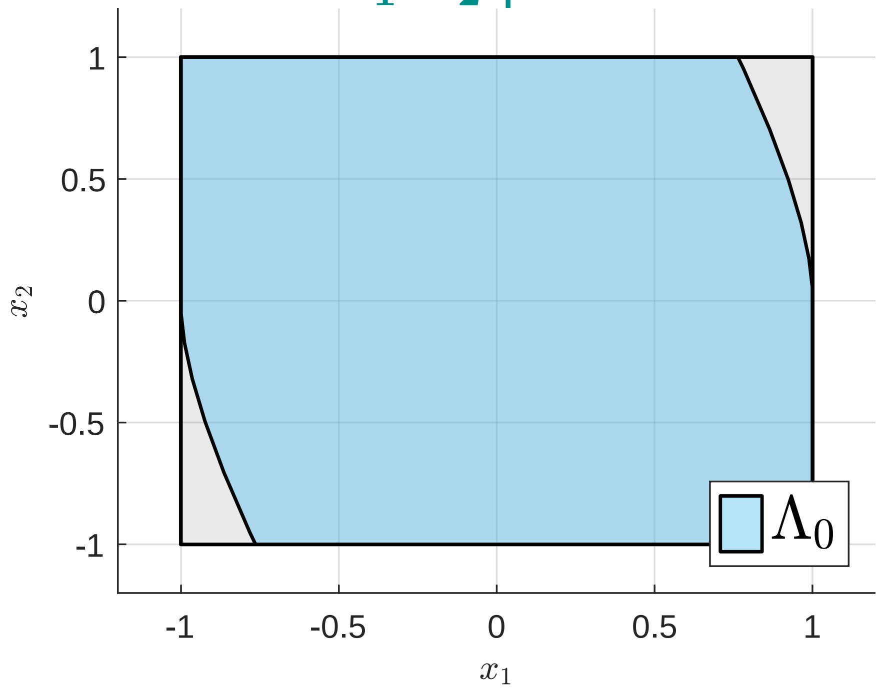

- Larger estimate for MFC

Motivating example - MFC

Sliding-mode MFC: $u = k^{\star\top} x^\star \; - \; \left(m\,(x_2 - x_2^\star) + \rho\,\mathrm{sgn}(s(x - x^\star))\right)\,, \quad k^\star = -\left[1, 2\right]^\top$

Model: $\dot{x}^\star = \left(A + B\,k^{\star\top}\right) x^\star, \;\; x^\star(0) = x(0)$

Closed loop: exact model tracking

$x \equiv x^\star$ whenever $x^\star(t) \in \mathcal{D}$ for all $t \geq 0$

- Estimate of region of attraction

$$\Lambda_0 = \left\{ x_0^\star \,\middle|\, x^\star(t) \in \mathcal{D} \text{ for all } t \geq 0 \right\}$$
$$= \left\{ x_0^\star \,\middle|\, e^{(A + B\,k^{\star\top})\,t} x_0^\star \in \mathcal{D} \;\text{ for all } t \geq 0 \right\}$$

  - Largest invariant set in $\mathcal{D}$ is computable

N. Athanasopoulos, G. Bitsoris, and M. Lazar, “Construction of invariant polytopic sets with specified complexity,” *International Journal of Control*, vol. 87, no. 8, pp. 1681–1693, 2014
L. Schäfer, F. Gruber, and M. Althoff, “Scalable computation of robust control invariant sets of nonlinear systems,” *IEEE Transactions on Automatic Control*, vol. 69, no. 2, pp. 755–770, 2024

x_1-x_2-plane

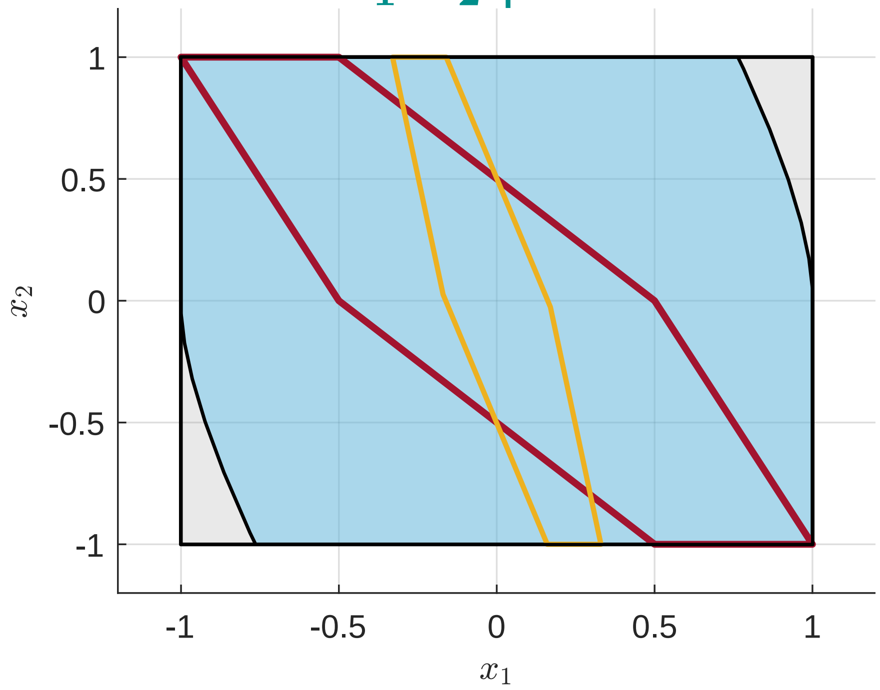

- Larger estimate for MFC

Outline

1 Model-following control architecture

2 First-order sliding-mode MFC
- Control design
- Stability
- Region of attraction

3 Super-twisting MFC
- Control design
- Stability
- Region of attraction

4 Conclusion

Model following control architecture

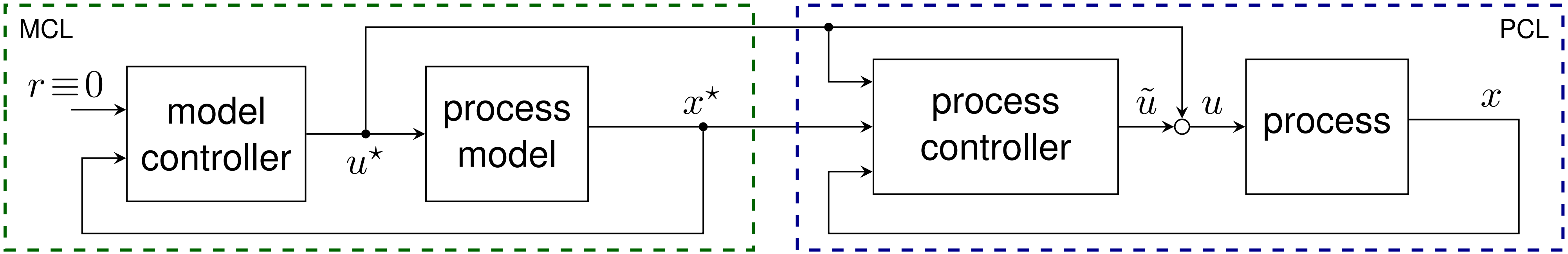

Model following control architecture

- 2-DOF structure
- Two control loops:
  - Model control loop (MCL)
  - Process control loop (PCL)

- MCL: no perturbation
- New reference $x^\star$
- Feedforward $u^\star$

H. Erzberger, "On the use of algebraic methods in the analysis and design of model-following control systems," National Aeronautics and Space Administration, Washington DC, Tech. Rep., 1968

J. Willkomm, K. Wulff, and J. Reger, "Quantitative robustness analysis of model-following control for nonlinear systems subject to model uncertainties," in *IFAC Conference on Modelling, Identification and Control of nonlinear Systems*, Tokyo, Japan, 2021, pp. 167–172

Model-following control architecture

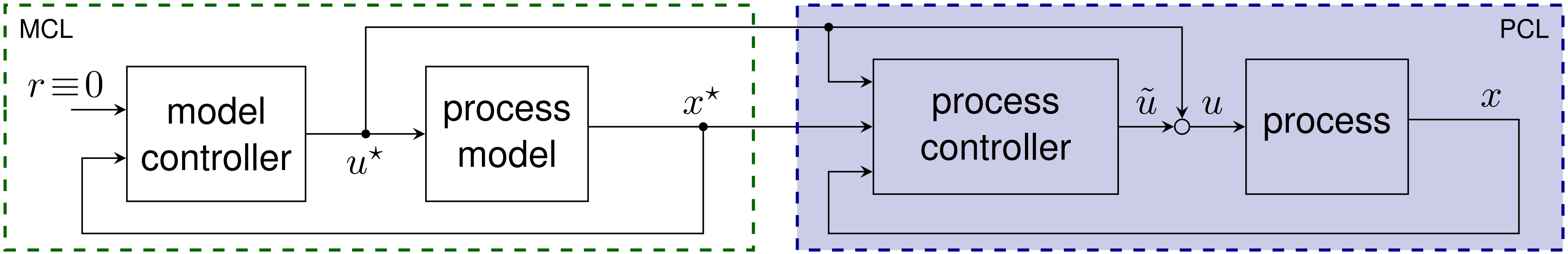

MCL: nominal stabilisation

- State $x^\star \in \mathbb{R}^n$, input $u^\star \in \mathbb{R}$

$$\dot{x}^\star = A\,x^\star + B\,u^\star$$

- Initial state $x^\star(0) = x_0^\star$
- Linear state-feedback: $u^\star = k^{\star\top} x^\star$

PCL: robust stabilisation

- State $\tilde{x} = x - x^\star$, input $\tilde{u} = u - u^\star$

$$\dot{\tilde{x}} = A\,\tilde{x} + B\,\big(\tilde{u} + \Delta(x, t)\big)$$

- Initial state $\tilde{x}(0) = \tilde{x}_0 = x_0 - x_0^\star$
- Control law $\tilde{u}$

Robust design of the process control loop

Continuous control

- High-gain control

J. Willkomm, K. Wulff, and J. Reger, "Set-point tracking for nonlinear systems subject to uncertainties using model-following control with a high-gain controller," in *European Control Conference*, London, United Kingdom, 2022, pp. 1617–1622

N. Tietze, K. Wulff, and J. Reger, "A model-following control approach to peaking attenuation in high-gain partial state feedback for nonlinear systems," in *IFAC Conference of Modelling, Identification and Control of nonlinear systems*, Lyon, France, 2024

Discontinuous control

- Lyapunov redesign

N. Tietze, K. Wulff, and J. Reger, "Dynamic partial state-feedback revisited for output tracking using Lyapunov redesign and model-following control," in *IEEE Conference on Decision and Control*, Milan, Italy, 2024

- Sliding-mode control

N. Tietze, K. Wulff, and J. Reger, "Local stabilisation of nonlinear systems with time- and state-dependent perturbations using sliding-mode model-following control," in *IEEE Conference on Decision and Control*, Milan, Italy, 2024

Sliding-mode design

1. First-order
2. Super-twisting

First-order sliding-mode model-following control

Process controller $\tilde{u} = -[0\ \tilde{m}^\top]\,\tilde{x} - \tilde{\rho}\,\mathrm{sgn}(\tilde{s}(\tilde{x}))$

- Linear sliding-variable: $\tilde{s}(\tilde{x}) = [\tilde{m}\ 1]^\top \tilde{x}$
- Gain: $\tilde{\rho} > \delta \geq \max_{x \in \mathcal{D}, t \geq 0} \left|\Delta(x,t)\right|$

Dynamics of the closed loop

- Reduced state $\tilde{z} = [\tilde{x}_1, ..., \tilde{x}_{n-1}]^\top \in \mathbb{R}^{n-1}$

$$\begin{aligned} \dot{\tilde{z}} &= A_\mathrm{z}\,\tilde{z} + B_\mathrm{z}\,\tilde{s}, \\ \dot{\tilde{s}} &= -\tilde{\rho}\,\mathrm{sgn}(\tilde{s}) + \Delta(x,t), \end{aligned} \qquad A_\mathrm{z} = \begin{bmatrix} 0 & 1 & \dots & 0 \\ \vdots & \ddots & \ddots & \vdots \\ 0 & & 0 & 1 \\ -\tilde{m}_1 & \dots & \dots & -\tilde{m}_{n-1} \end{bmatrix}, \quad B_\mathrm{z} = \begin{bmatrix} 0 \\ \vdots \\ 0 \\ 1 \end{bmatrix}$$

- Lyapunov function for $\tilde{z}$ (if $\tilde{s} = 0$)

$$\tilde{V}_\mathrm{z}(\tilde{z}) = \left(\tilde{z}^\top P_\mathrm{z}\,\tilde{z}\right)^{1/2}, \qquad A_\mathrm{z}^\top P_\mathrm{z} + P_\mathrm{z}\,A_\mathrm{z} = -\tilde{q}\,I, \quad \tilde{q} > 0$$

Sliding-mode model-following control - stability

Closed loop

- Candidates for positively invariant sets of the PCL

$$\tilde{\Omega}_{\tilde{c},\tilde{c}_\mathrm{z}} = \left\{ \tilde{x} \,\middle|\, \left|\tilde{s}(\tilde{x})\right| \leq \tilde{c} \wedge \tilde{V}_\mathrm{z}(\tilde{z}) \leq \tilde{c}_\mathrm{z} \right\}, \quad \tilde{c} \geq 0, \quad \tilde{c}_\mathrm{z} \geq \tilde{a}\,\tilde{c}, \quad \tilde{a} = 2\,\tilde{q}^{-1}\lambda_{\max}^{1/2}(P_\mathrm{z})\,\|P_\mathrm{z}B_\mathrm{z}\|_2$$

Theorem 1 (Stability of the closed loop).

Let $x_0 = x_0^\star + \tilde{x}_0$ with $\tilde{x}_0 \in \tilde{\Omega}_{\tilde{c},\tilde{c}_\mathrm{z}}$. The solution $x = x^\star + \tilde{x}$ converges to the origin and

$$x(t) \in \left(\{x^\star(t)\} \oplus \tilde{\Omega}_{\tilde{c},\tilde{c}_\mathrm{z}} \right) \text{ for all } t \geq 0, \qquad \text{whenever} \qquad \left(\{x^\star(t)\} \oplus \tilde{\Omega}_{\tilde{c},\tilde{c}_\mathrm{z}} \right) \subseteq \mathcal{D} \text{ for all } t \geq 0.$$

Idea of proof

- $\tilde{\Omega}_{\tilde{c},\tilde{c}_\mathrm{z}}$ invariant w.r.t. dynamics of closed PCL

$$\dot{\tilde{z}} = A_\mathrm{z}\,\tilde{z} + B_\mathrm{z}\,\tilde{s},$$
$$\dot{\tilde{s}} = -\tilde{\rho}\,\mathrm{sgn}(\tilde{s}) + \Delta(x^\star + \tilde{x}, t)$$

Sliding-mode model-following control - stability

Discussion

$\boxed{\tilde{x}_0 \in \tilde{\Omega}_{\tilde{c},\tilde{c}_z} \text{ and } \left(\{x^\star(t)\} \oplus \tilde{\Omega}_{\tilde{c},\tilde{c}_z}\right) \subseteq \mathcal{D} \text{ for all } t \geq 0} \Rightarrow \boxed{x(t) \in \left(\{x^\star(t)\} \oplus \tilde{\Omega}_{\tilde{c},\tilde{c}_z}\right) \text{ for all } t \geq 0}$

- Geometric condition using solution of unperturbed MCL to check stability of perturbed process

Geometric interpretation

- Solution x remains in tube around $x^\star$ whenever tube is subset of $\mathcal{D}$

Example: $n = 2$ with $k^\star = -[1, 2]$, $\tilde{m} = 3$

- Initial state $x_0^\star = \begin{bmatrix} -0.5 \\ -0.5 \end{bmatrix}$
- $\tilde{\Omega}_{\tilde{c},\tilde{c}_z}$ such that tube is subset of $\mathcal{D}$

$\boldsymbol{x(t)}$ in time domain

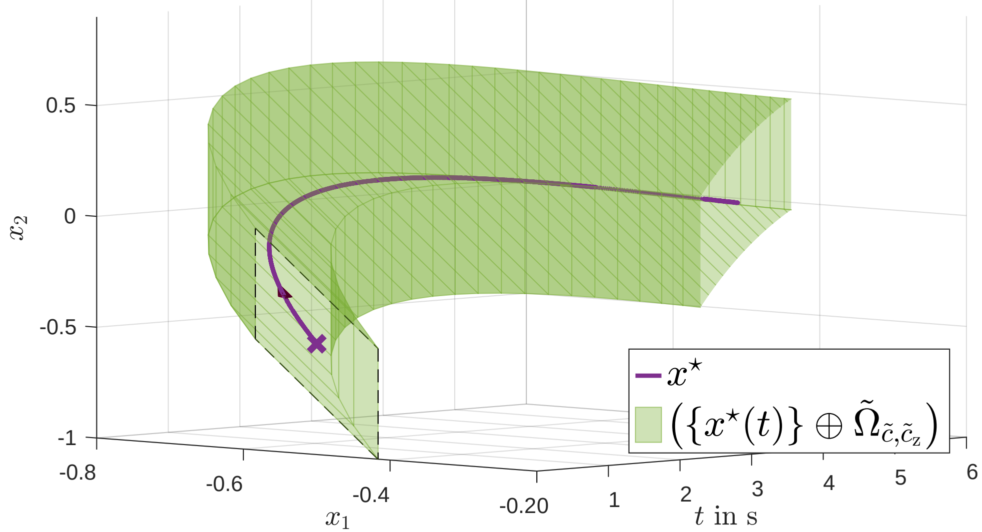

Sliding-mode model-following control - stability

Discussion

$$\boxed{\tilde{x}_0 \in \tilde{\Omega}_{\tilde{c},\tilde{c}_z} \text{ and } \left(\{x^\star(t)\} \oplus \tilde{\Omega}_{\tilde{c},\tilde{c}_z}\right) \subseteq \mathcal{D} \text{ for all } t \geq 0} \Rightarrow \boxed{x(t) \in \left(\{x^\star(t)\} \oplus \tilde{\Omega}_{\tilde{c},\tilde{c}_z}\right) \text{ for all } t \geq 0}$$

- Geometric condition using solution of unperturbed MCL to check stability of perturbed process

Geometric interpretation

- Solution x remains in tube around $x^\star$ whenever tube is subset of $\mathcal{D}$

Example: $n = 2$ with $k^\star = -[1, 2]$, $\tilde{m} = 3$

- Initial state $x_0^\star = \begin{bmatrix} -0.5 \\ -0.5 \end{bmatrix}$
- $\tilde{\Omega}_{\tilde{c},\tilde{c}_z}$ such that tube is subset of $\mathcal{D}$

x_1-x_2-plane

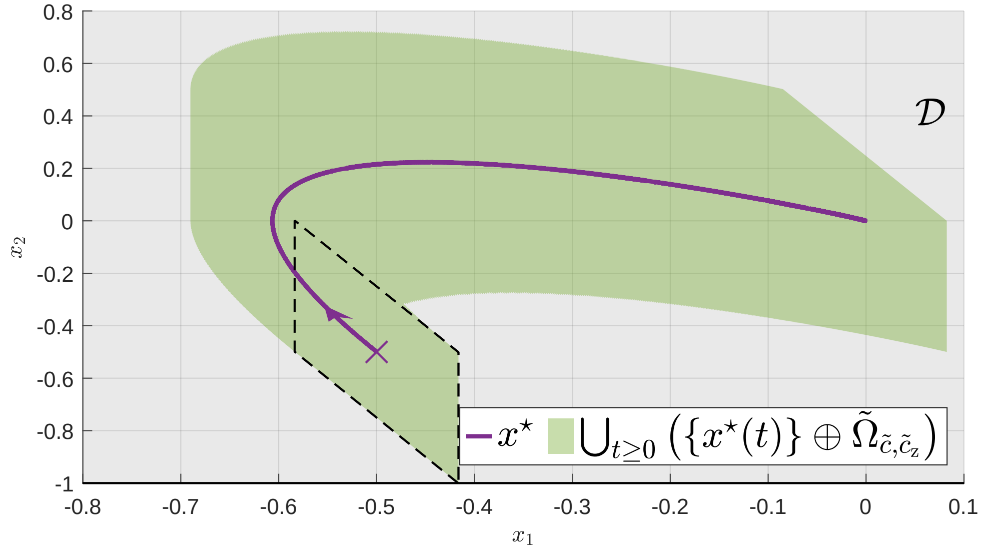

Sliding-mode model-following control - example

Second-order system: solution for different x_0 for one $x_0^\star$

$x(t)$ in time domain

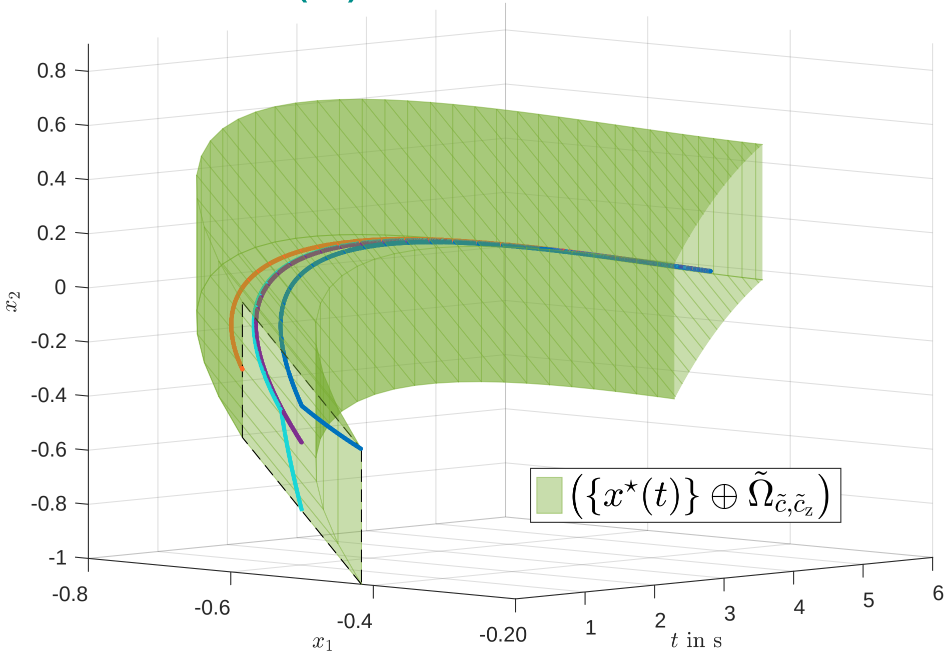

x_1-x_2-plane

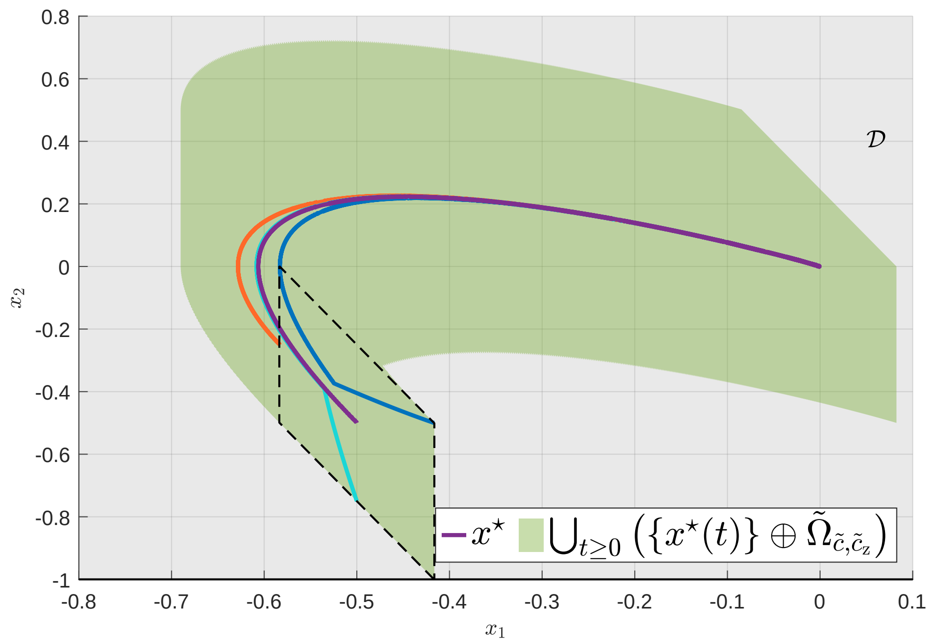

- Invariance: $x(t) \in \left(\{x^\star(t)\} \oplus \tilde{\Omega}_{\tilde{c},\tilde{c}_z}\right) \; \forall t \geq 0$
- Exact model tracking $x \equiv x^\star$ for $x_0^\star = x_0$

Sliding-mode model-following control - region of attraction

Region of attraction: Depends on x_0 and $x_0^\star$

$$\boxed{\tilde{x}_0 \in \tilde{\Omega}_{\tilde{c},\tilde{c}_\mathrm{z}} \text{ and } \left(\{x^\star(t)\} \oplus \tilde{\Omega}_{\tilde{c},\tilde{c}_\mathrm{z}}\right) \subseteq \mathcal{D} \text{ for all } t \geq 0} \quad \Rightarrow \quad \boxed{x(t) \in \left(\{x^\star(t)\} \oplus \tilde{\Omega}_{\tilde{c},\tilde{c}_\mathrm{z}}\right) \text{ for all } t \geq 0}$$

- Define:

$$\Lambda = \bigcup_{\substack{x_0^\star \in \mathcal{D}, \tilde{c} \geq 0, \tilde{c}_\mathrm{z} \geq \tilde{a}\,\tilde{c} \\ \text{s.t.} \left(\{x^\star(t)\} \oplus \tilde{\Omega}_{\tilde{c},\tilde{c}_\mathrm{z}}\right) \subseteq \mathcal{D} \ \forall\, t \geq 0}} \left(\{x_0^\star\} \oplus \tilde{\Omega}_{\tilde{c},\tilde{c}_\mathrm{z}}\right)$$

Theorem 2 (ROA with appropriately chosen $x_0^\star$).

For each $x_0 \in \Lambda$, there exists some $x_0^\star \in \mathcal{D}$ such that $\lim_{t\to\infty} x(t) = 0$.

Special cases: $x_0^\star = 0$

Idea of proof: Construction of the set Λ

- Given some $x_0 \in \Lambda$, select $x_0^\star \in \mathcal{D}$ s.t. $\tilde{x}_0 \in \tilde{\Omega}_{\tilde{c},\tilde{c}_\mathrm{z}}$ and $\left(\{x^\star(t)\} \oplus \tilde{\Omega}_{\tilde{c},\tilde{c}_\mathrm{z}}\right) \subseteq \mathcal{D}$ for all $t \geq 0$ for some $\tilde{c} \geq 0, \tilde{c}_\mathrm{z} \geq \tilde{a}\,\tilde{c}$

Sliding-mode model-following control - region of attraction

Region of attraction

$$\boxed{\Lambda \supseteq \bigcup_{\substack{x_0^\star=0,\tilde{c}\geq 0,\tilde{c}_\mathrm{z}\geq\tilde{a}\,\tilde{c} \\ \text{s.t.}\left(\{0\}\oplus\tilde{\Omega}_{\tilde{c},\tilde{c}_\mathrm{z}}\right)\subseteq\mathcal{D}\ \forall\, t\geq 0}} \left(\{0\} \oplus \tilde{\Omega}_{\tilde{c},\tilde{c}_\mathrm{z}}\right)}$$

Case: initialisation $\boldsymbol{x}_0^\star = \mathbf{0}$

- Trivial MCL $\boldsymbol{x}^\star \equiv \mathbf{0}$

$$x \equiv \tilde{x} \quad \Rightarrow \quad u = \overbrace{u^\star}^{\equiv 0} + \tilde{u} = -[0\ \tilde{m}^\top]\, x - \tilde{\rho}\,\mathrm{sgn}(\tilde{s}(x))$$

$\Rightarrow$ MFC is equivalent to single-loop design

$$\Psi_\mathrm{sl} = \boxed{\bigcup_{\substack{\tilde{c}\geq 0,\tilde{c}_\mathrm{z}\geq\tilde{a}\,\tilde{c} \\ \text{s.t.}\ \tilde{\Omega}_{\tilde{c},\tilde{c}_\mathrm{z}}\subseteq\mathcal{D}}} \tilde{\Omega}_{\tilde{c},\tilde{c}_\mathrm{z}} \subseteq \Lambda}$$

SM MFC - region of attraction without solution of the MCL

Discussion: estimate of the ROA

- Appropriately chosen $x_0^\star$: ROA MFC $\supseteq$ ROA SL ($\Lambda \supseteq \Psi_{\mathrm{sl}}$)

Requirement: solution $x^\star$ of the MCL

Idea: estimation of $\boldsymbol{x}^\star$

- Lyapunov function $V^\star(x^\star)$ of $\dot{x}^\star = \left(A + B\,k^{\star\top}\right) x^\star$
- Invariance of level-sets

$$V^\star(x_0^\star) \leq c^\star,\; c^\star \geq 0 \qquad \Rightarrow \qquad x^\star(t) \in \Omega^\star_{c^\star} \quad \text{with} \quad \Omega^\star_{c^\star} = \left\{ x^\star \,\middle|\, V^\star(x^\star) \leq c^\star \right\}$$

$\Rightarrow$ Evaluate geometric stability criterion for estimate $\Omega^\star_{c^\star}$ of $x^\star$

SM MFC - stability without solution of the MCL

Bound for the solution: $x^\star(t) \in \Omega^\star_{c^\star}$ for all $t \geq 0$

$$\left(\{x^\star(t)\} \oplus \tilde{\Omega}_{\tilde{c},\tilde{c}_z}\right) \subseteq \boxed{\left(\Omega^\star_{c^\star} \oplus \tilde{\Omega}_{\tilde{c},\tilde{c}_z}\right) = \Omega_{c^\star,\tilde{c},\tilde{c}_z}}$$

Corollary 3 (Stability of the close-loop).

Let $c^\star, \tilde{c} \geq 0$ and $\tilde{c}_z \geq \tilde{a}\,\tilde{c}$ such that $\Omega_{c^\star,\tilde{c},\tilde{c}_z} \subseteq \mathcal{D}$. Then, for all $x_0 = x_0^\star + \tilde{x}_0$ with $x_0^\star \in \Omega^\star_{c^\star}$ and $\tilde{x}_0 \in \tilde{\Omega}_{\tilde{c},\tilde{c}_z}$, the solution x converges to $x = 0$.

Example: $n = 2$ with $k^\star = -[1,2]$, $\tilde{m} = 3$

- $V^\star(x^\star) = x^{\star\top} P^\star x^\star$, $\quad A^{\star\top} P^\star + P^\star A^\star = -I$, $\quad A^\star = A + B\,k^{\star\top}$
- $\Omega^\star_{c^\star}$, $\tilde{\Omega}_{\tilde{c},\tilde{c}_z}$ such that $\Omega_{c^\star,\tilde{c},\tilde{c}_z}$ is subset of $\mathcal{D}$

x_1-x_2-plane

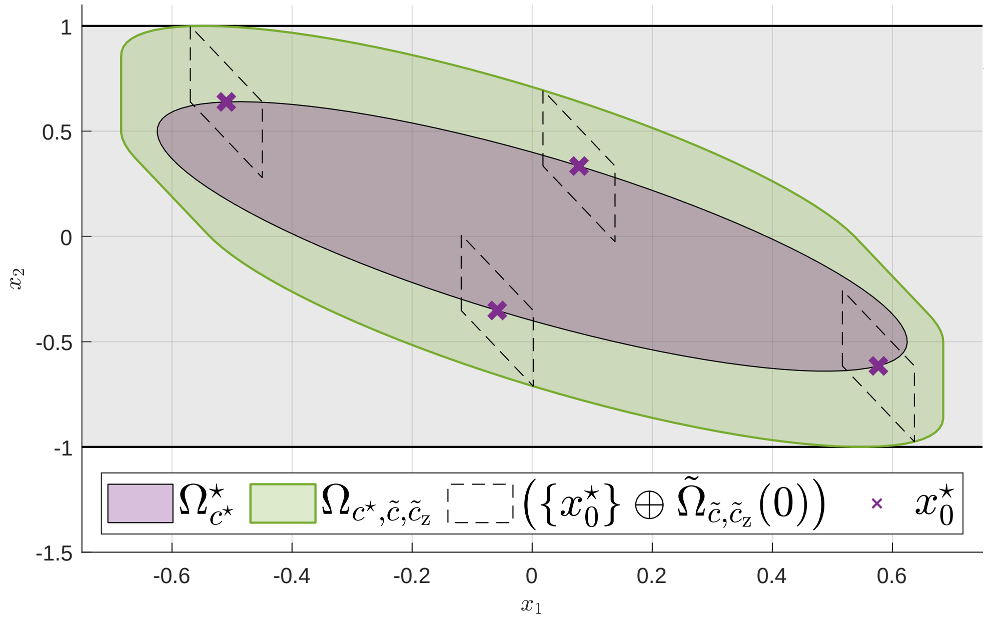

SM MFC - region of attraction without solution of the MCL

Region of attraction

$$\Psi_{\mathrm{sl}} = \bigcup_{\substack{\tilde{c}\geq 0, \tilde{c}_{\mathrm{z}}\geq \tilde{a}\,\tilde{c} \\ \text{s.t. } \tilde{\Omega}_{\tilde{c},\tilde{c}_{\mathrm{z}}}\subseteq \mathcal{D}}} \tilde{\Omega}_{\tilde{c},\tilde{c}_{\mathrm{z}}} \subseteq \Psi = \bigcup_{\substack{c^\star, \tilde{c}\geq 0, \tilde{c}_{\mathrm{z}}\geq \tilde{a}\,\tilde{c} \\ \text{s.t. } \Omega_{c^\star,\tilde{c},\tilde{c}_{\mathrm{z}}}\subseteq \mathcal{D}}} \Omega_{c^\star,\tilde{c},\tilde{c}_{\mathrm{z}}} \subseteq \Lambda = \bigcup_{\substack{x_0^\star\in\mathcal{D}, \tilde{c}\geq 0, \tilde{c}_{\mathrm{z}}\geq \tilde{a}\,\tilde{c} \\ \text{s.t. } \left(\{x^\star(t)\}\oplus\tilde{\Omega}_{\tilde{c},\tilde{c}_{\mathrm{z}}}\right)\subseteq\mathcal{D}\,\forall\, t\geq 0}} \left(\{x_0^\star\}\oplus\tilde{\Omega}_{\tilde{c},\tilde{c}_{\mathrm{z}}}\right)$$

Corollary 4.

For each $x_0 \in \Psi$, there exists some $x_0^\star \in \mathcal{D}$ such that $\lim_{t\to\infty} x(t) = 0$.

x_1-x_2-plane

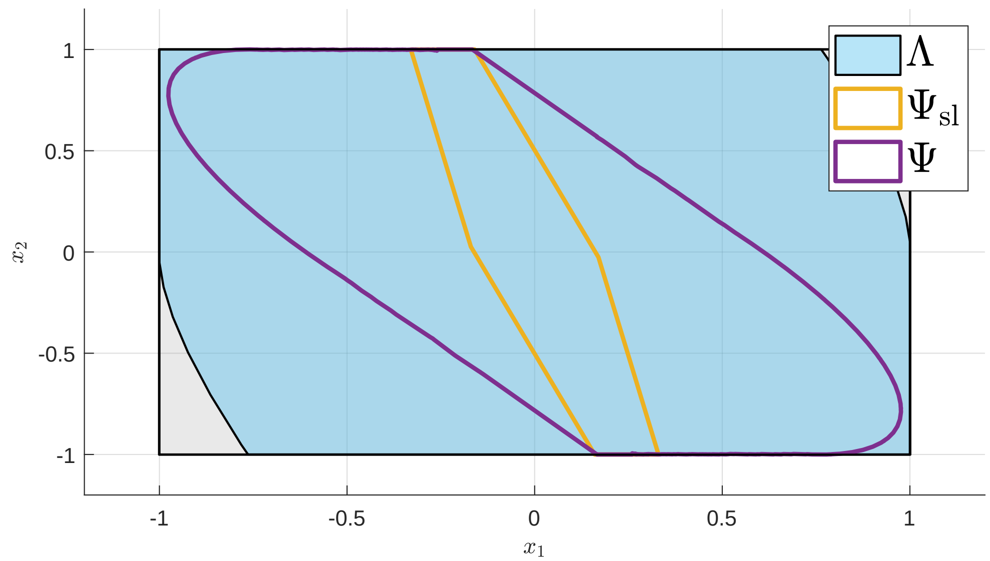

Note: inclusion $\Psi_{\mathrm{sl}} \subseteq \Psi$

- Restrict definition of Ψ to $c^\star = 0$

Example: $n = 2$ with $k^\star = -[0.25, 0.5]^\top$, $\tilde{m} = 3$

SM MFC - summary

First-order sliding-mode MFC

- Stabilisation by tracking solution of the stabilised process
  $\Rightarrow$ Geometric stability criterion for perturbed process using the solution of the unperturbed MCL
  $\Rightarrow$ Bound: x remains in tube around $x^\star$
- Region of attraction
  $\Rightarrow$ Appropriately chosen $x_0^\star$: ROA SL $\subseteq$ ROA MFC ($\Psi_{\mathrm{sl}} \subseteq \Psi \subseteq \Lambda$)

Outline

Super-twisting model-following control

Goal: stabilise PCL with super-twisting algorithm (STA)

- Perturbation $\Delta(x,t) = \Delta_x(x) + \Delta_t(t)$ satisfying local bounding conditions on $\mathcal{D}$

$$\max_{x\in\mathcal{D},t\in\mathbb{R}^+} |\Delta(x,t)| \leq \delta, \quad \max_{t\in\mathbb{R}^+} \left|\frac{\mathrm{d}\Delta_t(t)}{\mathrm{d}t}\right| \leq \delta_t, \quad \max_{x\in\mathcal{D}} \left|\frac{\partial\Delta_x(x)}{\partial x_i}\right| \leq \delta_{x_i}, \; i = 1, 2, ..., n$$

STA with state-dependant perturbation

- Typically non vanishing reaching-phase (even if initial value of sliding variable is zero)

  A. Chalanga, S. Kamal, and B. Bandyopadhyay, “A new algorithm for continuous sliding mode control with implementation to industrial emulator setup,” *IEEE/ASME Transactions on Mechatronics*, vol. 20, no. 5, pp. 2194–2204, 2015

- A-priori bound on the time-derivative of the perturbation $\Rightarrow$ may cause algebraic loop

$$\frac{\mathrm{d}\Delta(x,t)}{\mathrm{d}t} = \frac{\partial\Delta(x,t)}{\partial t} + \frac{\partial\Delta(x,t)}{\partial x}\dot{x} = \frac{\mathrm{d}\Delta_t(t)}{\mathrm{d}t} + \frac{\mathrm{d}\Delta_x(x)}{\mathrm{d}x}\Big(A\,x + B\big(u + \Delta(x,t)\big)\Big)$$

I. Castillo, L. M. Fridman, and J. A. Moreno, “Super-twisting algorithm in presence of time and state dependent perturbations,” *International Journal of Control*, vol. 91, no. 11, pp. 2535–2548, 2018

Super-twisting MFC - control design

Super-twisting design: special parametrisation

H. Liu and H. K. Khalil, “Output-feedback stabilization using super-twisting control and high-gain observer,” *International Journal of Robust and Nonlinear Control*, vol. 29, no. 3, pp. 601–617, 2019

- Integral sliding-mode control

  N. Tietze, K. Wulff, and J. Reger, “Local stabilization of systems with time and state dependent perturbations using super-twisting integral sliding-mode control,” in *European Control Conference*, Stockholm, Sweden, 2024, pp. 3676–3683

- Model-following control

  N. Tietze, K. Wulff, and J. Reger, “Local stabilisation of nonlinear systems with time- and state-dependent perturbations using sliding-mode model-following control,” in *IEEE Conference on Decision and Control*, Milan, Italy, 2024

Super-twisting MFC: $u = u^\star + \tilde{u}_0 + \tilde{u}_1$

- Gains $\tilde{\alpha}_1, \tilde{\alpha}_2 > 0$ and scaling $\tilde{\mu} > 0$

$$\tilde{u}_0 = -\begin{bmatrix} 0 & \tilde{m}^\top \end{bmatrix} \tilde{x},$$

$$\tilde{u}_1 = -\frac{\tilde{\alpha}_1}{\tilde{\mu}} |\tilde{s}|^{1/2} \operatorname{sgn}(\tilde{s}) + \tilde{v},$$

$$\dot{\tilde{v}} = -\frac{\tilde{\alpha}_2}{2\,\tilde{\mu}^2} \operatorname{sgn}(\tilde{s}), \quad \tilde{v}(0) = 0$$

Dynamics of the closed loop

- State $\tilde{z}$, auxiliary variable $\bar{v} = \tilde{v} + \Delta(x,t)$

$$\dot{\tilde{z}} = A_\mathrm{z}\,\tilde{z} + B_\mathrm{z}\,\tilde{s},$$

$$\dot{\tilde{s}} = -\frac{\tilde{\alpha}_1}{\tilde{\mu}} |\tilde{s}|^{1/2} \operatorname{sgn}(\tilde{s}) + \bar{v},$$

$$\dot{\bar{v}} = -\frac{\tilde{\alpha}_2}{2\,\tilde{\mu}^2} \operatorname{sgn}(\tilde{s}) + \frac{\mathrm{d}\Delta(x,t)}{\mathrm{d}t}$$

Super-twisting MFC - stability

Lyapunov function for STA: $\tilde{V} = \chi^\top \tilde{P}\,\chi, \quad \chi = [\chi_1, \chi_2]^\top = [|\tilde{s}|^{1/2}\,\mathrm{sgn}(\tilde{s}),\ \tilde{\mu}\,\bar{v}]^\top$

$$\tilde{A} = \frac{1}{2}\begin{bmatrix} -\tilde{\alpha}_1 & 1 \\ -\tilde{\alpha}_2 & 0 \end{bmatrix},\ \tilde{B} = \begin{bmatrix} 0 \\ 1 \end{bmatrix} \quad \text{with solution} \quad \tilde{P} = \begin{bmatrix} \tilde{p}_{11} & \tilde{p}_{12} \\ \tilde{p}_{12} & \tilde{p}_{22} \end{bmatrix} > 0 \quad \text{of} \quad \tilde{A}^\top \tilde{P} + \tilde{P}\,\tilde{A} = -I$$

J. A. Moreno, "A linear framework for the robust stability analysis of a generalized super-twisting algorithm," in *International Conference on Electrical Engineering, Computing Science and Automatic Control*, 2009, pp. 1–6

Theorem 5 (Stability of the closed loop for sufficiently small scaling $\tilde{\mu}$).

Given some $c^\star$, $\tilde{c}$ and $\tilde{c}_z \geq \tilde{a}\,\tilde{c}$ such that $\boxed{\Omega_{c^\star,\tilde{c},\tilde{c}_z} = \left(\Omega^\star_{c^\star} \oplus \tilde{\Omega}_{\tilde{c},\tilde{c}_z}\right) \subseteq \mathcal{D}}$, let $\boxed{x_0^\star = x_0 \in \Omega^\star_{c^\star}}$.

Then there exists some $\bar{\mu} > 0$ such that x remains in $\Omega_{c^\star \tilde{c},\tilde{c}_z}$ and $\boxed{\lim_{t\to\infty} x(t) = 0 \text{ for every } \tilde{\mu} < \bar{\mu}.}$

Idea of proof: overcoming the algebraic loop locally

- Bound $\bar{\mu}$ depends on parameters in Lyapunov equation and estimate of bounds of $\Delta(x,t)$

$$\dot{\tilde{V}} \leq \frac{1}{\tilde{\mu}\,|\chi_1|}\left(-\|\chi\|_2^2 + 2\boxed{\tilde{\mu}^2}\|\chi\|_2 \|\tilde{P}\,\tilde{B}\|_2\,|\chi_1| \boxed{\left|\frac{\mathrm{d}\Delta(x,t)}{\mathrm{d}t}\right|}\right), \quad \boxed{\left|\frac{\mathrm{d}\Delta(x,t)}{\mathrm{d}t}\right|} \leq \frac{\gamma_0}{\tilde{\mu}} \quad \text{for some } \gamma_0 > 0$$

Super-twisting MFC - stability

Theorem 6 (Stability of the closed loop for sufficiently small scaling $\tilde{\mu}$).
Given some $c^\star$, $\tilde{c}$ *and* $\tilde{c}_\mathrm{z} \geq \tilde{a}\,\tilde{c}$ *such that* $\Omega_{c^\star,\tilde{c},\tilde{c}_\mathrm{z}} = \left(\Omega^\star_{c^\star} \oplus \tilde{\Omega}_{\tilde{c},\tilde{c}_\mathrm{z}}\right) \subseteq \mathcal{D}$, *let* $x_0^\star = x_0 \in \Omega^\star_{c^\star}$ *and*

$$\tilde{\mu}_0 = \frac{1}{\delta\,\tilde{p}_{22}} \sqrt{\left(\tilde{p}_{11}\,\tilde{p}_{22} - \tilde{p}_{12}^2\right)\tilde{c}}\,, \qquad \tilde{\mu}_1 = \left(2\,\gamma\,\|\tilde{P}\tilde{B}\|_2\right)^{-1}$$

for some $\gamma \geq \gamma_0$ *with*

$$\gamma_0 = \Big(\max_{x^\star\in\Omega^\star_{c^\star}} |u^\star| + \max_{\tilde{x}\in\tilde{\Omega}_{\tilde{c},\tilde{c}_\mathrm{z}}} |\tilde{u}_0| + 2\,\delta\Big)\delta_{x_n}\tilde{\mu}_0 + \delta_t\,\tilde{\mu}_0 + \tilde{\mu}_0 \sum_{i=2}^{n} \max_{x\in\Omega_{c^\star,\tilde{c},\tilde{c}_\mathrm{z}}} |x_i|\delta_{x_{i-1}} + \delta_{x_n}\left(\tilde{\alpha}_1 + \sqrt{\frac{\tilde{p}_{11}}{\tilde{p}_{22}}}\right)\sqrt{\tilde{c}}.$$

Then x *remains in* $\Omega_{c^\star,\tilde{c},\tilde{c}_\mathrm{z}}$ *and* $\lim_{t\to\infty} x(t) = 0$ *for every* $\tilde{\mu} < \min\{\tilde{\mu}_0, \tilde{\mu}_1\}$.

Super-twisting MFC - region of attraction

Discussion

$$\boxed{x_0^\star = x_0 \in \Omega_{c^\star}^\star} \text{ with } \boxed{\Omega_{c^\star,\tilde{c},\tilde{c}_z} \subseteq \mathcal{D}} \xRightarrow{\tilde{\mu}<\bar{\mu}} \boxed{\lim_{t\to\infty} x(t) = 0}$$

Region of attraction

- Convergence for all $x_0 \in \Omega_{c^\star}^\star$

Challenges

- Non vanishing reaching-phase for exact initialisation $x_0^\star = x_0$
- Algebraic loop resolved (via scaling $\tilde{\mu}$)

x_1-x_2-plane

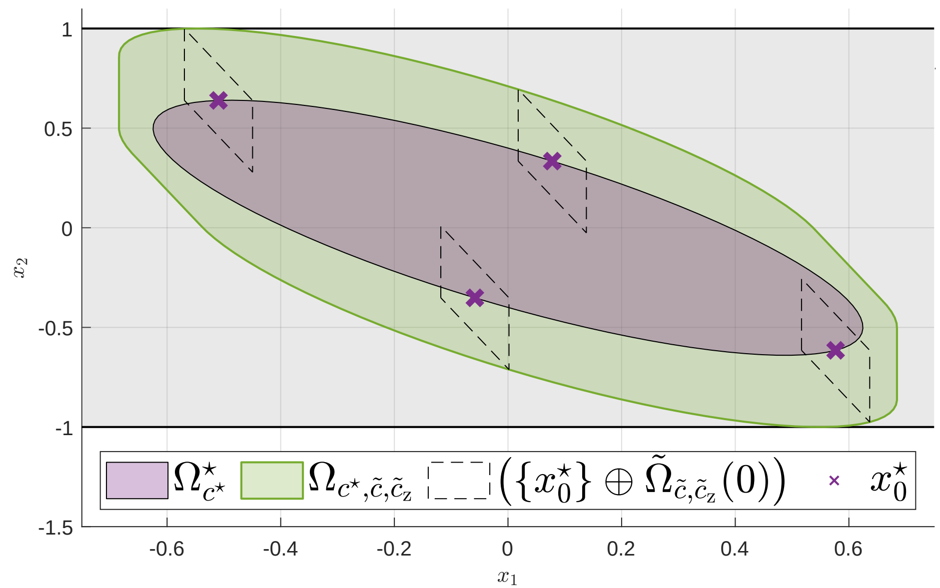

Conclusion - sliding mode MFC

Robustness of 2-DOF architecture with sliding-mode control

- Local stability and invariance properties using solution of MCL
  - $\Rightarrow$ First-order: region of attraction SL $\subseteq$ region of attraction MFC
  - $\Rightarrow$ STA: overcome problem of non vanishing reaching phase and algebraic loop

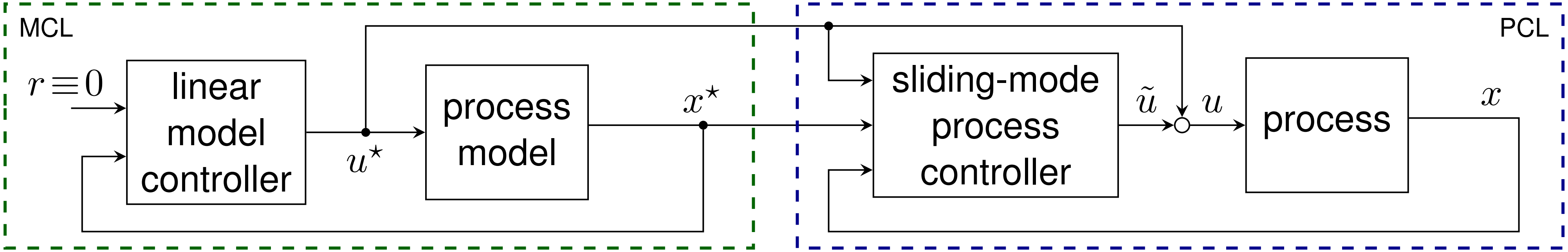

Outlook

- Lyapunov redesign: smaller gain for controller

  N. Tietze, K. Wulff, and J. Reger, "Dynamic partial state-feedback revisited for output tracking using Lyapunov redesign and model-following control," in *IEEE Conference on Decision and Control*, Milan, Italy, 2024

- High-gain control: peaking attenuation

  N. Tietze, K. Wulff, and J. Reger, "A model-following control approach to peaking attenuation in high-gain partial state feedback for nonlinear systems," in *IFAC Conference of Modelling, Identification and Control of nonlinear systems*, Lyon, France, 2024

XII. Super-Twisting Control in Practical Applications: An Alternative to PI-Control?

presenter: Benedikt Andritsch

Super-Twisting Control in Practical Applications: An Alternative to PI Control?

Benedikt Andritsch, Stefan L. Hölzl, Stefan Koch,
Markus Reichhartinger and Martin Horn,
Institut für Regelungs- und Automatisierungstechnik

23rd Styrian Workshop on Automatic Control
11 September 2024

Motivation

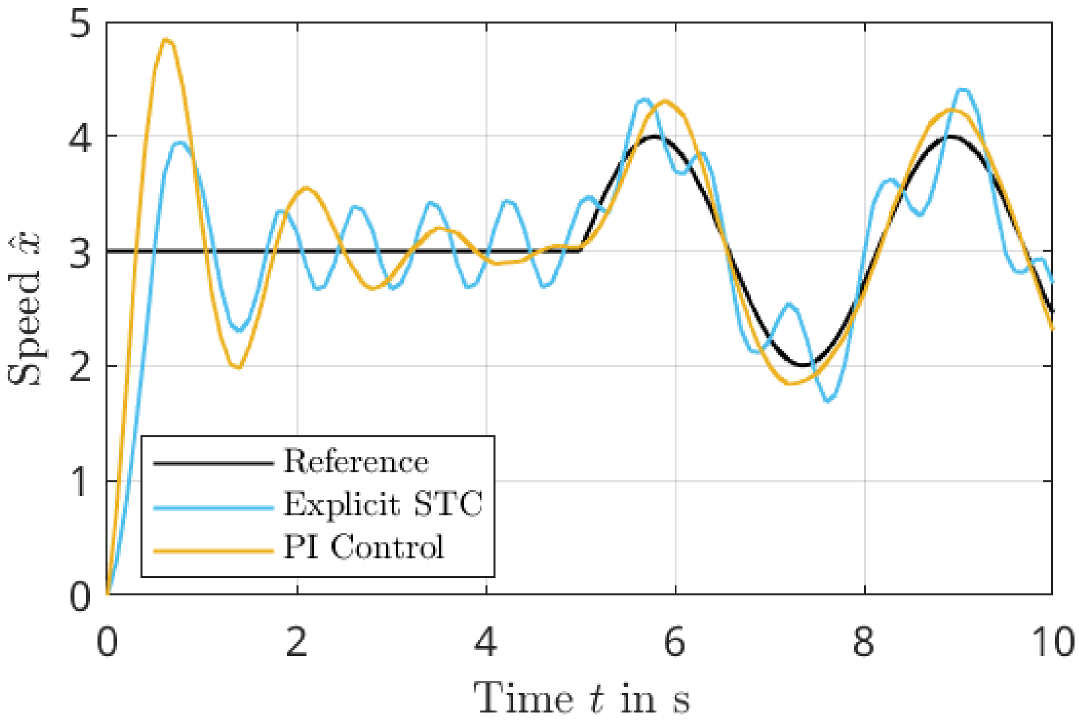

Objectives:

- Remove chattering in practical application of super-twisting control.
- Compare super-twisting control and PI control.

Problem Description

Plant

$$\begin{aligned} \dot{\mathbf{x}} &= \mathbf{f}(\mathbf{x}) + \mathbf{g}(\mathbf{x})(u + \varphi), \\ \sigma &= h(\mathbf{x}) - r(t), \end{aligned} \tag{1}$$

with unknown input disturbance φ and relative degree 1:

$$\dot{\sigma} = a(\mathbf{x}) - \dot{r}(t) + b(\mathbf{x})(u + \varphi) \tag{2}$$

Control goal: Stabilize output (control error) at $\sigma = 0$.
Assumptions:

- $b(\mathbf{x})$ positive and bounded,
- $b(\mathbf{x})\varphi(t)$ and $a(\mathbf{x}) - \dot{r}(t)$ Lipschitz-continuous in t.

Established Control Methods

PI Control & Super-Twisting Control

PI Control

$$
\begin{aligned}
u &= -k_1\sigma + v, \\
\dot{v} &= -k_2\sigma
\end{aligned} \tag{3}
$$

yields

$$
\dot{\sigma} = b(\mathbf{x})v - b(\mathbf{x})k_1\sigma + a(\mathbf{x}) - \dot{r}(t) + b(\mathbf{x})\varphi(t). \tag{4}
$$

- Can only reject constant disturbances,
- Well established and broadly used in industry,
- Many tuning rules exist.

High-Gain PI Control: Robust Linear Control

$$u = -k_1\sigma + v,$$
$$\dot{v} = -k_2\sigma$$

Robustness via high gains[1]

$$k_1 = \frac{h_1}{\varepsilon}, \quad k_2 = \frac{h_2}{\varepsilon^2}, \tag{5}$$

small $\varepsilon > 0$. Decreasing ε diminishes the effect of the disturbance on σ.

- Practically infeasible due to large control actuation and sensitivity to noise.

[1] Khalil, Chapter 14 in Nonlinear Systems. Upper Saddle River, New Jersey: Prentice Hall, 2002.

Super-Twisting Control (STC): Robust Nonlinear Control

$$
\begin{aligned}
u &= -k_1 \mathsf{sign}\left(\sigma\right)\sqrt{|\sigma|} + v, \\
\dot{v} &= -k_2 \mathsf{sign}\left(\sigma\right)
\end{aligned}
\tag{6}
$$

yields

$$
\dot{\sigma} = b(\mathbf{x})v - b(\mathbf{x})k_1 \mathsf{sign}\left(\sigma\right)\sqrt{|\sigma|} + a(\mathbf{x}) - \dot{r}(t) + b(\mathbf{x})\varphi(t). \tag{7}
$$

- Can reject any Lipschitz continuous disturbances,
- Can lead to chattering effects due to unmodeled dynamics and discretization.

Discrete-Time Super-Twisting Control

General discrete-time controller

$$\begin{aligned} u_k &= v_k - k_1 \Psi_1(\sigma_k), \\ v_{k+1} &= v_k - T k_2 \Psi_2(\sigma_k), \end{aligned} \qquad (8)$$

with discretization time T.

Explicit Euler discretization leads to discretization chattering:

$$\begin{aligned} \Psi_1^{\mathsf{exp}}(\sigma_k) &= \mathsf{sign}\,(\sigma_k)\sqrt{|\sigma_k|}, \\ \Psi_2^{\mathsf{exp}}(\sigma_k) &= \mathsf{sign}\,(\sigma_k)\,. \end{aligned} \qquad (9)$$

Implicit Euler[2,3] and Low-Chattering[4] methods

- produce no discretization chattering,
- yield linear controllers close to $\sigma = 0$, i.e. utilize high-gain PI control.

[2] Andritsch et al., Modified implicit discretization of the super-twisting controller. IEEE Transactions on Automatic Control, 2024.
[3] Seeber et al., Proper implicit discretization of the super-twisting controller ... 2024. https://arxiv.org/abs/2406.16094.
[4] Hanan et al., Low-Chattering Discretization of Homogeneous Differentiators. IEEE Transactions on Automatic Control, June 2022.

Input-Output Linearization: Compensate Output Dynamics

Recall output dynamics

$$\dot{\sigma} = a(\mathbf{x}) - \dot{r}(t) + b(\mathbf{x})(u + \varphi).$$

Applying control law

$$u = \frac{1}{b(\mathbf{x})}(-a(\mathbf{x}) + \dot{r}(t) + u^*) \quad (10)$$

yields

$$\dot{\sigma} = u^* + b(\mathbf{x})\varphi(t) \quad (11)$$

- Assume necessary state information given to compute $a(\mathbf{x})$ and $b(\mathbf{x})$.
- PI control still not robust against $b(\mathbf{x})\varphi(t)$.
- STC does not have to be robust against $a(\mathbf{x})$ but only $b(\mathbf{x})\varphi(t)$ (smaller gains).

Simulation Example

Speed Control of a DC motor

Speed Control of a DC Motor

First-order model yields error dynamics $\dot{\sigma} = \alpha x + \beta u - \dot{r}(t)$.

Speed x, reference r, error $\sigma = x - r$.

Parametrization[5]: $\alpha = -25.1$, $\beta = 28.5$.

Parameters: $k_1 = \sqrt{2k_2}$, $k_2 = 50$, $T = 0.01$

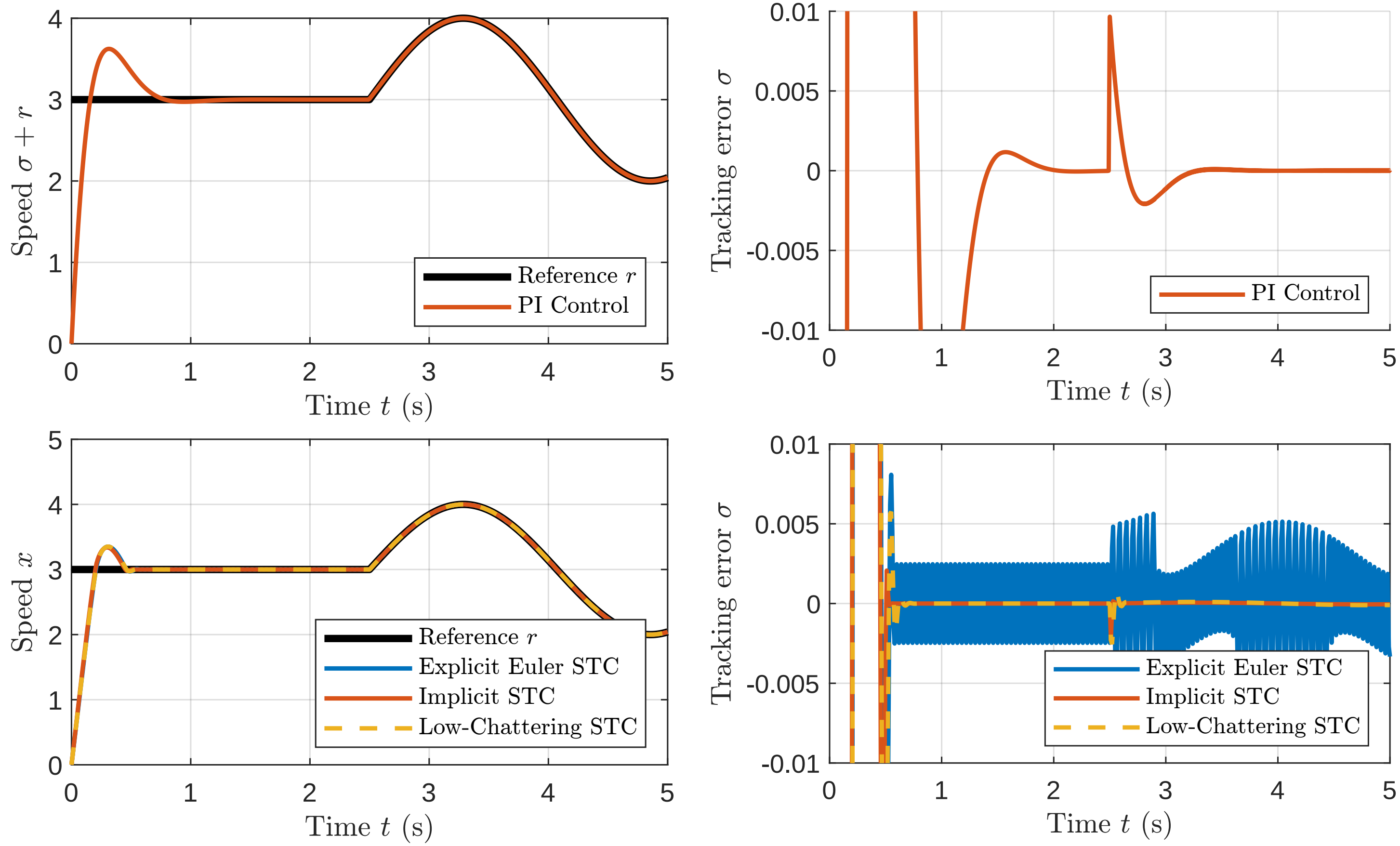

[5] Andritsch et al., Experimental comparison of sliding mode control dedicated discretization approaches. Accepted to International Workshop on Variable Structure Systems (VSS), 2024.

Discrete-Time Eigenvalues

Pseudo-Linear System Representation & State-Dependent Eigenvalues

Pseudo-Linear System Representation

Recall general form of discrete-time controller

$$u_k^* = v_k - k_1 \Psi_1(\sigma_k),$$
$$v_{k+1} = v_k - T k_2 \Psi_2(\sigma_k).$$

Defining $z_k = \varphi_k + v_k$ and $\psi_i(\sigma_k) = k_i \frac{\Psi_i(\sigma_k)}{\sigma_k}$ yields the closed-loop system

$$\begin{bmatrix} \sigma_{k+1} \\ z_{k+1} \end{bmatrix} = \begin{bmatrix} 1 - T\psi_1(\sigma_k) & T \\ -T\psi_2(\sigma_k) & 1 \end{bmatrix} \begin{bmatrix} \sigma_k \\ z_k \end{bmatrix} + \begin{bmatrix} 0 \\ T \end{bmatrix} \Delta_k \tag{12}$$

State-Dependent Eigenvalues under STC

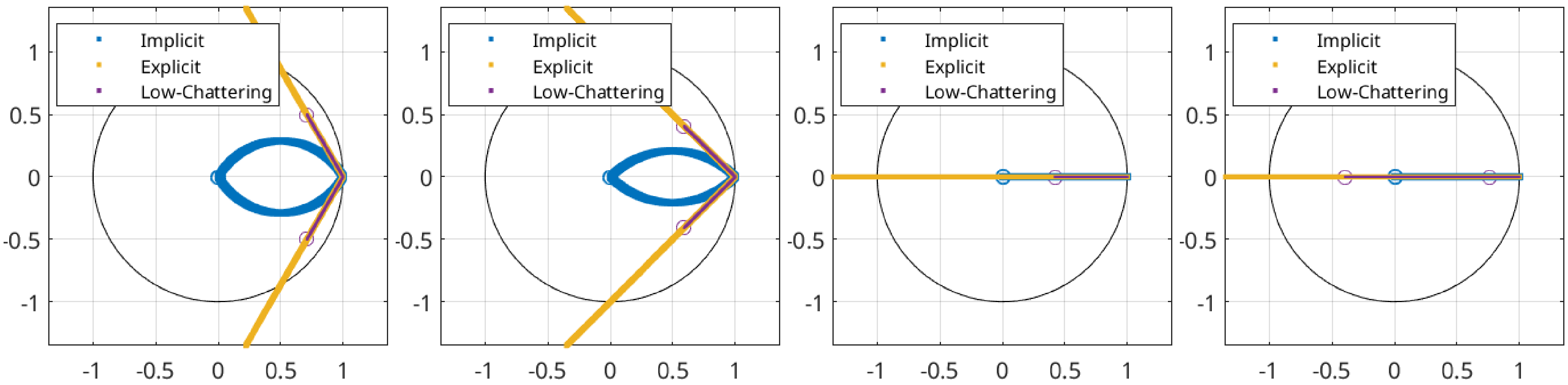

$k_1 = \sqrt{k_2}$ $k_1 = \sqrt{2k_2}$ $k_1 = \sqrt{4k_2}$ $k_1 = \sqrt{8k_2}$

Unmodeled Dynamics

Description, Effects & Chattering Reduction Method

Unmodeled Dynamics

- Originate from sensor and/or actuator (input/output dynamics).
- Often neglected as they are "fast" in comparison.
- Can be approximated by a first-order low pass.

E.g. sensor dynamics with time constant $\frac{1}{\omega}$:

$$\dot{\hat{\sigma}} = -\omega\hat{\sigma} + \omega\sigma. \tag{13}$$

Output $\hat{\sigma}$ is available for control.

Speed Control with STC and Unmodeled Dynamics

$$k_2 = 50,$$
$$k_1 = \sqrt{2k_2},$$
$$T = 0.01$$

Large time constant $\frac{1}{\omega} = 0.1\,$s. Small time constant $\frac{1}{\omega} = 0.01\,$s.

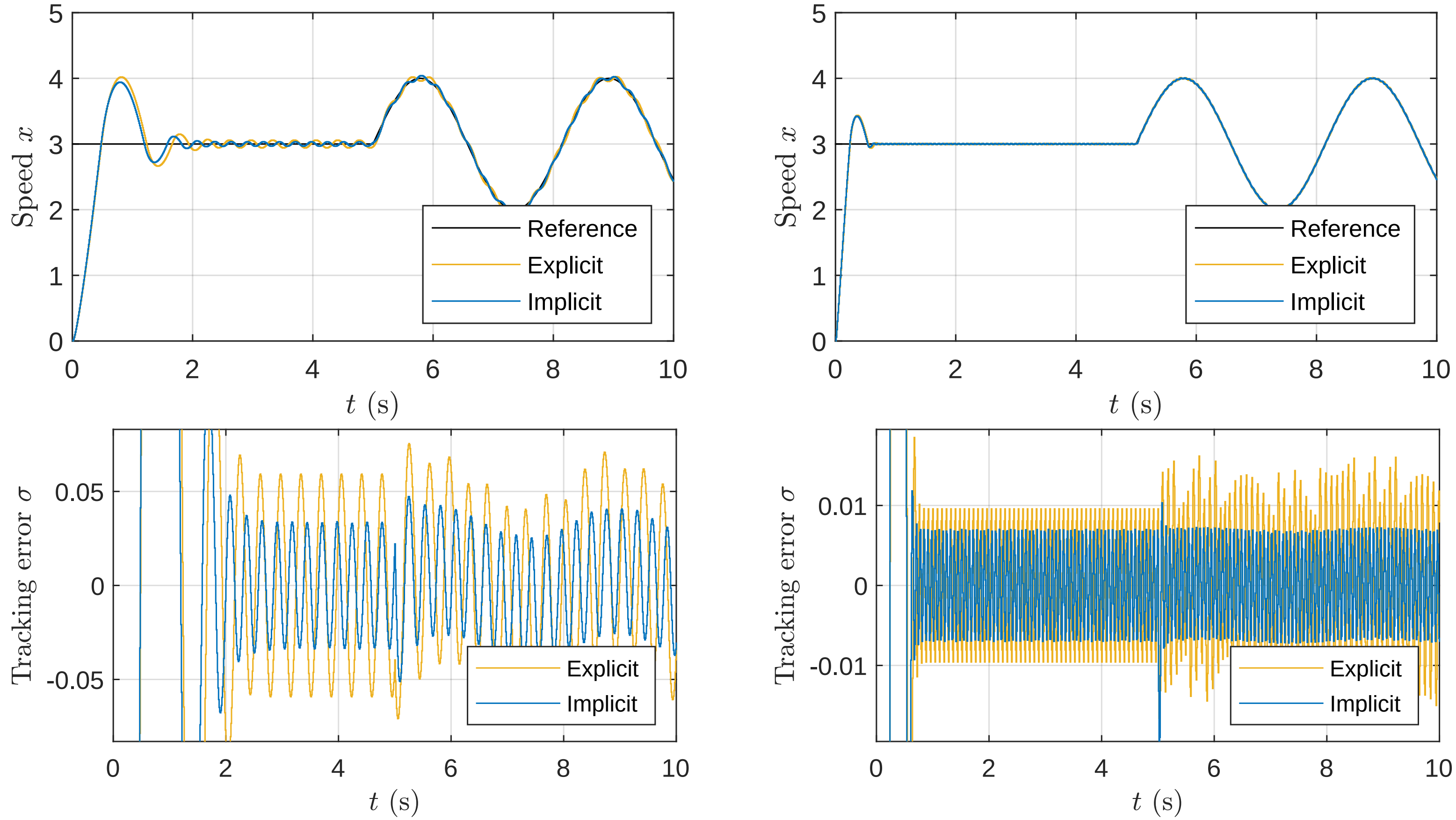

State-Dependent Eigenvalues under STC

Recall: Pseudo-linear system representation with $\psi_i(\sigma_k) = k_i \frac{\Psi_i(\sigma_k)}{\sigma_k}$, state-dependent closed-loop 3×3 system matrix.

Trajectory of explicit STC is equivalent to high-gain PI control over ε.

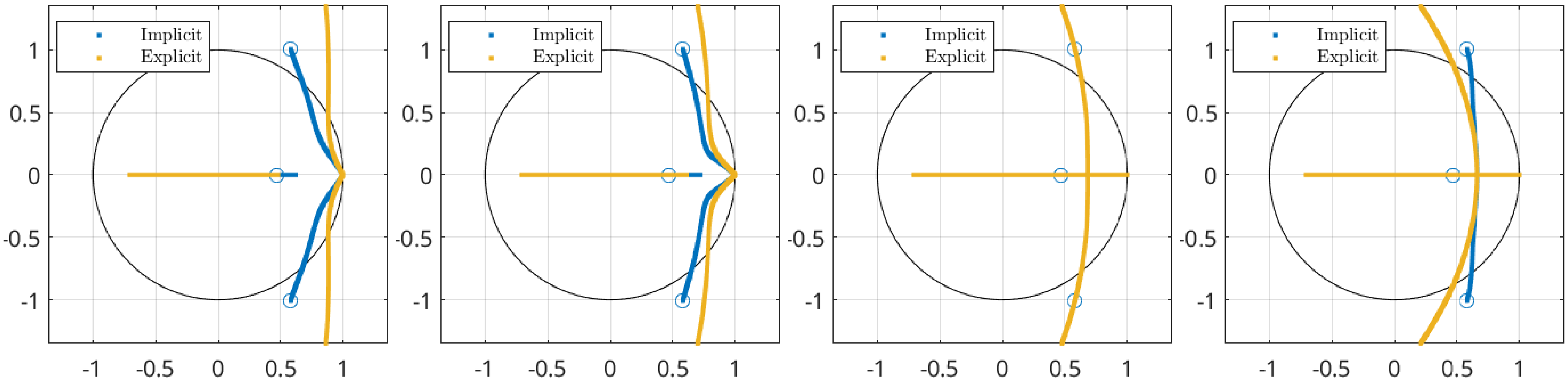

$k_1 = \sqrt{k_2}$ $\quad$ $k_1 = \sqrt{2k_2}$ $\quad$ $k_1 = \sqrt{4k_2}$ $\quad$ $k_1 = \sqrt{8k_2}$

Reduced-Chattering STC

Idea: Stop eigenvalue evolution within the unit disk, similar to[6].
Yields linear control when $\sigma \approx 0$: STC converges to high-gain PI control.

$$\Psi_i^{\text{r-}*}(\sigma) = \Psi_i^*\left(\text{sign}\left(\sigma\right)\max(|\sigma|,\gamma)\right)\frac{|\sigma|}{\max(|\sigma|,\gamma)}. \tag{14}$$

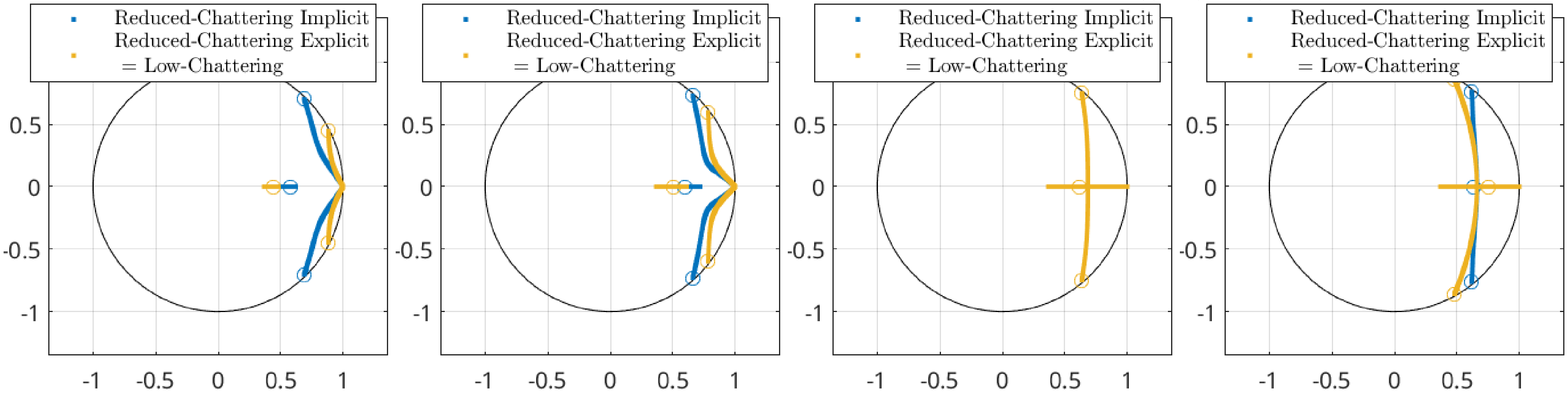

$k_1 = \sqrt{k_2}$ $\quad$ $k_1 = \sqrt{2k_2}$ $\quad$ $k_1 = \sqrt{4k_2}$ $\quad$ $k_1 = \sqrt{8k_2}$

[6] Rüdiger-Wetzlinger et al., Discrete-Time Implementations of Differentiators Homogeneous in the Bi-Limit. Springer Int. Publishing, 2023.

Speed Control with Reduced-Chattering STC

$$k_2 = 50,$$
$$k_1 = \sqrt{2k_2},$$
$$T = 0.01$$

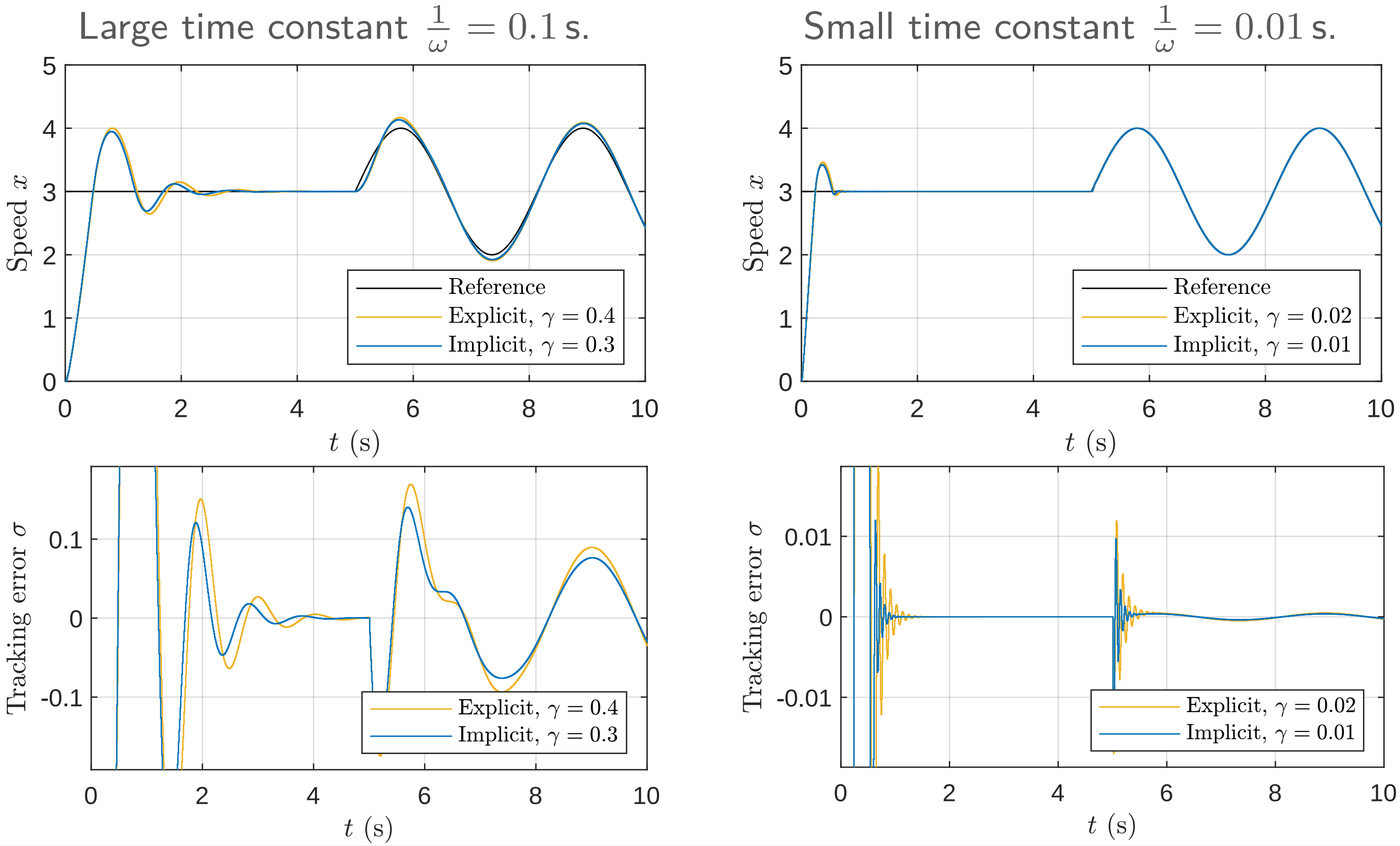

Tuning of STC

- Select controller gains $k_2 = \Lambda = \omega_0^2$, $k_1 = \rho\sqrt{\Lambda} = 2\zeta\omega_0$.
  - Pair (Λ, ρ) typical for SMC, pair (ω_0, ζ) typical for PI control.
  - Select $\rho > 2$ for convergence without oscillations.
  - Select $\rho < 2$ for convergence with oscillations.
  - Increase Λ for faster convergence.
  - Robust against input disturbance with a slope smaller than Λ.
- Select a discretization method (e.g. Explicit Euler or Implicit Euler).
- Select chattering-reduction parameter γ based on
  - closed-loop eigenvalues including estimated unmodeled dynamics or
  - the region $|\sigma| \leq \gamma$, in which the controller is linear.

Experiments

Speed Control of a DC Motor & Air Temperature Control for Fuel Cell Test Bed

Speed Control of a DC Motor (1)

$T = 0.01,\ \omega = 20,\ k_1 = \rho\sqrt{\Lambda},\ k_2 = \Lambda$ with $\rho = 4,\ \Lambda = 5$

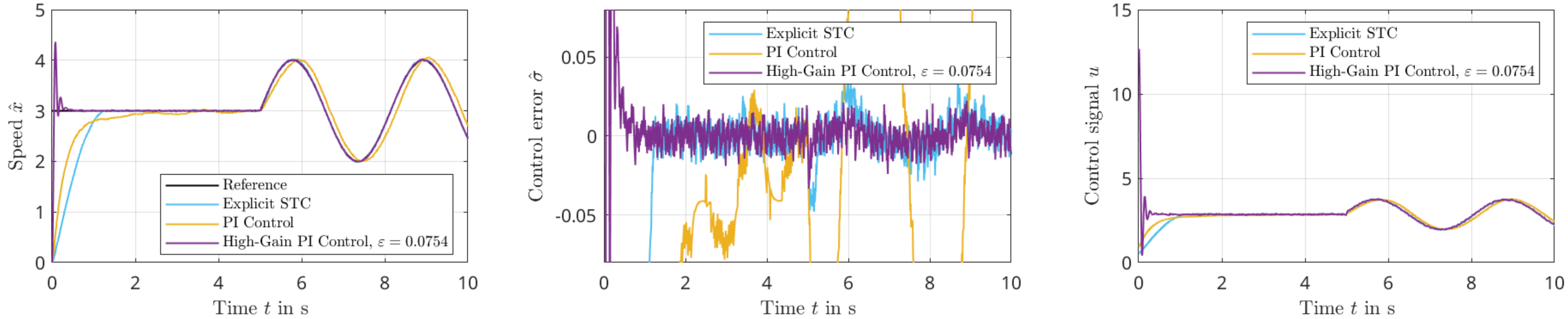

Unmodeled Dynamic: Output filter that differentiates the encoder signal.

Speed Control of a DC Motor (2)

$T = 0.01,\ \omega = 20,\ k_1 = \rho\sqrt{\Lambda},\ k_2 = \Lambda$ with $\rho = 4,\ \Lambda = 200$

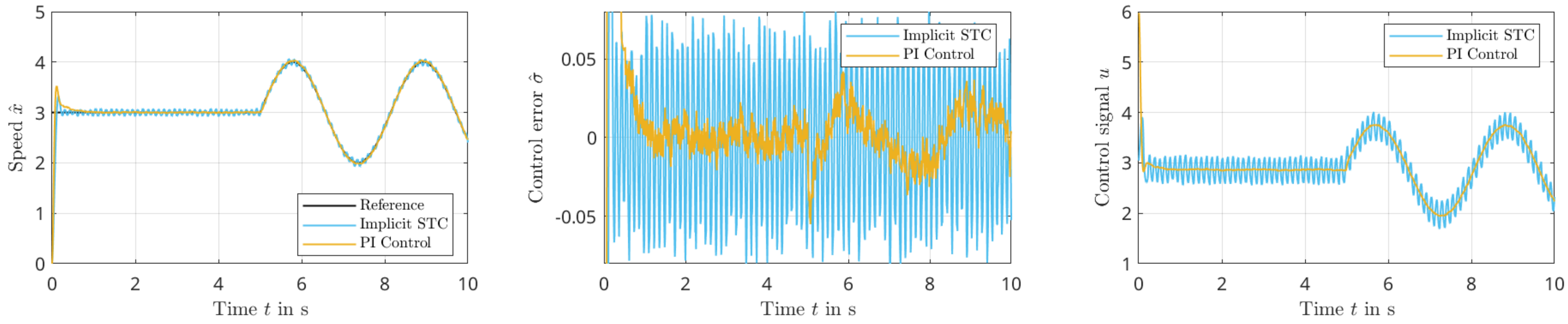

Speed Control of a DC Motor (2)

$T = 0.01,\ \omega = 20,\ k_1 = \rho\sqrt{\Lambda},\ k_2 = \Lambda$ with $\rho = 4,\ \Lambda = 200$

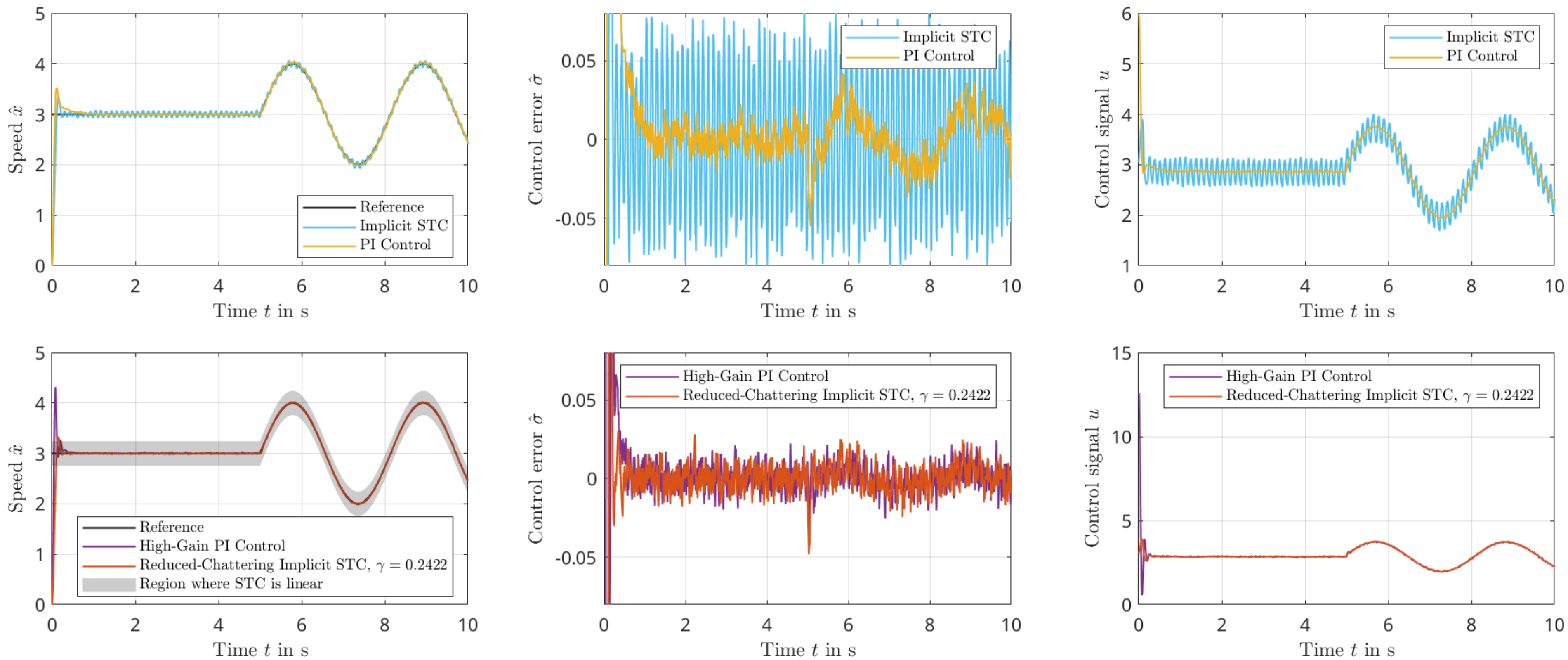

Air Temperature Control for Fuel Cell Test Bed

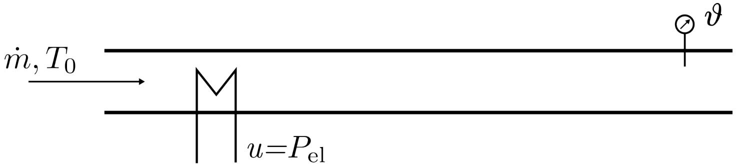

$$P(s) = \frac{0.0937}{529\,s+1} \Rightarrow 529\,\dot\vartheta = -(\vartheta - T_0) + 0.0937\,u,$$
$$T = 0.02,\ k_1 = \rho\sqrt{\Lambda},\ k_2 = \Lambda,\ \rho = 2,\ \Lambda = 0.001$$

Air Temperature Control for Fuel Cell Test Bed

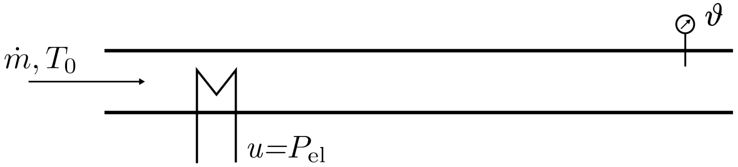

$$P(s) = \frac{0.0937}{529\,s+1} \Rightarrow 529\,\dot{\vartheta} = -(\vartheta - T_0) + 0.0937\,u,$$

$$T = 0.02,\ k_1 = \rho\sqrt{\Lambda},\ k_2 = \Lambda,\ \rho = 2,\ \Lambda = 0.001$$

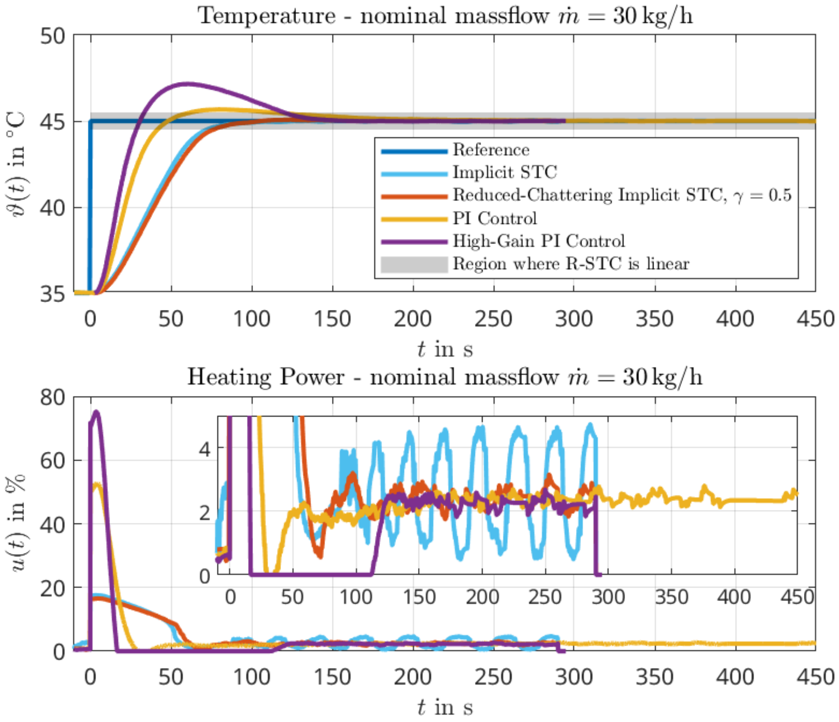

Air Temperature Control for Fuel Cell Test Bed

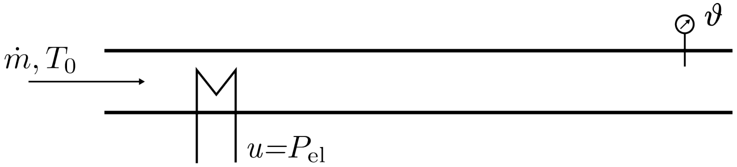

$$P(s) = \frac{0.0937}{529\,s+1} \Rightarrow 529\,\dot\vartheta = -(\vartheta - T_0) + 0.0937\,u,$$

$$T = 0.02,\ k_1 = \rho\sqrt{\Lambda},\ k_2 = \Lambda,\ \rho = 2,\ \Lambda = 0.001$$

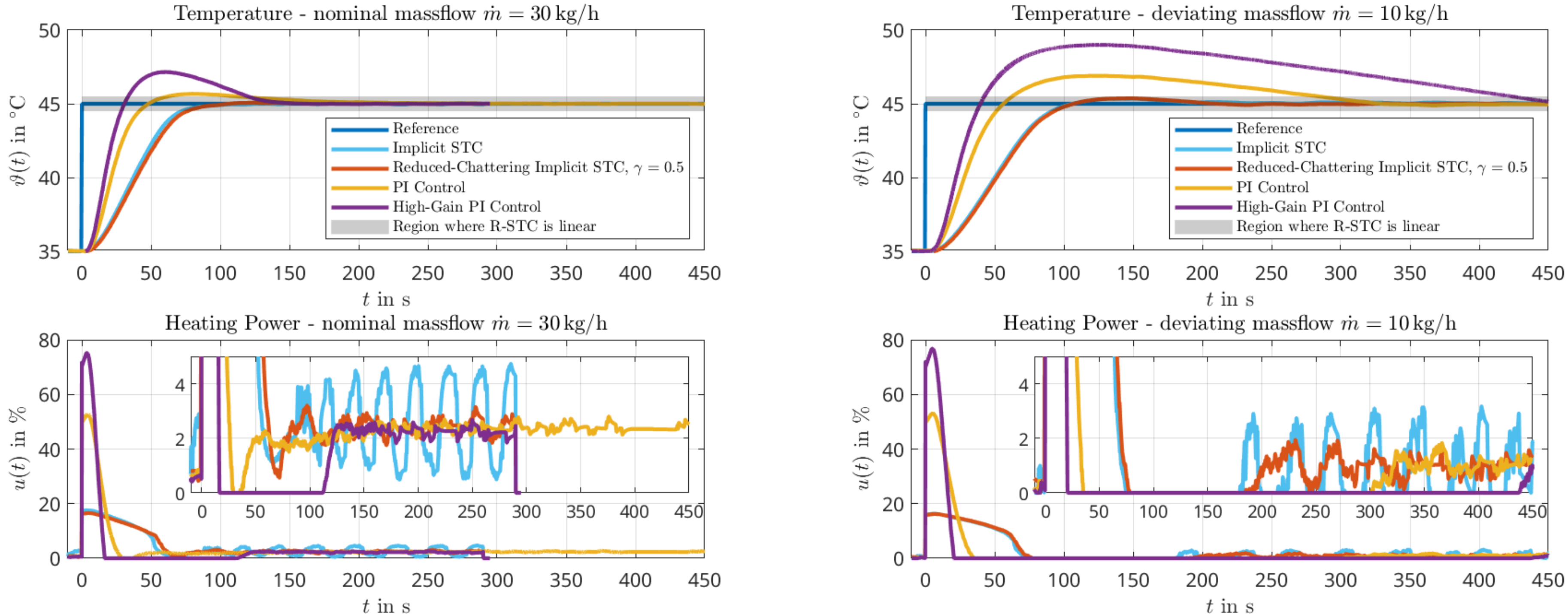

Conclusion

- Super-twisting control can successfully be deployed in practical applications.
- Chattering reduction method introducing one additional intuitive parameter.
- STC can outperform PI Control in transient behavior and remaining error.
- At $|\sigma| \leq \gamma$, reduced-chattering STC is equivalent to a PI controller.
- STC combines the benefits of PI control and high-gain PI control:
  - tolerable input actuation for the plant,
  - small overshoot in transient phase,
  - robustness against input disturbances.

Literature

[1] B. Andritsch, V. Holzner, S. Koch, M. Reichhartinger, and M. Horn, *Experimental comparison of sliding mode control dedicated discretization approaches*, in accepted to International Workshop on Variable Structure Systems (VSS), 2024.

[2] B. Andritsch, L. Watermann, S. Koch, M. Reichhartinger, J. Reger, and M. Horn, *Modified implicit discretization of the super-twisting controller*, IEEE Transactions on Automatic Control, 69 (2024), pp. 1–8.

[3] A. Hanan, A. Levant, and A. Jbara, *Low-Chattering Discretization of Homogeneous Differentiators*, IEEE Transactions on Automatic Control, 67 (2022), pp. 2946–2956.

[4] H. Khalil, *Nonlinear Systems*, Upper Saddle River, New Jersey: Prentice Hall, 2002.

[5] M. Rüdiger-Wetzlinger, M. Reichhartinger, and M. Horn, *Discrete-Time Implementations of Differentiators Homogeneous in the Bi-Limit*, Springer International Publishing, 2023, pp. 181–204.

[6] R. Seeber and B. Andritsch, *Proper implicit discretization of the super-twisting controller – without and with actuator saturation*, https://arxiv.org/abs/2406.16094, (2024).

Further Air Temperature Control Experiments

Similar rise time with $\Lambda = 0.02$, $\gamma = 1$ for STC

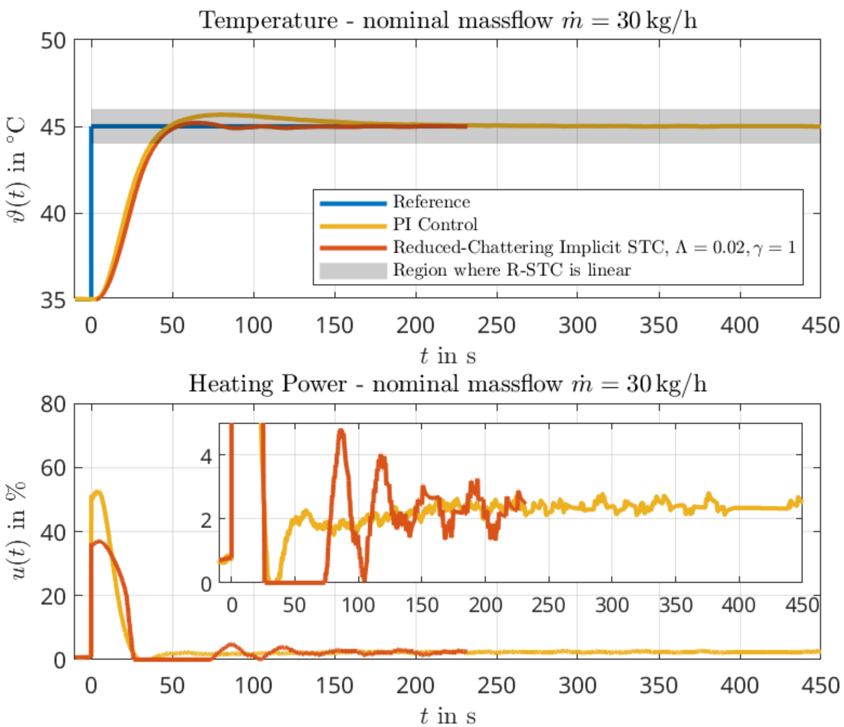

Response to 30°C step with $\Lambda = 0.001$, $\gamma = 0.5$